CRANFIELD INSTITUTE OF TECHNOLOGY

SILSOE COLLEGE

Ph.D. THESIS

ACADEMIC YEAR 1982-1985

Paulo Sergio Graziano Magalhães

An Investigation into the Grade Dynamics of Drainage Implements

Supervisor: R.J. Godwin

August 1985

This thesis is submitted in fulfilment of the requirements for the degree of

Doctor of Philosophy

ABSTRACT

The use of the trenchless plough drainage implement has increased in the past few years due to its efficiency and cost advantages over other methods. However, the performance of these machines when working in fields with irregular soil conditions is not yet satisfactory. It is important therefore to study the soil parameters and conditions which could affect the implement behaviour under these circumstances.

Therefore, a detailed investigation of the soil reaction forces acting upon a scale model of the trenchless plough was conducted under controlled conditions in a soil laboratory. The model was tested first under restricted conditions of movement, in order to observe and determine all the possible soil reaction forces.

The tine, due to its geometric characteristics, was classified as a very narrow tine, and an existing model to predict the soil reaction force acting on the front face of these tines was extended to predict the forces on the sides. Since the length of the failure plane ahead of the tine is often required in the investigation of the soil reaction forces, a mathematical solution based on the Coulomb principle of Passive Earth Pressure was presented to estimate the soil failure pattern. There was good agreement between the values of the angle of the shear plane predicted by this method and the experimental data obtained from the glass sided tank tests.

Dynamic tests were conducted with the implement assembled with a long floating beam arrangement assisted by a small link (free-link), used between the hitch-point and the pivoted end of the beam. These tests revealed that, when working over irregular soil conditions a better grade control can be obtained if the hitch-point is kept at constant level in reference to a desired line. In the case where field irregularities persist for long (step inputs), corrections in the hitch-point height might be necessary. These tests show that the implement depth changes in different proportion in relation to the hitch-point height. Where no control is imposed on the hitch-point, the path of the implement is attenuated in relation to the hitch-point position, where better results are obtained for high frequency of the hitch-point.

A mathematical solution based on these findings and on the dynamic balance of the forces acting on the system was presented. Since it is an interactive method and requires long and repetitive calculations, a computer programme was developed and used to predict the response of the implement under these uneven conditions. Good agreement between data and estimated values suggested that the method is acceptable.

ACKNOWLEDGEMENTS

The author is sincerely grateful and indebted to Professor R.J. Godwin for his supervision, criticism, encouragement and time spent during the development of this study.

Many thanks are expressed to Mr. A. Reynolds for his assistance in the preparation of the soil and recording of the data. To Mr. S. Miller and Mr. G. Soane for all their valuable suggestions, discussions and their general enthusiasm.

Thanks also to all other members of staff of the Silsoe College who have contributed for the development of the project, fear of omission prevents my mentioning names.

Gratitude is also due to Mrs. M. Maule for her proof-reading of the draft copy of this thesis. To J. Lamont and C. Lautenschlager for their friendly encouragement.

The author acknowledges the financial support of Conselho Nacional de Desenvolvimento Cientifico e Tecnologico CNPq (Brazil), and Oversas Research Awards (U.K.), both of which contributed grants, which made this research possible. Thanks also to Universidade Estadual de Campinas for giving me the oportunity to come to Silsoe College.

A very special thanks to my wife Adelaide, for her affectionate support and encouragement during the development of this work, and in particular for her suggestions and help with the writing and printing of the final thesis. Thank you, Adelaide, for your support patience and understanding, without which this thesis would never have been completed.

Table of Contents

List of Figures

List of Tables

SYMBOLS

a	distance of the pivoted end of the the beam to C.G., m
b	horizontal distance between the pivoted end of the beam and the bottom of the implement, m
b'	horizontal distance between the pivoted end of the beam and the centre of the resistance, m
C	resultant of the cohesion, N
c	cohesion, N/m^2
ca	soil interface adhesion, N/m^2
d	depth of the implement, m
dc	critical depth, m
de	equilibrium depth of the tine, m
do	initial depth of the tine, m
Δd	incremental change in depth, m
f	forward rupture distance ratio
F_h	total horizontal force reaction in the system, N
F_v	total vertical force reaction in the system, N
F_t	tangential soil reaction force, N
C.G.	centre of gravity
h	height of the hitch-point, m
H	horizontal force component of the crescent failure zone, N
H_T	total horizontal soil reaction force, N
H.P.	hitch-point
I	moment of inertia, kgm^2

Ko	ratio of horizontal to vertical stress on the soil at rest
L	length of the bottom plate of the tine, m
l	horizontal distance between the pivoted end of the beam and the tine tip, m
m	rupture distance ratio
M,Mo	moment about the pivoted end of the beam, Nm
N	normal soil reaction force, N
N	dimensionless number; Suffixes to N: = gravitational, c = cohesive, ca = adhesive, q = surcharge (Appendix 5)
N'	dimensionless number; Suffixes to N': q = gravitational, c = cohesive
P	resultant of the earth pressure, N/m^2
q	surcharge pressure, N/m^2
Q	force on the tine face, at depth greater than the critical depth, N
r	crescent radius = f, m
R	soil resultant force, N
R_F	frictional reaction, N
R_T	total resultant force, N
s	distance travelled by the implement, m
Δs	incremental change in the travelled distance, m
T	total force required to pull the implement, N
v	forward speed of the implement, m/s
V	vertical soil component of the crescent failure zone, N
V_T	total vertical soil reaction force, N

x	length of the side plate of the tine at depth z, m
w	tine width, m
W	weight of the system, N
z	depth, m
α	rake angle, deg
β	angle of the shear plane, deg
δ	angle of the interface-friction, deg
γ	soil bulk density, Kg/m^3
θ	angular deflection of the implement, rad
θ_o	initial angular deflection of the implement, rad
λ	angle between carriage and implement velocity vectors, rad
σ	angle of shearing resistance, deg
ρ	angle of crescent element from the direction of travel, deg

CHAPTER 1

INTRODUCTION

1.1 Introduction

A good soil physical environment is a prime requirement for a high level of crop production and this is synonymous with good soil structure and where high natural moisture levels occur, subsurface drainage is critical. Agricultural drainage gained a great impetus when the use of steam power became available for trench excavation. In the past twenty years a lot of improvements have been introduced to the drainage enterprise. The appearance of corrugated plastic pipes in the middle sixties and the application of laser beam grade control systems had a considerable influence on the development of high-power, high-speed trenching and trenchless ploughs. However, these machines are still not free from performance difficulties, which usually arise from inadequate knowledge of the dynamic behaviour of the implement, which is affected by the design and operational characteristics of the machine and by the condition of the soil.

1.2 The Implement

The machinery used to perform or to assist subsurface drainage includes the following:

i) mole-plough drainers

ii) trenching machines to assist tile-laying or pipe laying

iii) trenchless pipe-laying machines

The mole-plough technique which consists in producing a stable channel at depth in the soil, on a desired grade, is most satisfactorily applied on clay soil. The method is more successful when used as a secondary drainage in conjunction with the main pipe drains laid below the working depth of the mole-plough, providing an economic and satisfactory way of draining heavy land. The implement, a cylindrical foot attached to a vertical leg, is usually followed by an expander of great diameter (attached to it to enlarge the cavity and smooth the walls). It is generally fixed to a long beam which could be either sliding along the surface or in a floating position above the soil. The most important disadvantage of the method is the fact that the tunnels are liable to collapse particularly in a less stable soil and when there has been water logging.

The trenching machines are designed for excavating narrow trenches with parallel walls, up to 20 cm wide and at a depth of 1.4-1.8 m, using a bucket-wheel or a cutting chain. After placing the drain pipe into the open trench the ditch is refilled with gravel and soil. Depending on the available power and the soil conditions, these machines can work at a rate of 50-400 m/h. The disadvantages of the method are the high soil disturbance which induces a low rate of work and the increase in the cost of drainage.

In the trenchless drainage technique the pipe is fed into the ground in soil disturbed but not excavated by a special blade designed to lift and split the soil as it moves forwards. The equipment is generally heavier and more powerful than the trencher, and permits pipe-laying at a rate of 200-3,000 m/h, at depths of 1.4-1.7 m. The method can frequently offer significant cost advantages over the other techniques, specially because it reduces the consumption of expensive gravel backfill. Its use has largely increased in the past few years bringing up the necessity of a better understanding of its characteristics and performance.

1.3 The Plough-beam Arrangement

A uniform gradient for subsurface drainage is essential for the efficiency of the drainage implements. The control of the grade line established by the drainage machine, called grade control, varies according to the different types of plough-beam arrangement.

Childs (1942) suggested that improvements in the grade control could be obtained if the implement was operated with its beam floating. The floating beam, which is not sliding along the soil surface, is a physical or an imaginary beam depending upon the plough design. As the plough is pulled through the soil the forces acting on the blade and gravitational forces are in balance with the tractor resultant force. Godwin et al (1981), investigating the force mechanisms of the mole-

plough, reported that draught forces of a long sliding beam plough could be up to 85% greater than those of the plough with its beam clear of the surface.

There are several types of trenchless ploughs that utilize the floating beam principle, basically they can be categorized in relation to the type of link and hitch point location (Reeve, 1978), as:

i. Real hitch-point
    a) fixed
    b) moveable
ii. Virtual hitch-point
    a) double roller
    b) double link system

The fixed hitch-point plough utilizes a shorter beam than the other ploughs usually pivoted at the rear of the crawler track, Fig. 1.1a. The attitude control in these machines is achieved by tilting the plough blade about its heel where the hitch-point remains fixed, and the beam is in a free floating condition. In the movable real hitch-point plough, grade control is achieved by raising or lowering the hitch-point, which is a pivoted connection, with the hydraulic system, Fig. 1.1b.

In the virtual hitch-point arrangement the actual beam is replaced by a system of converging linkages, which still use the same principle of the long floating beam with a large distance between the hitch point, usually located at the front of the tractor, and the implement. Ede

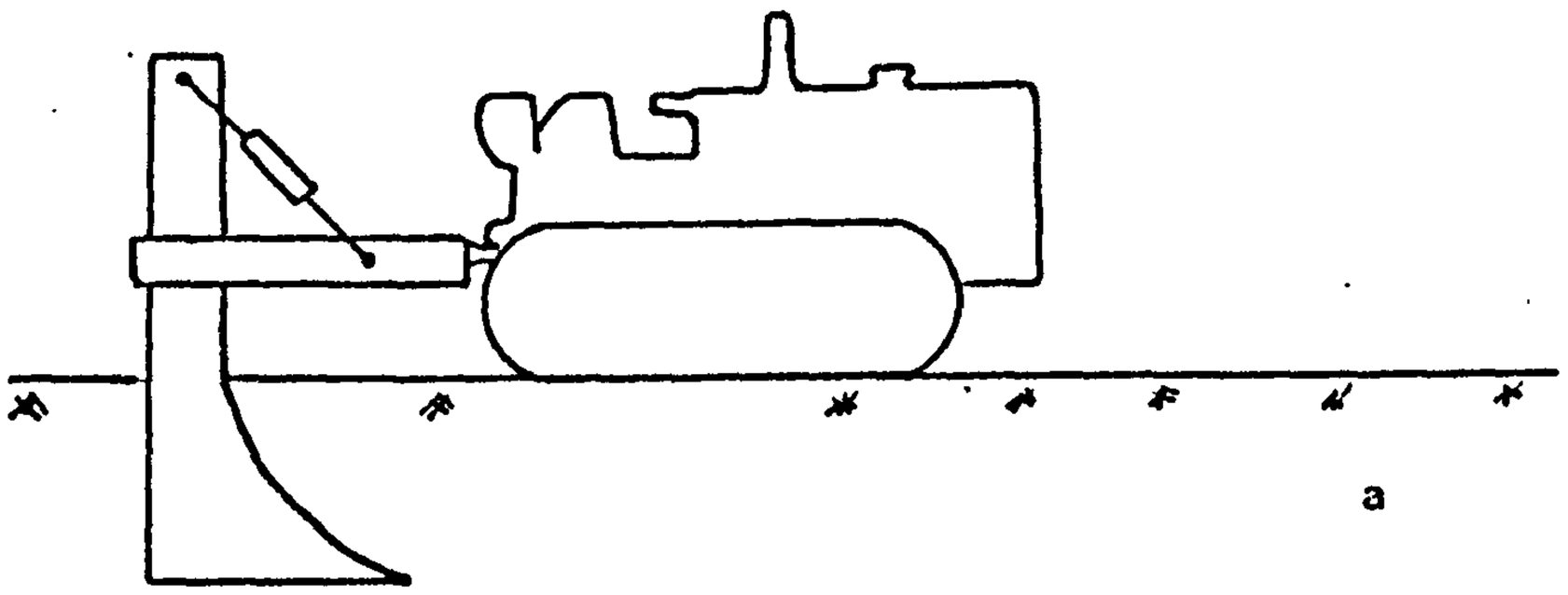

a

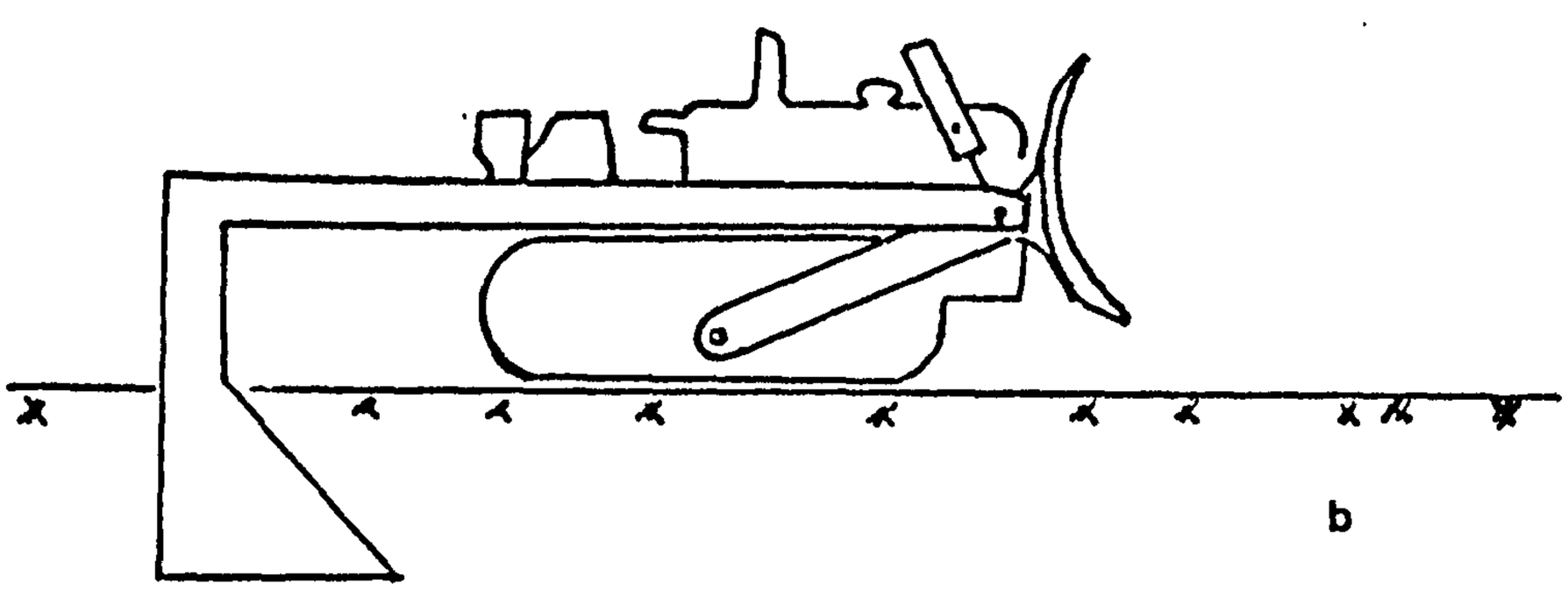

b

FIG. 1.1 Trenchless drainage implement with a real hitch-point

a) fixed

b) moveable

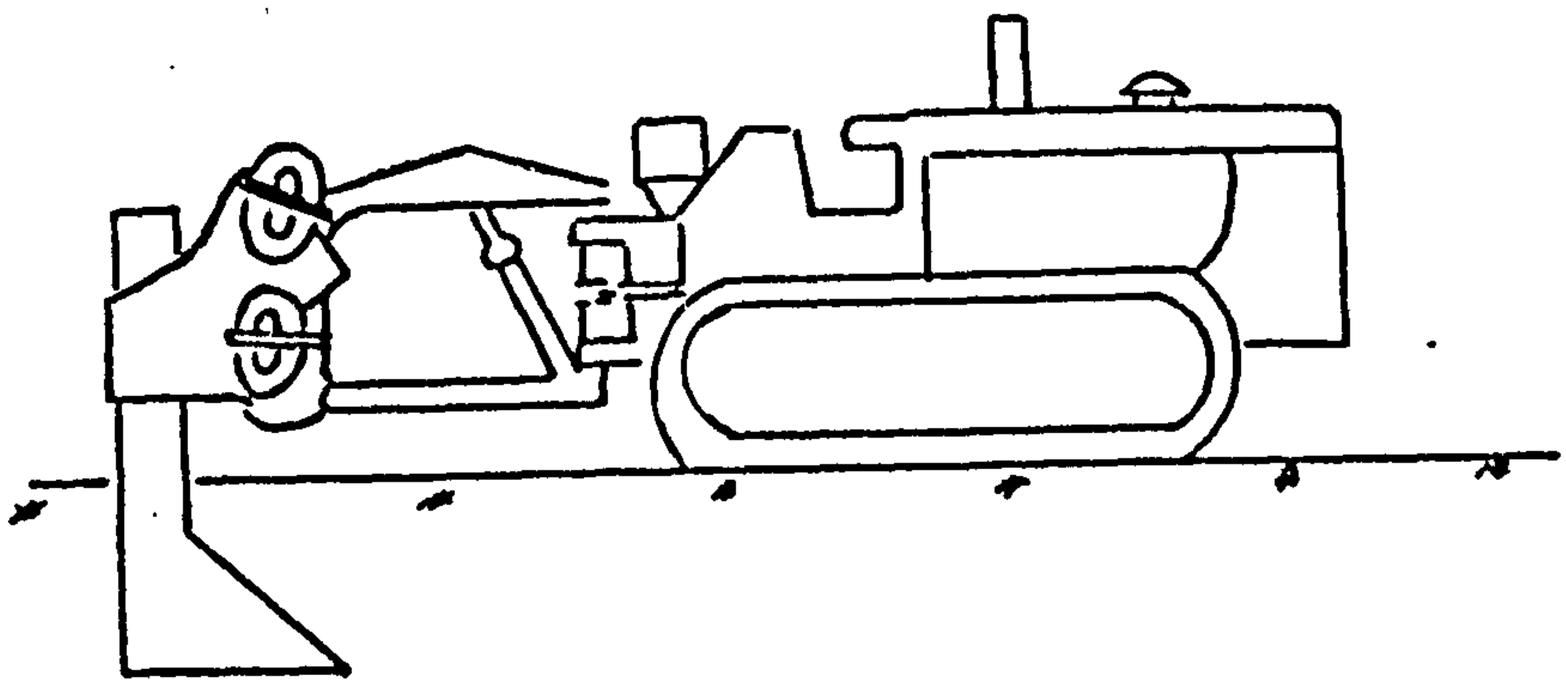

a

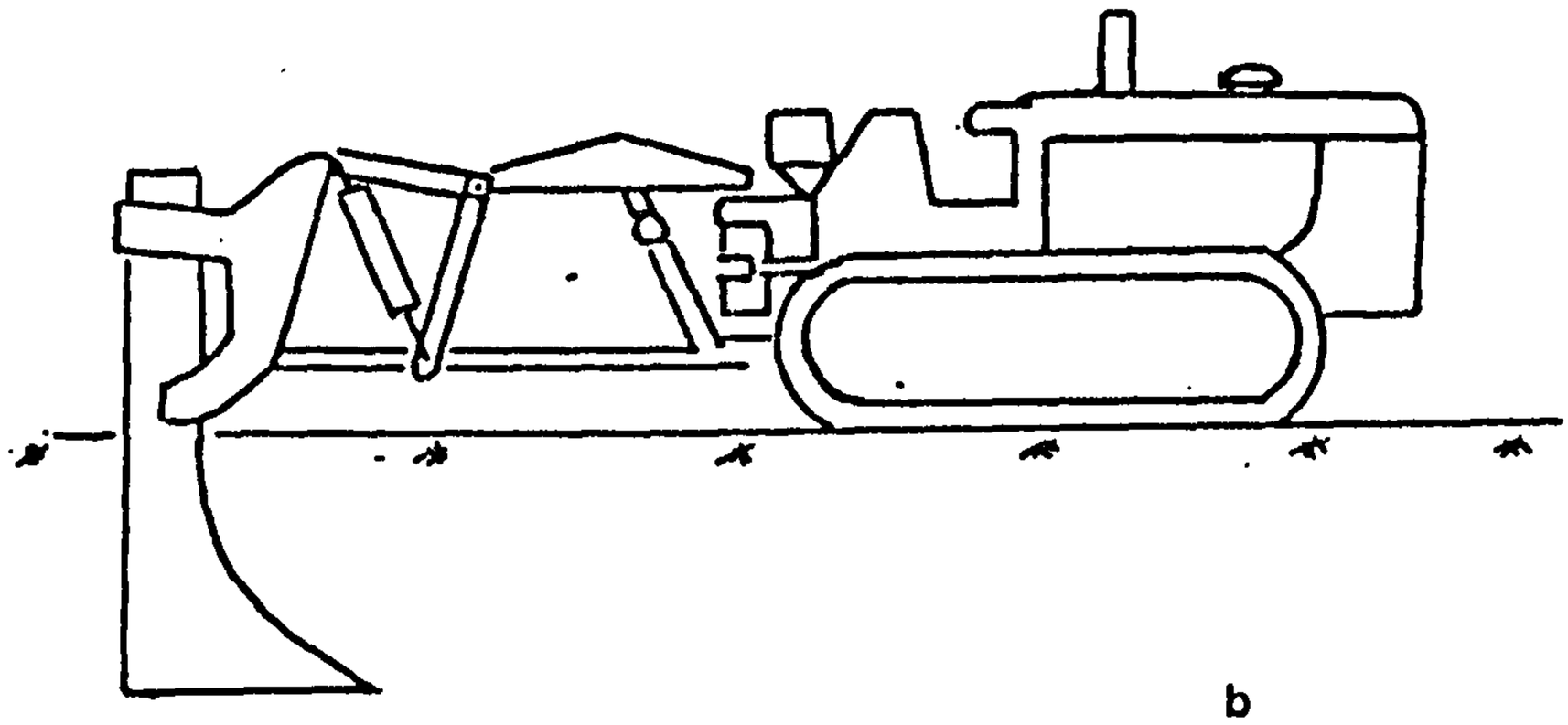

b

FIG. 1.2 Trenchless drainage implement with a virtual hitch-point

a) double roller

b) parallel converging linkage

(1961) developed the concept of a roller type floating plough where the implement and tractor are connected through a pair of rollers which run on a curved vertical track mounted at the rear of the tractor, Fig. 1.2a. The double link system utilizes two non-parallel links that provide depth control combined with free floating action, where the rear link simulates plough rotation about the virtual hitch point, Fig. 1.2b.

1.4 Grade Control

Grade control on drainage machines is essential for quality work. In the past, the grade of the implement was controlled manually through the hydraulic system by sighting to target rods, placed traditionally by levelling of height piles. This method was acceptable for the standards of the time. With the increasing demand for improvement in this sector, a better system had to be designed.

Ede (1965) developed a semi-automatic optical radio control system. The observer, stationary behind the drainage machine, could sight on a marker fixed to the plough blade and maintain it on the sight line directly by controlling the tractor hydraulic system. Delayed reaction of the observer and limited effective range were the major problems.

Fouss et al (1964) developed an "A" frame, based on a fluid damped pendulum device for automatic control of the trench machine and a floating beam type mole plough. The system worked well in slow motion, but was inadequate for high speed, and its tendency to make accumulative

errors was the main limitation.

In the middle sixties, laser beam light began to be used as a grade control for the drainage machine. The system consists of a low-power laser beam projector to emit the light line datum, and a machine-mounted electronic receiver which adjusts the elevation of the plough through the hydraulic system. The drain gradient was obtained by tilting the laser plan to the desired grade of slope. At present, the majority of drainage contractors utilize this grade control technique, Fig. 1.3.

1.5 Quality Survey

The efficiency of field drainage demands particularly careful work. It has been found that several parameters affect the quality of work among which, those relative to soil and machines appeared to be the most important ones.

It is clear that a negative slope could lead to stagnation of water at the end of the drainage period. In addition, the slope change lowers the mean water velocity and provides sedimentation of solids transported. Another common problem is laying error which is caused by an increase or decrease of drain slope.

Cros et al (1978) reported a survey conducted in France where they concluded that the drain laying quality is not mainly influenced by the type of machine and control system, but by the physical soil conditions,

FIG. 1.3 Laser beam grade contol

a) transmitter

b) the trencher implement with a laser receiver

such as slope and topography. These problems are normally caused by the pitching action of the tractor over uneven ground where the delayed activity of the control system to respond to some changes causes a considerable loss in time and of the desired standards.

1.6 Objectives

A possible solution to these problems could probably be found if better scientific knowledge about the soil condition effects on the drainage implement performance was acquired.

Therefore the main objectives of this study are:

i) Study of the magnitude and direction of the resultant soil forces acting upon the drainage implement in the dynamic situation, considering different soil profile conditions and hitch-point trajectories.

ii) Attempt to present a mathematical solution to predict the implement behaviour which does not need the introduction of empirical coefficients to explain the system, and could be valid for the most adverse conditions. The equation should be based on results obtained in the first objective and the existing information for narrow tines and the dynamics of soil engaged implements.

CHAPTER 2

LITERATURE REVIEW

2.1 Introduction

The majority of previous research projects on drainage implements performance have concentrated on flat surface conditions. Although some studies have been conducted, very little information has been given about the effect of irregularities on the surface profile or soil conditions on the implement. However, only the grade control was observed and studied, no one had measured the forces acting on the implement under these circumstances. Where force measurements were necessary, they were introduced as a package without reference to the soil conditions, moisture content, texture and topography, factors which may affect the dynamic behaviour of the plough.

2.2 Drainage Implements

One of the first investigations on drainage implements was a study of the nature of the forces acting on the mole plough by Childs (1942). Working with a 1/24 scale model, he estimated the forces acting on the implement based on the assumption that the condition for a static equilibrium is that the algebraic sum of forces and moments about any point should be separately zero. Using empirical relations to solve the

equations, he related the results with a full scale model. Childs also compared the behaviour of the long floating beam and the sliding beam over some soil irregularities and based on his analysis of forces and moments, gave the following explanation for the dynamic behaviour of the floating beam. When the mole plough passes through small soil irregularities in comparison with the length of the beam, the difference in the soil reaction will cause an imbalance in the moment, therefore, the tendency will be for the implement to raise or penetrate to compensate for it. However, the slight movement of the foot will immediately increase the moment in the other direction. The moments are therefore brought into equilibrium again, without significant movement of the cartridge from its path.

Later Wells (1951) investigated the forces distribution on the mole-plough. Using the theory commonly applied to determine the bearing strength of building fundations, together with laws of friction, he developed a simple equation to predict the draught force. From that he concluded that the friction must account for a very high proportion of the total draught. The average draught force distribution will be approximately 48% in the leg, 24% in the foot and 28% underside of the beam where the vertical force is 24% of the total draught.

He also suggested that the mole plough penetration obeys a first order differential equation of which the solution is:

$$y = D\left(1 - e^{x/l}\right) \qquad \ldots(1)$$

Where **l** is the beam length, **D** is the depth of the mole and **y** is the depth of the mole in the soil after a travel distance **x**. From his experimental work he noticed that the mole reached its working depth more quickly than was predicted by equation (1).

After analysing the performance of the mole-plough, Ede (1961) conducted some experiments with the floating beam and described the experimental aspects of the depth controlling qualities. He explored the possibilities of obtaining depth regulation by variation of the height of the point of draught. Ede found that the grade control of the implement could be satisfactorily activated by maintaining the correct level of the pivot point. The author then tested two scale models in a soil bin, the models having the long beam holding the tine replaced by an imaginary beam comprising the radius from the blade to an instantaneous center of rotation of this mounting. These tests led to a design in full scale of a "role track mole-plough" to be mounted on the tractors.

A deeper dynamic analysis of the mole-plough was carried out by Fouss (1971). Assuming that the forces are a function of the moling depth ($R_h = Kd^p$), he developed the following equation of linear second order system to simulate the dynamic response of the floating beam mole-plough.

$$\ddot{d} + \frac{(c\ b^2)}{JH}\ \dot{d} + \left(b\ K\ \left(\frac{r\ do + hs - n}{JH}\right)\ (do)^{p-1}\right)\ d = 0 \qquad ...(2)$$

Where: d = moling depth; do = specific steady state moling depth; $\dot{d}$ = velocity of change in moling depth; $\ddot{d}$ = acceleration of change in moling depth; b = effective beam length; c = damping coefficient for the mole plough; JH = moment of inertia about hitch point; K = coefficient of soil resistance; hs = any given steady-state hitch height; n = distance below the plough hitch; H where the soil resistance force acts on the blade; p = exponent coefficient in draught equation.

The solution of this equation is similar to the one for damped system, where he estimated the plough damping to be five times the critical damping coefficient Cc. From the experimental work he estimated the unkown variables, and used them in a simulation study on an analogue computer obtaining very satisfactory results. Fouss then developed a mathematical model for a "Laserplane" grade control system mounted on a drainage plough which incorporated the first model.

Later Fouss (1978), using this simulation technique, studied the best position of receiver along the beam. The origin of this study came from the fact that he observed changes in soil consistency within the path of the plough caused by a change in forces which may affect the working depth without affecting the hitch point height.

2.3 Soil Mechanics Theory

The determination of the cutting forces in the process of cutting soil is a complex task. However, much work has been conducted and the relationship between the soil mechanical properties and the performance of cultivation implements are reasonably well understood as is explained by the following.

Kostritsyn (1956) was one of the first to suggest that below a certain depth, soil movement changes from predominantly forward and upward form, to a mainly forward and sideways forms. He also proposed some mathematical equations for calculating the draught force of narrow tines in cohesive soil, where the constants were determined based on empirical relations.

Based on a series of experiments with vertical tines, both narrow and wide, Payne (1956) studying the influence in the soil behaviour, suggested a hypothesis to explain the soil resistance, using existing soil mechanics theories developed for retaining walls. After a series of practical experiments were conducted to test his hypothesis, he found that ,the model was only valid for tines sufficiently wide to bring the soil into plastic equilibrium, therefore it was invalid for very narrow tines which do not press the soil sufficiently to bring it to this state. Later, this work was extended (Payne and Tanner, 1959) for tines with different rake angles. They reported experimental results which showed that the draught force is relatively insensitive to

changes in a rake angle between 20^{o} and 50^{o}, increasing very rapidly thereafter. They also found that at less than 45^{o}, the soil resultant force acts downwards assisting penetration, but at greater angles acts in the opposite direction. Dranfield et al (1964) confirmed these findings when they examined the effect of tine rake angles on the soil rection.

O'Callaghan and Farrelly (1964) proposed a mechanism of soil cleavage by tined implements. They confirmed the existence of two regimes of soil failure (Kostritsyn 1956), and found that the region of transition occurs at an aspect ratio of 0.6 for vertical tines. They suggested a mathematical equation to predict the draught force which considers these two different zones. Through a series of experiments they confirmed that the equation can be applied over a wide range of soil conditions. This work was later extended (O'Callaghan and McCullen,1965) to include both plane and wedge-shaped tines with rake angles varying from 0^{o}-45^{o}.

The complexity of the available methods to calculate soil forces, where solutions cannot be obtained without recourse to laborious graphical methods or use of a digital computer, led Hettiaratchi et al (1966) to propose a method for two dimensional soil failure based on the General Soil Mechanics Equation postulated by Reece (1965)

$$P = (\gamma\, d^{2}\, N\gamma + c\, d\, Nc + ca\, d\, Na + q\, d\, Nq) \qquad ...(3)$$

where the "N-factors" are dimensionless constants affected by soil

cohesion, adhesion and tine rake angle. Later Hettiaratchi and Reece (1967) extended the work for a three-dimensional analysis, narrow tines, where a semi-empirical solution is given. The model is based on the two failure regimes found for tines working below a certain depth, called critical depth. The first zone is called forward failure regime, where the forces can be calculated from the equation used for two dimensional-failure in front of the wide cutting blades. For the other zone, the sideways failure, one equation similar to that presented by O'Callaghan and Farrely (1964) was derived. A simple equation to predict the main rupture ratio has also been derived, where he showed that both forward and sideways rupture distance ratios area linear function of depth. The results presented from experimental work done with tines at several depths up to an aspect ratio 6, and for different rake angles, showed that a reasonable prediction of the forces can be made.

Studying the soil failure caused by very narrow tines for different tine widths and rake angles, Godwin and Spoor (1977) confirmed the existence of two failure zones for tines working below certain depths, and going beyond this they found that the critical depth is dependent upon the aspect ratio and the tine rake angle. They also showed that the ratio between the forward rupture distance and the critical depth (rupture distance ratio) is constant for a given rake angle, i.e. independent of the aspect ratio. Assuming that the soil worked by the tines obeys the Mohr-Coulomb failure criterion, and using the knowledge obtained from the experimental work, the authors then proposed equations to calculate the forces acting on these tines. For the upper failure zone (crescent

zone), based on the solution proposed by Hettiaratchi and et al (1966, 1974), to estimate the passive force, they derived two equations to calculate the horizontal and vertical forces, acting on the tine face. For the zone below the critical depth (lateral failure), considered to fail in two dimensional ways which is independent of the rake angle, the total force acting on the tine face in this zone was calculated by the integration of Meyerhof's (1951) solution for deep narrow footing orientated through 90^{o}. The total horizontal force component of the soil reaction will then be the sum of the forces acting in these two zones. The comparison between the predicted and measured forces from a range of 90^{o} rake angle tines are presented, and seem to be in good agreement. Godwin and Spoor (1977) also presented a model to estimate the position of the critical depth based on the assumption that the soil ahead of the tine fails in such a way that the horizontal force will be minimum. This model had not been sufficiently developed for precise prediction of the critical depth of tines with rake angles different from 90^{o}, although the critical depth could be estimated from experimental data provided.

Later Godwin et al (1984) extended the model to improve the estimation of the disturbed zone in the crescent failure with better results for the horizontal force. Although the model could be expanded for the vertical force no results were presented.

McKyes and Ali (1977), assuming that the surface side failure crescent is circular instead of elliptical, proposed a theoretical model to

predict the forces in the crescent failure zone. The model is based on the principle that the soil fails on the path of least resistance. They divided the crescent failure zone into two sections and did a force balance for each section deriving an expression with the same form as proposed by Reece (1965), where the **N** values are functions of the tine and soil characteristics.

Spoor and Fry (1983) showed that the type of disturbance produced by a trenchless tine is dependent upon whether it is working above or below critical depth. Below critical depth, significant lateral soil disturbance can occur beyond the failure plane, which could result in compaction and consequently poor drainage performance. The design geometry of the trenchless drainage tines used in practice varies, but they usually have an aspect ratio (working depth/tine width ratio) from about 6-18, and a rake angle between 15^{o} and 50^{o}, and can be classified as a narrow tine, (Godwin and Spoor, 1977; Spoor and Fry, 1983).

2.4 The Dynamics of Soil Engaged Implements

The relation between tractor, implement and soil is an important aspect often forgotten when drainage implements are studied. Research conducted in order to investigate the dynamics of the tractor and implement, and some of the relevant aspects available in the literature, are summarized below.

Childs (1942) investigated the condition of equilibrium of the mole

plough. Assuming the system similar to a rigid body under the external system of forces, where the condition of equilibrium is that the algebraic sums of the horizontal force, the vertical force and the moments about any point shall be separately zero. When the equilibrium condition is not satisfied, the implement is lifted from its equilibrium position.

Generally speaking, researchers divide the implement dynamic behaviour into two categories:

i) the vertical longitudinal plane, where they are concerned about how the rate of penetration and the depth of penetration are affected by the linkage mechanism.

ii) lateral dynamic of the implement, where they are concerned about the lateral stability of the implement.

Reece et al (1966) carried out an analysis considering the simplest kind of soil engaging implement, a point fixed to a bar pivoted at the hitch point. Assuming a linear relation between the restoring torque and the angular deflection in which the implement is moving, they developed a second order differential equation with constant coefficients

$$\ddot{\theta} + 2\mu\theta + wn^2 = 0 \qquad \ldots(4)$$

which has the same form of the equation representing a damped harmonic

motion. In practice, the damping coefficient is large and the equation becomes a first order one. The solution for the initial conditions $\theta=\theta o$ at t=0 is a first order system

$$\theta = \theta o \, e^{-s/l} \qquad \ldots(5)$$

where s = the travelled distance.

l = the length of the beam.

They also mentioned that although the damping is mathematically equivalent to viscous damping, it is physically different. This work was later extended by Cowell and Makanjuola (1966) for a three point linkage system.

Crolla and Pearson (1975) studied the penetration of mouldboard ploughs, and showed results of tests performed on a three furrow mouldboard plough which indicated that the initial rate of entry increases with the forward angle of inclination of the plough.

Cowell and Sial (1976) presented a theory to explain the vertical dynamic behaviour of the mouldboard plough, based on the works mentioned above, where a first order differential equation is derived to describe the movement of a single point implement during penetration. In this analysis they considered only the kinematics of the implement and no mention was made about the soil parameters and forces involved in the process.

Considering the results presented by Cowell, Singh (1982) decided to conduct his experiment using the same approach for the trenchless drainage plough moving in a vertical plane. From the analysis of the forces involved in the dynamic movement of the implement, he derived a second order differential equation to predict the travel distance and the time response of the implement due to vertical displacement of the hitch point. This equation is a function of the plough mass, geometry, speed and soil resistance, and is similar to the response of a compound pendulum oscillating in a vertical plane, where the damping coefficient is very large. The solution for this equation could be presented in the following form:

$$\theta = \theta o \, e^{-wm^2 t/2\mu} \qquad \ldots(6)$$

where θ is the angular displacement of the implement, θo is the initial angular displacement of the implement and **t** is the time. Using a 1/6 scale-model of the trenchless drainage machine, he tested the theory in a soil tank, and found a good relation between the predicted and experimental values for a tine with a relieved bottom. He reported that the predicted time response for an implement with a relieved bottom to achieve its equilibrium position during penetration, and for both relieved and non relieved bottom tines to correct reduction in depth was in excess when compared with the experimental data. This discrepancy was shown to be due to generation of unbalanced stress condition on the supporting soil mass. He also found that the relation between the soil resistance force and the unbalanced force for a small angular deflection

is linear.

2.5 Similitude Studies

Developments of aerodynamics and hydrodynamics have been largely benefited from the use of scale-models, where models are used not only to provide information about certain aspects, but also to support the evolution of the theory.

Recently many studies have been conducted to develop techniques for the use of the principle of similitudes in soil engaging implements. Freitag et al (1970) pointed out the difficulties and limitations of using a scale-model for soil machine studies, usually, because there are elements, particularly of the test medium, that cannot be scaled. Two systems will exhibit similar behaviour if geometric, kinematic, and dynamic similarity are activated.

Young (1968) discussed the techniques and problems associated with the development of modelling laws for systems in which there is a dynamic interaction between soil and machines. He stated that reliable data can be obtained a from small scale-model system and useful quantitative prediction of prototype behaviour can be made, but some or perhaps the majority of the models are distorted.

To overcome this problem, Schafer et al (1969) presented an approach to solve the distorted model. After the analysis and interpretation of the

distortion in a general soil-mechanic system, they devised a technique for using distorted models. The prediction factor obtained was related to length scale in the form

$$\mathcal{S} = n_{\lambda}^{s} \qquad \ldots(7)$$

where $\mathcal{S}$ is the prediction factor

n_{λ} is the length scale

s is a function of soil and machine

Based on this model Verna and Schafer (1969) exteded the model for a situation where there is no need to have a uniform soil condition through the test section. The extended model includes a new term t on the equation (7) exponent, **(s-t)**, where t is a multiplicity exponent, relating to Pi terms containing dimensional soil variables and tool geometric and operational variables. Results of their tests indicated that the term **(s-t)** remains constant irrespective of the soil type, soil strength profile and moisture content. This statement was not in agreement with the results found by the same authors in 1968, where s was found to be independent of the apex angle of a triangular chisel tine, but varies in different soil treatments.

Godwin (1974) compared his experimental results obtained from tests with narrow tines, to see if they were in agreement with the procedures for handling distortion suggested by Schafer et al (1969). From the analysis, he found that the exponent s on equation (7) was constant for the range of tine geometry studied in a particular soil treatment. He concluded that if s is only a function of soil type and condition and

independent of tine geometry, it will be possible to estimate the performance of a large tine scale based only on tests with scale-models.

2.6 Conclusion

The theory developed to explain the dynamic behaviour of soil engaged implements seems to introduce the soil dependent constant as empirical values, which usually are only suitable for the specific case studied. No mention is made of the use of soil mechanics theory to estimate the forces involved in the process. The trenchless drainage plough due to its dimensions and normal working conditions, can be classified as a very narrow tine, for which the soil mechanics theory is well explained, as mentioned previously. If it is possible to establish a link between these theoretical approaches an advance in soil-implement-tractor dynamics in general, and trenchless drainage machine design in particular, can be reached.

CHAPTER 3

METHOD of INVESTIGATION and EXPERIMENTAL EQUIPMENT

3.1 Plan of Investigation

To fulfil the objectives of this project, i.e. to understand the nature, magnitude, and effect of the physical parameters involved in a trenchless drainage machine operation, it is necessary to monitor the behaviour of the implement. However, due to its dimensions and characteristics, the measurement of the forces involved as well as the linear and angular displacement, involves some difficult tasks in field experiment, requiring considerable technician assistance and the use of large sophisticated equipment which is unavailable and would be expensive to construct for a project of this nature.

Scale model tests represent one method by which this problem could be overcome and the study of various elements of the system can be fulfilled. It enables a easy control over the implement and instrumentation, and observation of the model behaviour can be used to predict accurately the performance of the physical system in the desired respect. To make use of the model in this sense, it is necessary that a certain relationship is satisfied between the model and the full size implement.

Usually there are two ways of interpreting scale model studies, by similitude principles or by quantitative analysis. The first method consists in the development of valid similitude requirements using modeling laws, either by dimensional analysis or by the analysis of the characteristic equation which governs the system. However, this method requires the use of corrective procedures to determine the effect of non-scale elements and to compensate for them. Schafer (1969) has developed a method for handling distortion in such a system, where the prediction factor obtained is a function of length scale, as mentioned in section 2.5, and Godwin (1974) has proved that this distortion factor can be considered as a constant for a given soil condition. The second method consists in the use of fundamental soil physics equations which are valid for a wide range of tines, but are not restricted to the problems of similitude prediction by requiring tests at different scales in order to determine the distortion factor.

In order to evaluate these methods when working with soil engaging tools, the forces of a very narrow tine were calculated by both methods and are compared in Table 3.1. The results shown in this table have proved that it is possible to estimate the soil reaction forces acting on the narrow tine either by using the similitude principle or by direct applications of the fundamental theory of narrow tines with very close results. Taking this into consideration the trenchless model in this project was studied with no concern about the similitude requirements, having only been reduced geometrically.

TABLE 3.1

Relation between H/wd and tine scale, for experimental and predicted values

Tine scale	Dist. factor $S = n^s$	Experimental H/wd (N/mm^2)	Theoretical value (full scale) applying the dist. factor H/wd (N/mm^2) col. (2x3)	error % comparing to tine scale 1
(1)	(2)	(3)		
1	1.00	0.60	0.60	--
2	1.15	0.54	0.62	3.0
4	1.32	0.45	0.59	-1.6
8	1.52	0.40	0.61	1.6

Predicted value for a full scale tine applying the theory of narrow tines

H/wd (N/mm^2) = 0.59

Experimental data from Godwin (1974).

s = 0.20 (from experimental values, Godwin 1974)

Aspect ratio (d/w) = 8

Tine caracteristics - rake angle = 90^o
smallest tine width = 6.35 mm

Soil properties

ϕ = 34^o	N = 4.4		m = 1.65
c = 4.6 KN	Nc = 7.5		Nc' = 200
δ = 22^o	Nq = 0		Nq' = 165
ca = 0	γ = 1500 Kq/m^3		

Nevertheless, the design conditions involving soil properties could present problems. Clearly the best way to overcome these difficulties of scaling, producing and measuring soil properties would be to conduct all the tests in the same soil conditions, as suggested by Godwin (1974). Soil types and conditions often vary considerably within a single field. Even if the soils are of the same type, their strength properties are not likely to be the same at any given time. The solution for this question would then be to conduct this investigation in a laboratory soil bin, where soil properties are within the control of the experiment to a much greater degree with standardized treatment to enable an extensive number of tests to be conducted in a homogeneous media.

The use of a soil bin represents further benefits. It permits a better control over the implement behaviour, and most of the instruments necessary to monitor it are available or could be easily developed. Tests can be conducted independent of weather conditions and only require two men for operation. The soil surface profile can be measured without trouble, and what is more significant is that it can be easily prepared to suit the experiment requirements.

Soil conditions and topography are some of the key factors which affect the implement performance. The irregular soil profile usually causes a pitching action of the crawler tractor and/or an undesired reaction of the implement. Fouss (1971) showed that changes in the hitch height causes changes in the plough depth in different proportions. To evaluate the influence of the soil condition and topography, it is

then necessary to simulate a variable soil profile and movement of the hitch-point in the soil bin.

The simplest way to introduce such variation is to have step inputs in the soil surface, where differences in depth during the continuous movement of the implement show the effect of soil forces on the implement behaviour. In addition, a more realistic type of soil surface profile, i.e. a continuous change in depth, in the form of a sine wave, was used. This has the advantage of a relatively easy mathematical representation and is an adaptation of the commonly found field undulation.

However, before testing the implement in a dynamic situation, like the one suggested in the previous paragraph, it would be logical to test the implement in a restricted motion condition. The idea of these tests was to compare the results obtained from them with the ones predicted using the theory of the narrow tines. These kinds of tests permit the evaluation of the possible soil forces involved in the tine reaction and in which range they are presented. This could provide valuable information later in the dynamic analysis.

In the study of the dynamic behaviour of the implement, it is compulsory not to evaluate only the effect of soil surface, but also other factors which could influence its behaviour and performance, or could even only help in the process of analysis. Such factors as system weight and soil density should then be investigated.

The work conducted in the past, and explained in the literature review, discloses very little information about the measurement of the soil force acting on an implement or its behaviour when working in a dynamic situation. Therefore, it was necessary to conduct some pilot studies which clarified some information about the trenchless plough and helped in the establishment of a link between the known theories and in the development of the theoretical study of this project.

3.2 Experimental Equipment

3.2.1 Introduction

The equipment necessary to carry out the experimental part of this project was partly available in the soil physics laboratory. This consists of commercially available instrumentation (to measure force and displacement and to record data) and specific equipment designed in the College for exclusive use in soil implement investigations. This equipment developed by other researchers and used in this experiment, e.g. the soil bin, the soil processor and the extended octagonal ring transducer, whose characteristics are fully presented in the cited literature, is only briefly described in this chapter.

However, some of the equipment used had to be designed specially for this project. The description of this equipment, as well as the way in which it was used is presented as follows.

3.2.2 The general dynamic assembly description

To achieve the objectives of this project there is no need, as explained earlier, to differentiate between the real and the virtual hitch point. So, a real hitch point arrangement with a long floating beam was used in the system mainly because it is simple to engineer.

Figs. 3.1a and 3.1b show the arrangement of the assembled system. The trenchless plough implement (1) was rigidly mounted to a long floating beam, 670 mm long (2). To measure the forces and moment acting on the implement, an extended octagonal ring transducer (3) was mounted at one end of the beam close to the trenchless tine. To measure the soil reaction forces on the bottom of the implement a "L-shaped" cantilever beam (4) was machined inside the tine. The system was connected to the carriage through a small link called a "free-link" (5), which was replaced later by a tension transducer, allowing the measurement of the total force required to pull the plough. The angular displacement of the tine and the "free-link" was recorded using an angular displacement transducer (7), and a linear displacement transducer was used to measure the vertical movement of the tine and the hitch-point, when this was the case (8).

The minimum scale rate which allows the use of the existing soil bin with a variable soil profile and at reasonable implement depth was 1/6. Therefore, the dimensions of the model were chosen in order to maintain the model as closely as possible to a common shape of the trenchless

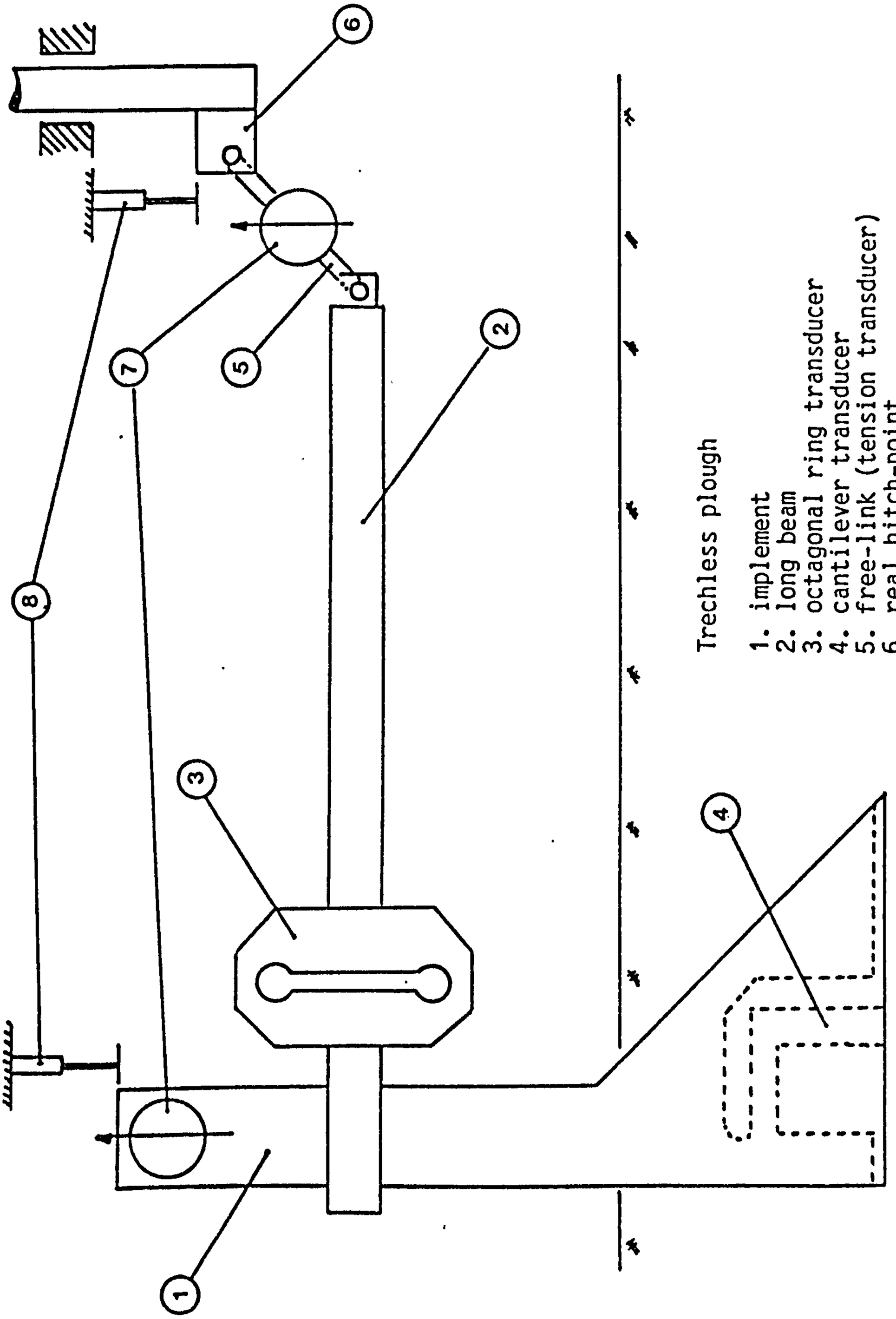

FIG. 3.1a Implement dynamic assembly

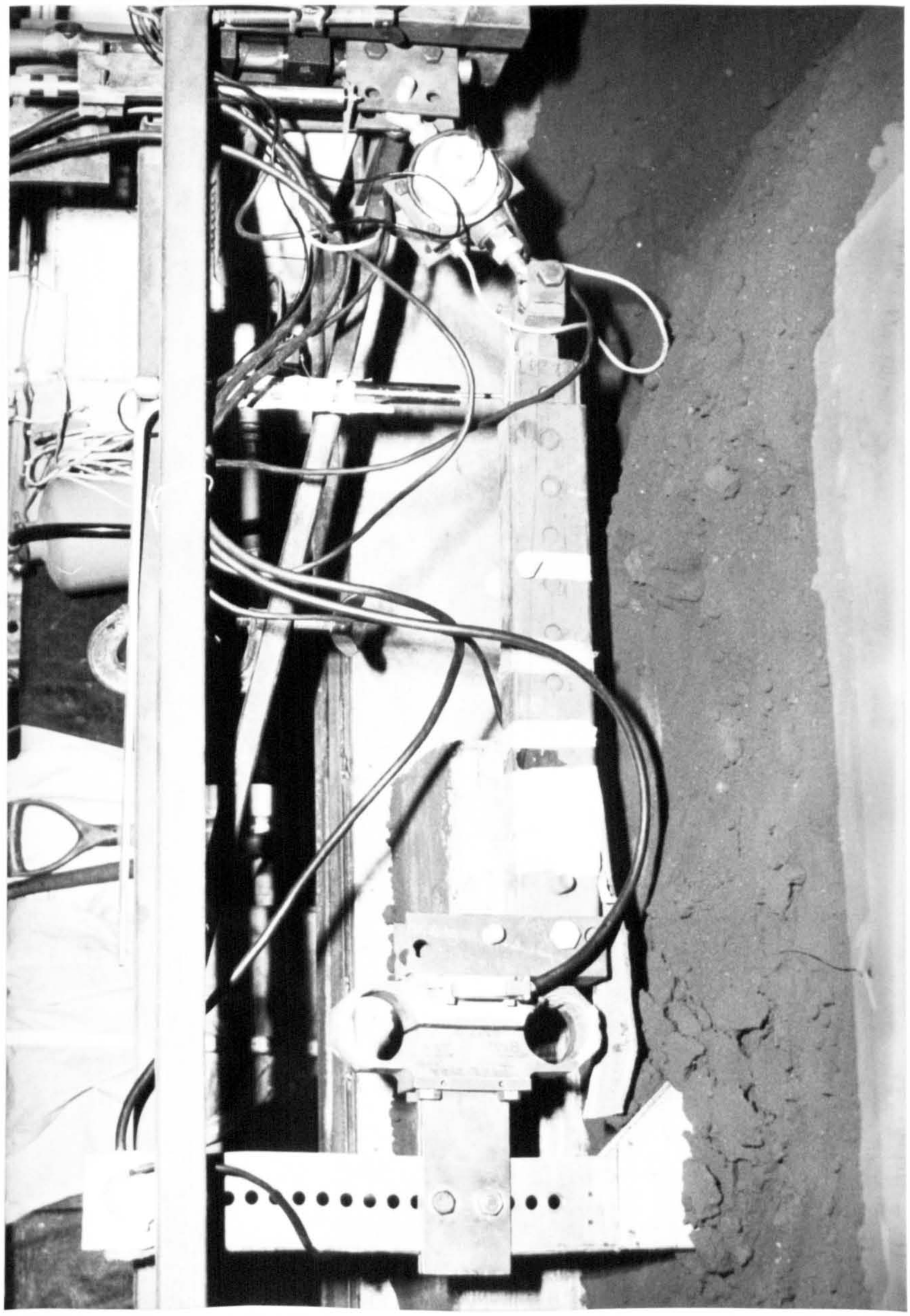

FIG. 3.1b Implement dynamic assembly

plough in full scale, and permit some instrumentation inside the leg. The soil engaging implement was at 45^{o} rake angle tine 10 mm wide and with a flat bottom 300 mm long. Holes in the tine leg permitted an adjustment of the position where the octagonal ring transducer was fixed. The whole system weighs 236 N.

3.2.3 The restricted motion assembly

In the special case when the implement was studied in a restricted motion condition, the general assembly was modified to fulfil the requirements. The tine was rigidly mounted in the soil bin tool bar, with the extended octagonal ring transducer (Fig. 3.2), and all the other parts removed. A series of holes in the clamp, used between the tine and the octagonal ring, permitted the setting of the tine inclination, in relation to the vertical, on a desired position for the run without affecting the position of the transducer.

3.2.4 Hitch-point movement

A system was designed to introduce the step-input displacement in the hitch point as it travels forwards. It consists of a four arm linkage system, driven by hand (Fig. 3.3). The hitch-point (1) is connected to the lower arm (2) which has a vertical displacement when the upper arm (3) rotates about the point 'O' Due to its construction the maximum displacement of the hitch-point is obtained by a rotation of $60\text{-}40^{o}$, dependent upon the step height, of the upper arm. That gives a very fast

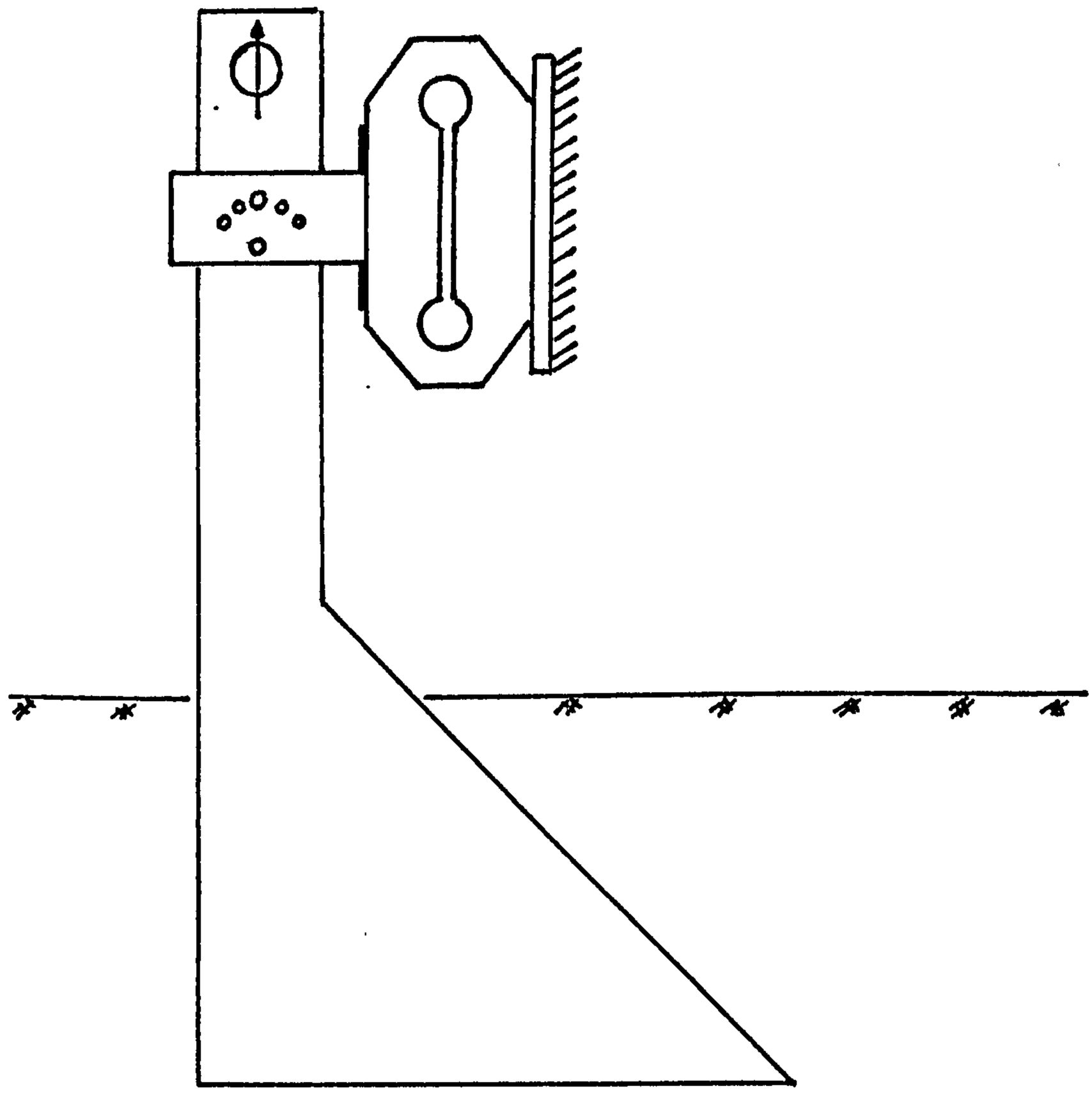

FIG. 3.2 Implement restricted motion assembly

change in the hitch-point position, which was considered almost instantaneous. In order to adjust the height of the step the upper arm has a variable length.

To simulate the sine wave displacement a constant diameter cam was designed (Fig. 3.4). This consisted of a circular plate with the camshaft hole eccentrically located. The amount of eccentricity determines the amount of displacement of the follower, which has a positive action, and a harmonic motion is produced. This type of arrangement, Scotch Yoke mechanism (1), which is shown in Fig. 3.5, was driven by a capstan (2) connected to a cable (3) fixed along the side of the bin. The reason for this kind of power transmission to the Scoth Yoke mechanism was to maintain the position of the hitch-point as close as possible to a perfect sinusoidal form, without being affected by the velocity of displacement of the carriage. Due to the low torque required at the capstan, it was observed that the error caused by any slip of the cable was less than 1%. Different diameters of the capstan permitted the simulation different wavelengths.

3.3 Soil and Soil Preparation

The soil used in the experiment was a sandy-loam which characteristics are shown in Table 3.2 (Godwin 1974).

All the tests were conducted with the soil prepared with a bulk density of 1500 kg/m^3 and 10.5% ±1% of moisture content, unless otherwise

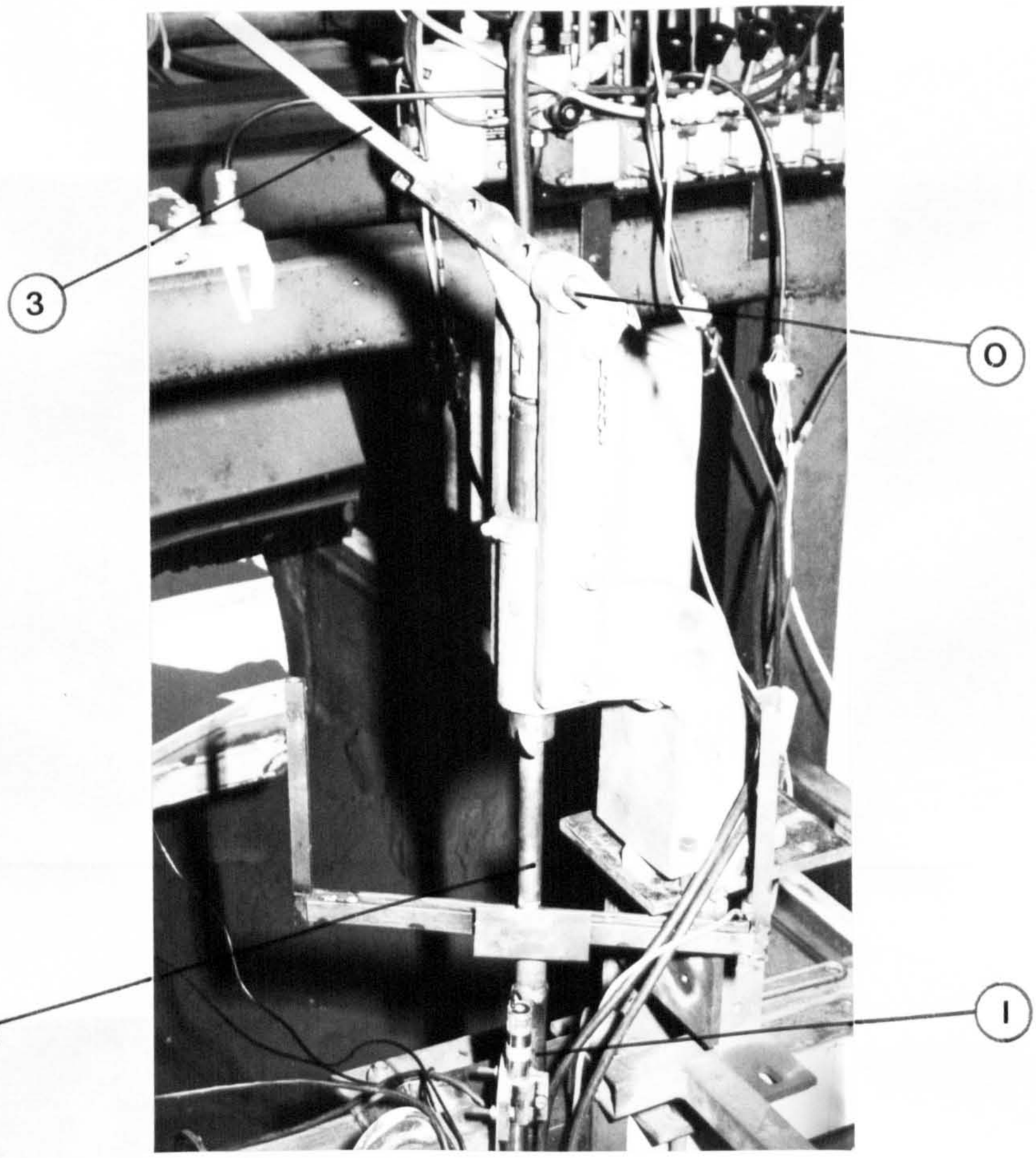

FIG. 3.3 Mechanism used to simulate a step-input in the hitch-point

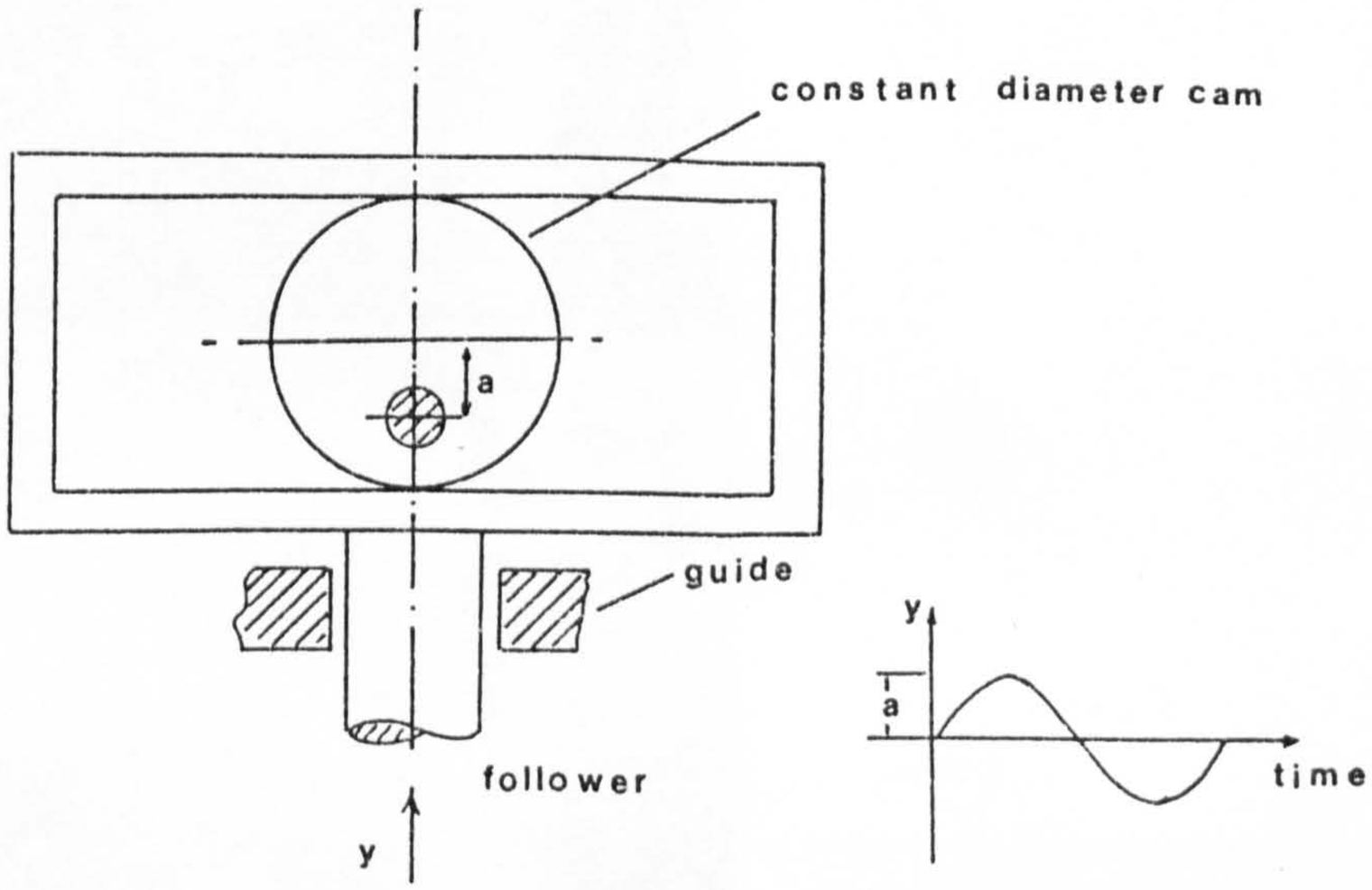

FIG. 3.4 Scotch Yoke mechanism used to simulate the sinusoidal movement of the hitch-point

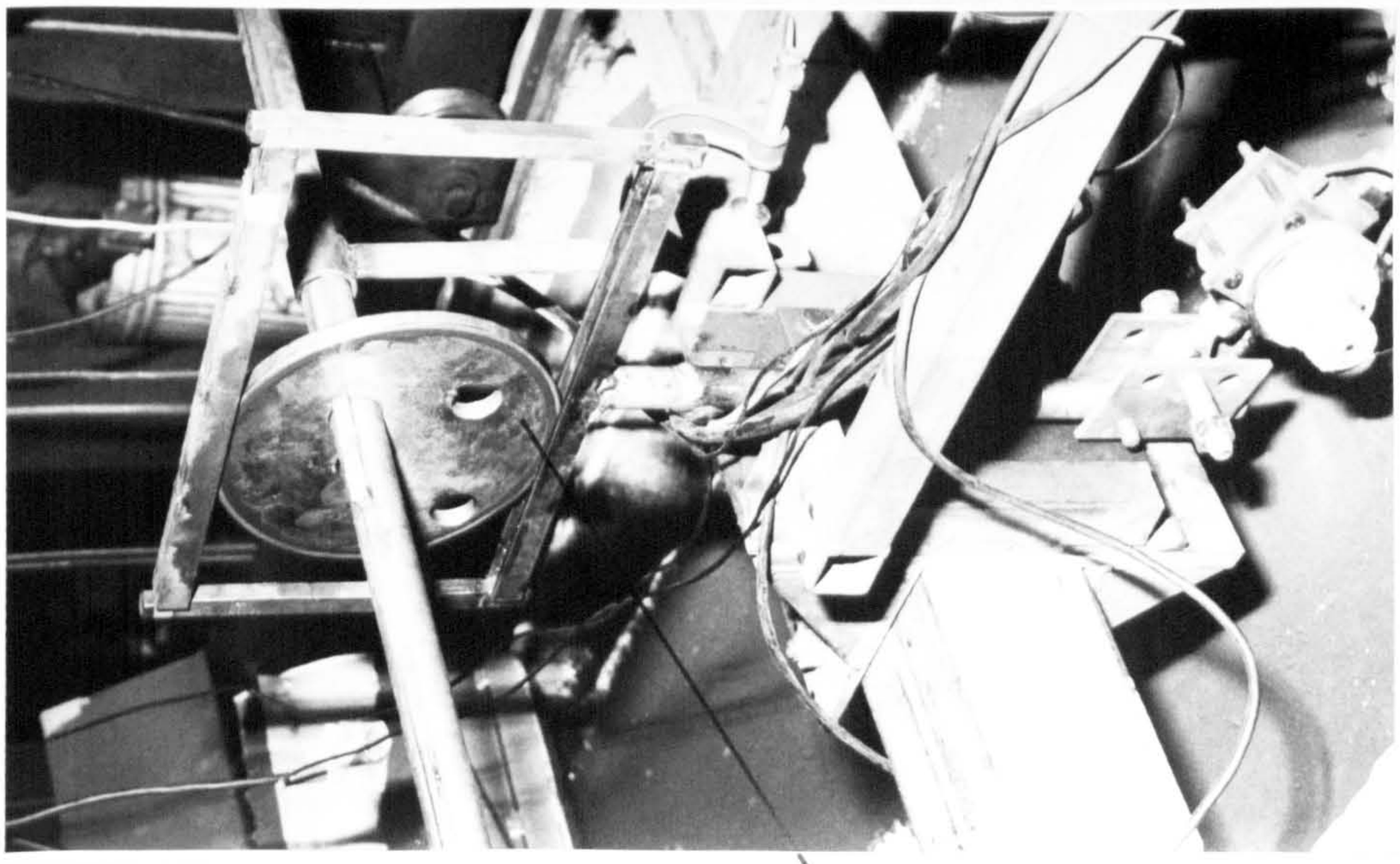

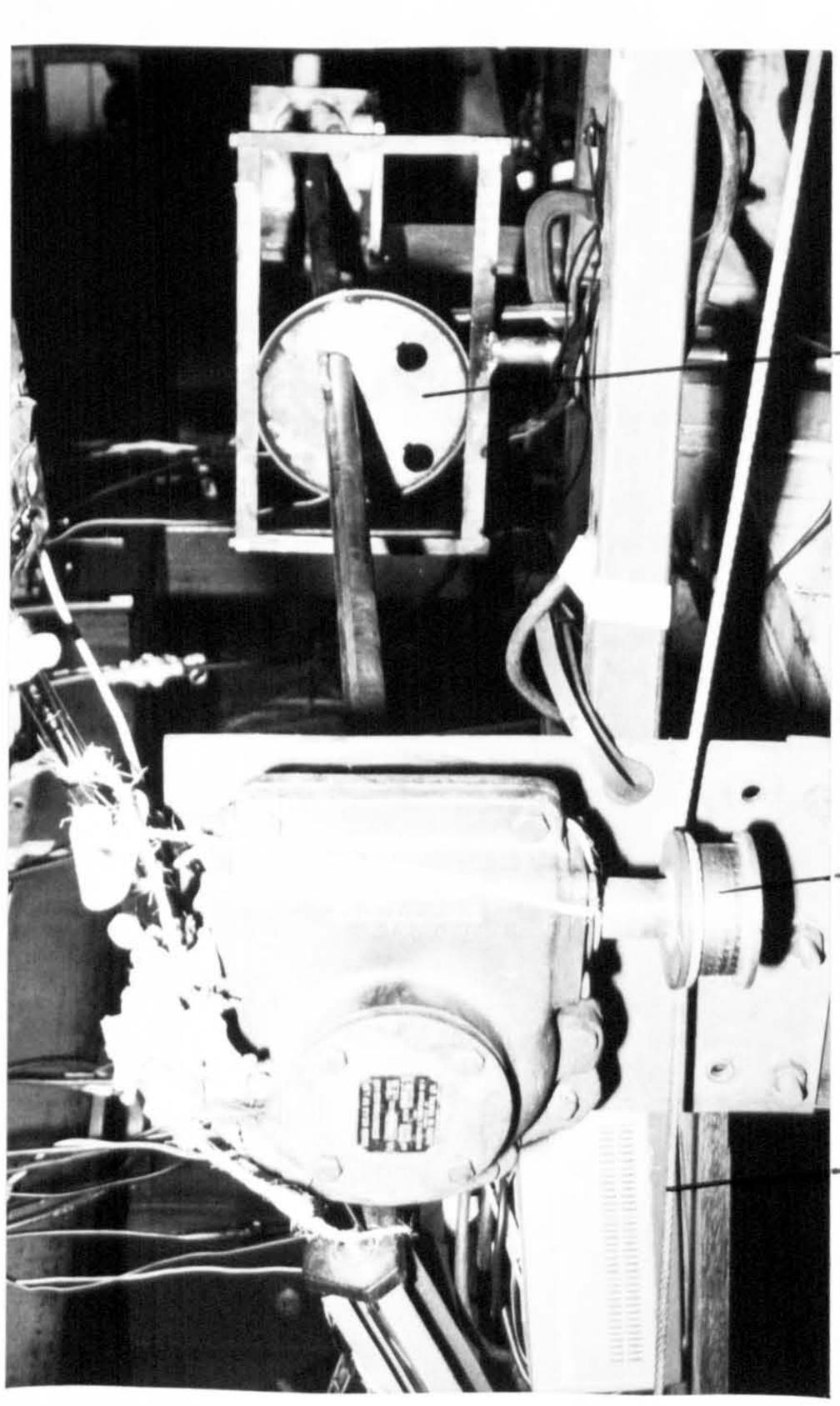

FIG. 3.5 General assembly of the scotch Yoke mechanism

TABLE 3.2

Mechanical analysis by 'Bouyoucous Method'

Fraction	Mean	Adjust percentage
silt	10.00%	10.25%
clay	17.00%	17.44%
sand-coarse	38.09%	39.05%
-fine	32.44%	33.26%
	97.53%	100.00%

Mechanical properties relating to operation of tillage tools

	Soil bulk density Kg/m^3		
Mechanical properties	1200	1500	1680
Angle of shearing resistance, Deg.	37.2	37.6	42.37
Cohesion, KN/m^2.	0.0	4.616	7.56
Adhesion	0.0	0.0	0.0
Angle of soil-metal friction, Deg.	-	22	-

(Godwin, 1974)

stated. Using the soil processor existent in the soil bin (Godwin, Spoor and Kilgour 1980), the soil, usually packed up to 250 mm depth, was prepared in layers of 50 mm and then compacted using a pavement roller in order to get a uniform density. The surface of each layer was scarified to obtain a bond with the next layer. When not in use, the soil was covered with a polythene sheet to reduce evaporation. Water loss was replaced by controlled hand digging with water being applied from knapsack spray giving a firm and relatively even application.

To prepare the soil surface profile with a step input, the soil was prepared in the same way as described above up to the third layer, then a large board with the desired thickness and length was used as a form to fill in the gap between the layers in part of the soil bin . After loading the soil and compacting it to the board thickness, the latter was removed, Fig. 3.6.

The sine wave soil profile was prepared using the mechanism described above to simulate the hitch-point sine wave movement. The soil was prepared as usual up to the desired level, and then loosened using a rake fixed to the Scotch Yoke mechanism. Finally, a scraper fixed to the same device, removed the unnecessary soil, and if needed a small roller was used to compact the soil. The result was a smooth sine wave soil profile, Fig. 3.7.

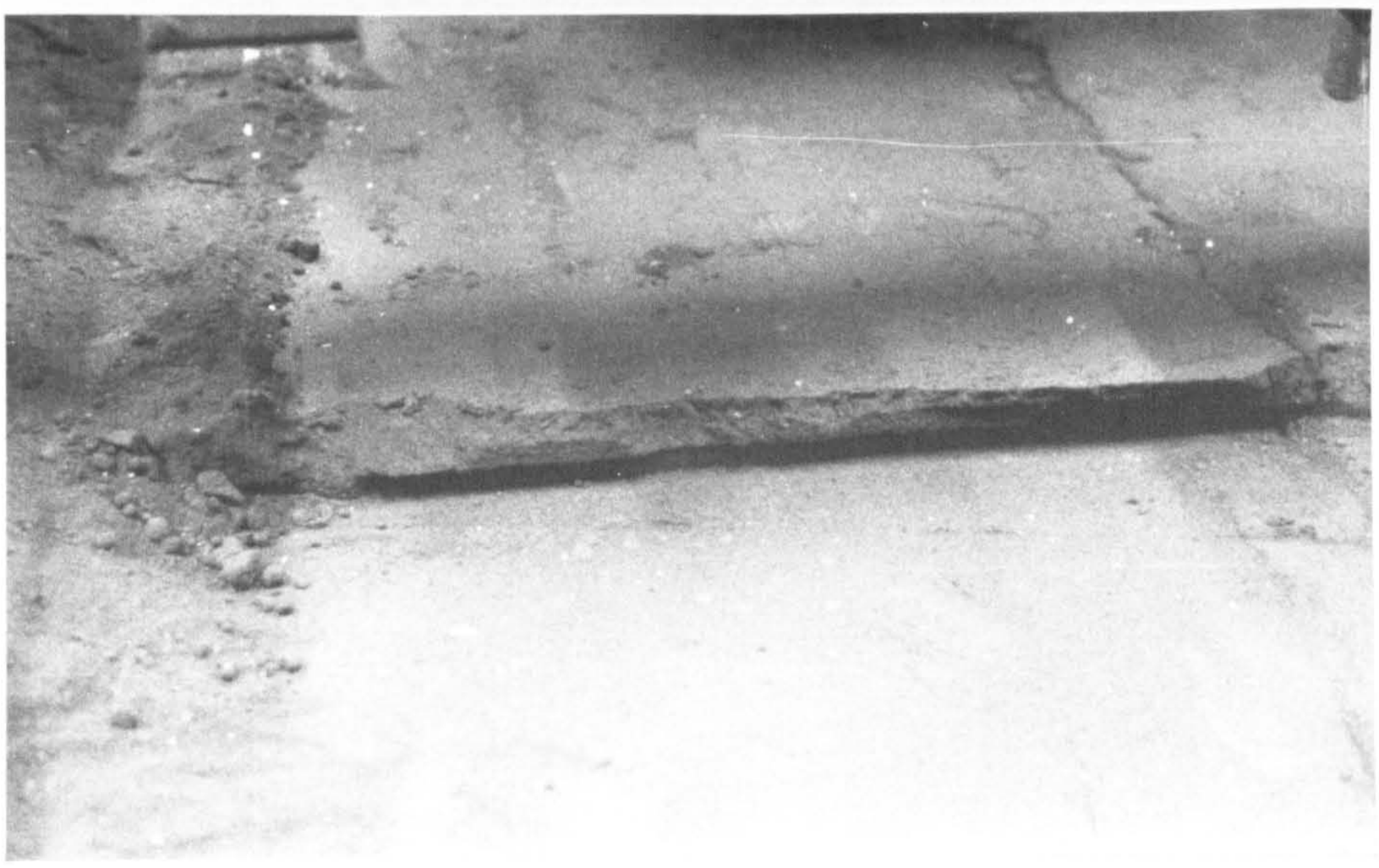

FIG. 3.6 Soil prepared with a step input

FIG. 3.7 Soil prepared with a sine wave profile

3.4 Instrumentation

The equipment to measure forces and displacement was arranged to give the maximum information possible during the test, and was used as described below.

A tension compression strain gauge transducer load cell with ball joints in both ends, replacing the "free-link", was used to measure the total force required to pull the implement through the soil.

To measure the total forces acting on the implement, independent of the system weight, an extended octagonal ring transducer (Godwin, 1975) was mounted between the leg and the beam. Due to its construction, the octagonal ring measures the horizontal and vertical forces component of the resultant force and the moment about the geometric centre of the transducer.

To verify the influence of the supporting forces underneath the implement, a special measuring device had to be designed. In a cantilever beam machined inside the tine, Fig. 3.8, strain gauges were bonded and connected into three four arm bridge networks, as shown in Fig. 3.9, to measure the differences in strain caused by normal and frictional forces acting on the bottom plate, and the moment about its neutral axis, separately from the other forces acting on the plough (Appendix 3). It is capable of supporting forces up to 600 N and a moment of 50 Nm with a safety factor of 2.5 to ensure linearity within

the working range. It has a cross section of 240 mm^2, and the position of the strain gauges was determined in order to give maximum sensitivity. After loading tests the following characteristics were found in the transducer:

i) cross sensitivity of less then 2%.

ii) variation in channel output due to position of the forces N and Ft less than 3%.

iii) the output from the moment bridge was independent of the origin of the eccentric force N or Ft.

The output from each strain gauge bridge circuit was amplified using a strain gauge high impedance output amplifier, which also provides 10 V dc excitation for the strain gauge circuit.

To record the angular displacement of the system, two high sensitivity dc/dc variable transformer type tilt sensors utilising a 10 V dc input with a 2 V dc output were used, Fig 3.1a. One fixed to the blade with a measurement range of 20^o, sensitivity of 340 $mV/^o$ and linearity of $\pm$0.5%, permitted a precise measurement of the leg movement in relation to the vertical. The other inclinometer fixed to the "free-link" with measurement range of 60^o, sensitivity of 140 $mv/^o$ and linearity of $\pm$0.5%, permitted a reading of the "free-link" angle at any time. Two 9 V batteries connected in parallel were used as

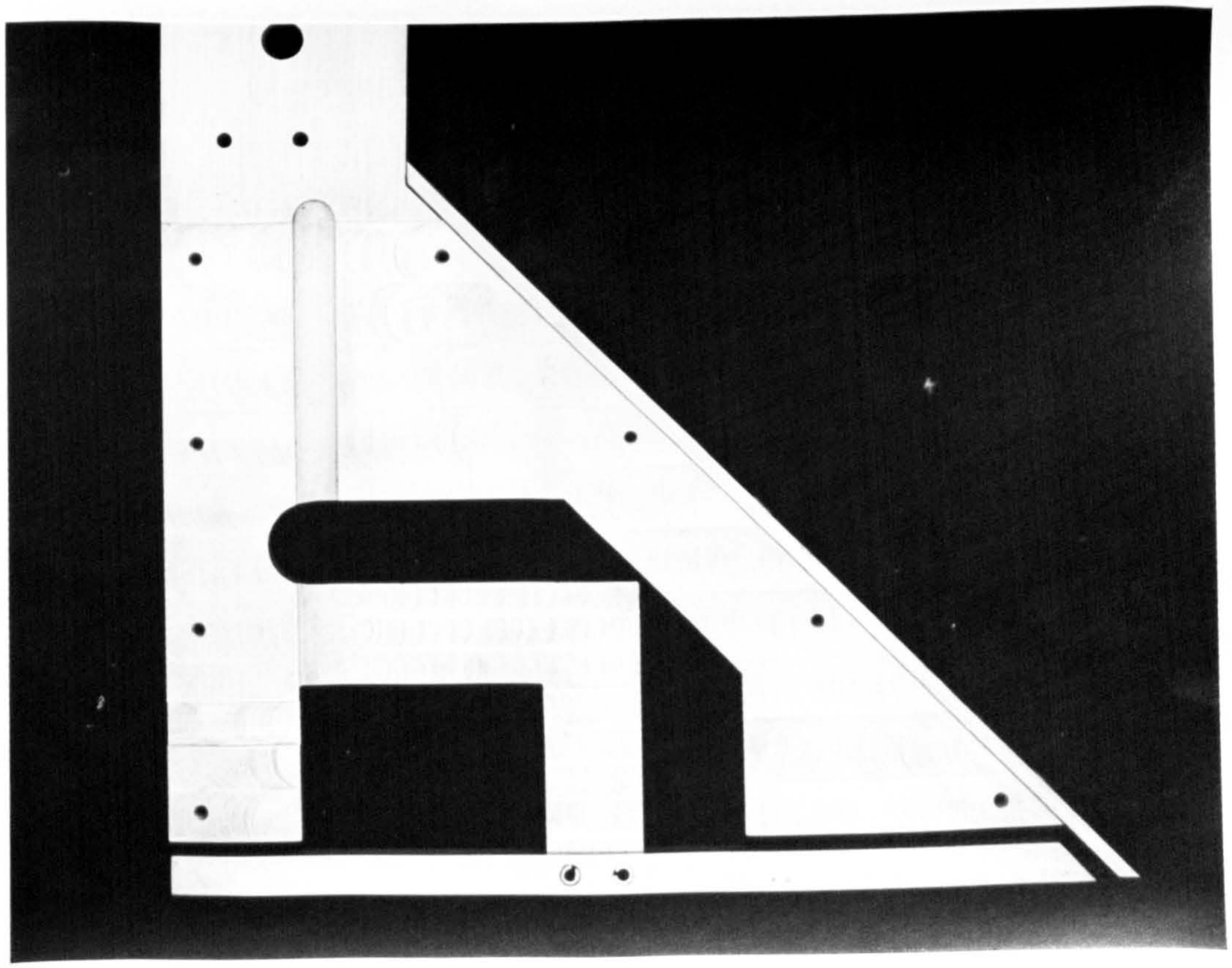

FIG. 3.8 Details of the cantilever beam machined inside the trenchless tine

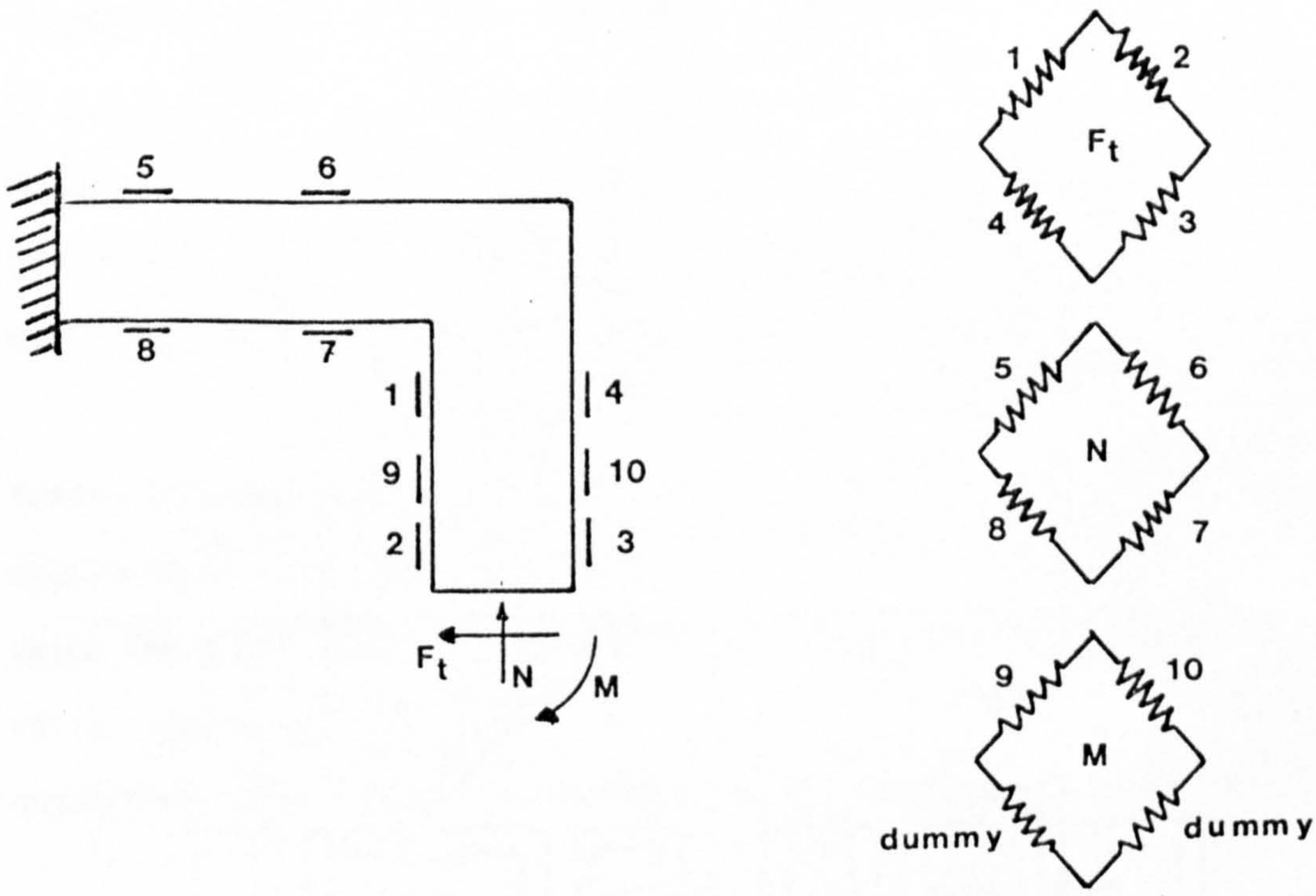

FIG. 3.9 Strain gauge assembly

a power supply for the inclinometers.

To measure the relative movement of the implement and hitch-point, when this was the case, in relation to a fixed reference plan, two L.V.D.T. (Linear Variable Displacement Transducer) dc/dc were used. A power convertor supplied 10 volts DC to this equipment.

The speed and travel distance of the carriage was measured using an on/off switch energized by a 1.5 V battery, fixed to the carriage. Equal length and distance plates fixed on the side of the soil bin were used to switch the device on and off.

3.5 Recording and Listing System

Recording data direct in a digital form is a great improvement which was introduced in the past few years. The use of microcomputer and analogue to digital converter have proved to be a very successful way of helping to get a fast and more precise data analysis. But this kind of equipment has to be very carefully selected in order not to distort the relevant data, which leads to a false conclusions.

Tests conducted by Godwin (1974) showed that the cyclic variation in the magnitude of the forces component was as much as ±25% about the mean value for tines with a small ratio, and tended to reduce as the aspect ratio increased. In terms of time response, these cyclic variations could correspond as much as 10 Hz, when working at speed of 1 m/s

and ten to reduce as the carriage velocity reduces. To overcome these cyclic variations, it is then advisable to use at least double the cyclic rate, i.e. 20 Hz, and more reliable results would be obtained as this rate increases.

The analogue output from the strain gauge amplifiers, and the other instruments, were converted into digital form by an analogue digital converter included in a data logger unit that was designed to receive up to 16 channels simultaneously at a rate of 100 Hz (or 1 channel at 1600 Hz), for the duration of approximately 20 sec, utilizing a microcomputer memory for temporary data storage. Due to this limitation, for the tests with a time length of over 20 seconds, the sampling rate had to be reduced and a compromise between time and cyclic variation problems had to be made, and a sampling rate of 40 Hz was chosen as a minimum to be used.

The results of all the sixteen channels could be listed after the run was finished by a printer connected to the microcomputer. The results could then be presented in integers computer units or engineer units, and in addition simple graphics could be plotted, Fig. 3.10.

Due to the microcomputer limitations in memory and speed of calculation, and considering the quantity of information to be processed, all the data from the tests was later transferred to the Vax 11/750 computer, where it was possible to compare the results from different tests and also compare those with the predicted results.

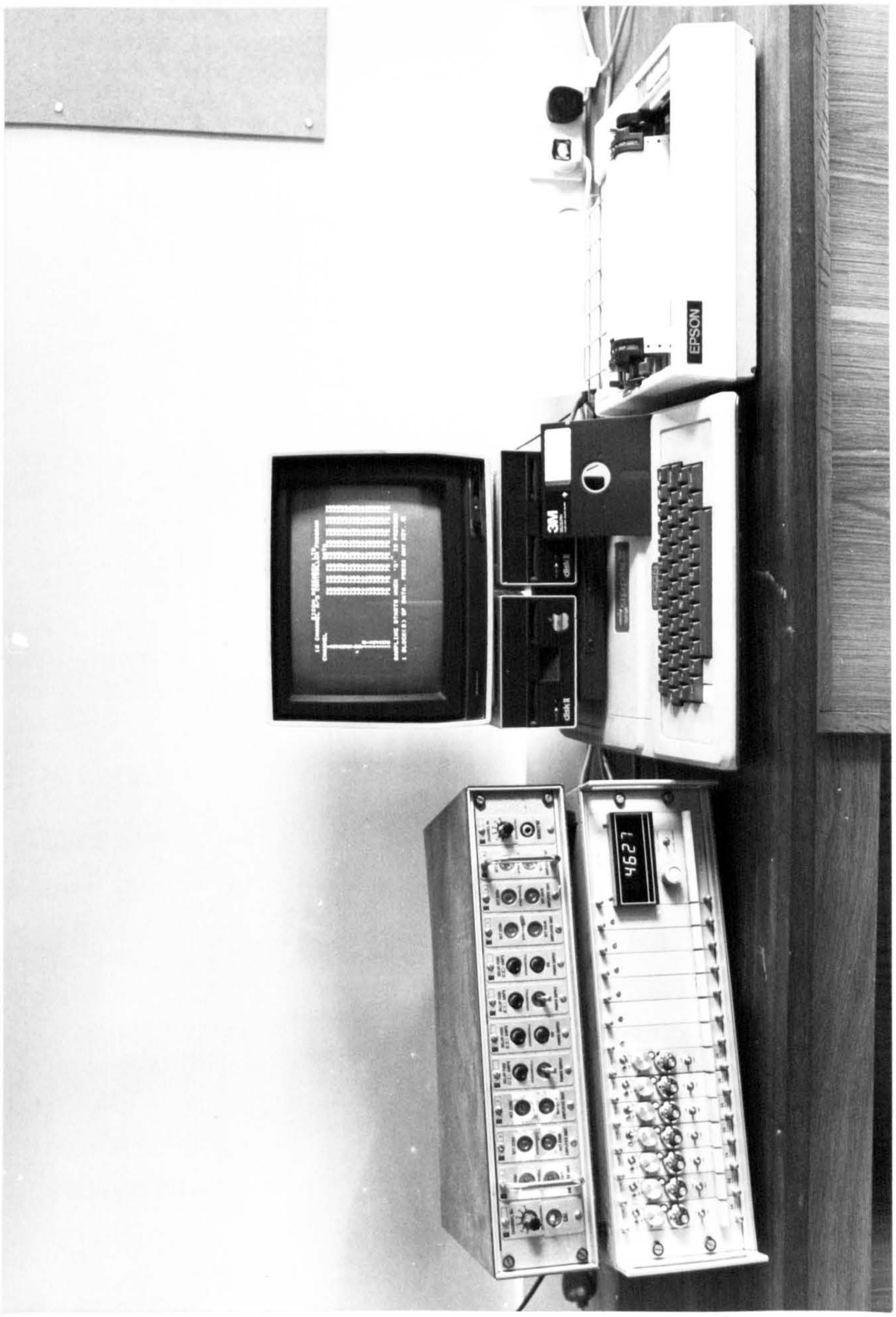

FIG. 3.10 Data record equipment

CHAPTER 4

QUANTITATIVE EXPERIMENTS to DETERMINE the BEHAVIOUR of the TRENCHLESS PLOUGH

4.1 Introduction

Preceding any advance in the main theoretical study, it was necessary to conduct a series of investigations into the basic aspects of the implement behaviour. Research conducted in the past with different soil engaging tools; by Childs (1942), Reece et al (1966), Cowell et al (1966, 1976), Fouss (1971) and Singh (1982); to study the influence of some external parameters on the dynamic response of these implements, revealed very little about the effect of soil reaction on the implement dynamic behaviour. Therefore, preliminary experiments were conducted to observe the influence of various factors that might affect the soil reaction on the tine and consequently the dynamic response of the implement when working with its beam in a floating position.

4.2 Experimental Method

These tests were divided into three sections, the first to determine the forces acting on the tine independent of the system weight or any factor other than soil. For this the implement was rigidly mounted on the soil bin carriage, without the long beam. The forces were measured when the plough was held at different depths at several deflected

positions in relation to the vertical, using the extended octagonal ring transducer to measure the main soil reactions, and the cantilever transducer machined inside the tine to measure the forces acting on the bottom of the implement.

The second section was a dynamic situation with the full implement assembly where the forces were measured in the following situations:

i) at various constant depths

ii) during increasing and decreasing of depth

iii) implements with different weights

iv) in soil with different shear strengths

The experimental apparatus used in these experiments is fully described in section 3.2 and the method of soil preparation in section 3.3. The soil surface was level for all these tests.

The third section was tests conducted in a glass sided soil bin to observe the pattern of the failure plan ahead of a cutting blade, with different soil profiles.

4.3 Experimental Results

4.3.1 Rigidly mounted tine

The objective of these tests was to determine the nature and magnitude of the soil reaction forces acting on a tine, geometrically similar to the trenchless blade, working at different depths and angles of

inclination. The results of these tests are presented in Figs. 4.1 and 4.2., and in particular this data illustrates:

a) Forward tilt of the implement at constant depth

i) As the tine is tilted forward the development of the clearance angle between the bottom plate and the soil reduces the horizontal force for inclinations up to 5^{o}. The physical basis of a large horizontal force at zero clearance is the frictional force between the bottom plate and the soil.

ii) A distinct change in the slope of the horizontal force curve occurs at 10^{o} of deflection, where the relationship becomes more dependent upon the rake angle. Godwin (1974) showed similar results when testing narrow tines at different rake angles, and proved that the effect of the rake angle on the horizontal forces is relatively small for angles between 45^{o} - 60^{o}.

iii) The vertical soil reaction acts downwards for an inclination angle of 0^{o} and becomes smaller in magnitude as the rake angle increases approaching zero and then changing direction at the rake angle in excess of 67^{o}, agreeing with the findings of Godwin (1974) for plane tines in the same soil.

b) Backwards tilt of the implement at constant depth

i) When the implement is tilted backwards, the magnitude of the horizontal and vertical forces change very significantly. Initially the vertical force reduces to zero and on futher displacement produces a very large upwards (negative) force. Similar response is noted on the soil reaction forces on the bottom plate, with a large increase in the normal reaction force upwards, and also on the tangential force. Due to design limitation on strength of the tine transducer, inclination greater than -3^{o} was not tested.

c) Forward tilt of the implement at different depths

i) Fig. 4.2 shows the results of tests conducted with the tine fixed at different angles of inclination running at different depths of work. The response of the horizontal and vertical force components to change in depth is similar to the results presented by Godwin (1974) and Singh (1982) indicating that this relationship is non-linear for a working depth range between 110-210 mm.

ii) The results show that at shallow depths the clearance angle influence is less than the change in rake angle. It is noticeable in this figure that at 110 mm deep the horizontal force is reduced up to 4^{o} of inclination only, and then increased for further inclinations; at 6^{o} it is already bigger than at 0^{o}. As the depth of work increases the relation between the rake angle and clearance angle slightly changes,

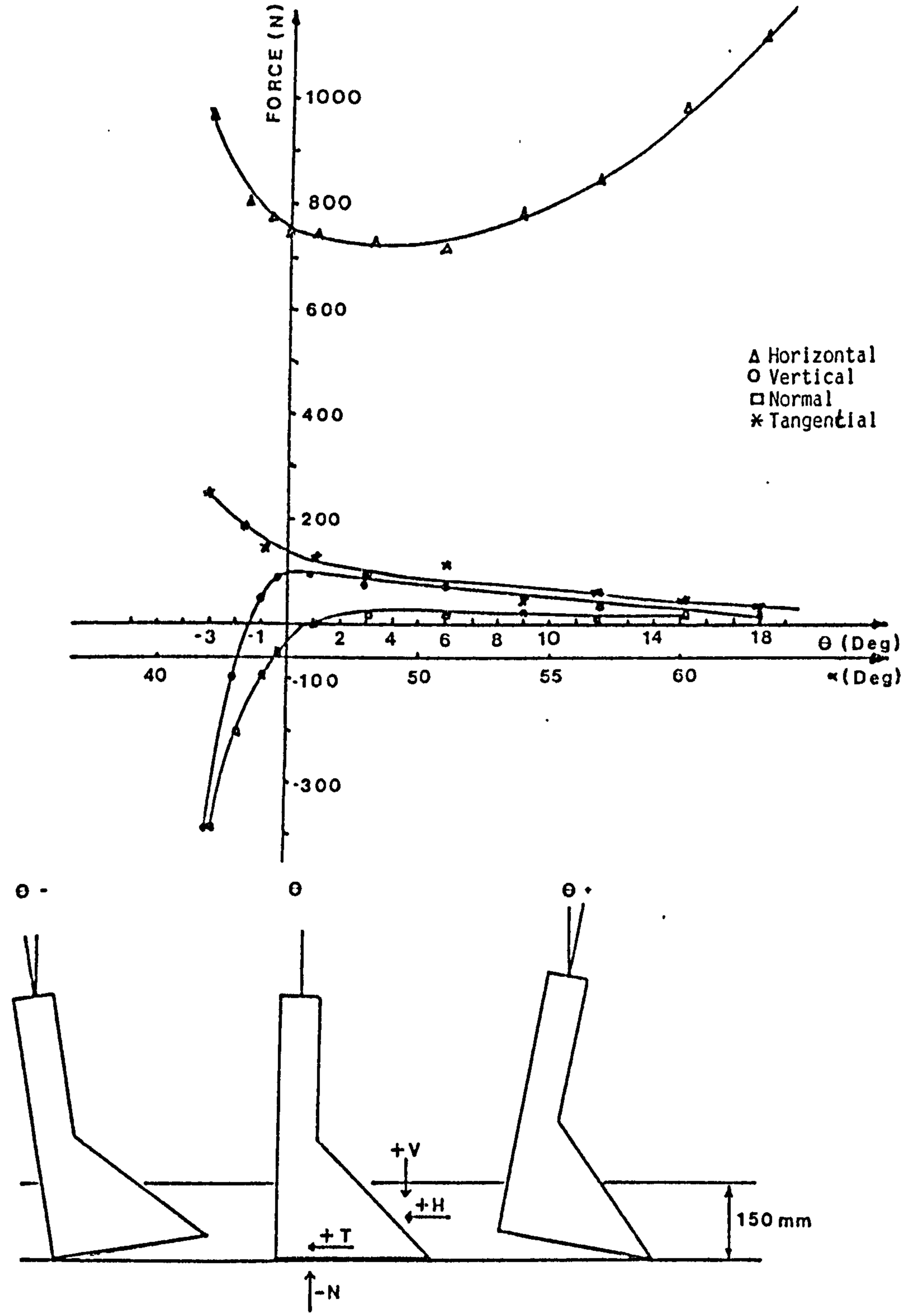

FIG. 4.1 Results of the restricted motion study. Soil reaction forces at different angle of inclination of the tine (θ), and constant depth of 150 mm

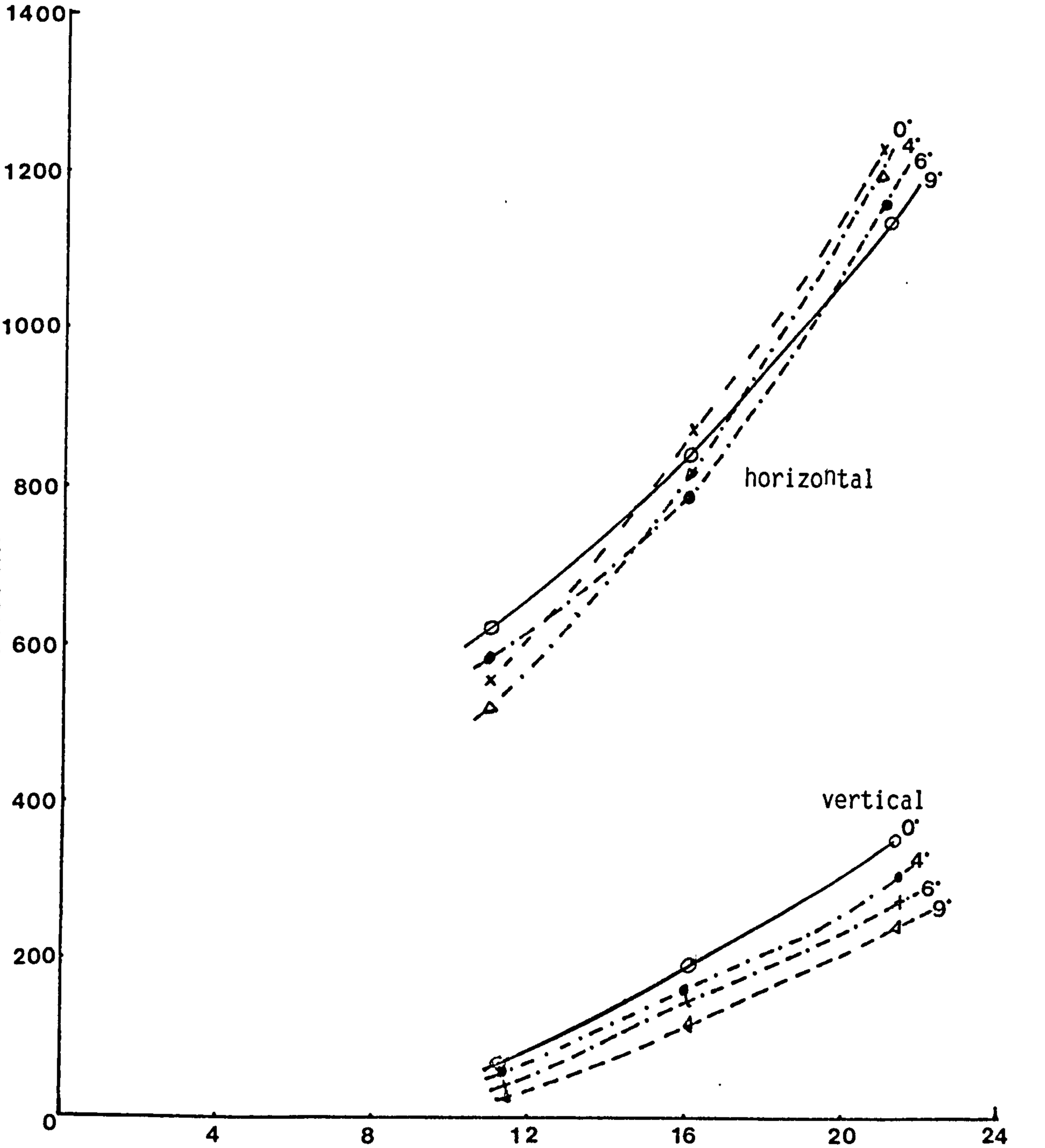

FIG. 4.2 Results of the restricted motion study. Soil reaction forces at different depth d, and angle of inclination θ

and it can be observed that at 210 mm the inclination of 9o still causes a reduction in the horizontal force.

From these results it was possible to conclude the following:

Although there is a small difference in the horizontal force when the tine is tilted forwards due either to the clearance angle or to the difference in the rake angle for large inclinations, for depths bigger than 130 mm, the error in considering the horizontal force constant in a range of 0-10o for a given depth is less than 8%, and this error tend to reduce as the depth increases. At shallow depths, below 130 mm, it is adivisable to take the difference into account.

The same consideration is not valid when the implement is tilted backwards, in this case the increase in forces is significantly greater and could certainly influence the implement behaviour.

4.3.2 Dynamic motion studies

4.3.2.1 Introduction

A limited number of experiments were conducted with the tine in the dynamic situation to examine the influence of the forces observed in section 4.3.1, and relate them with the behaviour of the trenchless drainage plough.

4.3.2.2 Equilibrium situation

The free-body diagram of the trenchless tine is shown in Fig. 4.3. The nature of the forces exerted on the system by the soil is determined by the physical properties of the latter. By symmetry the resultant of the sideways components is zero, giving only the forces acting on the implement in the horizontal and vertical directions. Since the point **'O'** and the hitch-point are pivoted, and the resultant force must pass through the latter, the angle of the "free-link" and the total resultant force are the same.

The desired position for the trenchless plough to work is at equilibrium condition with its bottom parallel to the grade of the drainage project. Tests conducted in the soil bin with a fixed hitch-point over a flat soil surface, showed that the implement maintains its desired position independent of the working depth up to a certain limit, called the maximum working depth. An explanation for this is that the free-link used between the real hitch-point and the point **'O'** gives the beam some degree of freedom in vertical and horizontal directions. Consequently, when the weight of the system, combined with the vertical force, induces the implement to penetrate, this movement is opposed by the soil resistance on the bottom of the tine, and sustains the weight of the implement, creating a support force sufficient to compensate and balance the forces. This balanced situation can be upset in two ways. If the implement is forced to run below the maximum working depth, by means of reducing the height of the hitch-point, the increase in the horizontal

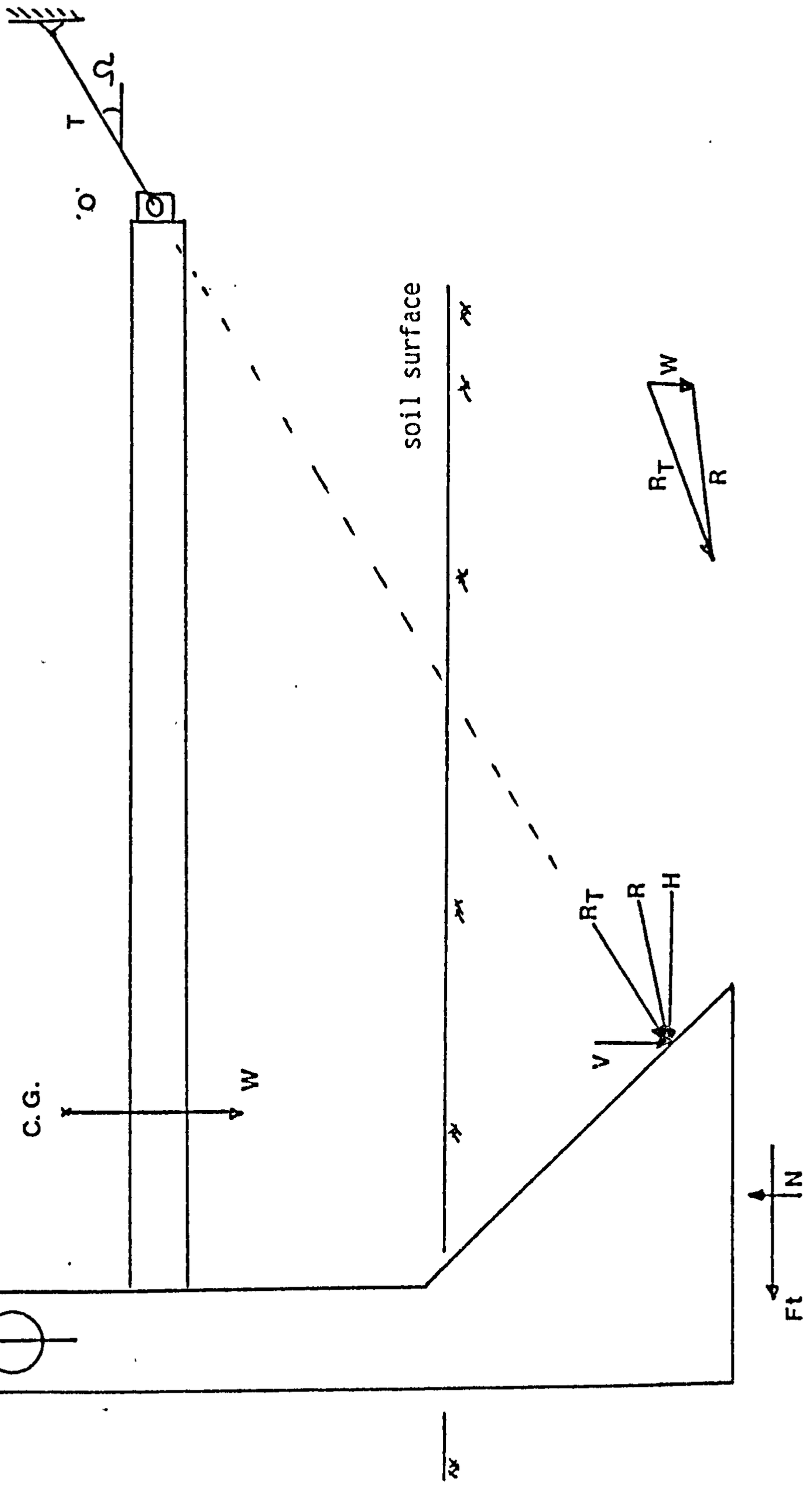

FIG. 4.3 Soil reaction forces at a desired equilibrium position

force unbalances the forces and the moments involved in the system and the implement turns forwards, but does not penetrate. The other situation would be if the soil structure is not sufficiently strong to support the implement weight, then the tine sinks and compacts the soil until the bearing capacity is reached, and the balance is restored.

In this work, the equilibrium condition is considered the one achieved when the implement is working at its desired condition above the maximum working depth.

The trenchless tine, due to its aspect ratio (depth of work/tine width), can be classified as a narrow tine, and although its way of assembly and condition of work differ from the cultivation tine, it was decided to check how the values obtained experimentally fitted in the theory proposed by Godwin and Spoor (1977) for rigidly mounted narrow tines.

The basic differences between these tines are that, the cultivation tine is a blade with a relieved bottom fixed to a frame, where generally the weight of the system is supported by a rigid attachment; on the other hand the trenchless plough is a blade with a non-relieved bottom and a relatively wide side plate, and is self supported, i.e., all the weight of the system is an active force in the process of cutting soil.

The forces recorded during these tests in the horizontal and vertical direction, and the one calculated from the equation for narrow tines (Godwin and Spoor 1977), are plotted on Fig. 4.4. Although the theory of

narrow tines could be used to predict the forces acting on the tine face, and are in close agreement with the results obtained at large depths. As the depth of work reduces the influence of the forces acting on the bottom plate and on the side plates of the implement increases, and the results of the experimental values start to present some variations, especially for the vertical forces. The reason is, as explained above, that it is not the purpose of the model to predict all the forces which are involved with the tine shape used in the trenchless plough beam arrangement.

Comparing the overall forces in the horizontal and vertical direction with the results predicted by the narrow tine theory for the tine face, the difference between the curves suggests that it is necessary to find a way to predict the resultant force acting on the tine in the horizontal and vertical direction to complement the results obtained from this theory.

4.3.2.3 Position of the resultant force

The magnitude, direction and point of action of the total resultant force, R, acting on the trenchless plough is a function of the tine working depth. However, it is possible to observe in Fig. 4.5a that the ratio of the depth of the centre of resistance and the implement depth remains fairly constant. The results presented in Table 4.1 show that the ratio cr/d has an average value of 0.877, where 92% of the values are within + 2 standard deviation for depths between 138-198 mm. It is also noticeable in Fig. 4.5b (Table 4.1) that the angle of the resultant force tends to decrease with the increase in depth, and this

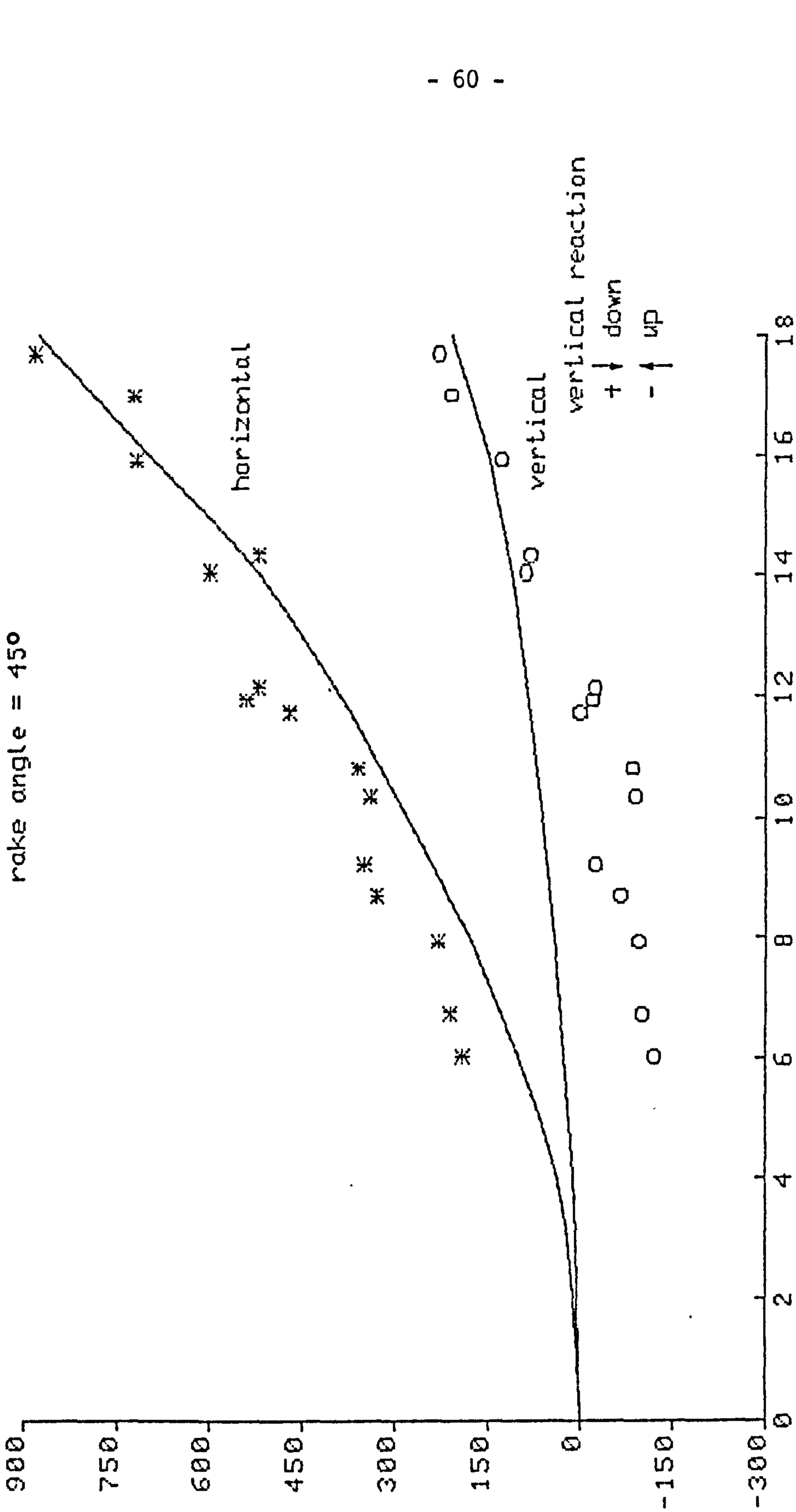

FIG. 4.4 Soil reaction forces on the trenchless tine model assembled with a long floating beam. *; o Experimental results. —— Results obtained from the theory of the narrow tines (Godwin and Spoor, 1977)

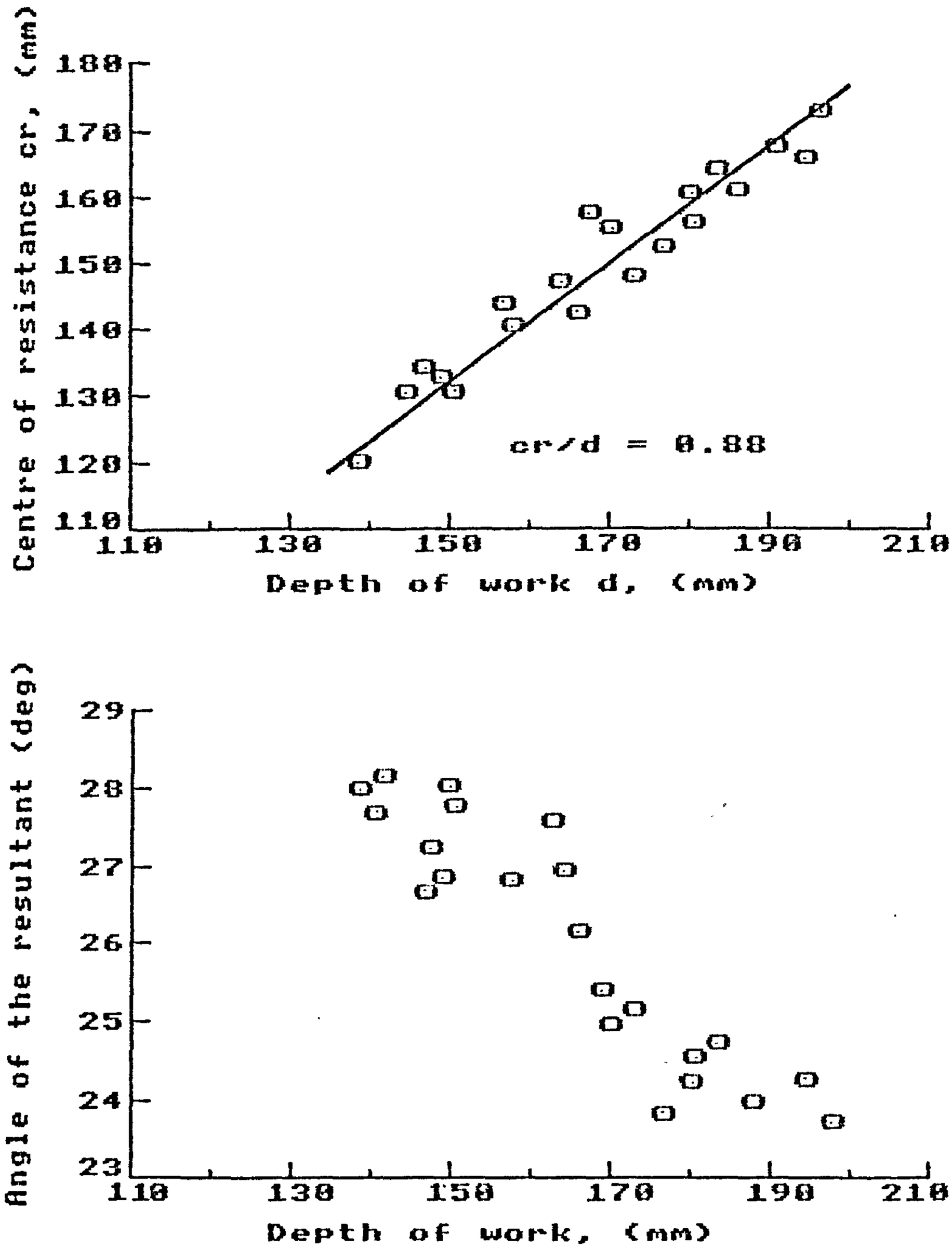

FIG. 4.5 Relation between resultant force and depth of work
a) center of resistance
b) angle of the resultant force

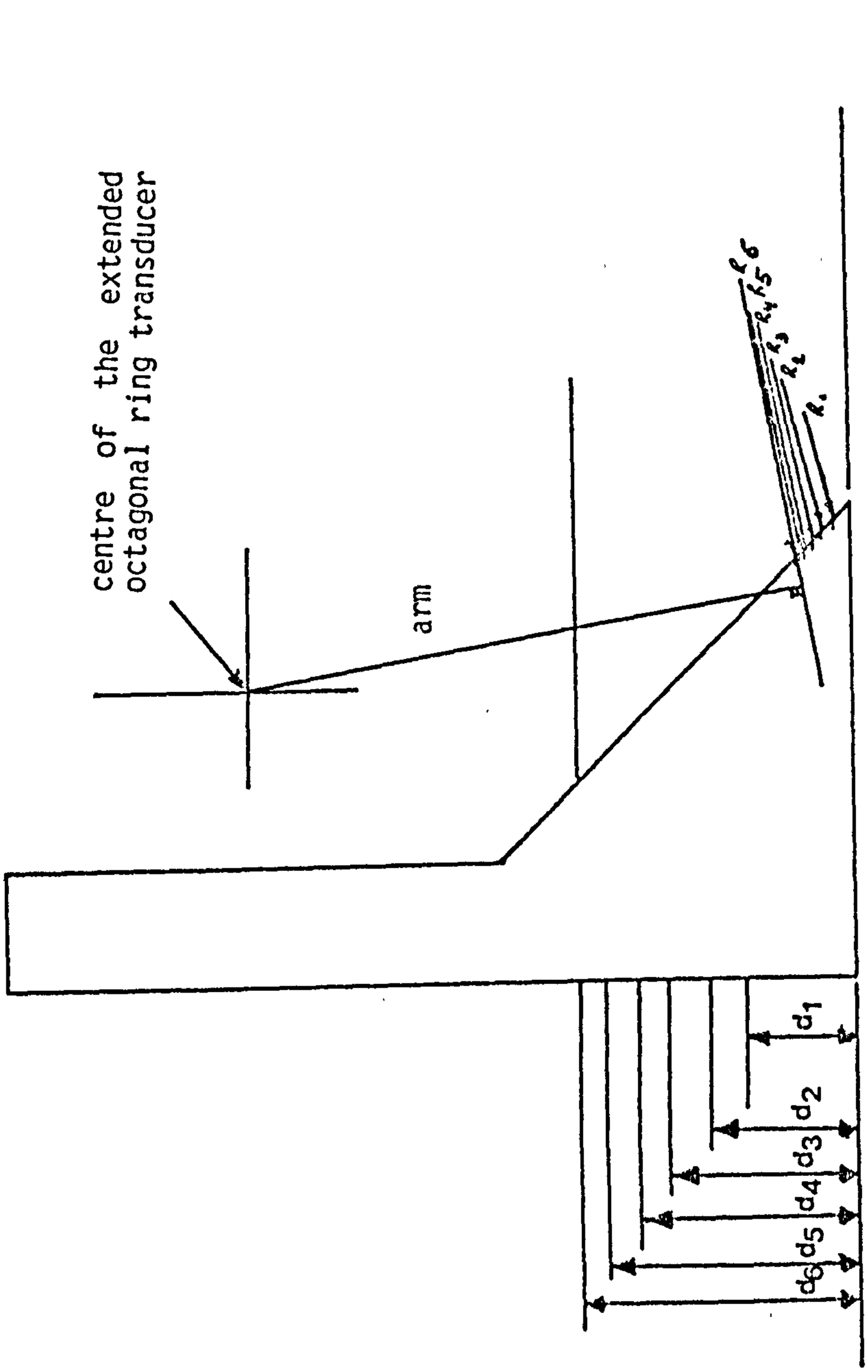

FIG. 4.6 Position of the centre of the resistance

relationship appears to be non-linear. Fig. 4.6 illustrates the relationship between depth, position of the centre of resistance, direction and magnitude of the resultant force.

4.3.2.4 Force response to changes in hitch-point height

An important factor in the dynamic behaviour of the implement is its response to changes in the hitch-point level, and the soil reaction forces to these changes. Singh (1982) in his hypothesis on the dynamics of the trenchless implement suggested that the angular response of the model drainage plough could be represented by a second order linear differential equation. As a result of the tests, he found that the implement achieved 63.2% and 99% of the desired correction after travelling 0.9 and 4.5 times the beam length respectively, and these figures were independent of the forward speed of the implement.

There are fundamental differences between the model of trenchless plough being studied here and the one studied by Singh. One important aspect which differs in Singh's plough model was that due to its configuration the implement could achieve the equilibrium condition at any angle of the tine or the long beam, dependent only on the position of the hitch-point; Singh's model was a relieved bottom tine, and the hitch-point 'O' was fixed to the carriage, without the use of the free-link. Therefore, it is important to repeat some of this test, in order to verify if his findings are applicable to a tine with the characteristics presented here.

To observe the response of the implement to a change in the hitch-point height, the implement was settled at its equilibrium position before starting the run, and then the hitch point was raised or lowered, so when the carriage started to move forwards the implement moved up or down, until a new equilibrium position was reached.

The results obtained when testing the penetration, Figs. 4.7 and 4.8, and the raising response of the tine, Fig. 4.9, are consistent with the results reported by Singh. It is possible to observe in these figures that the distance travelled to achieve its equilibrium, for the same deflection, is practically the same whether the tine is moving upwards or downwards, suggesting that there is no significant difference between the upwards and downwards responses of the implement.

In order to have a better comparison between the results obtained for penetration or raising of the implement, the angular deflection of the tine against the travelled distance is plotted in the same graph (Fig. 4.10 top), disregarding their signs. In this figure the green line represents the results obtained during the raising of the tine, and it is possible to observe that it has the same pattern as the other two curves which represent the penetration of the tine. The "time constant", the distance necessary for the implement to achieve 63.2% of its equilibrium, is equivalent to 0.86 times the length of the beam, and it needs 3.75 times this value to achieve 99% ofthe desired condition. Fig. 4.10 (bottom) shows the path of the implement correspondent to the

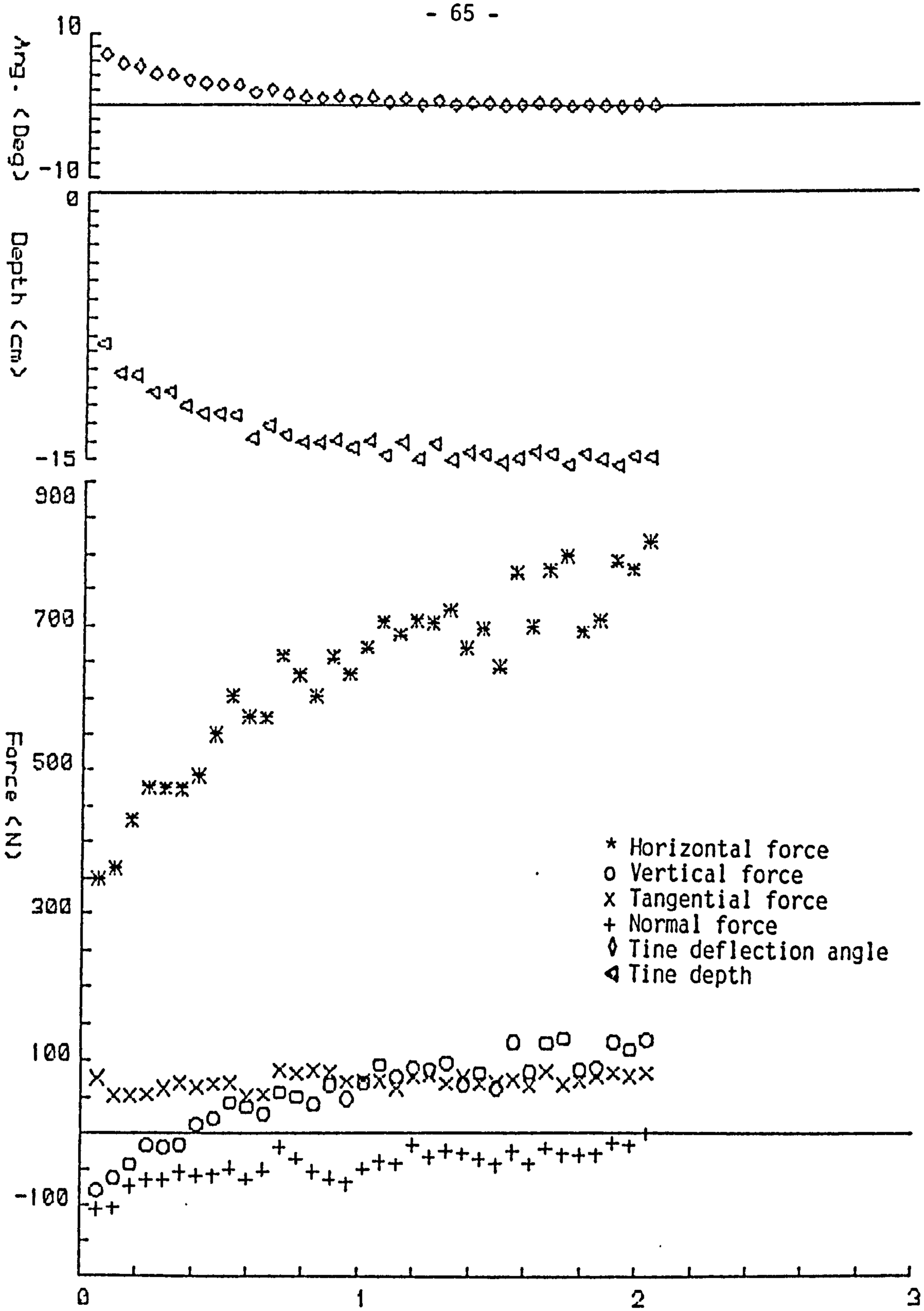

FIG. 4.7 Results of the dynamic motion study, downwards response of the implement. Equilibrium depth 155 mm

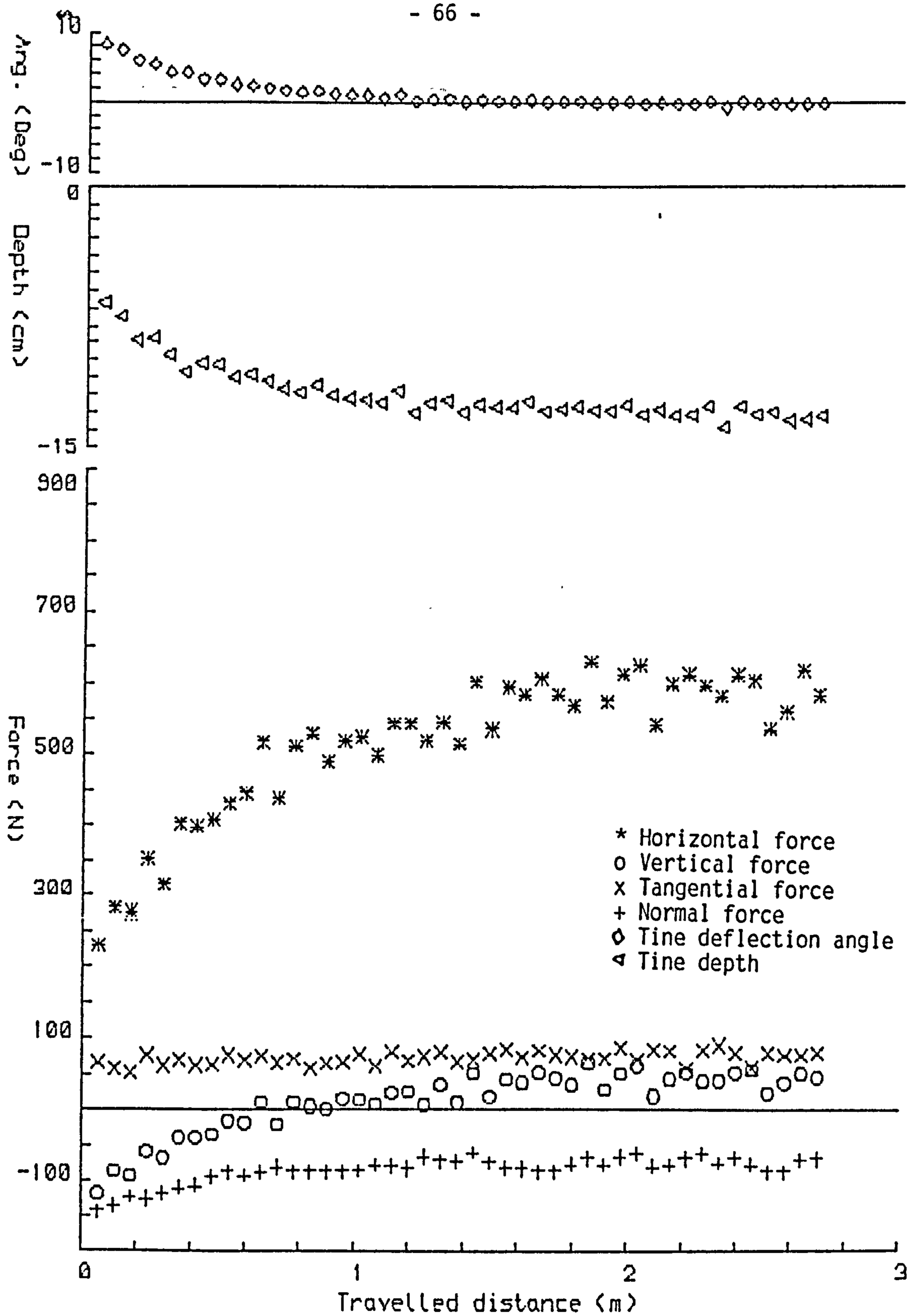

FIG. 4.8 Results of the dynamic motion study, downwards response of the implement. Equilibrium depth 130 mm

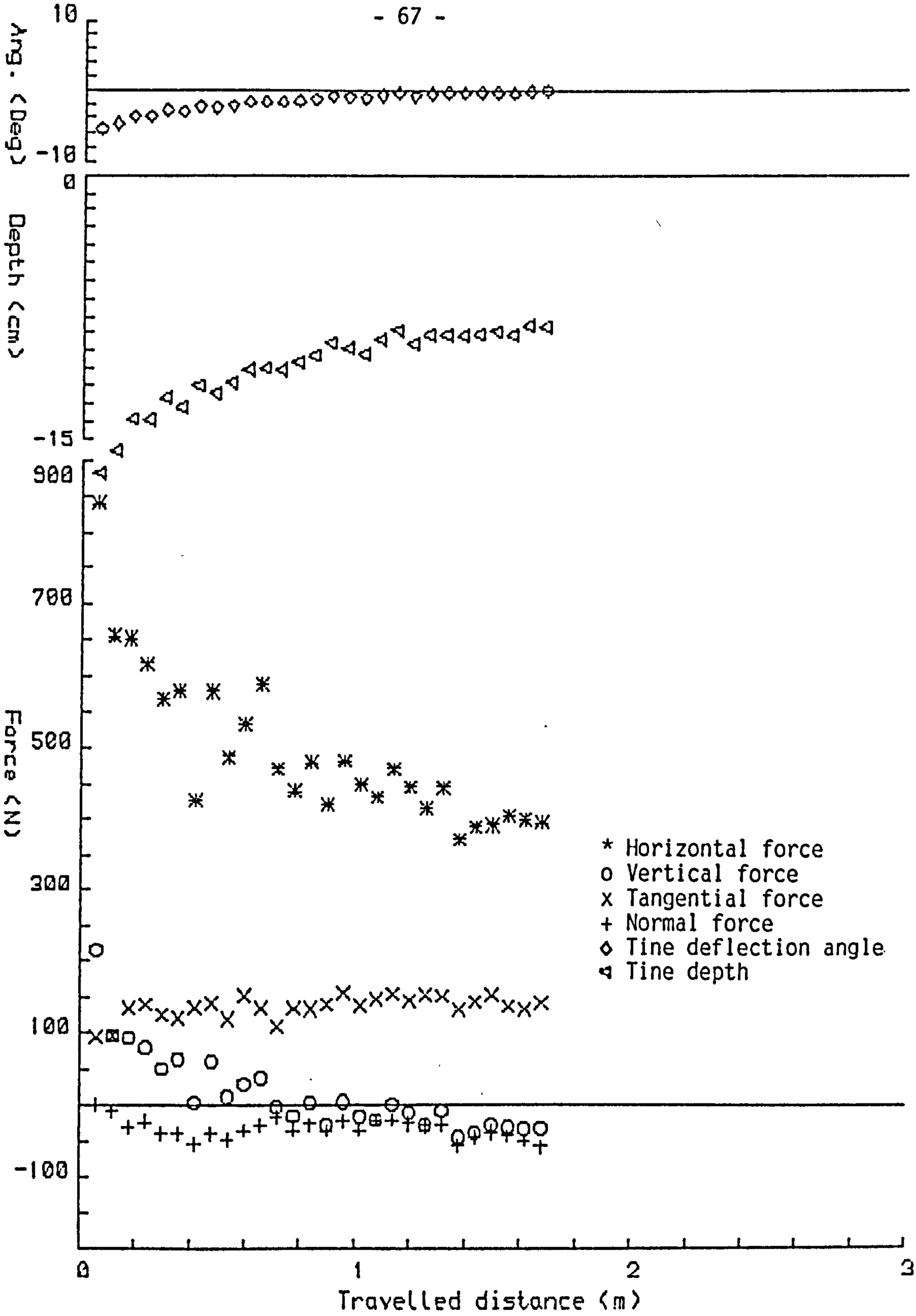

FIG. 4.9 Results of the dynamic motion study, upwards response of the implement. Equilibrium depth 90 mm

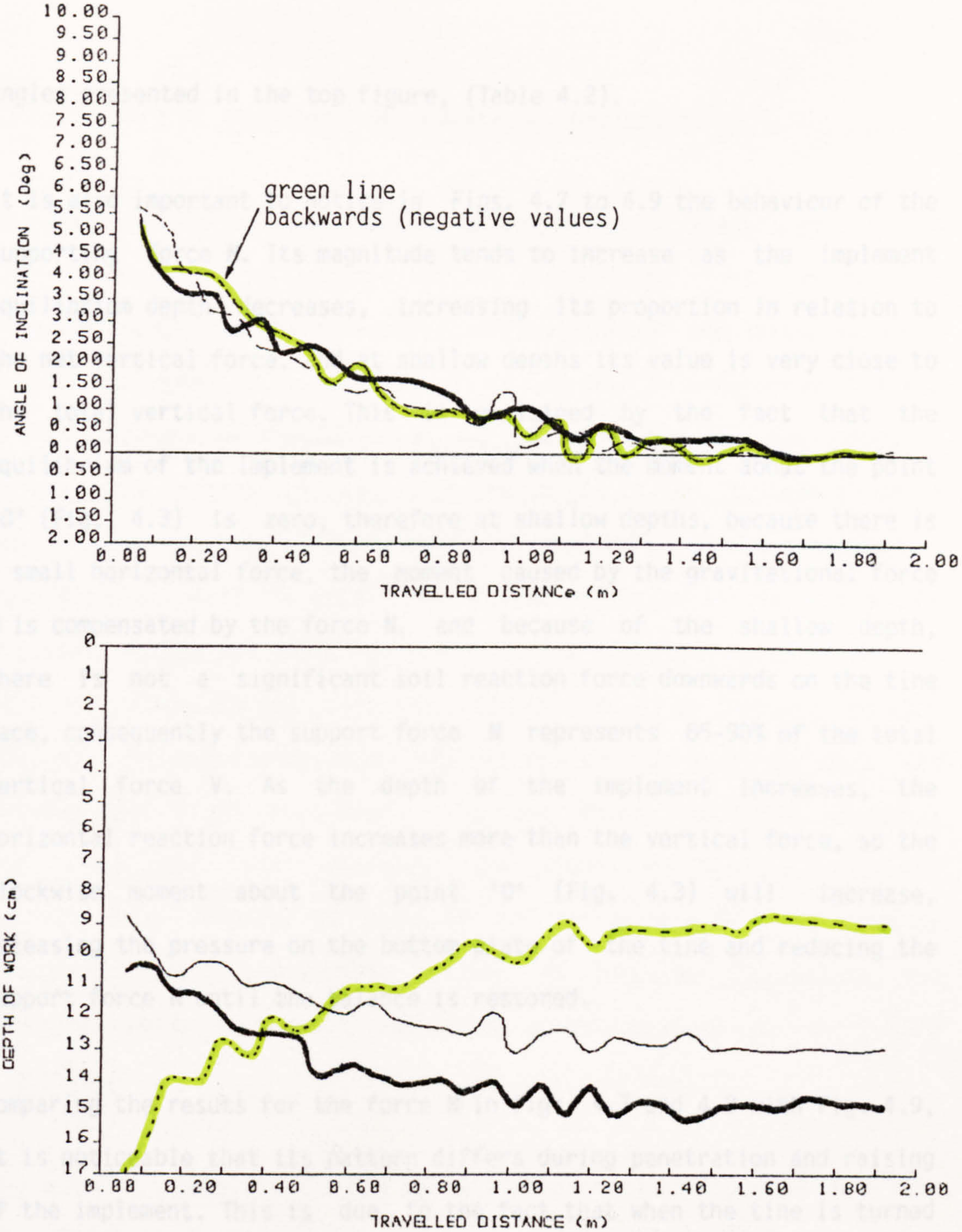

FIG. 4.10 Results of the tests during penetration and raising of the implement. Top: Travelled distance with the tine angle of inclination. Bottom: Travelled distance with the tine working depth. ▬ Penetrating to an equilibrium depth equal to 130 mm. -- Penetrating to an equilibrium depth of 150 mm. ▬ Raising to an equilibrium depth of 90 mm

angles presented in the top figure, (Table 4.2).

It is also important to notice in Figs. 4.7 to 4.9 the behaviour of the supporting force **N**. Its magnitude tends to increase as the implement equilibrium depth decreases, increasing its proportion in relation to the net vertical force, and at shallow depths its value is very close to the total vertical force. This is explained by the fact that the equilibrium of the implement is achieved when the moment about the point **'O'** (Fig. 4.3) is zero, therefore at shallow depths, because there is a small horizontal force, the moment caused by the gravitational force **W** is compensated by the force **N**, and because of the shallow depth, there is not a significant soil reaction force downwards on the tine face, consequently the support force **N** represents 85-90% of the total vertical force V. As the depth of the implement increases, the horizontal reaction force increases more than the vertical force, so the clockwise moment about the point **'O'** (Fig. 4.3) will increase, releasing the pressure on the bottom plate of the tine and reducing the support force **N** until the balance is restored.

Comparing the resuts for the force **N** in Figs. 4.7 and 4.8 with Fig. 4.9, it is noticeable that its pattern differs during penetration and raising of the implement. This is due to the fact that when the tine is turned forwards and starts to penetrate, the bottom plate is pressing an undisturbed soil. On the other hand when it is raising, turned backwards, although the bottom plate is still pressing the soil, it is a disturbed soil, and therefore weaker.

4.3.2.5 Effect of the moment of inertia of the system

One way of testing the effect of the moment of inertia in a system dynamic behaviour, is by comparing the response of this system with different masses in the same physical condition. If the system response remains unaltered, or very similar, it can then be considered that the dynamic behaviour of the implement is not affected by the moment of inertia. The effect of changes in the weight of the implement, which remains with the same size and geometric configuration, is presented in Figs. 4.11 to 4.13. To obtain the desired variation in the mass of the implement, weight was added or removed, therefore the normal weight of 236 N was reduced to 60% (142 N), and 80% (186 N) or increased to 200% (432 N). For experiments with less weight, the long metal beam was replaced by a light wood beam of the same length, and the octagonal ring transducer was removed. The wooden replacement beam was carefully made in order to maintain the centre of gravity as close as possible to that of the original system. To increase the weight, the implement was ballasted with additional weight attached near the centre of gravity.

The result of these tests can be better observed in Fig 4.14 where the path of the implement for the tests with different weights is plotted on the same graph. Although the soil reaction forces and the equilibrium depth increased with the increase in weight, the motion of the implement remained heavily damped with little change in the total travelled

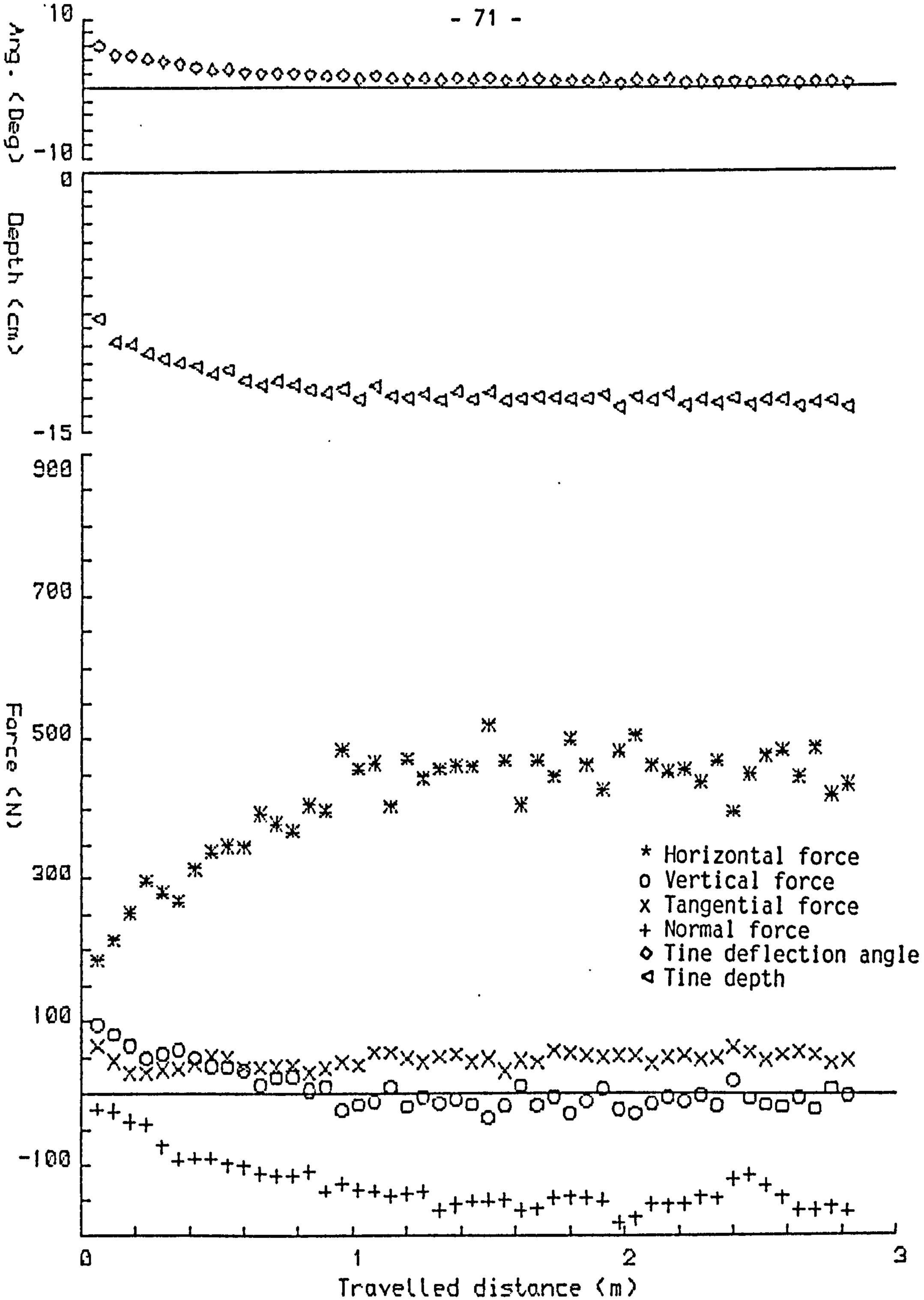

FIG. 4.11 Results of the dynamic motion study, downwards response of the implement. Weight equal to 142 N, (60% of the normal weight). Equilibrium depth 130 mm

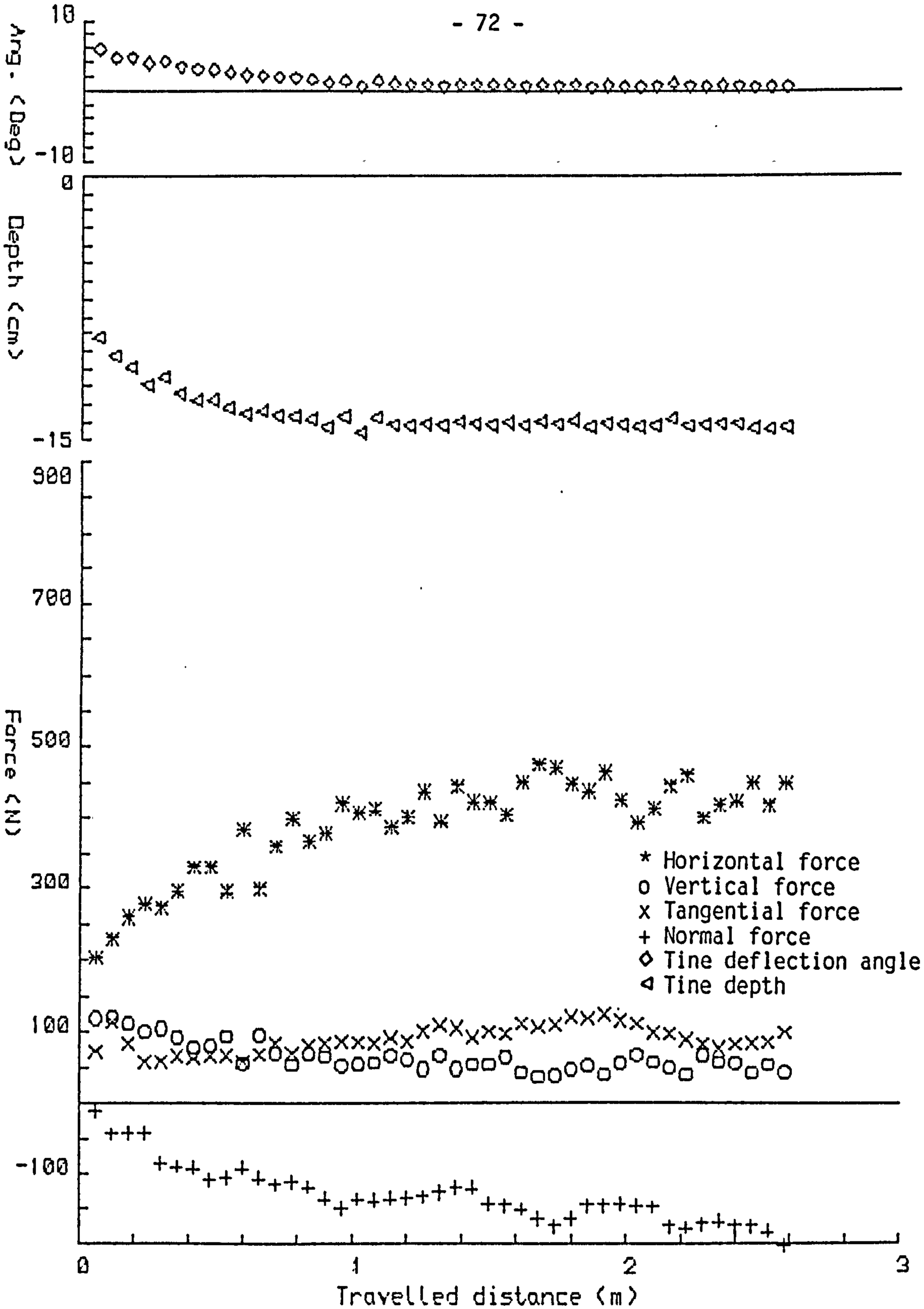

FIG. 4.12 Results of the dynamic motion study, downwards response of the implement. Weight equal to 186 N, (80% of the normal weight). Equilibrium depth 135 mm

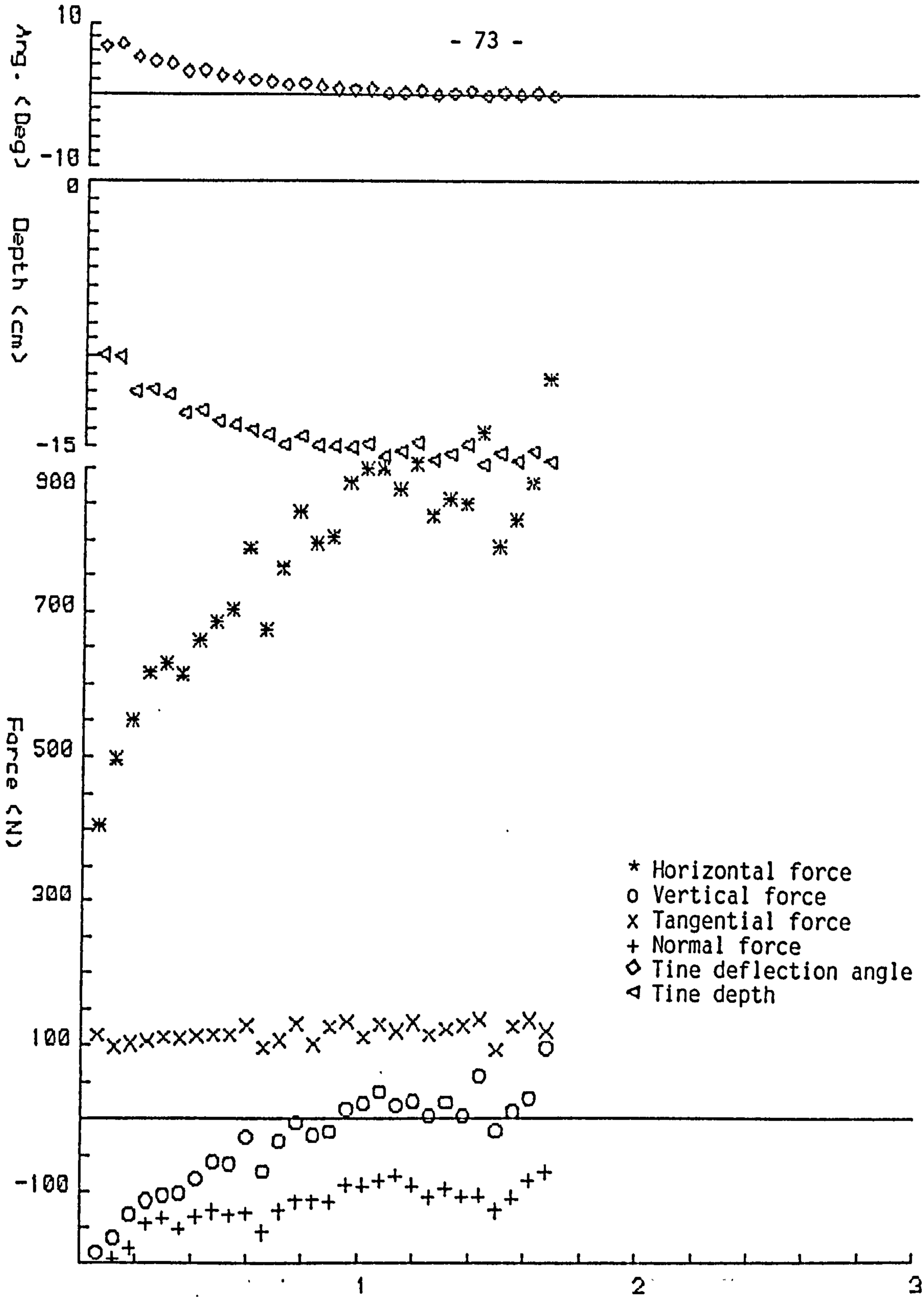

FIG. 4.13 Results of the dynamic motion study, downwards response of the implement. Weight equal to 432 N, (200% of the normal weight). Equilibrium depth 160 mm

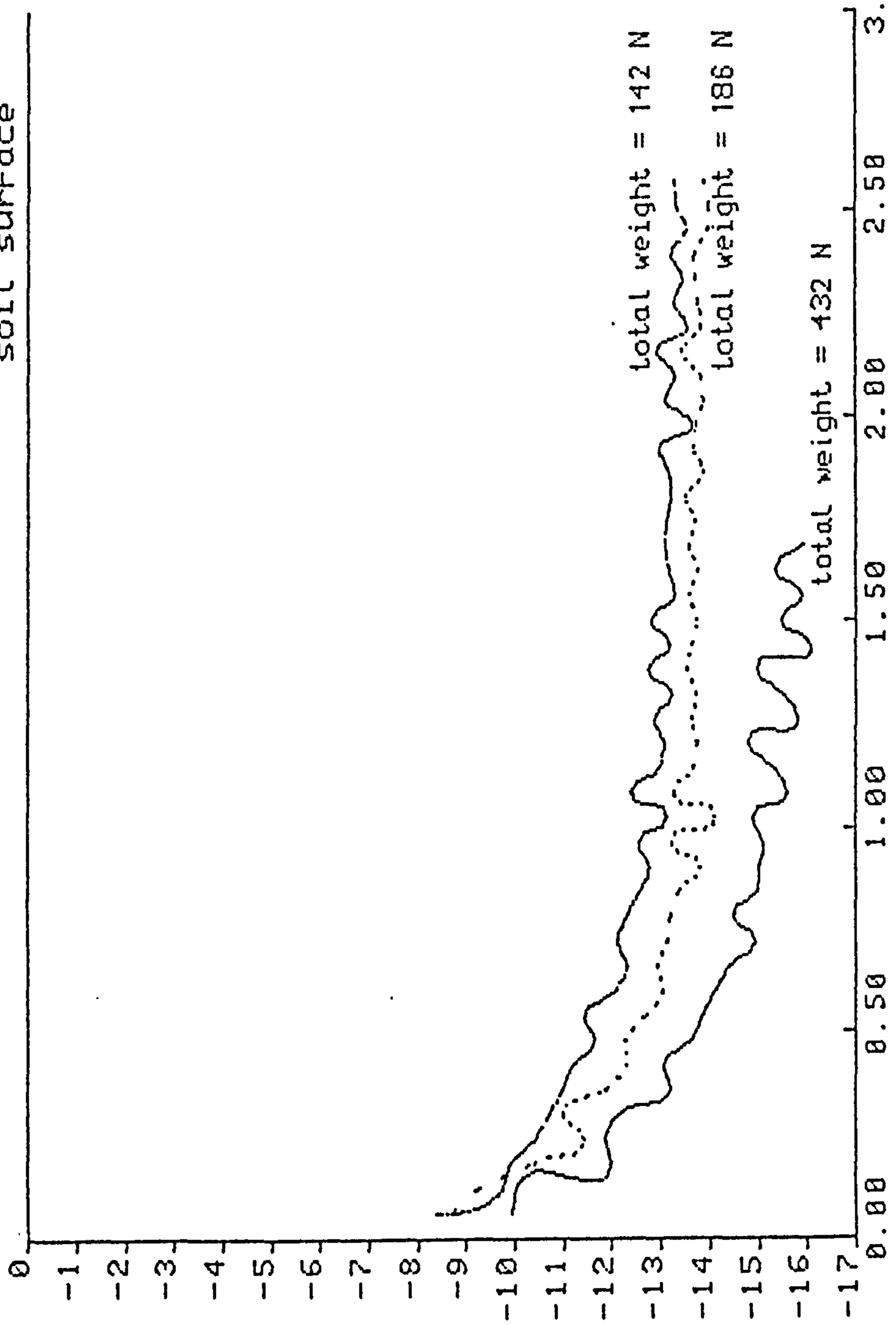

FIG. 4.14 Path of the implement with different weights during penetration on a flat surface. Hitch-point height constant equal to 210 mm

distance necessary for the implement to reestablish its equilibrium, (Table 4.3).

These results suggested that the dynamic response of the implement is independent of the moment of inertia of the system, because its displacement occurs at a slow speed. This is in consensus with the report presented by Cowell (1976) in his theory for the dynamic behaviour of mouldboard ploughs, and Singh's (1982) for the drainage plough. Those authors actually did not test but inferred, based on the fact that the inertia force exerted on the implement is negligible in comparison with the forces exerted by the soil and gravity.

4.3.2.6 Effect of the soil shear strength

The response of the implement to changes in soil shear strength in the same run was investigated with the aim of observing the implement behaviour in a situation commonly found in the field. Altering the soil density is one way of altering the soil shear strength, and this was the method chosen in this project.

The soil density was varied in the range 1680-1200 Kg/m^3, prepared very carefully so that the boundary region was as small as possible in order to give an instantaneous change between the zones with different shear strength.

The results presented in Figs. 4.15 to 4.17, are for tests conducted in

the soil bin packed with different soil densities. The effect of the differences in the soil shear strength are clearly noticeable in the response of the soil reaction force acting on the tine. These forces changed abruptly when the zone with different soil density was reached, but the response of the implement in changing to a new depth was observed to be very slow. Fig. 4.18 shows the values of the horizontal force and depth of the implement for different tests plotted in the same graph for better comparison. It is noticeable in this figure that although the soil forces vary about 30-40% from the zones with different density, the difference in depth of work is no greater than 10%.

The explanation for this is that, alteration in the value of the forces acting on the tine causes a variation in the magnitude and direction of the resultant force, and consequently in the balance of the moment about the point 'O' (Fig 4.3). This makes the implement move to find a new equilibrium depth. The slow change in depth is due to the fact that the vertical displacement of the implement has a very large damping effect, therefore a relatively large travel distance is necessary before the equilibrium is restored. Because the proportion of change in the horizontal and vertical forces, due to the variation in soil density, is similar, there is not a great alteration in the direction of the resultant force, and consequently the change in the equilibrium depth is smaller compared to the amount of change in the forces in the horizontal and vertical direction (Table 4.4).

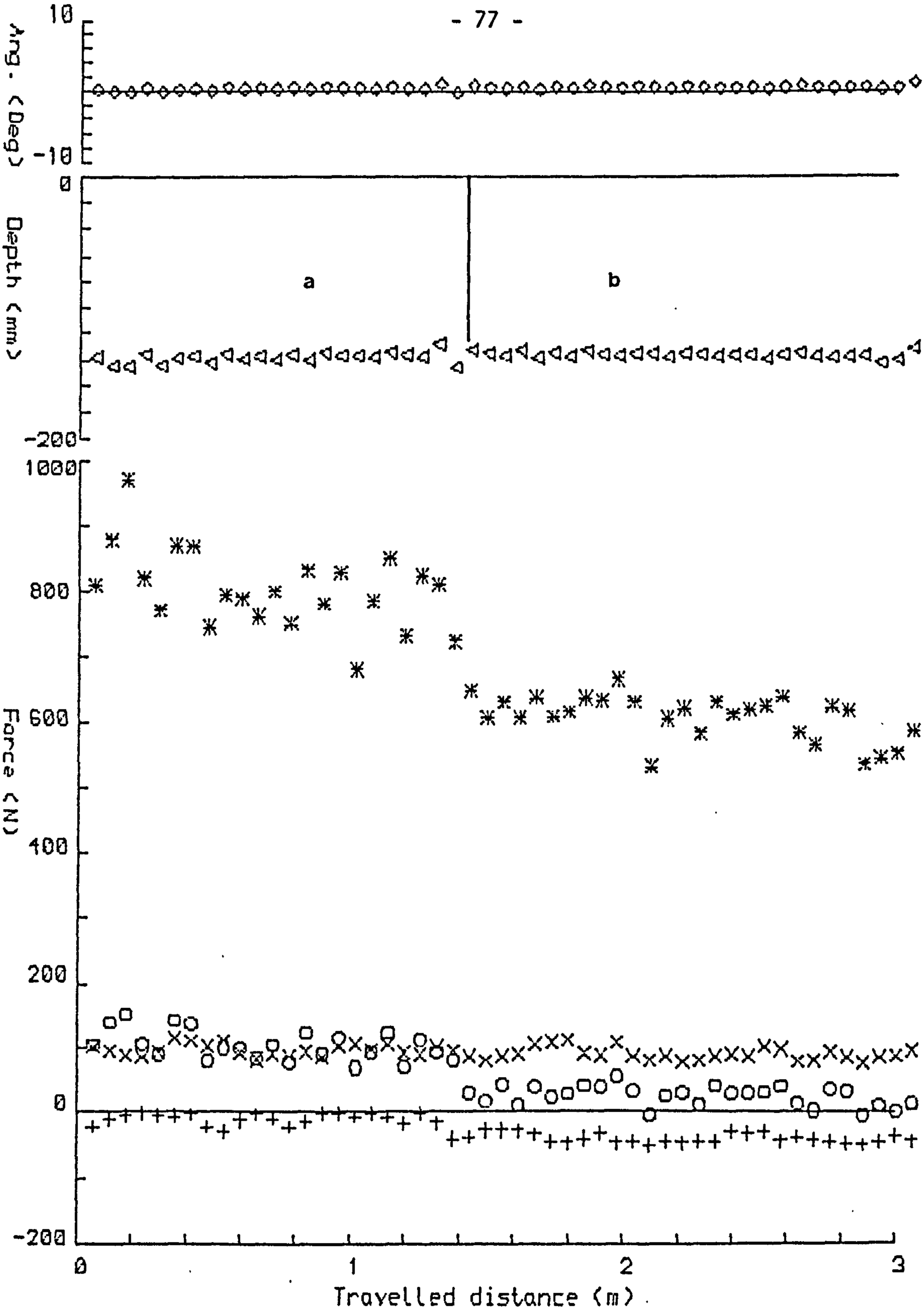

FIG. 4.15 Results of the dynamic motion study, soil with different density. Section (a) 1500 kg/m^3 and section (b) 1350 kg/m^3

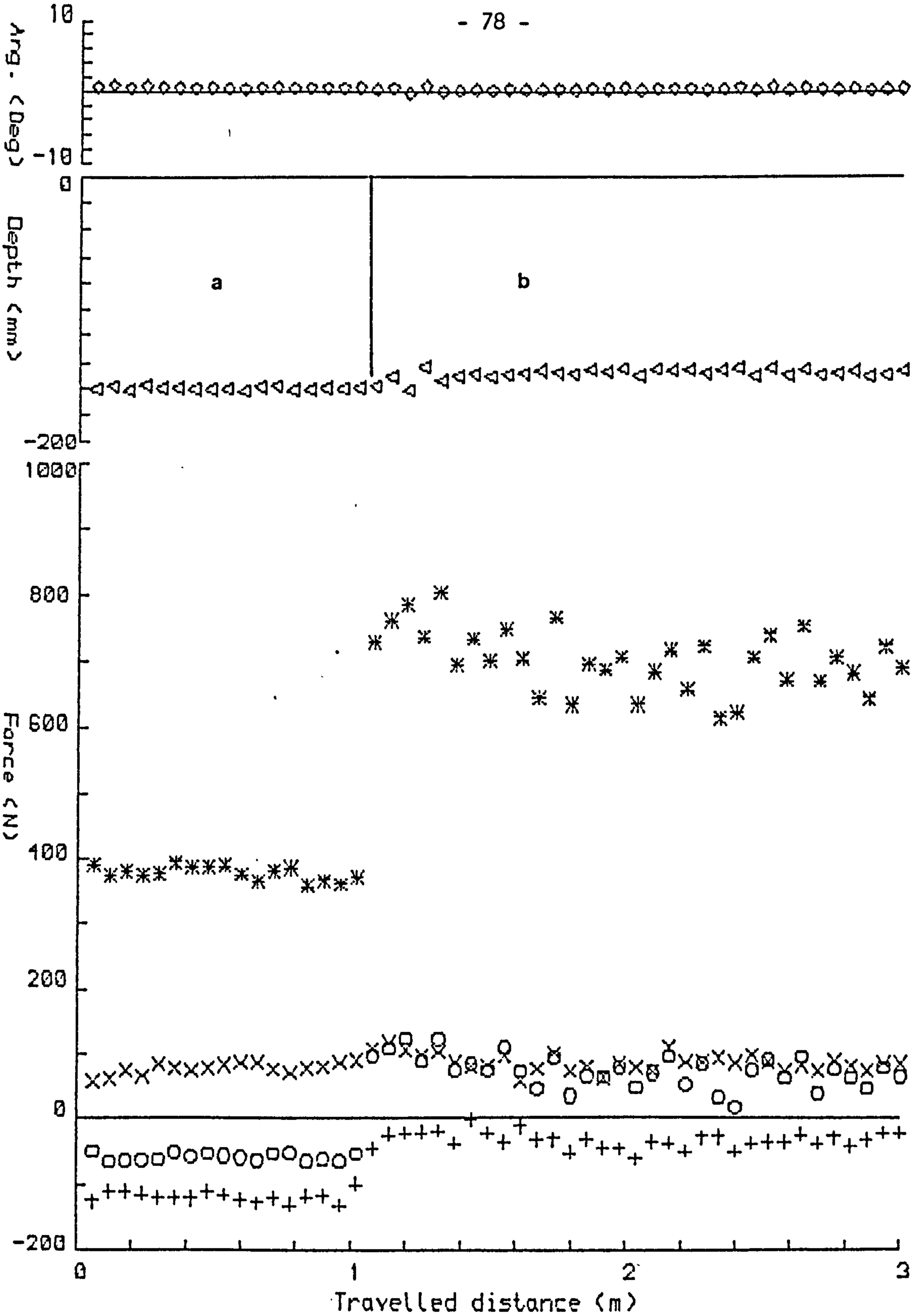

FIG. 4.16 Results of the dynamic motion study, soil with different density. Section (a) 1200 kg/m^3 and section (b) 1500 kg/m^3

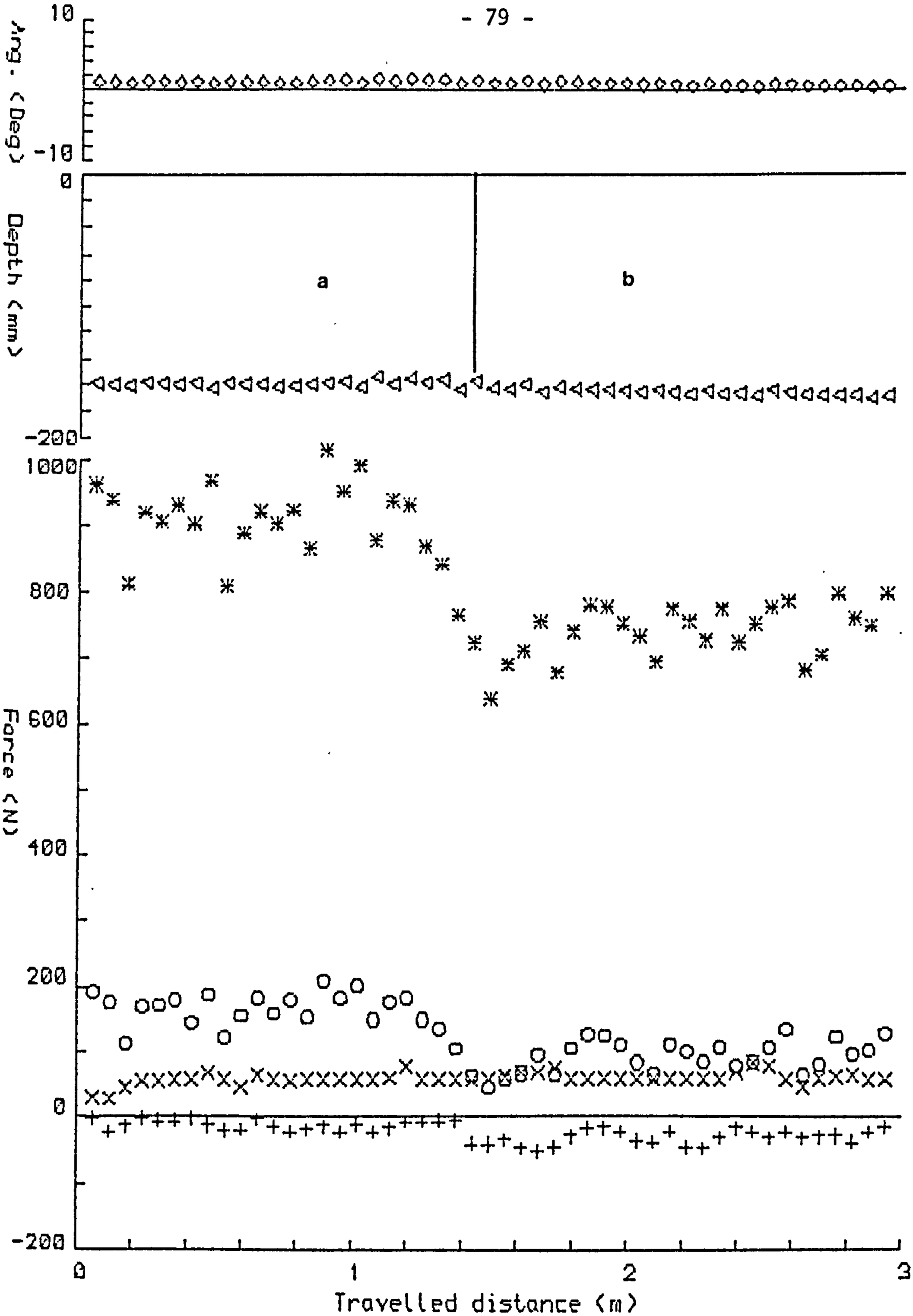

FIG. 4.17 Results of the dynamic motion study, soil with different density. Section (a) 1680 kg/m^3 and section (b) 1350 kg/m^3

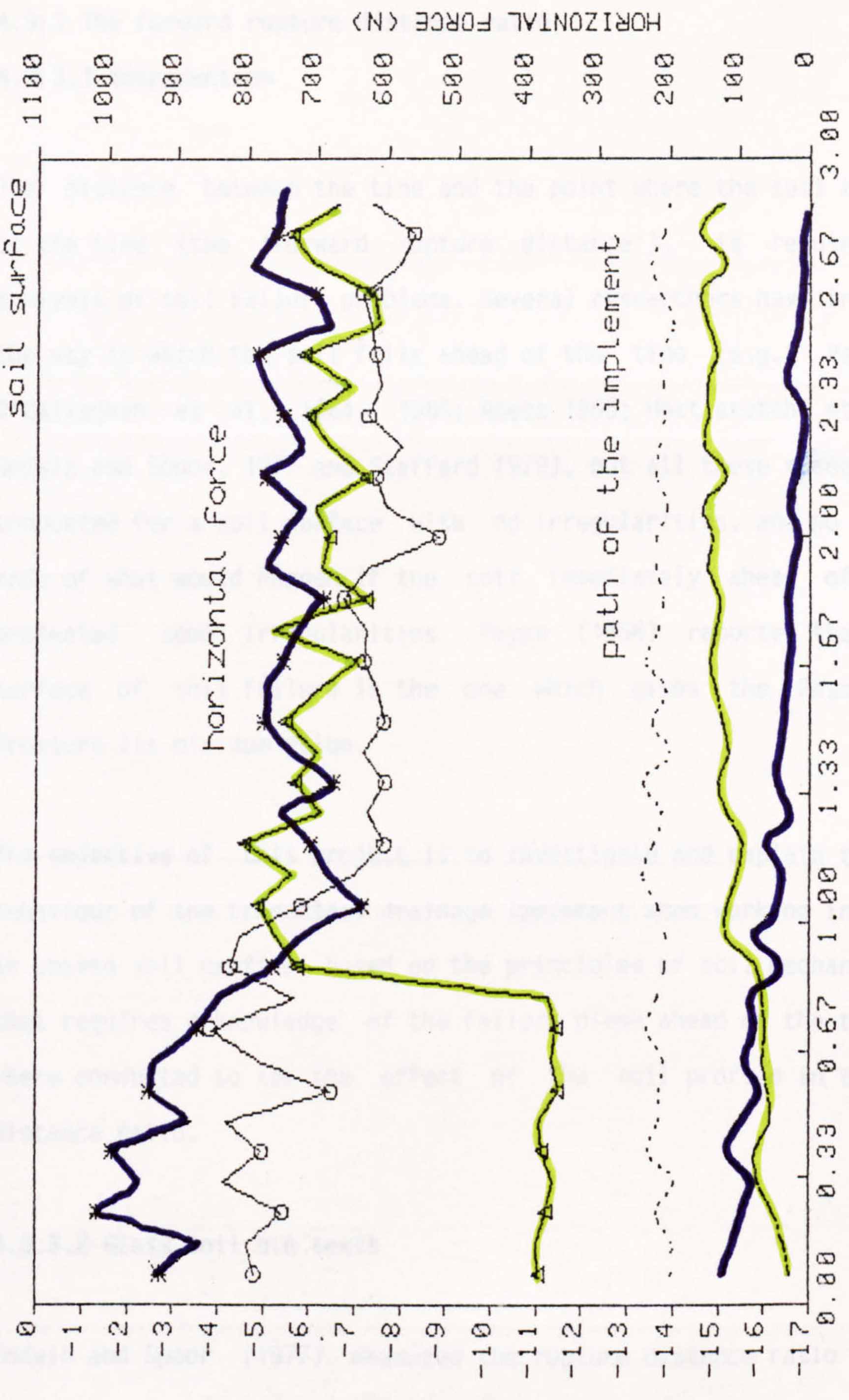

FIG. 4.18 Effect of the soil density in the tine depth of work and horizontal force. o --- 1500 to 1350 kg/m3; Δ —— 1200 to 1500 kg/m3; * —— 1680 to 1350 kg/m3. The lines with symbols (*, o, Δ) represent soil reaction force

4.3.3 The forward rupture distance ratio

4.3.3.1 Introduction

The distance between the tine and the point where the soil fails ahead of the tine (the 'forward rupture distance'), is required in the analysis of soil failure problems. Several researchers have investigated the way in which the soil fails ahead of the tine (e.g.; Payne, 1956; O'Callaghan et al, 1964, 1965; Reece 1965; Hettiaratchi et al, 1966; Godwin and Spoor, 1977 and Stafford 1979), but all these researches were conducted for a soil surface with no irregularities, and no mention is made of what would happen if the soil immediately ahead of the tine presented some irregularities. Payne (1956) reported that the true surface of soil failure is the one which gives the Passive Earth Pressure its minimum value.

The objective of this project is to investigate and explain the dynamic behaviour of the trenchless drainage implement when working in soil with an uneven soil profile, based on the principles of soil mechanics. Since that requires a knowledge of the failure plane ahead of the tine, tests where conducted to see the effect of the soil profile in the rupture distance ratio.

4.3.3.2 Glass soil bin tests

Godwin and Spoor (1977) measured the rupture distance ratio in a glass sided box, and reported that the results were not significantly

different, at 95% confidence level, from those made in a normal large soil bin filled with similar soil. This indicated that soil/glass friction had not significantly affected the failure pattern.

Therefore, tests, to evaluate the rupture distance ratio, were conducted in a small glass sided soil tank, which was available in the soil physics laboratory. The soil was packed in a similar way as that described in section 3.3 for the normal large soil bin, and when a different soil profile was required the soil surface was cut to give the desired variation. The trenchless tine was replaced by a 45^{o} rake angle tine 6.7 mm wide with a relieved bottom. The reason for this replacemnt was that using this technique only half of the soil failure can be observed, consequently the disturbance produced by the experimental tine width is equivalent to the soil failure caused by a tine with the double width in the field.

Tests were conducted for three different types of soil surfaces: flat, step and sinusoidal inputs. The results are presented below, and the tests for a flat and step soil surface profile are illustrated in Fig. 4.19, and in Fig. 4.20 are the ones for a sinusoidal soil profile.

The nature of the failure mechanism was recorded using a video apparatus. The video tape was studied latter and the length of the forward rupture distance and the angle of the failure plane measured at both slow replay and static. In addition the pattern of the failure plane was copied onto an acetat film on the glass plate.

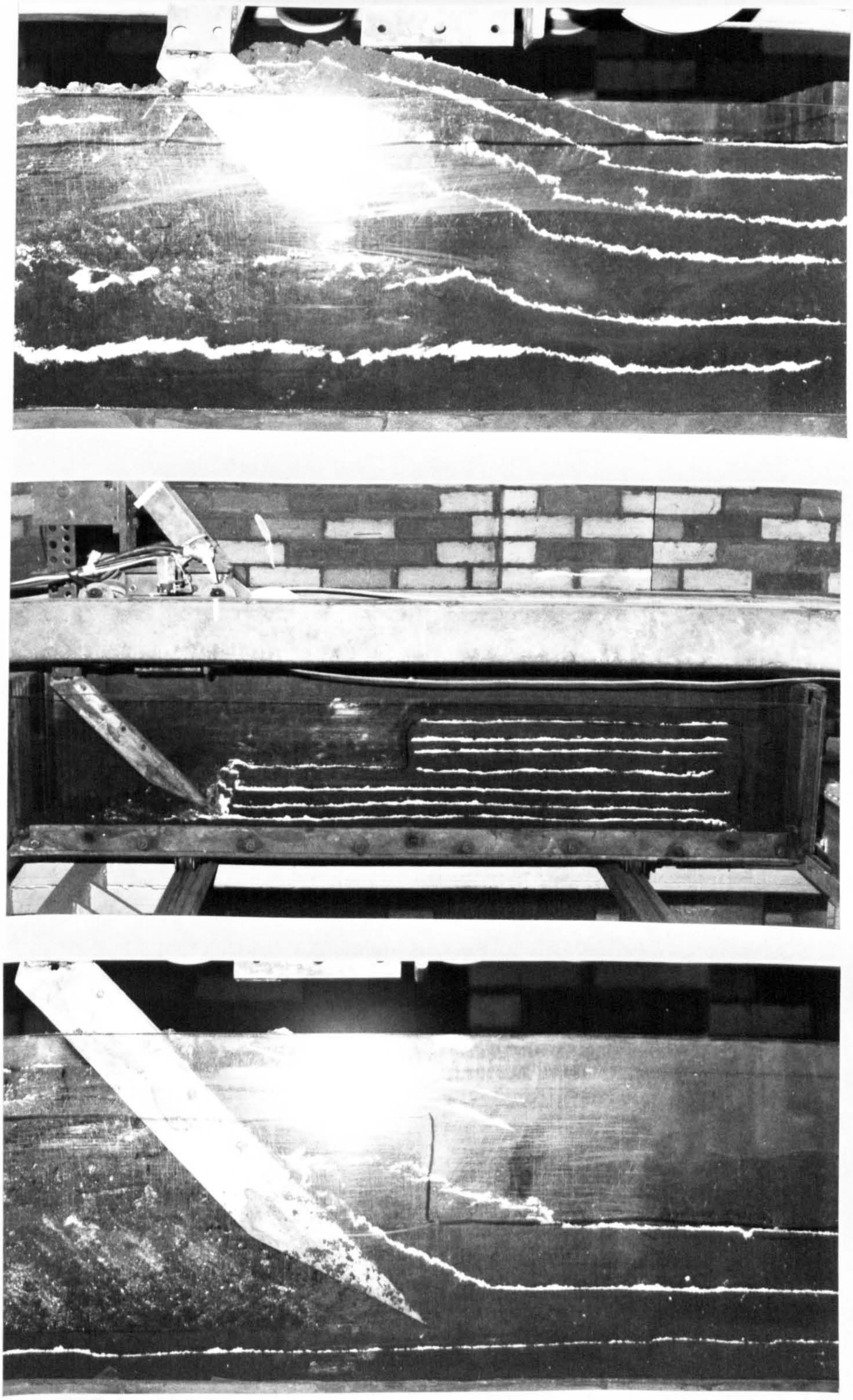

FIG. 4.19 Glass sided soil tank. Top: shear plane in a soil prepared with a flat surface profile. Middle: step input soil profile. Bottom: shear plane pattern in a step input soil profile

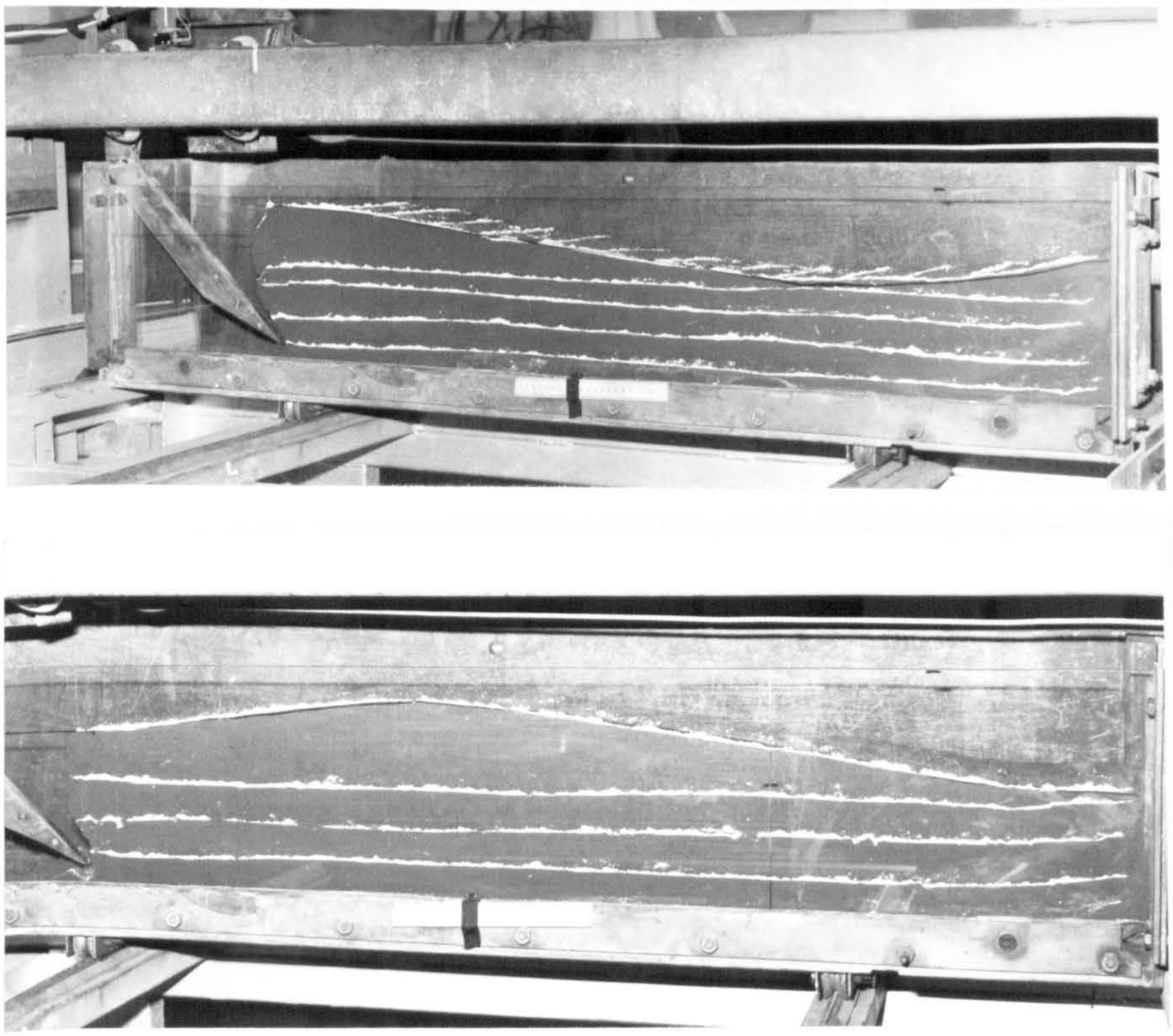

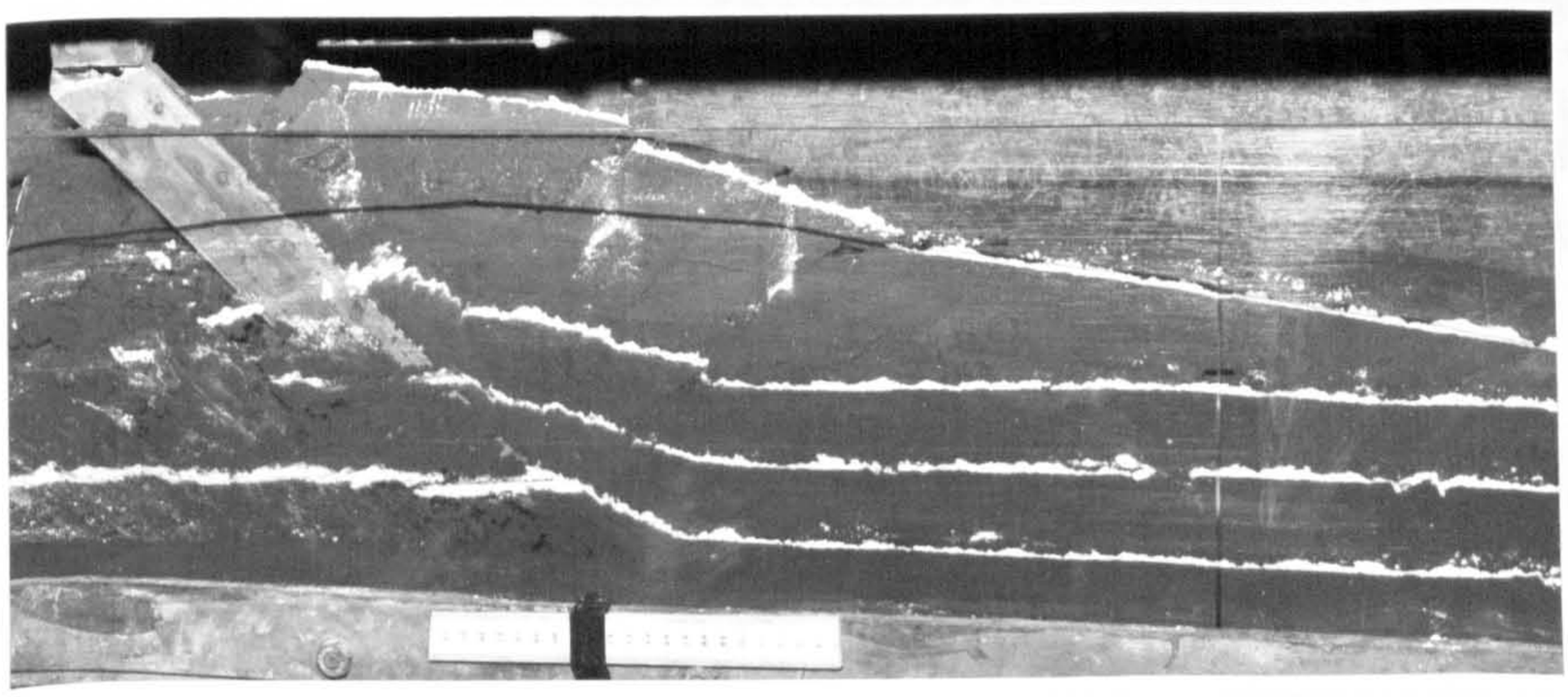

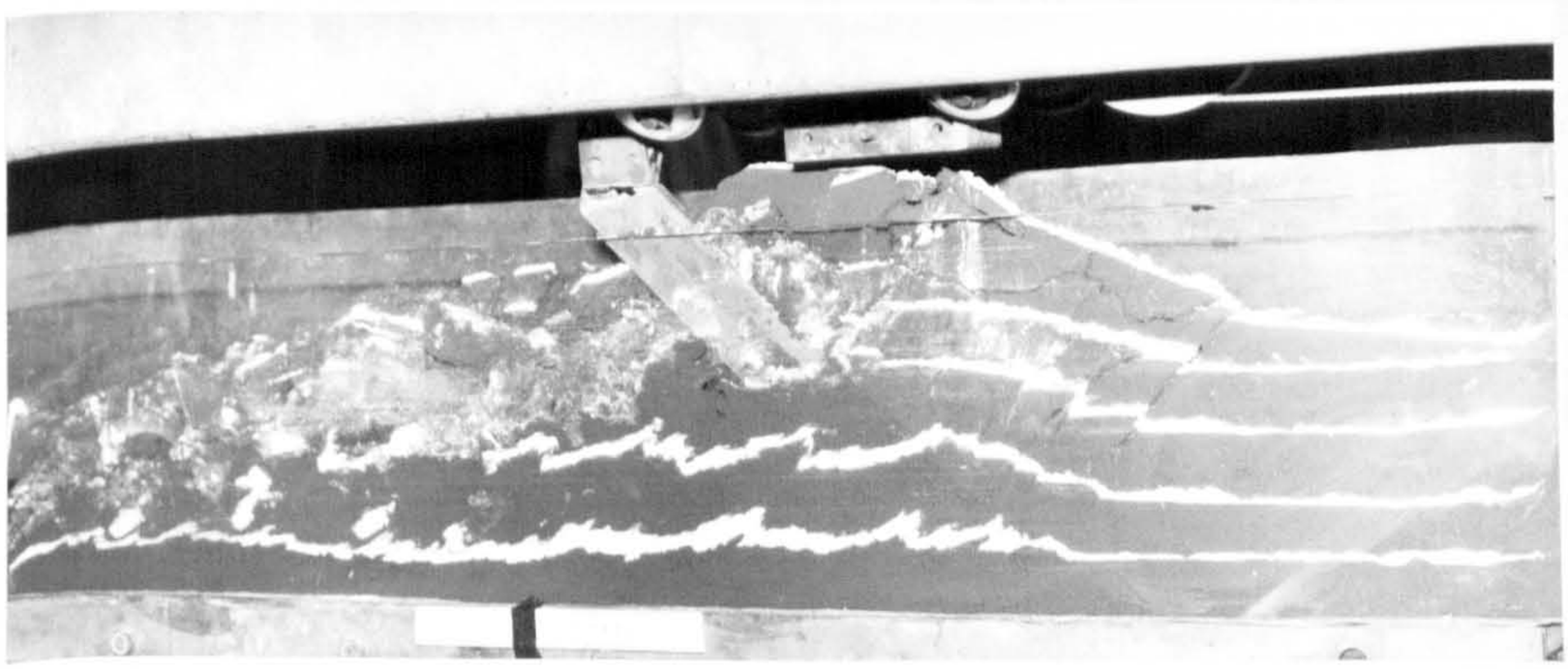

FIG. 4.20 Glass sided soil tank, with a sine wave soil profile. (a) and (b) soil preparation, (c) and (d) soil shear plane

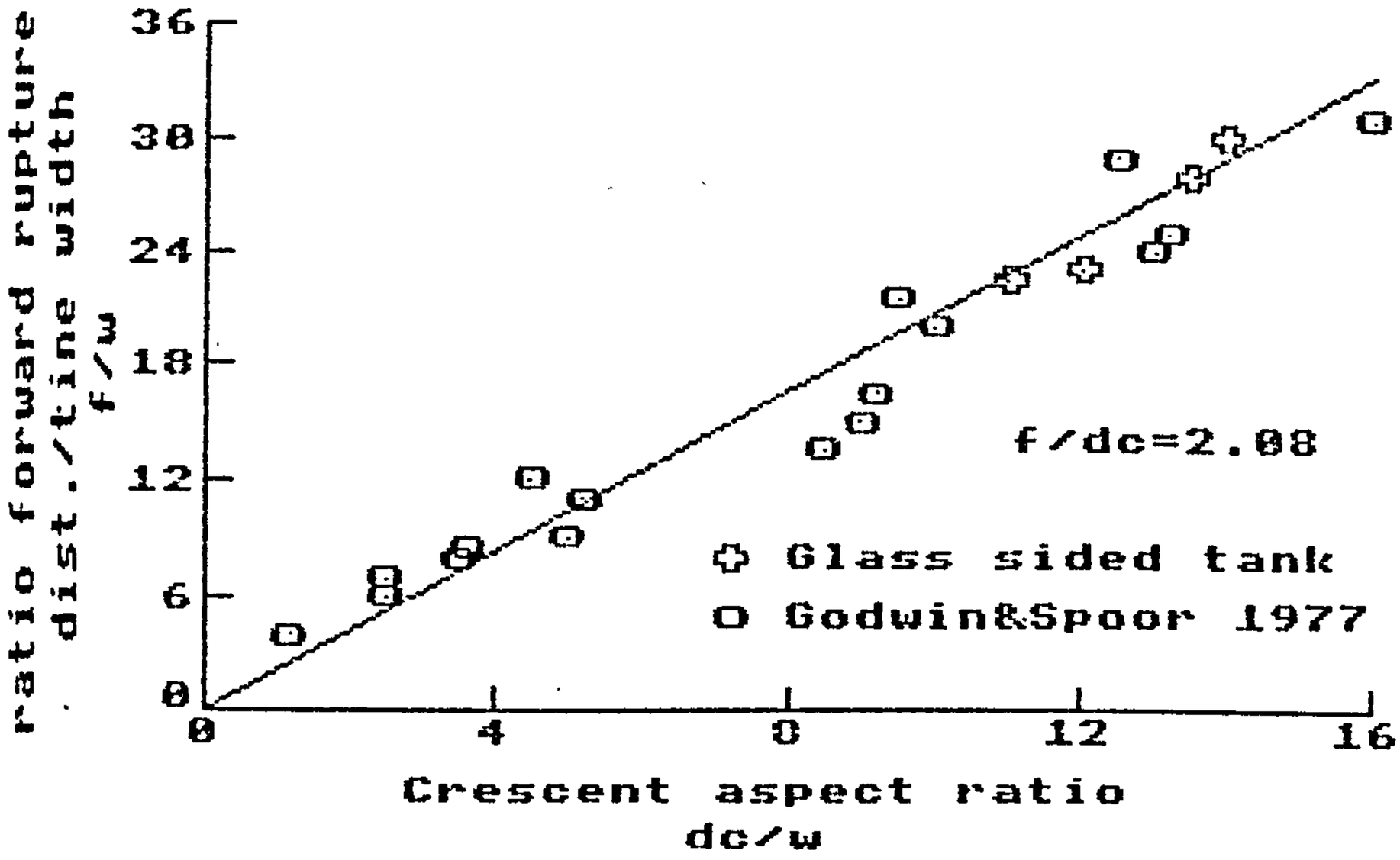

FIG. 4.21 Relationship between the ratio of the foward rupture distance/tine width and crescent aspect ratio for a 45^{0} rake angle, working in a flat surface soil profile

i) Flat surface

The results obtained from tests in the glass sided soil bin prepared with a flat surface showed that the length of the forward rupture changes with changes in the depths of work. However, as shown by Godwin and Spoor (1977), when the ratio of the forward rupture ratio/tine width is plotted against the tine crescent aspect ratio (dc/w) they have a linear relationship. Therefore, Fig. 4.21 shows the data obtained in these tests compared with the results obtained by Godwin and Spoor (1977). The close agreement between the two sets of data gives confidence in the technique used to measure the rupture distance.

ii) Step input soil profile

Tests were conducted with the soil surface prepared with different heights of the step and for implements running at different depths. Fig. 4.22 illustrates the way in which the soil fails and this is explained below:

1) step upwards

a) At tine positions where there are no soil irregularities in the plane formed between the failure plane **ab** and the tine face **ac**, (i) and (ii), the failure plane behaves as for a flat surface, because there is no reason for it to change. The angle β is constant and independent of the depth of work, but it is possible to observe in those tests that the critical depth is dependent on the depth of work.

b) As the tine approaches the step, (iv), and b coincides with e, the plane of failure starts to change. The plane of failure tends to be the one of least resistance and that is the plane formed by angle β'. The angle between the failure plane and the horizontal line will continue to increase, (v), until the plane formed between the critical depth and the bottom of the step, e, is no longer the one of least resistance, then the soil will start to fail again as described in (1a), (iii).

2) step downwards

a) A similar failure pattern to the one described in (1a) is observed when the tine is far from the step. As the implement approached the step and the distance be became smaller than the step height, the soil started to fail as shown in (vi). Since this behaviour of the failure plane did not repeat for all the steps down, it suggests that the reason for doing that can probably be explained by the way in which the soil was packed, in layers of 50 mm, creating a plane of least resistance between gd, where the principal failure plane maitained the angle of inclination β.

As the tine continued to move forward and be became very small, the angle of soil failure increased to β', (vii), and then started to decrease until the normal angle β' was reestablished, (viii), after that the soil failure pattern would be similar to the one described in 1a, (viii).

iii) The sinusoidal surface

The soil was prepared with a sinewave soil profile and the tests were conducted for different depths of the implement. Fig 4.23 illustrates the way in which the failure plane behaves when there is a constant alteration in the depth of work.

When the soil depth ahead of the tine increases, i.e. there is a bump, the angle between the failure plane and the horizontal line, ϕ, has a larger value than the one measured for a flat surface, and it tends to increase as the tine moves forwards, (iii) and (iv). When the failure plane bc approaches the top of the bump and the relative depth ahead of it starts to decrease, the angle ϕ will also decrease, (v), and the rupture distance will increase, and it will continue to do so, (i) and (ii), until the soil ahead of the plane bc starts to increase its relative depth again, (vi).

So, it was possible to observe in these tests that the failure plane is constantly altered and adapts itself to the line of least resistance for each position of the tine in relation to the wavelength.

The results of these tests for step soil surface profile and sine wave profile are presented in the next chapter. They are compared in Tables 5.1 and 5.2 with the results obtained from a theoretical approach to the problem, in order to predict the rupture distance ratio. See section 5.3.4.

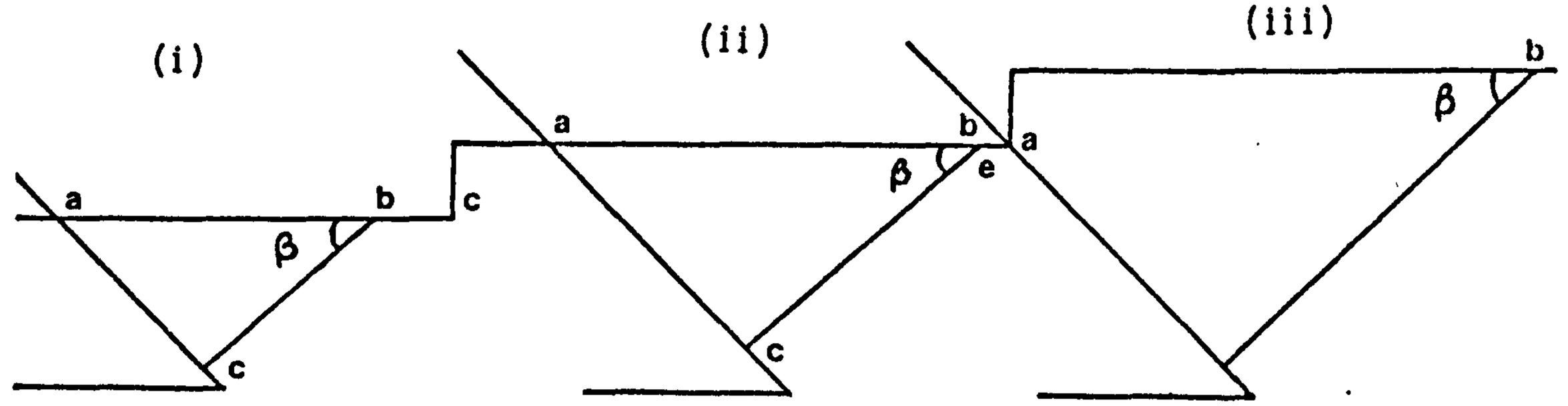

FIG. 4.22 The effect of the step soil profile in the angle of inclination of the shear plane

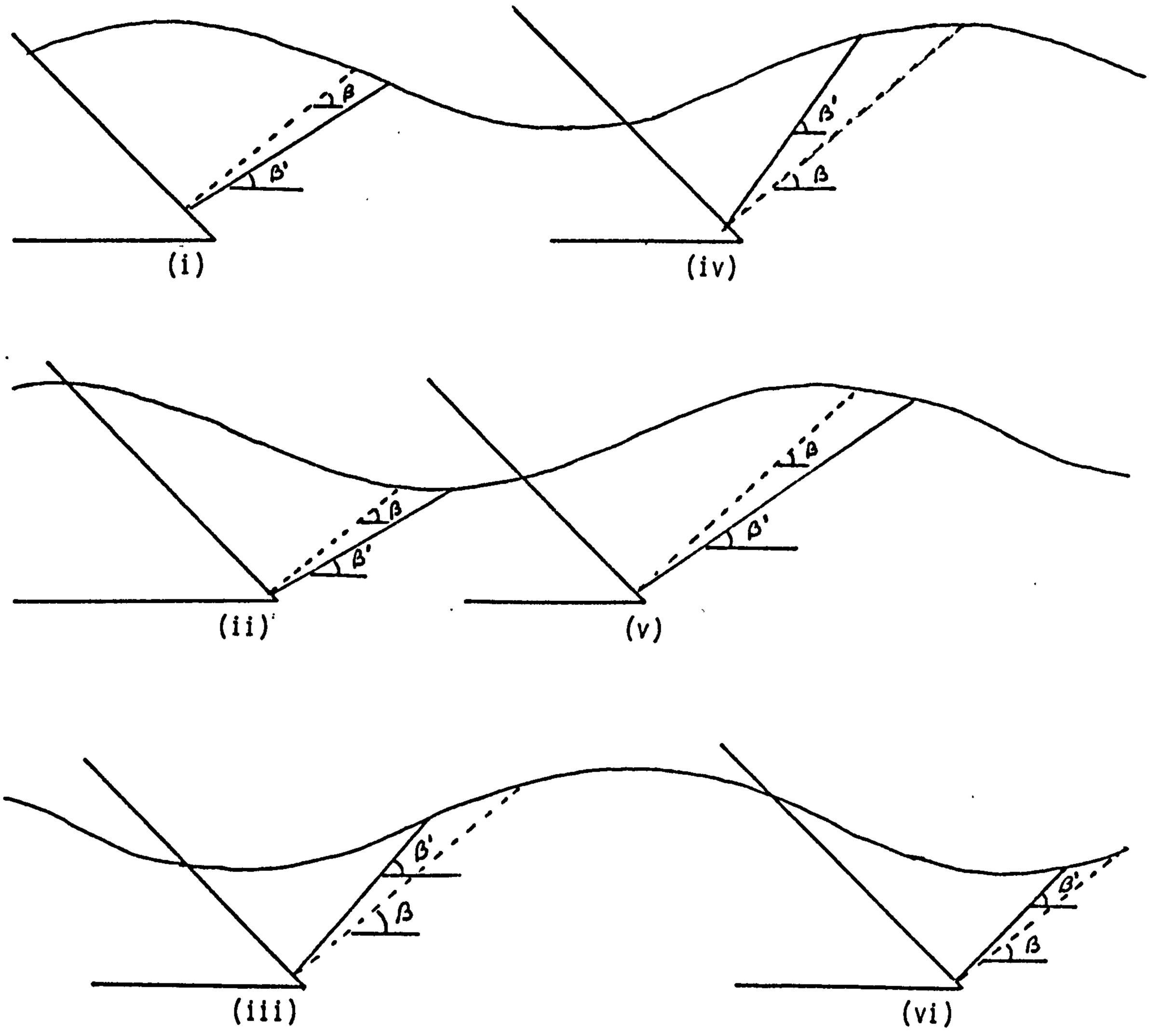

FIG. 4.23 The effect of a sinusoidal soil profile in the angle of inclination of the shear plane. (β) the angle of the shear plane in a flat soil surface. (β') the angle of the shear plane in a sinusoidal soil profile

4.3.4 Conclusion

Based upon the results of this study, it is possible to conclude the following:

i) The restricted motion study proved that soil reaction forces on the tine are potentially large when it is turned backwards. These extreme forces are not present in the dynamic situation, basically because the implement has a degree of freedom in the vertical direction, and when any unbalanced force is generated on the bottom plate, it forces the implement to move upwards, and in so doing that compensates the forces and moments again.

ii) The equation presented by Godwin and Spoor (1977) and Godwin et al (1984) for the calculation of soil forces acting on narrow tines predicts the forces acting on the face of the implement very satisfactorily. Although this model was not developed for an implement working in a dynamic situation, it covers the major part, but there are other forces involved in the system, which requires the development of equations to enable full predictions to be made.

iii) The motion of the implement is heavily damped, as predicted by Singh, and there is no significant difference in the response of the implement between the upwards and downwards movement of the tine, where the force response seems to obey a similar function.

iv) The effect of the moment of inertia of the system is very small and can be neglected in further calculations.

v) The soil shear strength has a great effect on the soil reaction forces, but very little change has been observed between the original equilibrium depth and the final one. The reason for that was explained to be due to the fact that tines with 45^{o} rake angle present little difference in the ratio of change in the horizontal and vertical forces caused by alteration of the soil properties.

vi) The size of the crescent failure ahead of the cutting blade changes when the soil surface profile is irregular. The shear plane tends to be the one which gives the least resistance to the Passive Earth Pressure.

CHAPTER 5

THEORETICAL ANALYSIS

5.1 Introduction

The aim of this investigation was to study the soil reaction forces affecting the dynamic response of a long floating beam trenchless plough and, based on this study, develop a mathematical model to simulate its response when working over an uneven field. The analysis of the implement behaviour in this chapter was based on a trenchless plough submitted only to the soil reaction force, the weight of the system and the pulling force of the carriage. The plough adjusts itself in the vertical plane under the net influence of these forces and it has no other external force to help it to penetrate, raise or maintain its equilibrium.

To investigate the influence of an uneven soil profile on the behaviour of the implement or the movement of the hitch-point over this surface, three types of soil profile and hitch-point movement were studied; horizontal level,and step and sinusoidal inputs. The reason for the selection of these profiles was because they permit a much simpler mathematical analysis of the situation and, at the same time, represent a wide range of field conditions.

As a result of the investigation explained previously (Chapter 4), where some aspects of the implement behaviour were revealed, the following assumptions could be made:

a. the implement achieves its desired condition of equilibrium when there is no movement in the vertical direction as the plough moves forward. As this position is reached, the resultant of its weight and soil forces pass through the point 'O' and its angle is the same as the 'free-link' (Fig. 5.1).

b. for each position of the hitch-point there is one equilibrium position of the implement, which is the function of the geometric configuration of the system and soil condition.

c. the effect of the inertia forces could be neglected, without affecting the results of this analysis.

5.2 Mathematical Analysis

The objective of this project was to estimate the path of the implement when there was an alteration in the equilibrium depth caused by either soil physical alteration or hitch-point movement.

From the free-body diagram of the implement shown in Fig. 5.1 the equations for the static-state situation can be written in the following form:

$$\Sigma F_h = T_h - H_T = 0 \qquad \ldots(1)$$

$$\Sigma F_v = T_v - V_T - mg = 0 \qquad \ldots(2)$$

$$\Sigma M_o = (mg)a + V_t e - H_t b' = 0 \qquad \ldots(3)$$

In the dynamic situation any alteration in the soil condition or other factors, which could induce a change in the soil reaction force would consequently alter the magnitude and direction of the resultant force, R. Since the forward displacement of the implement is slow, the assumption that the changes in the hitch-point cause an instantaneous reaction in the point **'O'** can be made, (i.e. $\ddot{O}=0$), with no effect on the dynamic analysis of the implement response. Then the principle of angular momentum can be applied:

$$M = I \frac{d^2\theta}{dt^2} \qquad \ldots(4)$$

Considering the velocity diagram of the system, Fig. 5.2, for a small value of **'θ'** it is acceptable to take the approximation $\cos\theta = 1$, $\sin\theta = 0$ and $\tan\lambda = \lambda$, and the following equations could be written

$$\tan \lambda = \frac{l\ d\theta/dt - v \sin\theta}{v \cos\theta}$$

$$\lambda = \frac{l}{v}\frac{d\theta}{dt} \qquad \ldots(5)$$

Following the work presented by Reece et al (1966), and assuming a linear relation between the torque and deflection is assumed where

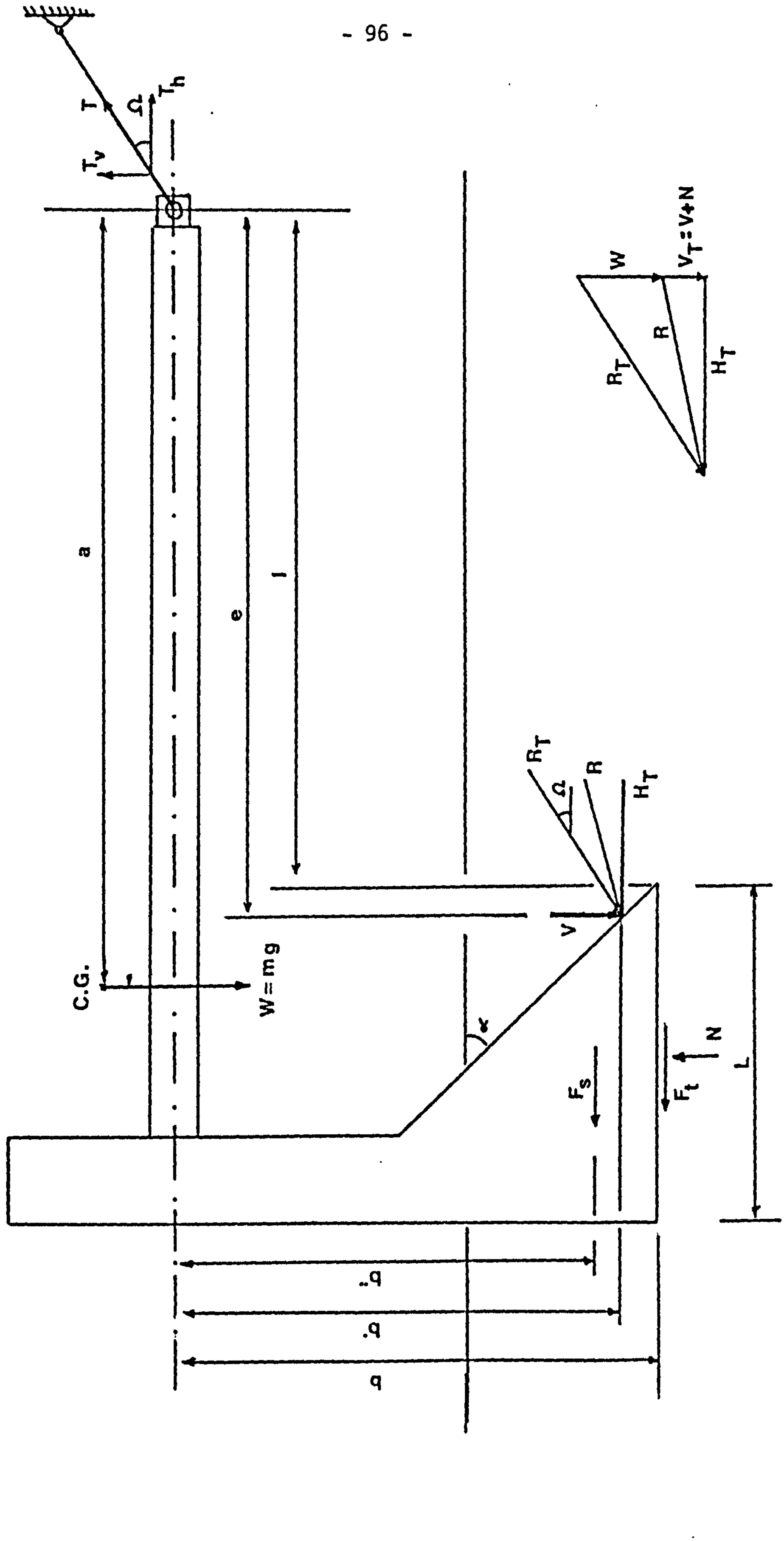

FIG. 5.1 Free-body diagram

$$M = -K(\theta + \lambda) \qquad \ldots(6)$$

Substituting equations (4) and (5) into (6) leads to:

$$\frac{d^2\theta}{dt^2} + \frac{lK}{vI}\frac{d\theta}{dt} + \frac{K\theta}{I} = 0 \qquad \ldots(7)$$

which represents damped harmonic motion. As has been reported by several researchers; (Reece et al 1966, for a simple tine engaging tool; Cowell 1976, for the mouldboard plough; Fouss 1971, for the mole plough; and Singh 1982, for the trenchless plough) and confirmed in the previous chapter, soil engaging implements usually have a very large damping constant, therefore the inertia force becomes relatively insignificant, and can be neglected.

So, the solution for equation (7), wich is dependent upon the magnitude of the damping coefficient, and in this case greater than 1, has the classical solution (Thomson, 1973) represented in the form of:

$$\theta = \theta o \exp(-v/l)t \qquad \text{or}$$

$$\theta = \theta o \exp(-s/l) \qquad \ldots(8)$$

where s is the travelled distance.

From the practical point of view there is more interest in predicting the path of the implement than in its angular deflection, so equation

(8) should be extended. Fig. 5.3 shows the implement out of equilibrium after the hitch-point has been raised. The vertical displacement due to the change in the hitch-point position can be expressed by

$$\Delta d = l \tan \theta \qquad \ldots(9)$$

Assuming $\tan\theta = \theta$ for small values of θ, and substituting for θ in equation (8), gives:

$$\Delta d/l = \theta o \exp(-s/l) \qquad \ldots(10)$$

and Fig. 5.3 shows

$$\theta o = (do - de)/l$$

which becomes

$$\partial \Delta d = (do-de) \exp(-s/l) \qquad \ldots(11)$$

This is a similar equation to the one presented by Cowell and Sial (1976) for the penetration of the mouldboard plough, where it could be used only to predict the path of the implement in the vertical and horizontal direction between two experimentally measured positions of the implement.

To solve equation (11) it is necessary to estimate the equilibrium depth

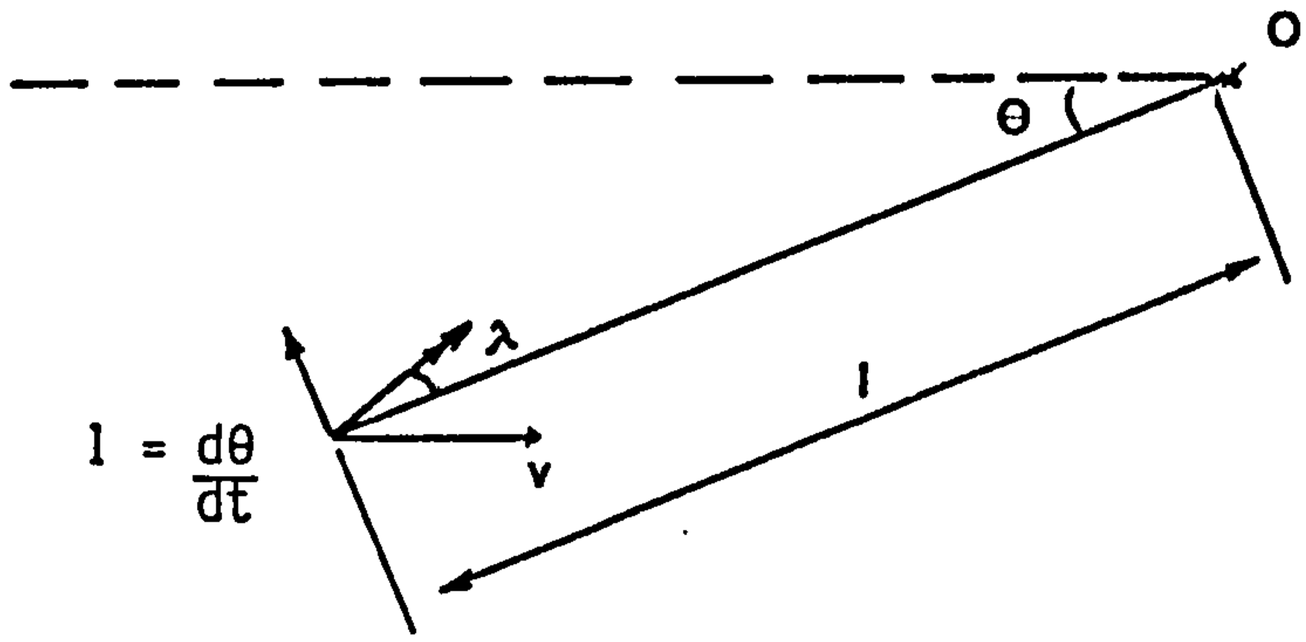

FIG. 5.2 Velocity diagram

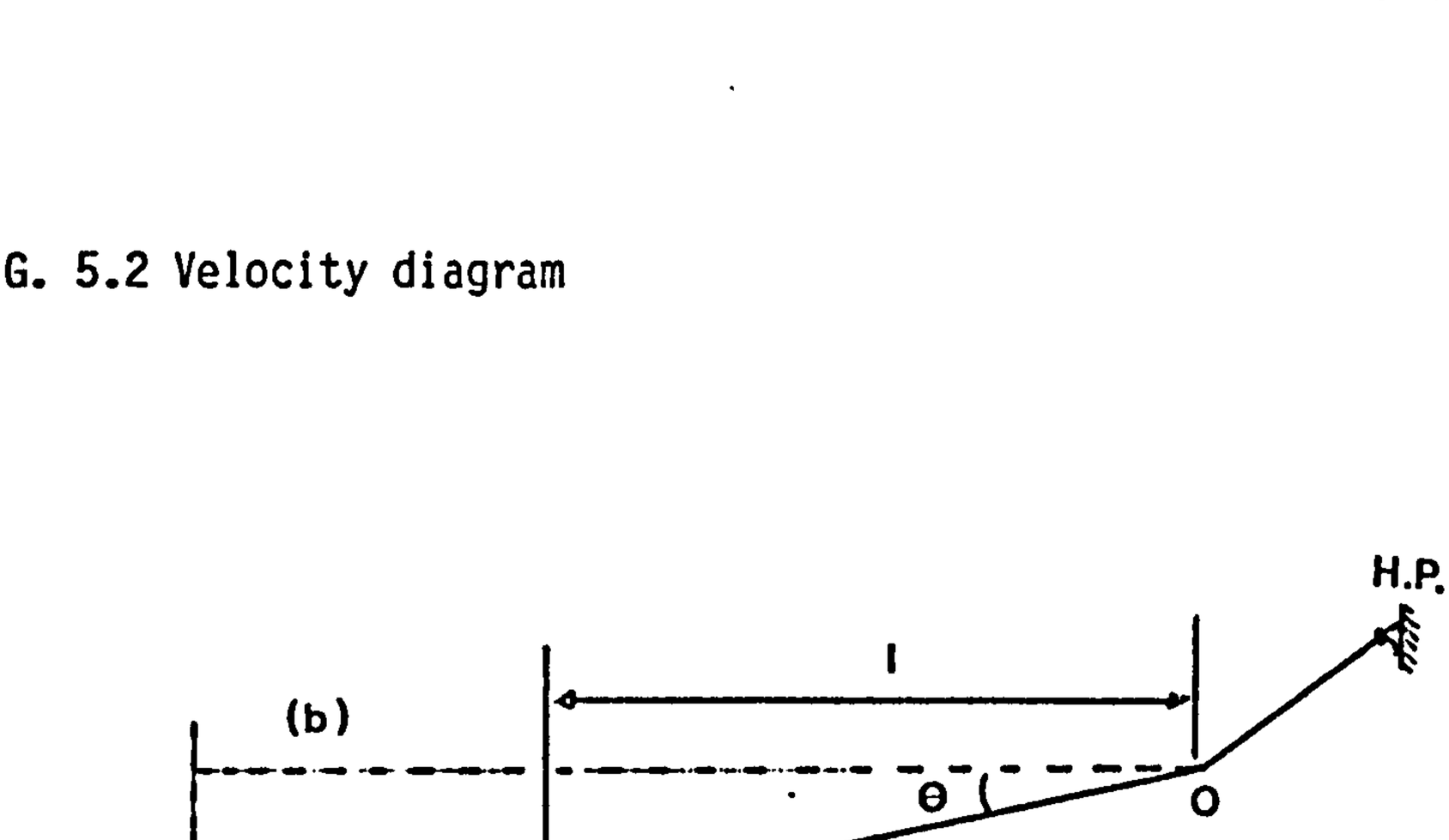

FIG. 5.3 Vertical displacement of the implement due to the change in the height of the hitch-point (a), and after the equilibrium is restored (b)

of the system at any point, which is dependent on the soil condition, and the geometric configuration of the implement system, and consequently it is also dependent on the soil reaction forces as is proved in the section below.

5.3 Forces Estimation

From Fig. 5.1 the equations for the equilibrium condition of the implement can be rewritten in a more convenient form :

$$F_h = 0 = H_T + F_s + F_t + T \cos \Omega \qquad ...(12)$$

$$F_v = 0 = V + W - N - T \sin \Omega \qquad ...(13)$$

$$M_0 = 0 = W\,a + V\,e - N(l + L/2) - F_t\,b - F_s(b - \tfrac{1}{3}\,d) - H_T\,b \qquad ...(14)$$

with the following assumptions for terms in the above equation 14 (not previously discussed):

i) The support force **N**, acting on the bottom of the implement is considered to be a uniform distributed load, because the bottom of the tine is in contact with the soil independent of the tine angle. That is the reason why the distance between the point of application of this force is considered to act midway along the base, this argument being further supported by the fact that any error in this assumption is proportionally reduced because of the length l, so any slight alteration in the position of **N** in relation to the bottom plate will have a minimum effect on the total moment about the point **'O'**.

ii) The force F_s is the result of adhesion and friction of the soil and the side plates in a disturbed and consequently cohesionless soil. Therefore it can be considered that F_s is distributed along the depth of work dependent on the normal pressure, which increases with the depth of work, and area of contact between the soil and the tine. Since the tine has a triangular shape, the point of application of the force F_s is at three quarters of the depth of work (Fig. 5.10).

iii) The front face of the trenchless plough corresponds to a narrow tine. Therefore to estimate the magnitude of the forces H, Q and V, which are acting on the face of the tine, the mathematical solution for calculating the forces on the front face of a narrow tine with a relieved base, available from Godwin and Spoor (1977) and Godwin et al (1984), can be applied.

The theory of narrow tines identifies two zones of soil failure. The crescent zone, where the displaced soil has forwards, sideways and upwards components, and the lateral failure; a lower zone where the displaced soil has components in the direction of travel and sideways. The depth where the division between the two zones occurs is called critical depth.

5.3.1 The crescent failure zone

In the crescent zone a simple passive failure is considered to occur,

where the magnitude of the resultant passive force can be estimated from the equation of plane failure in front of a wide cutting blade, using the equation proposed by Hettiaratchi et al (1966, 1974).

$$P = (\gamma d^2 N\gamma + cdNc + cadNa + qdNq) \qquad ...(15)$$

Based on this equation, Godwin and Spoor (1977) derived one equation to predict the soil forces reaction acting in the horizontal and vertical direction. Later, Godwin et al (1984) extended the model based upon a modification to the upper crescent soil failure. A more appropriate expression for the crescent boundary was proposed, Fig. 5.4, where

$$r = f - (f - s) \sin^2 \rho \qquad ...(16)$$

For tines with predominant crescent failure, (the trenchless tine should work at a depth very close to the critical depth, Spoor and Fry (1983), Payne and Tanner (1959) showed that:

$$s = d \qquad ...(17)$$

Substituting this into the previous equation, Godwin et al (1984) obtained the following results:

$$H = (\gamma\, dc^2\, N\gamma + c\, dc\, Nc + q\, dc\, Nq)\, [w + dc(m - \tfrac{1}{2}(m - 1))]$$
$$\sin(\alpha + \delta) + ca\, w\, dc\, (Na \sin(\alpha + \delta) + \cos\alpha) \qquad ...(18)$$

which could be extended to the vertical direction

$$V = (\gamma\, dc^2\, N\gamma + c\, dc\, Nc + q\, dc\, Nq)\,[w + dc(m - \tfrac{1}{3}(m - 1))]$$
$$\cos(\alpha + \delta) - ca\, w\, dc\, (Na \cos(\alpha + \delta) - \sin\alpha) \qquad ...(19)$$

The N factors in each of the terms are considered dimensionless numbers and their magnitudes, which are dependent upon the magnitude of λ, ϕ and δ, can be calculated using the graphical solution presented by Hettiaratchi et al (1966) and presented in Appendix 5.

5.3.2 The lateral failure

In the zone below the critical depth, the sort of failure which exists, is in two dimensional ways in the horizontal plane, and it is independent of the rake angle of the tine. This kind of soil failure is similar to that of a deep narrow footing orientated at 90^o to the normal direction of application, for which the equation given by Meyerhof (1951) is quite acceptable to predict the forces. Based on this solution Godwin and Spoor (1977) presented the following equation to estimate the forces in the lower zone, between the limits of the critical depth and the total working depth.

$$Q = w\, c\, Nc'\, (d - dc) + 0.5\, Ko\, \gamma\, w\, Nq'\, (d^2 - dc^2) \qquad ...(20)$$

The values of Nc' and Nq' can be determined from the graph presented in Appendix 5 (Godwin, 1974).

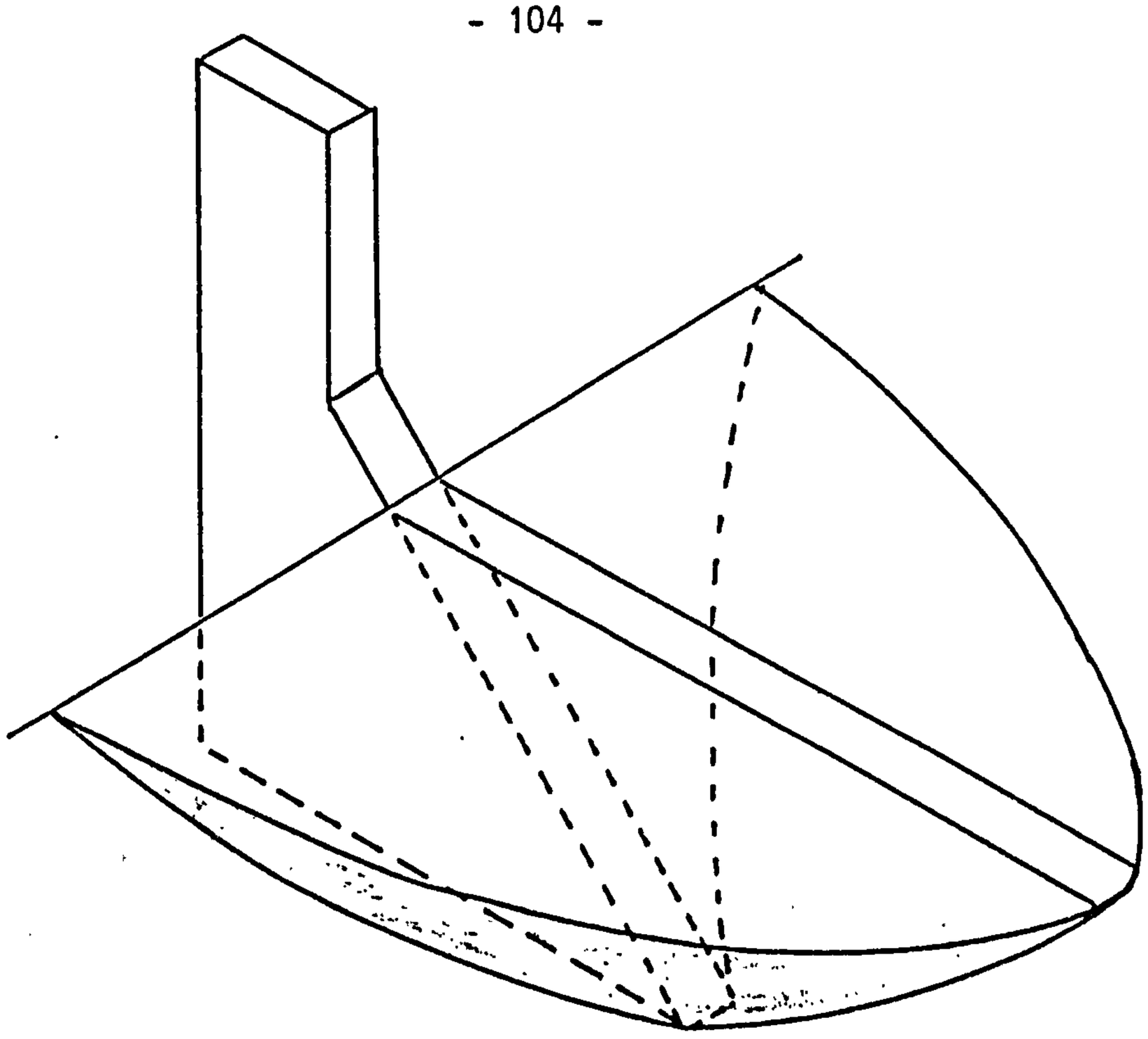

(a)

(b) (c)

FIG. 5.4 Crescent boundaries: (a) general view; (b) top view; (c) front view (Godwin et al, 1984). —— Experimental data; - - - r=f=md after Godwin and Spoor (1977); — · — · · r=f-(f-s)$\sin^2\rho$ after Godwin et al (1984)

So, the total horizontal force component of the soil reaction on the face of the tine, is given by:

$$H_T = H + Q \qquad \ldots(21)$$

5.3.3 Critical depth estimation

It is necessary to have a knowledge of the critical depth for a particular tine in a given soil to apply the equations proposed by Godwin and Spoor (1977) presented in sections 5.2.1 and 5.2.2. The mathematical solution given by Godwin and Spoor (1977) to estimate the critical depth does not give the necessary sensitivity to predict the accurate position of the critical depth, for a 45^{o} rake angle tine, therefore it could not be applied in this case.

It was then decided to use the practical solution, where the position of the critical depth can be found, using a glass soil technique. This method was used by Godwin and Spoor (1977) to estimate the critical depth in the same sand-loam soil used in this experiment. As a result of these tests they found that although the critical depth is a function of the width of the tine and depth of work, it could be represented in a function of the critical aspect ratio (dc/w) and aspect ratio (d/w). Fig. 5.5 shows the results of tests conducted by Miller (1971) and Godwin (1974). From this graph it is possible to estimate the critical depth, and this was the method used in this analysis.

5.3.4 Forward rupture distance ratio

Another requirement for using the equations proposed by the theory of narrow tines, is the knowledge of the ratio between the length of the forward rupture **f** and critical depth **dc.** To date, there is no satisfactory method for predicting the rupture distance ratio for three dimensional soil failure. Although the model proposed by Hettiaratchi et al (1966, 1967) works satisfactorily for wide tines, it gave errors up to 50% for narrow tines. Therefore, Godwin and Spoor (1977) presented a graphical solution based on experimental values to estimate the rupture distance ratio for different rake angles on a flat surface (Fig. 5.6).

The tests conducted on the soil glass sided tank, explained in the previous chapter, proved that the size of the crescent failure is irregular if the soil ahead of the tine has an uneven profile. Therefore, to be able to use the equations (18) and (19), the failure rupture distance ratio **m** had to be predicted, and for that it was necessary to know the shape of the boundary failure surface.

In order to predict the forward rupture distance the concepts explained below, developed to predict the passive force by Coulomb, were used to estimat the size of the shear plane.

The concept of passive earth pressure indicates the resistance of a mass of soil against displacement by lateral pressure, and Coulomb proposed a principle that the soil failure occurs in such a way that the Passive Earth Pressure is minimum.

Terzaghi and Peck (1967) suggested that the most likely failure pattern

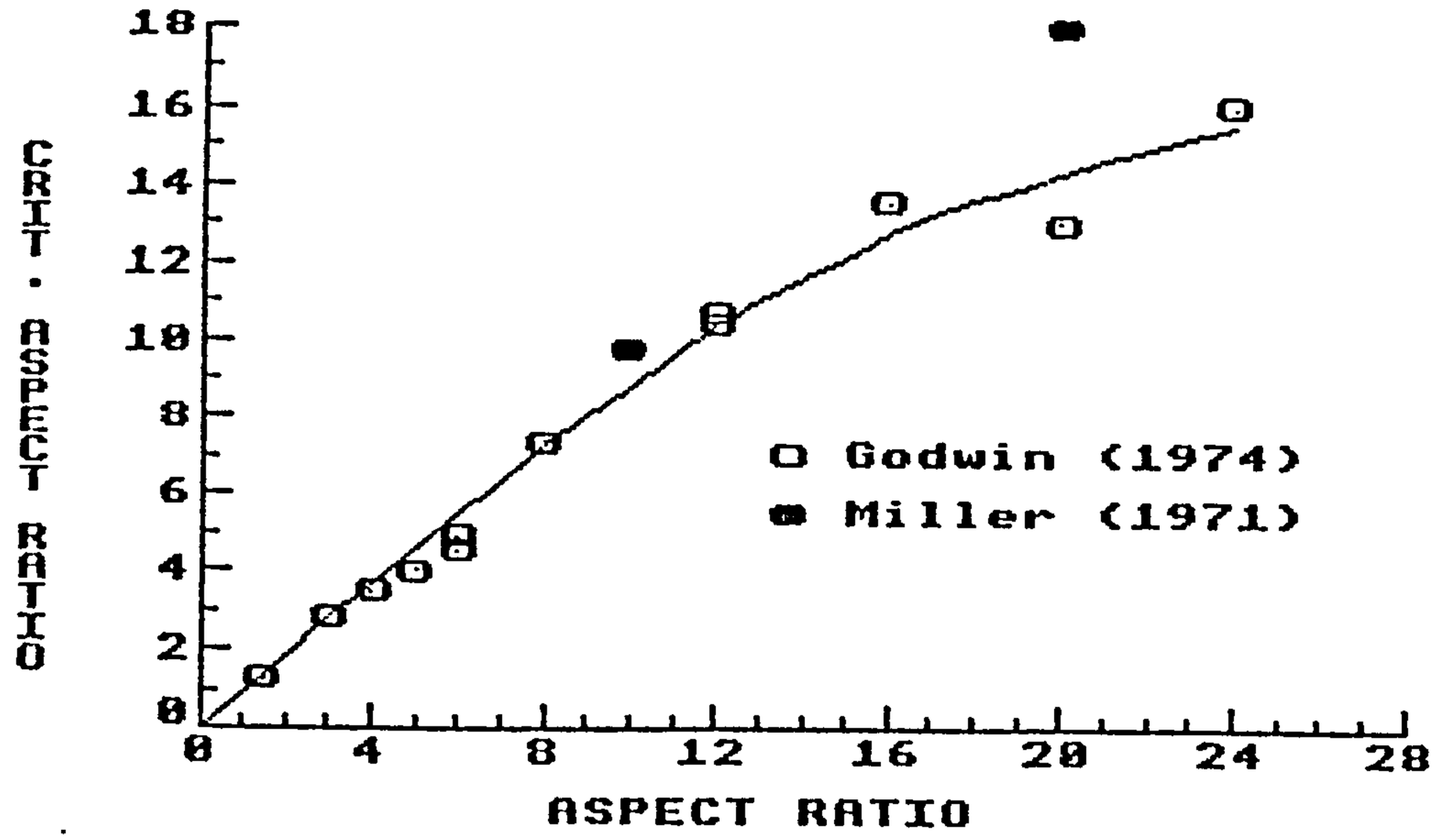

FIG. 5.5 The relationship between critical aspect ratio and aspect ratio (Godwin and Spoor, 1977)

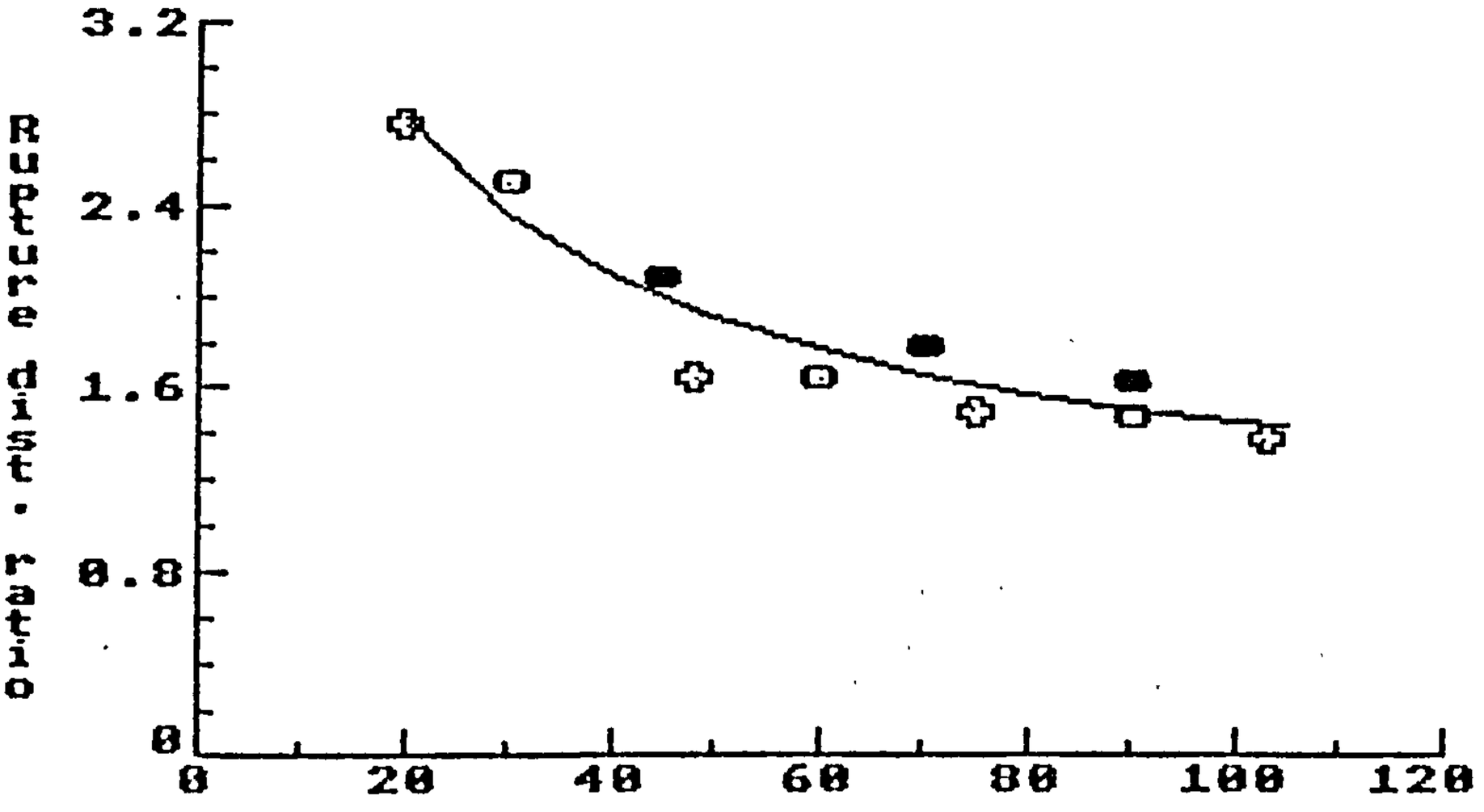

FIG. 5.6 Experimental relationship between distance ratio and tine rake angle. ● From Godwin and Spoor (1977), O from Hettiaratchi and Reece (1967), ⌖ from Payne (1956) and Payne and Tenner (1959)

for a soil under an external pressure is that shown in Fig. 5.7, for a static equilibrium situation, which includes a passive Rankine zone whose inclined boundaries rise at an angle of $45^{o} - \phi/2$ to the horizontal, and a lower boundary of the wedge-shaped zone, which is curved, located between the Rankine zone and the contact face.

Reece (1964) showed that the application of this consideration could be extended to the cutting blade problem, but that the failure zone suggested by the passive theory does not even fulfil the conditions of static equilibrium.

Considering the crescent failure zone ahead of a 45^{o} rake angle tine, and investigating only the linear section immediately ahead of the tine width, Coulombs principle can be applied, and the following analysis can be done in order to determine the length of the crescent failure.

Fig. 5.8 shows the forces acting ahead of the tine for a width equal to the blade (w). The surface of sliding in a real situation is slightly curved. Coulomb, however, computed the passive earth pressure against rough contact face on the simplified assumption that the surface is plane. If the rake angle of the tine is less then $(90^{o} - \phi)$, the failure plane is really almost straight and the error is acceptable.

The straight line BD, shown in Fig. 5.8 is arbitrarily assumed to represent the failure plane. The wedge ABD is in equilibrium under the weight W, the reaction to the resultant earth pressure P, the frictional

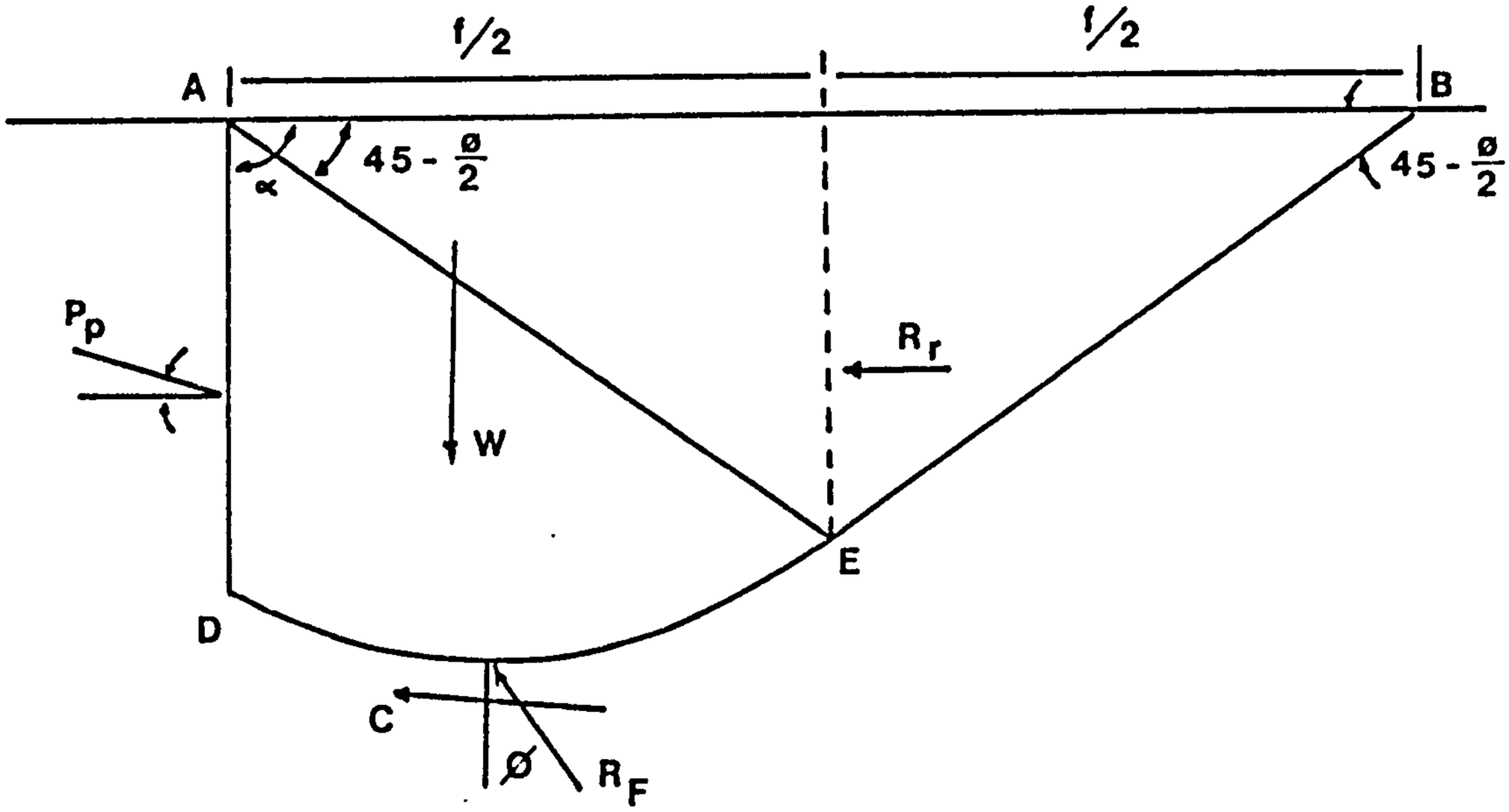

FIG. 5.7 Diagram illustrating assumptions on which theory of Passive Earth Pressure against rough contact forces is based

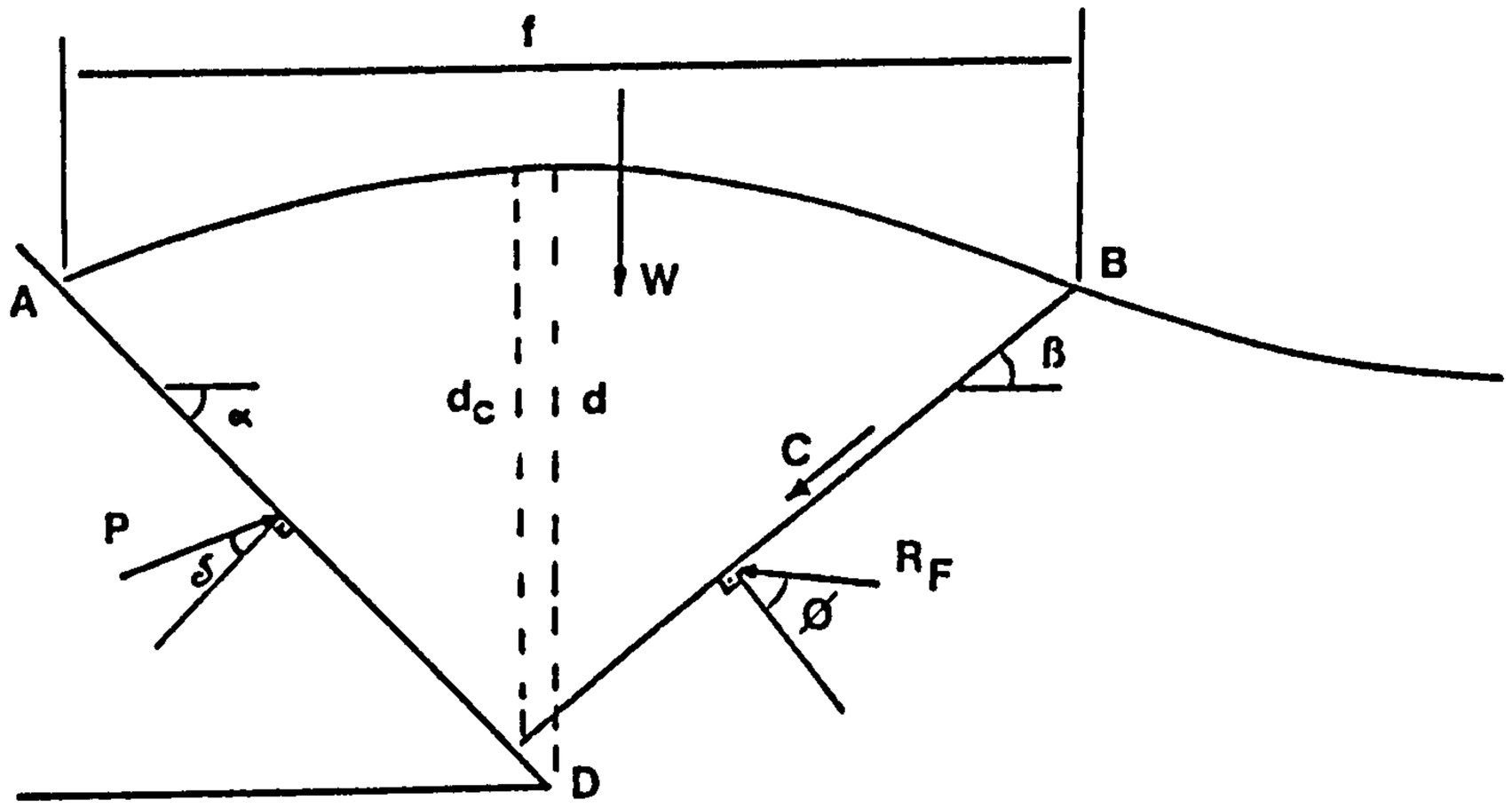

FIG. 5.8 The forces acting on the soil in the failure zone in front of a trenchless tine with a 45^{o} rake angle

reaction R_F and the resultant C of the cohesion along BD. The reaction R_F is inclined at the angle $\emptyset$ to the normal BD, because the frictional resistance is assumed to be fully developed along the surface of the plane. The forces can be resolved as follows:

i) in the horizontal direction

$$P \sin(\alpha + \delta) = R_F \sin(\beta + \emptyset) + c\, w\, BD \cos\beta \qquad \ldots(22)$$

ii) in the vertical direction

$$P \cos(\alpha + \delta) + R_F \cos(\beta + \emptyset) = (\text{area ABD})\, w + c\, w\, BD \sin\beta \qquad \ldots(23)$$

From 22 and 23

$$P = \frac{(\text{area ABD}) + c\, BD\, (\sin\beta + \cos\beta \cot(\beta + \emptyset))}{\sin(\alpha + \delta)\cot(\beta + \emptyset) + \cos(\alpha + \delta)}\, w \qquad \ldots(24)$$

$$H = P \sin(\alpha + \delta)$$

$$H = \frac{(\text{area ABD}) + c\, BD\, (\sin\beta + \cos\beta \cot(\beta + \emptyset))}{\cot(\beta + \emptyset) + \cot(\alpha + \delta)}\, w \qquad \ldots(25)$$

Since the plane BD is not necessarily the real failure plane, similar analyses are made for different planes and B is chosen for the minimum value of H. From that it is possible to calculate f

$$f = dc/\tan\alpha + dc/\tan\beta$$

and m is given by

$$m = f/dc \qquad \text{or}$$

$$m = \cot\alpha + \cot\beta \qquad \ldots(26)$$

For the uneven soil profile the computation is conducted in the same way

where the difference in the mass of the wedge **ABD** and the length of the plane **BD** is taken into account.

For the flat surface soil profile, where the experimental results of the tests conducted in the glass sided soil bin were presented in Fig. 4.20, the rupture distance ratio 'm', calculated from this technique is equal to 2.03. This value is in very close agreement with the value presented by Godwin and Spoor (1977) for tines with 45^{o} rake angle, where m was equal to 2.08.

Tables 5.1 and 5.2 present the results for the step input and sinusoidal soil profile respectively, where the experimental values can be compared with the results obtained using the technique explained above. Fig. 5.9 presents the angle of the shear plane plotted against the tine position for predicted and experimental values obtained for the sinusoidal soil surface.

Although in this case the results presented some variations, especially in the sine wave soil profile it seems to be a good approximation to evalulate the unknown value of **f**.

5.3.5 The force balance

Some other forces would still have to be calculated to complete the force balance in equations (4) to (6) .

TABLE 5.1
Effect of the step input soil profile in the shear plane angle

Distance from the step mm	angle of the shear plane measured	predicted	m f/dc
Implement depth 145 mm; step -75 mm			
300	45	44	2.036
250	--	25	3.124
220	22	27	2.930
200	33	30	2.707
150	--	38	2.271
100	45	44	2.036
Implement depth 135 mm; step -55 mm			
300	45	44	2.036
250	--	23	3.100
200	22	28	2.846
150	--	36	2.376
110	30	40	2.036
100	--	44	2.036
0	45	44	2.036
Implement depth 100 mm; step 70 mm			
200	43	44	2.036
150	45	44	2.036
100	--	44	2.036
80	55	52	1.781
50	--	61	1.554
0	40	44	2.036
Implement depth 130 mm; step 40 mm			
200	--	44	2.036
150	34	44	2.036
100	--	48	1.900
80	55	58	1.625
30	40	44	2.036
Implement depth 80 mm; step 95 mm			
200	45	45	2.000
150	--	45	2.000
100	40	45	2.000
80	45	46	1.966
40	--	61	1.550
0	45	44	2.036

TABLE 5.2
Angle of the shear plane in a soil with a sinusoidal soil surface

Depth (m)	Predicted Angle β (deg)	Experimental Angle β (deg)			mean	m -	f (m)
0.1500	41.0	38	40	--	39	2.173	0.264
0.1693	38.5	30	43	38	37	2.244	0.293
0.1838	37.5	38	--	--	38	2.235	0.304
0.1899	33.0	37	34	--	35.5	2.415	0.333
0.1862	32.5	37	30	36	34.3	2.514	0.334
0.1735	31.5	35	36	30	33.6	2.484	0.329
0.1550	30.0	35	30	--	32.5	2.598	0.323
0.1353	31.0	30	28	--	29.0	2.635	0.298
0.1192	34.5	36	41	--	38.5	2.554	0.261
0.1105	37.5	36	46	--	41.0	2.455	0.236
0.1120	40.0	41	38	--	39.5	2.329	0.226
0.1226	43.5	41	--	--	41.0	2.109	0.221
0.1401	41.5	41	45	--	43.0	2.175	0.252

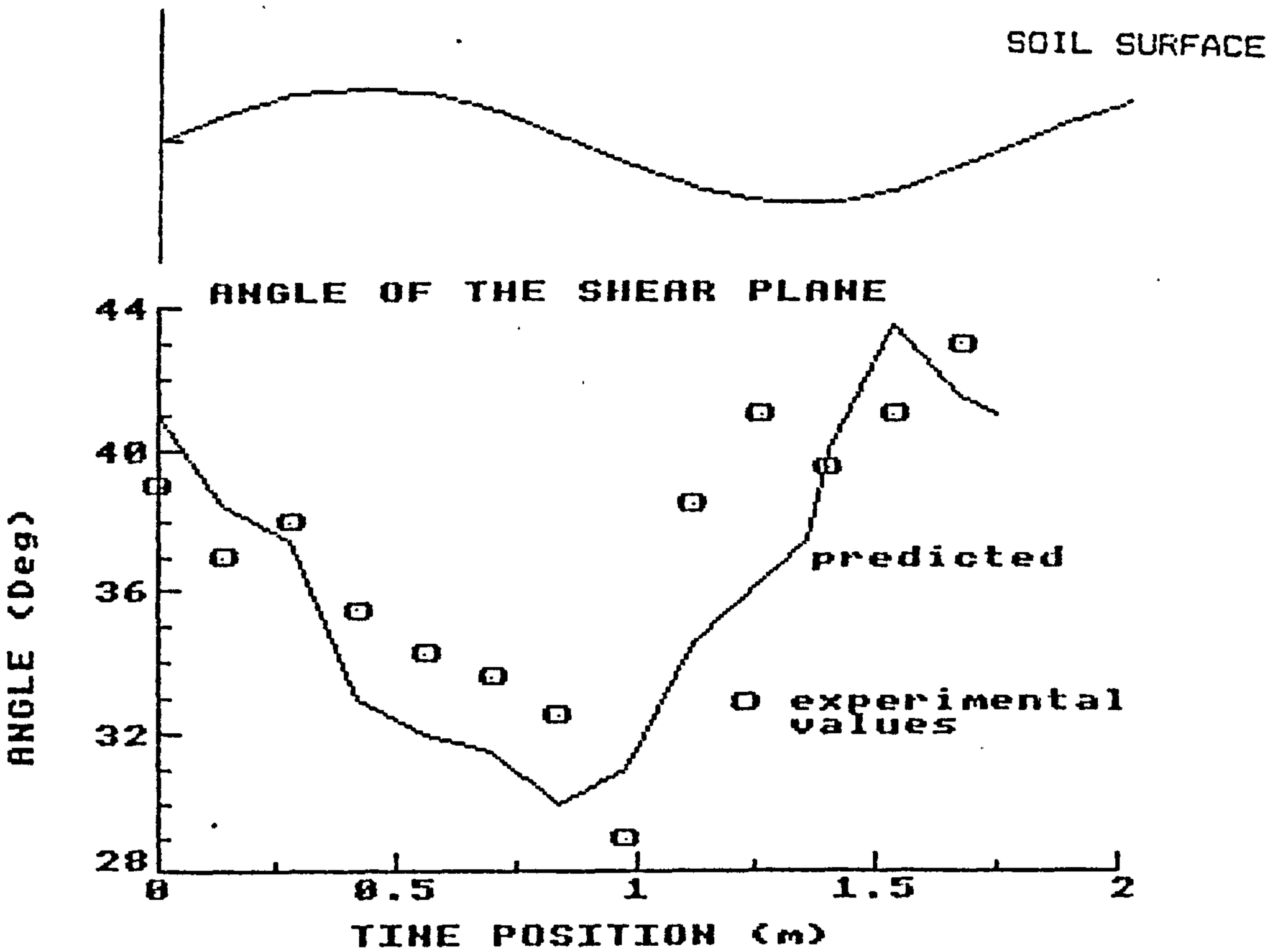

FIG. 5.9 Angle of the shear plane in relation to a sinusoidal soil surface

The value of Fs, the force acting on the side plate of the implement due to adhesion and friction can be calculated by using a solution similar to the one presented by Godwin (1974) to estimate the sliding resistance force acting on a uniform shaped tine, modified to adapt to the trenchless tine geometric shape. The force acting upon an elemental area, shown in Fig. 5.10, is given below in equation 27

$$dF_s = ca \times dz + \sigma h \times dz \tan\delta \qquad ...(27)$$

where

$$x = f(z) = (L - (d-z) \cot\alpha) \qquad ...(28)$$

and the horizontal stress is given by

$$\sigma h = Ko\ \gamma\ z \qquad ...(29)$$

then substituting (27) and (28) in (29)

$$dF_s = ca\ (L - (d-z) \cot\alpha)\ dz + Ko\ \gamma\ z \tan\delta\ (L - (d-z) \cos\alpha)\ dz \qquad ..(30)$$

F_s can be calculated by integrating equation (30), and the total sliding resistance force for a trenchless tine of bottom length L, working at depth d, can be represented by

$$F_s = ca\ d\ (2\ L - d \cot\alpha) + \tan\delta\ Ko\ \gamma\ (L\ d^2 - \tfrac{1}{3}d^3.\cot\alpha) \qquad ...(31)$$

The value of Ft the friction force between the bottom plate and the soil can be determined by:

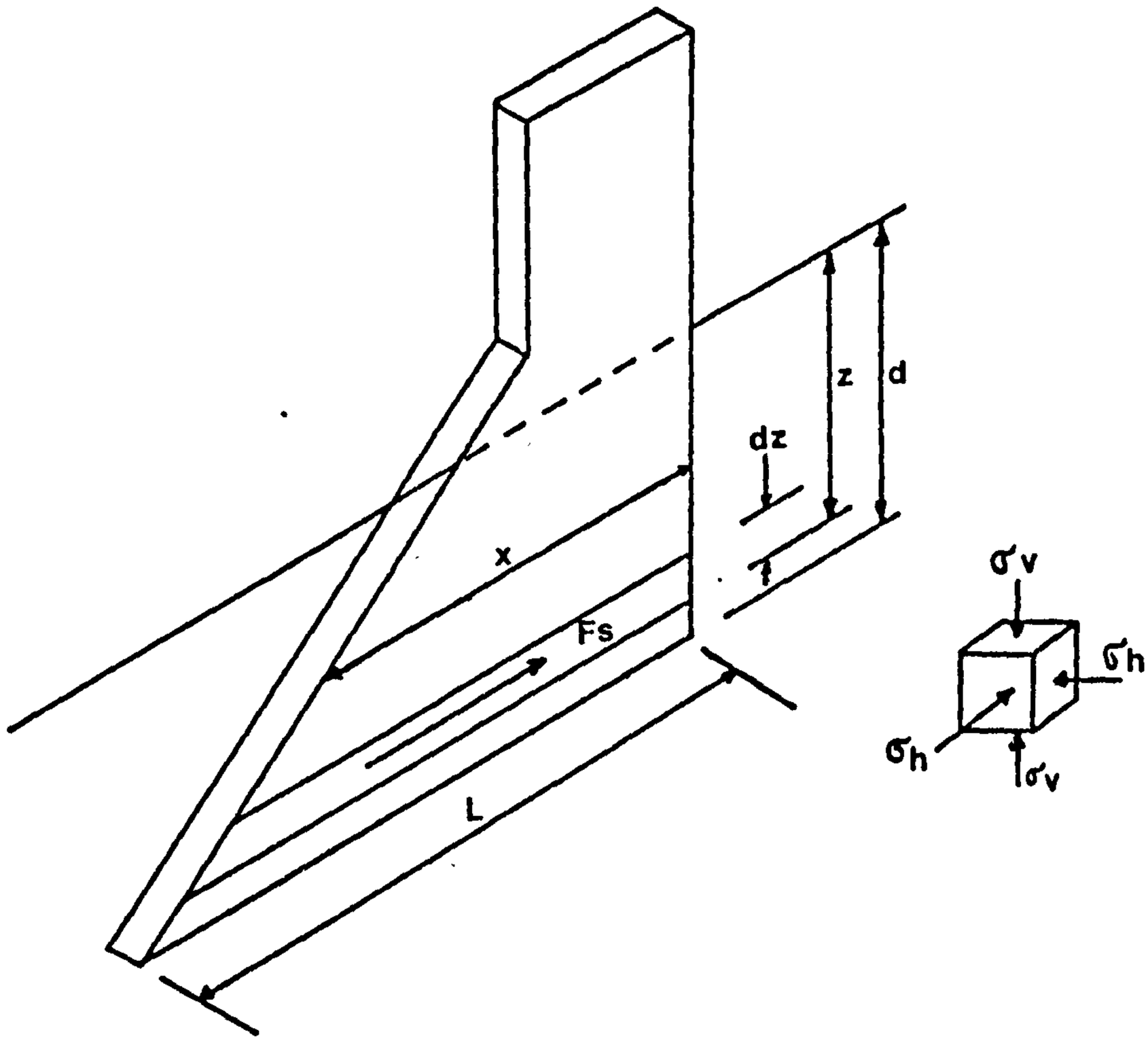

FIG. 5.10 Lateral force acting on the side plate

$$F_t = N \tan \delta \qquad \ldots(32)$$

To solve equation 14 the values of the moment arm have to be known. Therefore, a relation between these variable length arms and the fixed points, the hitch-point position, h1, and distance where the implement is fixed to the beam and its base, b, should be drawn. The value of the centre of gravity, a, can easily be determined experimentally or calculated from the geometric configuration of the system.

Results presented in the previous chapter showed that the centre of resistance of the soil reaction forces on the tine face, is dependent on the actual depth of the implement, but the ratio cr/d can be considered constant, with the average value of 0.88. So the distance between the hitch-point and the centre of resistance, b' in the vertical direction and e in the horizontal direction, can be expressed by the equations below

$$b' = b - (0.88d) \qquad \ldots(33)$$

$$e = l - (L - 0.88d \cot \alpha) \qquad \ldots(34)$$

Leaving only three values unknown, N, T, and Ω, and three equations to solve, so a Real solution is possible from the equations

$$\Sigma F_h = 0 = H + Q + F_s + F_t + T \cos \Omega \qquad \ldots(12)$$

$$\Sigma F_v = 0 = V + W - N - T \sin \Omega \qquad \ldots(13)$$

$$\Sigma M_0 = 0 = W a + V e - N(l + L/2) - F_t b - F_s(b - \tfrac{1}{3} d) - H_T b' \qquad \ldots(14)$$

5.4 The dynamic situation

The mathematical solution using the theory described above estimates the value of the soil reaction forces acting on the implement in a given position. It was observed, in experiments conducted earlier and described in the previous chapter, that the implement would react, changing its equilibrium depth , if there is any alteration in the soil forces resultant. Therefore, it is necessary to explain how these changes in forces would affect the implement behaviour.

It was shown in section 5.3 that it is possible to estimate the forces acting on the tine when the working depth of the implement and the height of the hitch-point are known. However, it was proved in section 5.3 that for a given height of the hitch-point there is a different working depth which is dependent on the physical conditions of the soil and implement characteristics

$$dc = f(\emptyset, S, \gamma, c, l, h, b) \qquad \ldots(36)$$

Since at the desired equilibrium depth the angle of the total resultant force acting on the implement and the angle of the free-link are the same, and the bottom of the implement is parallel to the horizontal line, it is possible to determine the equilibrium depth using an interactive method, for a known soil condition and hitch-point height, as described below.

5.5 The programme computer concepts

The theory so far described enables the forces acting on the tine to be estimated, using the principle of soil mechanics, the theory of narrow tines, and the dynamic balance of forces. Since it was found that the equilibrium condition of the implement is with its bottom parallel to the horizontal line for a given position of the hitch-point, it is possible to predict the equilibrium depth of the implement based on the fact that the angle of resultant force is the same as that of the 'free-link'. The model goes even further and utilizing the Coulomb Principle of Passive Earth Failure, estimates the length of the rupture distance. With the knowledge of these values it is then possible to estimate the path of the implement.

However, when working in adverse soil conditions any alteration in one of these values would affect the whole system, since they are interrelated. Consequently the solution for this interactive calculation was the development of a computer programme (Appendix 6) whose block diagram is shown in Fig. 5.11 and the basic principles are described below.

a. The first step of the programme consists in estimating the equilibrium condition of the implement for a given height of the hitch-point, assuming that the plough is working in a flat soil surface profile. The calculations are based on the equations presented in the

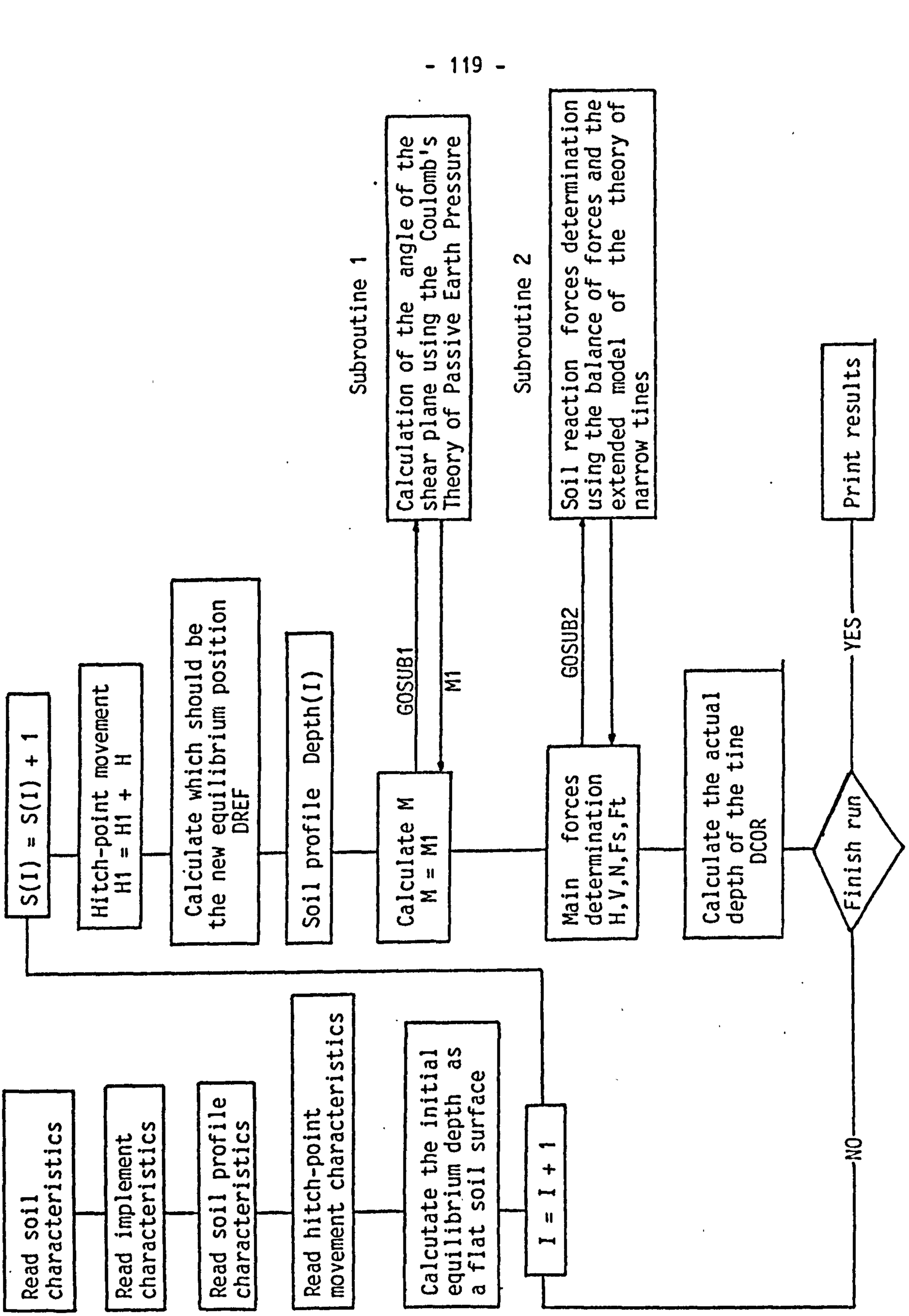

FIG. 5.11 Block diagram

section 5.2 and 5.3, where the soil physical conditions are known. It is an interactive method where the increments in depth are introduced until the moment about the point 'O' Fig. 5.1 is zero.

b. In the next step the programme verifies the conditions of the soil surface ahead of the tine for a displacement Δs in the travelled distance s. If there is any alteration in the soil profile it calculates the forward rupture distance ratio m using the method described in section 5.3.1, and then with the value of m and d calculates the resultant force, and which should be the new equilibrium condition .

c. For the same position of the tine, the programme checks the position of the hitch-point, and in case of any alteration it calculates which should be the new equilibrium position.

d. The actual depth of the implement is calculated using equation 11 where Δd is calculated for a depth do, the depth of the implement at point s, and de the new equilibrium depth if there is no other alteration in the further Δs displacement. The programme than assumes that do is equal to do $+\Delta d$ and s is equal to s $+\Delta s$

e. It then checks if the run has finished, and in a negative case it returns to section b.

CHAPTER 6

EVALUATION OF THE MODEL AND DISCUSSION OF RESULTS

6.1 Introduction

A series of tests were conducted in the soil bin in order to evaluate the mathematical model presented in the previous chapter, and to establish the fundamental kinematics of the behaviour of the trenchless plough. The results presented in this chapter are, therefore, a combination of appreciation of the model and a discussion of the behaviour of the implement under the circumstances tested.

Ede (1961) observed that grade control can be satisfactorily achieved by maintaining the correct level of the pivot point of a floating beam mole plough, and that the implement only runs in equilibrium at a single depth of about 660 mm for a beam length of 3.4 m. He conducted a limited number of tests for small soil irregularities and did not give further explanation of his findings and/or their possible implications in the behaviour of similar implements. It was therefore necessary to conduct tests under undulating conditions in order to analyse the behaviour of the trenchless plough.

The tests were divided into two main groups to study the effect of:

a. soil surface with constant hitch-point level

b. hitch-point movement over a flat soil surface

These are summarized in the table below:

Test	Soil surface	Hitch point
1		
2		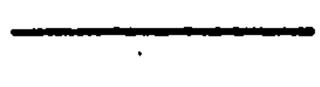
3		
4		

6.2 The effect of the soil surface

6.2.1 Introduction

To simulate the trenchless plough working in a field with an irregular soil surface, tests were conducted in the soil bin with the soil surface in both step and sinusoidal form. The method of preparation of the soil surface is fully described in section 3.4. The objectives of these tests were to observe the effect of the difference in the soil level on the implement response, and to compare the results with those obtained from the mathematical model for similar circumstances.

6.2.2 Step input soil profile

The length of the soil bin surface was prepared with two steps, with a

plateau sufficiently large between the steps to allow the implement to reachieve its equilibrium before another soil irregularity was reached. The steps, 0.05 m height, which represent a difference of 0.3 to 0.6 times the working depth of the implement (dependent on the original position of the tine), were constructed in both directions, i.e. increase and decrease in the soil depth. The tests were conducted for different hitch-point heights, in relation to the reference level, in order to vary the initial working depth of the implement. The hitch-point remained level during the run.

An example of the implement response to soil step input is presented in Fig. 6.1 (step down) and Fig. 6.2 (step up). It is possible to observe in these figures that the soil reaction forces H, V and N start to present some variation before the implement reaches the step. The distance between the point where the soil forces start to change and the point at which the soil step occurs, was found to be same as the length of the forward rupture distance for a flat surface. Since the forward rupture distance ratio can be considered constant for a flat surface, and has the value of 2.03 for a 45^{o} rake angle tine, it is possible to affirm that the soil reaction forces start to change their magnitude at the distance approximately equal to two times the critical depth before the implement reaches the step. As a consequence of this change in the soil reaction forces the implement reacts and starts to move even before it crosses the soil irregularity.

This behaviour of the soil reaction forces is explained with the support

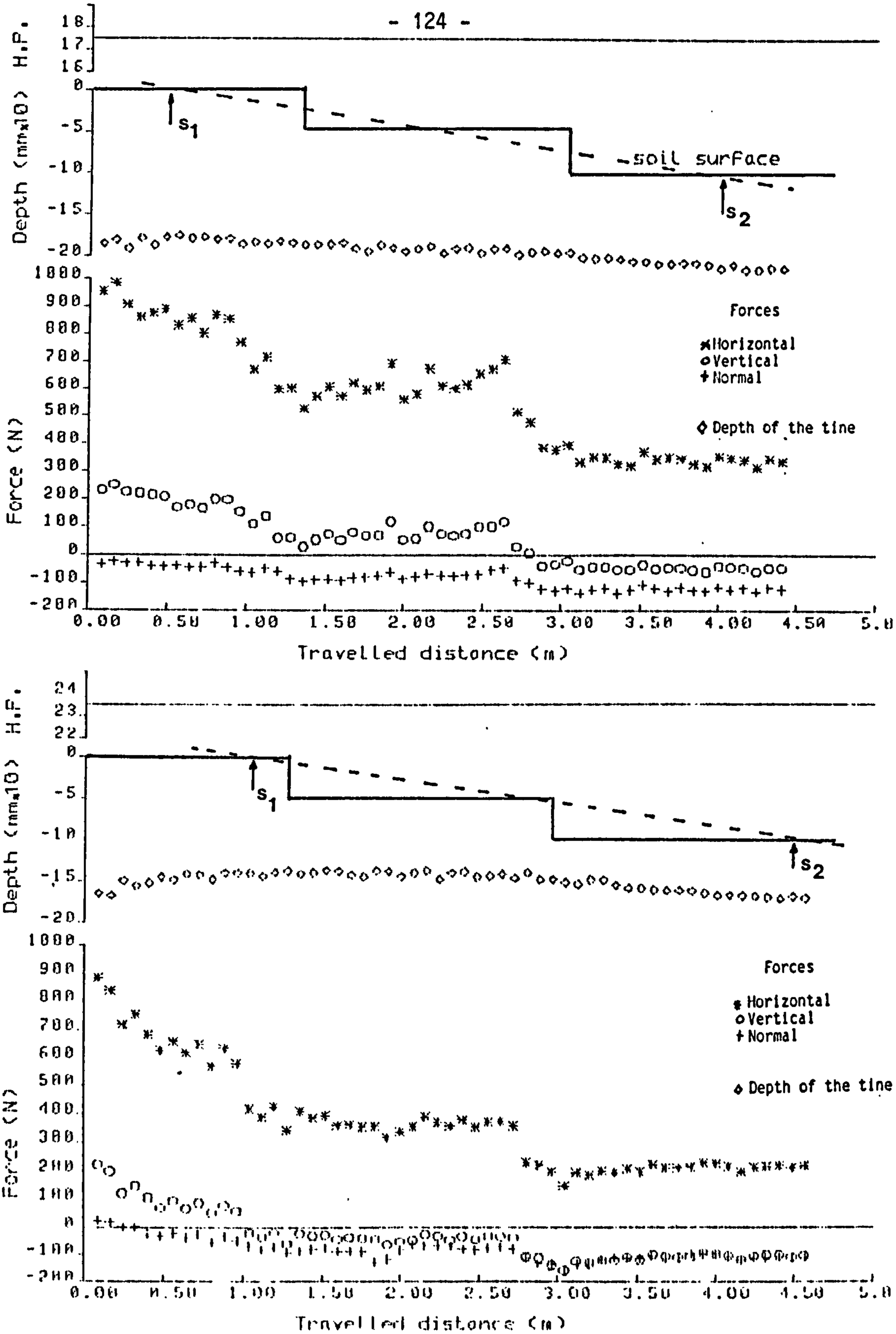

FIG. 6.1 Results of a step soil profile descent. Top: hitch-point height equal to 175 mm in relation to level 0 (zero) of the soil surface, and bottom: hitch-point height equal to 235 mm

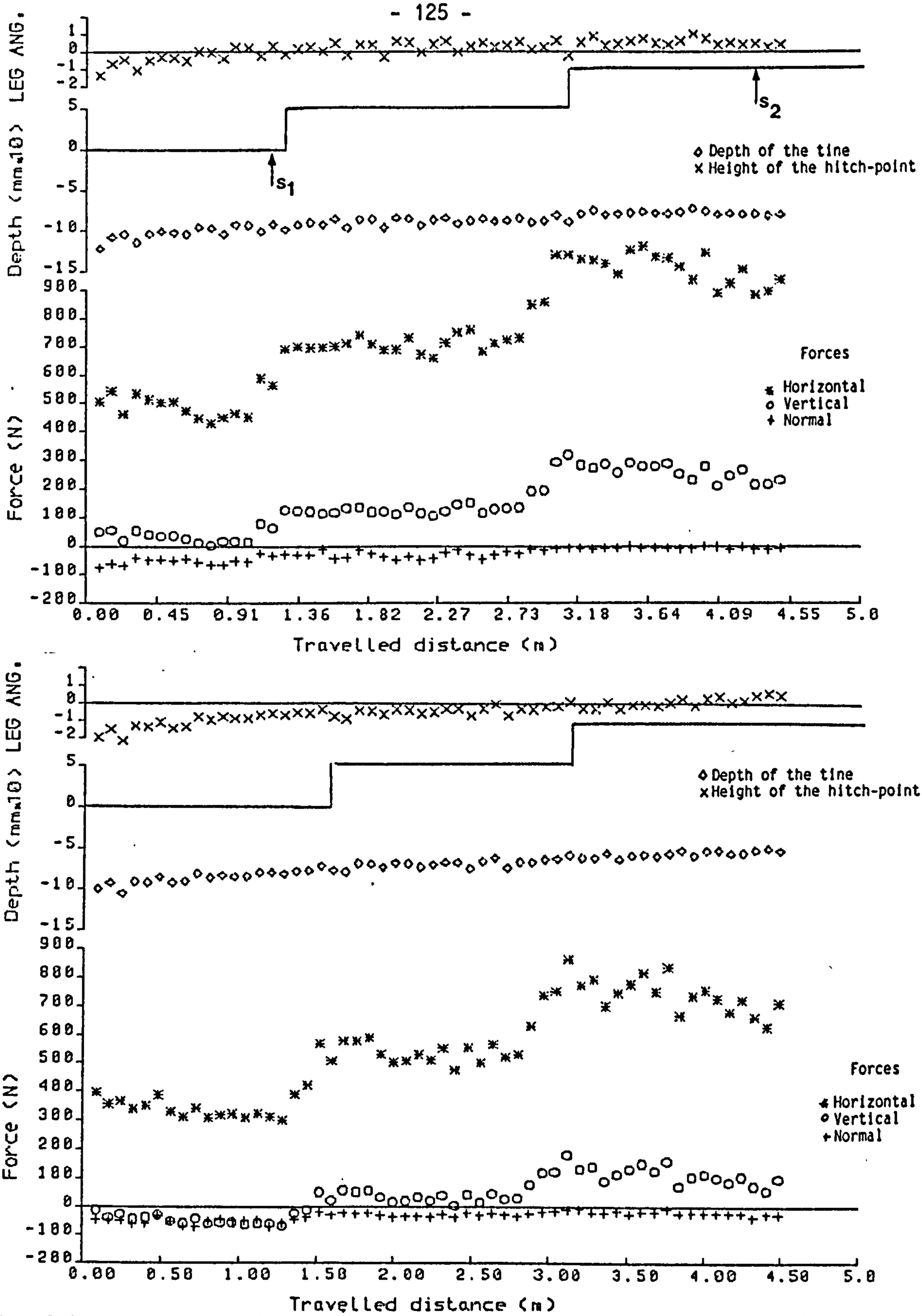

FIG. 6.2 Step input soil profile ascent. Top: hitch-point height equal to 270 mm in relation to the soil level (0), and bottom: hitch-point height equal to 300 mm

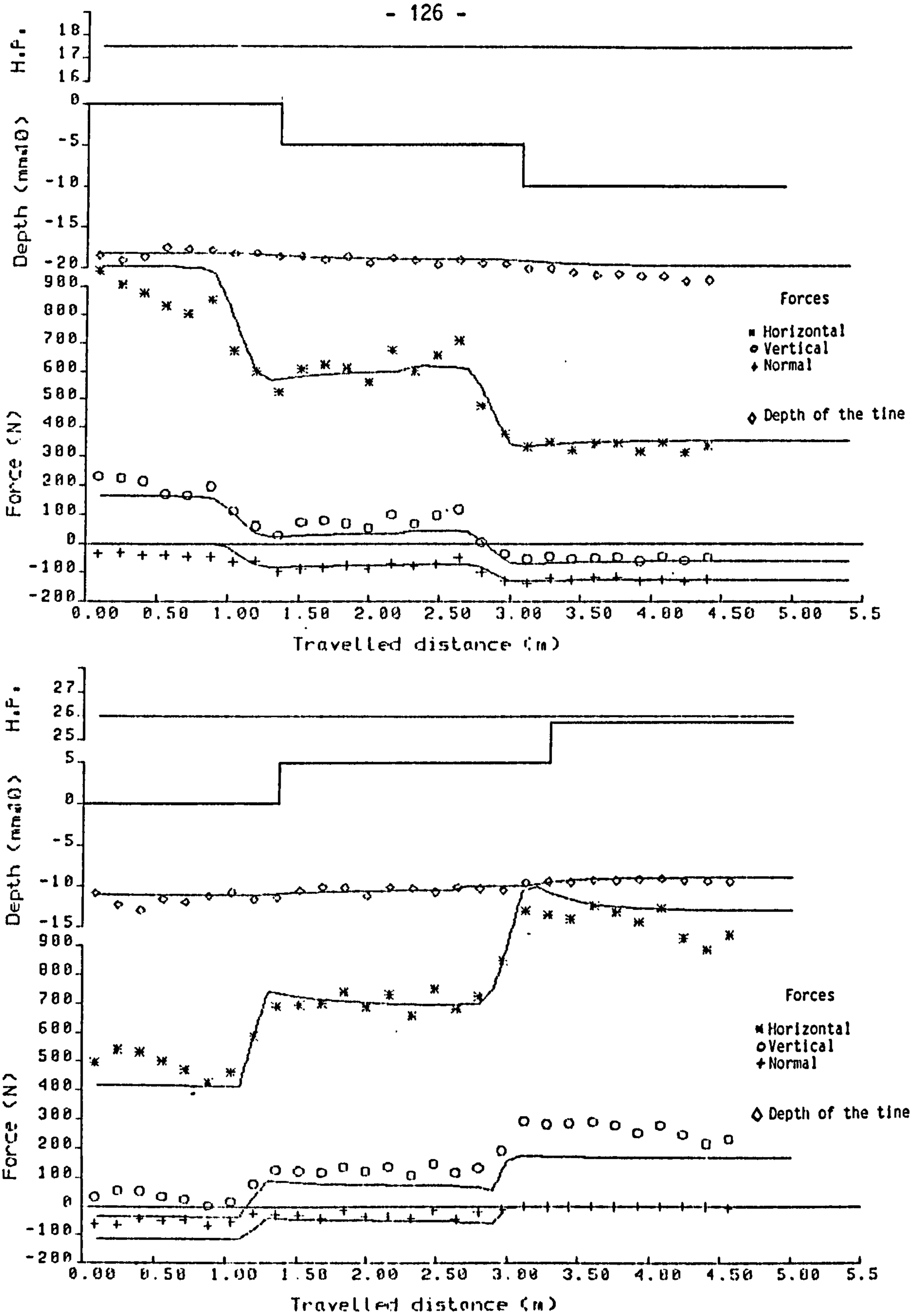

FIG. 6.3 The theoretical results for the step input soil profile compared with the experimental data

of the results obtained in the soil glass-sided tank (section 4.3.3), where it was found that the angle of inclination of the shear plane changes as the tine approaches the soil irregularity, because the soil fails in the plane of least resistance. This means that there must be an alteration in the soil reaction forces as the tine approaches the step input, and this change is proportional to the distance between the tine and the soil step and to the amount of change in the soil depth.

A theoretical approach for this problem was proposed in section 5.3.4, where a model based on Coulomb's theory of soil failure in the passive state was used to predict the alteration in the shear plane angle, and consequently in the soil reaction forces. The experimental and theoretical results are presented in Fig. 6.3. There is general agreement between the two sets of results and for the horizontal soil force in particular. The fact that it took a short distance (0.75 m) for thee implemant to reach equelibrium explaines the discrepancy between the two sets of data. The vertical soil reaction force estimation agrees with the experimental value in 70% of the cases and in 30% it was underestimated, although all the step changes were predicted. This agrees with the results obtained by Godwin and Spoor (1977).

As a consequence of this alteration in the soil reaction forces, there is an alteration in the total moment about the hitch-point '0' (Fig. 5.1). Since the change in angle of direction of the soil resultant force, due to changes in the depth of work, is small, the change in the balance of the moment and change in the position of the height of the point '0' is minimal. The result of these small alterations represents a slight change in the angle of the tine in relation to the horizontal plane, which induces the tine to penetrate or raise to re-establish the

equilibrium condition. This can be observed in Figs. 6.1 and 6.2. The difference in the soil reaction forces from the first soil level to the last one are nearly 100%, but only a small alteration in the depth of work, in relation to a reference level, can be noticed. It is important to observe that, because of the damped effect on the implement the change in depth is very slow and the slope of the channel is constant with no backward inclined grade.

It is also noticeable in these figures that the grade of the drainage pipe line differs from the grade of the soil surface. In Fig. 6.1 (top) if a linear decrease in depth between the point s1 at 0.45 m and s2 at 4.00 m is considered, the soil slope is 2.8% where the pipe line grade is only 1%. In Fig. 6.2 (top) the depth of the implement at point s1 is 96.4 mm, and at point s2 it is 74.9 mm in relation to the origin, where the difference in soil level is 100 mm. This suggests that the relationship between the hitch-point and the implement depth is non-linear.

The evidence from the results obtained in the experiments conducted with the hitch-point at different heights in relation to the soil surface (Fig. 6.4), suggested that the relationship between these values can be represented in parabolic form where the following empirical equation could be fitted to the experimental data:

$$Y = a + bx + cx^2 \qquad \ldots (6.1)$$

where the coefficients are:

Y = d = equilibrium depth in mm; x = HP = height of the hitch-point in mm; a = 220.5753; b = 4.865 E-2; c = -1.757 E-3

The reason for this behaviour of the implement with regard to the

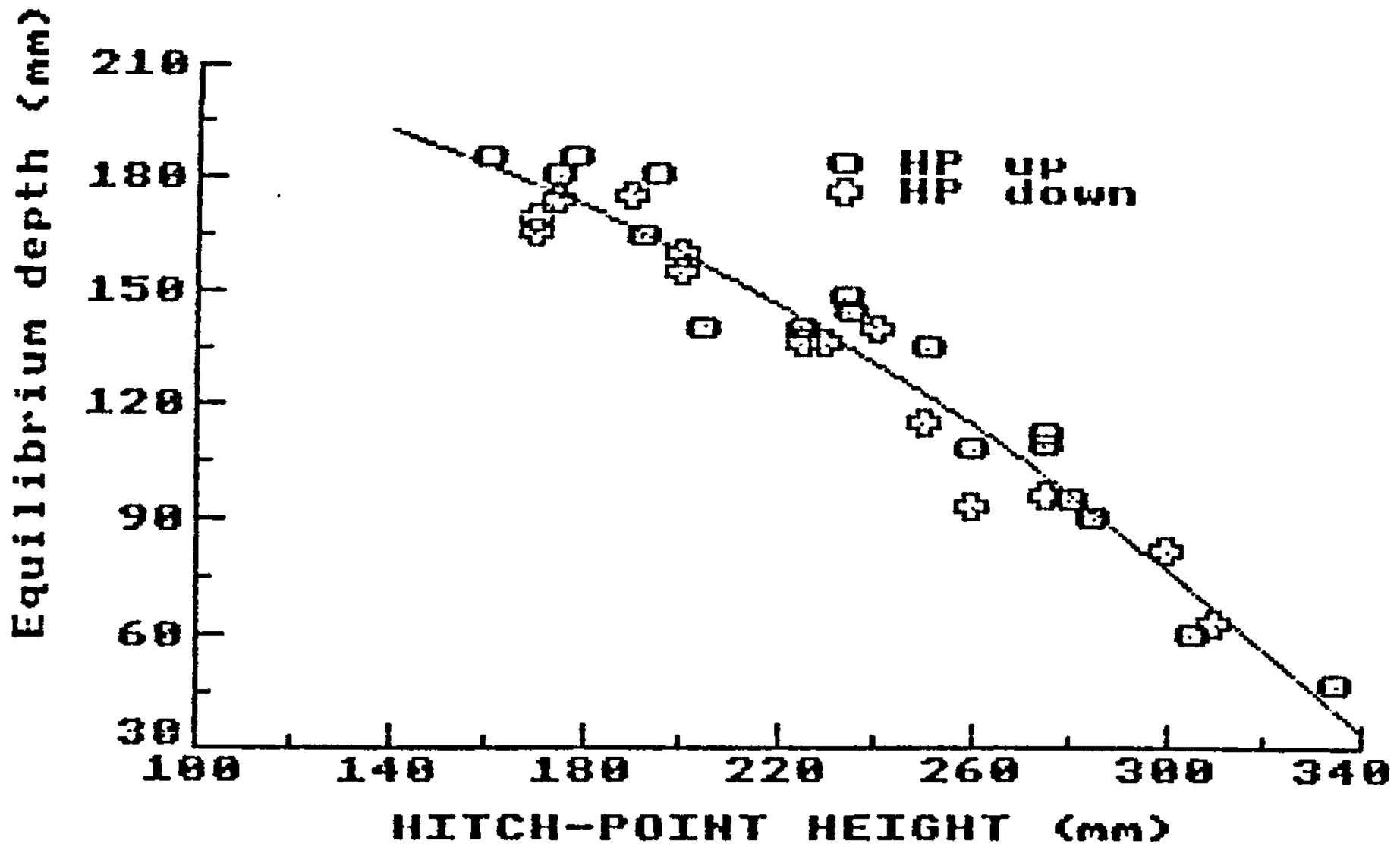

FIG. 6.4 The relation between the hitch-point height and equilibrium depth of the implement

hitch-point position is explained by the fact that the relation between soil reaction forces and depth of work is non-linear. What happens is that as the depth of the implement is reduced, by means of reducing the height of the hitch-point, the horizontal soil reaction force increases in a slightly bigger proportion than the vertical soil reaction. As a consequence the angle of the resultant force decreases and the implement is able to find an equilibrium position at a shallower penetration. This will happen up to a certain limit, i.e. the maximum working depth, after which the vertical forces acting on the implement, due to the soil reaction and weight of the system, would not be sufficient to compensate the moment generated by the horizontal force and the implement will no longer penetrate. However, the error in assuming a linear relationship, in the working range of 170-290 mm for the height of the hitch-point, i.e. between the operational depth of 80-170 mm, is very small; 1.25% for the two extremities. It can also be observed in Fig. 6.4 that the response of the implement to alterations in the height of the hitch-point is independent of direction of movement of the latter.

These results are similar to the ones obtained by Fouss (1971) for the mole plough tine; he reported that changes in the hitch-point height cause changes in the plough depth in different proportion.

6.2.3 The sine wave soil profile

The second series of tests were conducted in a sinusoidal soil surface

profile, with two different wavelengths, 1.75 and 3.00 m and two different wave amplitudes, 0.04 and 0.06 m, bringing it to a total of four different tests. The soil surface profile was prepared as described in section 3.3, and a small plateau of approximately 1 m long was left at the beginning of the bin, so that the implement could adjust itself to the equilibrium depth before the uneven surface started. In order to change the original equilibrium depth before the uneven soil surface started, the height of the hitch-point was varied between each run, but was kept at a constant level during the run.

Figs. 6.5 and 6.6 show the results of some of these tests. These figures illustrate particularly well that the implement can maintain its path of equilibrium if the hitch-point is kept at constant level in reference to a horizontal plane, independent of the soil profile. This is specially valid when the soil irregularities are most frequent. The short wavelength represents two beam lengths (Fig. 6.5 top, and Fig. 6.6 bottom). In Fig. 6.5 (top) the difference in the implement depth, between the shallowest point (d1) and the highest point (d2) is 80 mm, where the initial depth of work is only 100 mm. This represents a variation in depth of work of 130% between d1 and d2, and an alteration in magnitude of the soil reaction forces of 140%, where the path of the implement can be considered constant with less than 2% variation. This is due to the fact that the damped effect of the implement prevents the tine from moving in the vertical plane. When the moment about the hitch-point changes in one direction and the tine starts to move to respond to the alteration, the implement has already moved forward enough for the

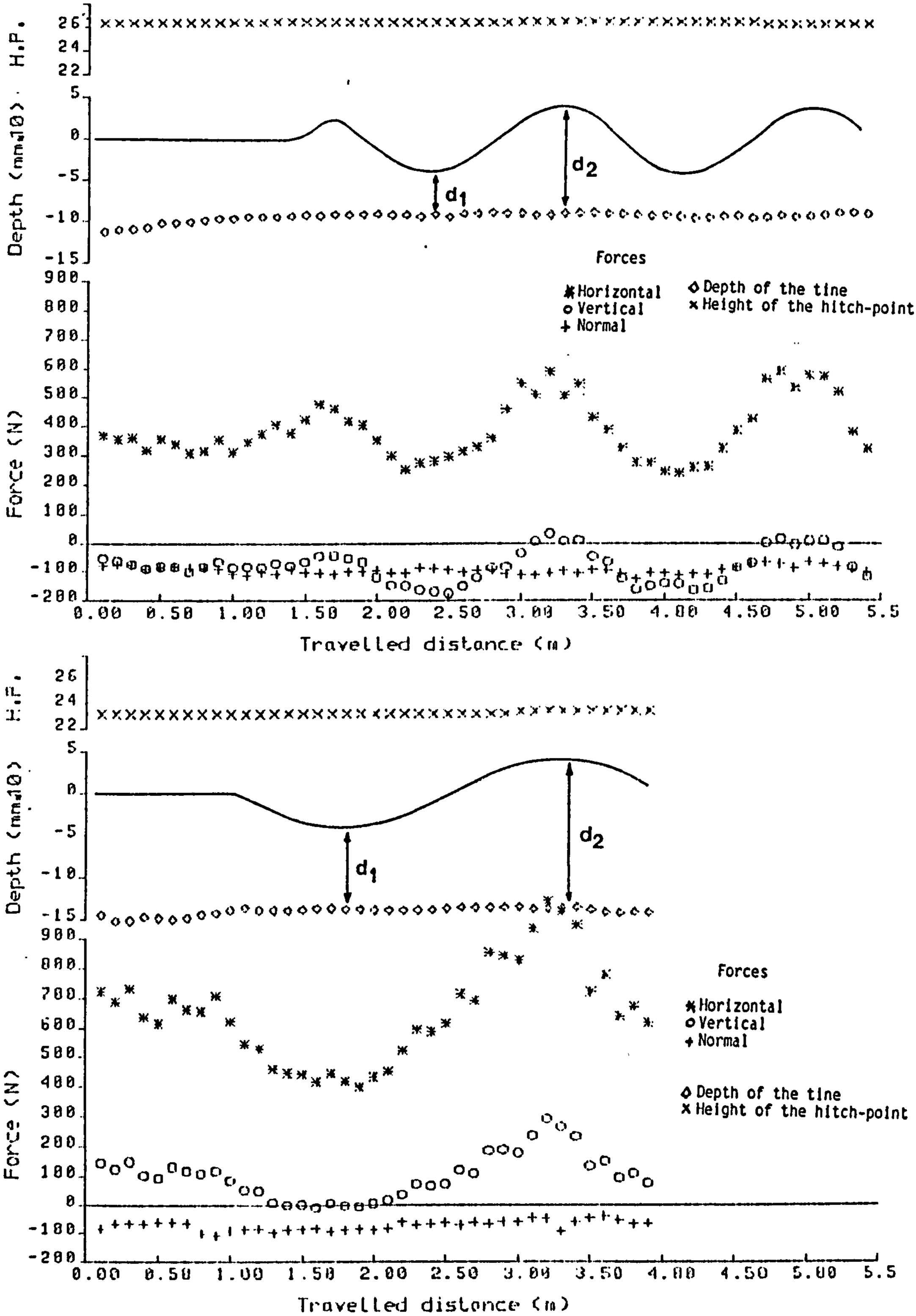

FIG. 6.5 Results from a sinusoidal soil profile. Top: wavelength equal to 1.7 m and amplitude 40 mm. Bottom: wavelength equal to 3.0 m and amplitude 40 mm

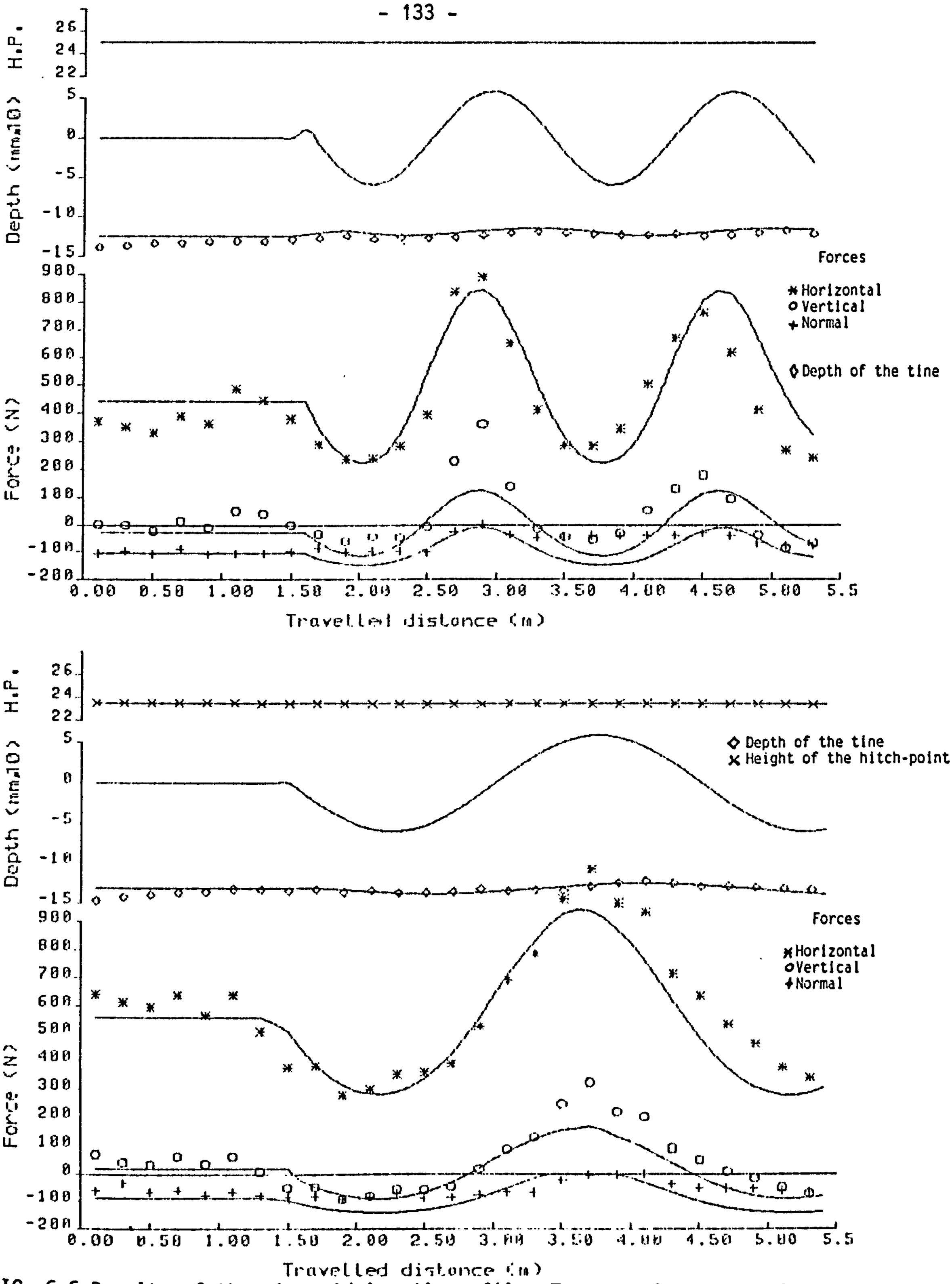

FIG. 6.6 Results of the sinusoidal soil profile. Top: wavelength equal to 1.7 m and 60 mm. Bottom: wavelength equal to 3 m and amplitude 60 mm. Full line results from the mathematical model

soil reaction forces to change in the opposite direction so that the tine does not have time to react to this soil variation. Therefore, the alteration in the grade of the drainage line is very small.

It is possible to observe in figures 6.5 and 6.6 that although the soil reaction forces have a sinusoidal response similar to the soil surface profile, with the same frequency, they differ in amplitude, which is dependent on the implement depth; e.g., the soil amplitude is the same in Fig. 6.5 top and bottom, but the soil reaction force has a bigger amplitude in the bottom figure because the implement is working at greater depth.

It is also noticeable, in the same figures, that the soil reaction forces are slightly out of phase in relation to the soil surface. The soil reaction forces tend to change in magnitude ahead of the actual change in soil profile, and it was observed that the amount out of phase of the soil reaction forces in relation to soil surface is dependent on the working depth, i.e. it is a function of the length of the forward rupture distance. This is explained by the fact that the shear plane ahead of the tine changes its angle of inclination as the soil surface profile varies. This was observed in the tests conducted in the glass sided tank and explained in section 4.3.3. This change in inclination of the shear plane induces a change in the soil reaction forces before the change in soil surfaces occurs. Therefore at a relatively deep working depth, where the length of the forward rupture distance is great, the amount out of phase is expected to exceed the amount out of phase at

shallow depth. As an example in Fig. 6.5 (top) the peak of the sinusoidal wave produced by the soil reaction forces differs by over 200 mm from the top of the soil bump (d2), and at the shallowest depth of work, the out phase, is only 100 mm, (d1).

The path of the implement in the case of a soil profile with a long wavelength (3.00 m, equivalent to 3.6 times the beam length, shown in Fig. 6.5 bottom and Fig. 6.6 bottom) presents a slightly bigger variation than the other case. The reason for this is that the distance between the soil bumps and depressions is sufficient to allow the implement to start moving in order to re-establish its equilibrium condition. Despite this, it is important to emphasize that although the difference between the depths d1 and d2 in figure 6.5 (bottom) is 120 mm (150% of the depth d1, or 95% in relation to the original depth of the implement), the difference in the drainage line is only 17 mm, which is less than a pipe diameter in the case of a normal size implement.

The results of the test conducted in the most adverse circumstance, i.e. the large soil sinusoidal wave length and amplitude, is presented in Table 6.1. There it is possible to observe that the variation of the free-link between the lowest and highest soil depth is 2^{o}, and the change is slow and gradual. This means that the alteration in the height of the pivoted end of the beam, which is directly dependent on this angle, is very small and also slow and gradual. A smaller alteration in the angle of the free-link was observed in the other tests conducted over smaller sinusoidal wavelengths and amplitudes.

The response of the normal soil reaction force at the bottom plate of the implement was observed to be smaller in comparison to the other soil reaction forces. Being a balance force to compensate for the moment about the hitch-point, this force was not expected to change a great deal as the soil depth varied. The reason for this is explained by the fact that the reduction in the horizontal force, which could induce an increase in the normal force because of the reduction of the moment about the hitch-point, is always associated with reduction in the vertical force.This in turn reduces the moment about the hitch-point in the opposite direction to the horizontal force, so that the alteration in the normal force is relatively small.

The results shown in Fig. 6.6 are a comparison between the data obtained from the experimental work carried out in the soil bin (the symbols) with the results obtained from the mathematical model (full line). To estimate the values of forces and the position of the implement, the length of the bin was divided into small segments equal to 0.06 m, and for each point the computer programme calculated the rupture distance ratio, the soil reaction forces, the resultant direction, the position of the end of the beam, the new equilibrium position and the actual position of the implement. The close agreement between the values proved that the approach adopted is entierly sufficient to adequately predict the dynamic performance of the implement.

6.2.4 Conclusions

These experiments cover a much broder range of situations than the ones find in the field, where the differences in the tine working depth of 100%, are not expected to occur, they were specially designed to help with the understanding of the dynamics of the implement. Inducing extreme conditions to study the implement behaviour is one way of extracting the information necessary to delimit the influence of the several external factors which are present in the process of pipe installation.

From the results presented here, it is possible to conclude that the behaviour of the trenchless drainage implement is not only dependent on topography and physical conditions of the soil, but is also dependent on the frequency with which these conditions change during the course of the implement. In situations where the field irregularity is more constant, up to 2-3 times the beam length, once the equilibrium depth is achieved by the tine then if the hitch-point is kept at a constant level in relation to a reference plane, the implement will maintain its desired position of work. In case of long field irregularities, over 3 times the beam length, (long bumps and depressions, or a permanent change in level), it might be necessary to correct the hitch-point level by a certain amount in order to maintain the implement at its desired position. This correction is unlikely to be equal to the difference in the soil level.

The results presented in section 6.2.2 showed that the relationship

between the working depth of the implement and height of the hitch-point can be considered linear within the working range of 80-170 mm, where the relationship can be expressed by 1/1.50. This means that to obtain the desired grade of the drainage line the hitch-point has to be kept at a different grade line.

6.3 The effect of the hitch-point movement

6.3.1 Introduction

Maintaining the hitch-point with reference to a design grade using the conventional equipment currently available for drainage work is a very difficult, if not impossible, task, in a field with an irregular soil surface. Therefore, to complete the objective of this project it is necessary to study the behaviour of the implement when the hitch-point is moving in the vertical plane following the ground as it does in the field.

However, the analysis of the system would be very complex and difficult to do if the number of variables was not kept to a minimum during each of the tests conducted in an experiment. So, it was decided to carry out this analysis with a variable hitch-point in a soil with a flat surface, constant density and regular physical properties.

The variations imposed on the hitch-point were similar to the ones used in the investigation of the effect of the soil profile, with step and sinusoidal inputs in the movement of the hitch-point. The equipment used

to simulate these movements is fully described in section 3.2.4.

6.3.2 The step input

The step movement in the hitch-point was introduced after the implement had achieved its equilibrium depth at the beginning of the run, and the distance between the steps was sufficient to allow the system to reachieve its equilibrium depth, or at least come very close to it. Since during the run, apart from eye judgement, there was no other way to decide if the implement was or was not in equilibrium, the minimum distance left between the steps was always over two beam lengths. The movement imposed on the hitch-point in the vertical plane was introduced in both directions, i.e. upwards and downwards, and had different step height. The velocity of the carriage was kept constant during the run, so the change in the hitch-point level was conducted without stopping.

From the results of these tests (Figs. 6.7 to 6.9), it was possible to extract information to explain the behaviour of the implement, or to confirm previous results and/or hypotheses.

First of all they confirm the damping effect of the implement when an instantaneous change in the hitch-point height is introduced. As predicted in chapter 4 from the preliminary tests conducted during penetration and raising of the implement, using a fixed hitch-point, the damping factor is likely to be large. Comparing these results with the ones obtained from equation 11 (chapter 5), they show a very good

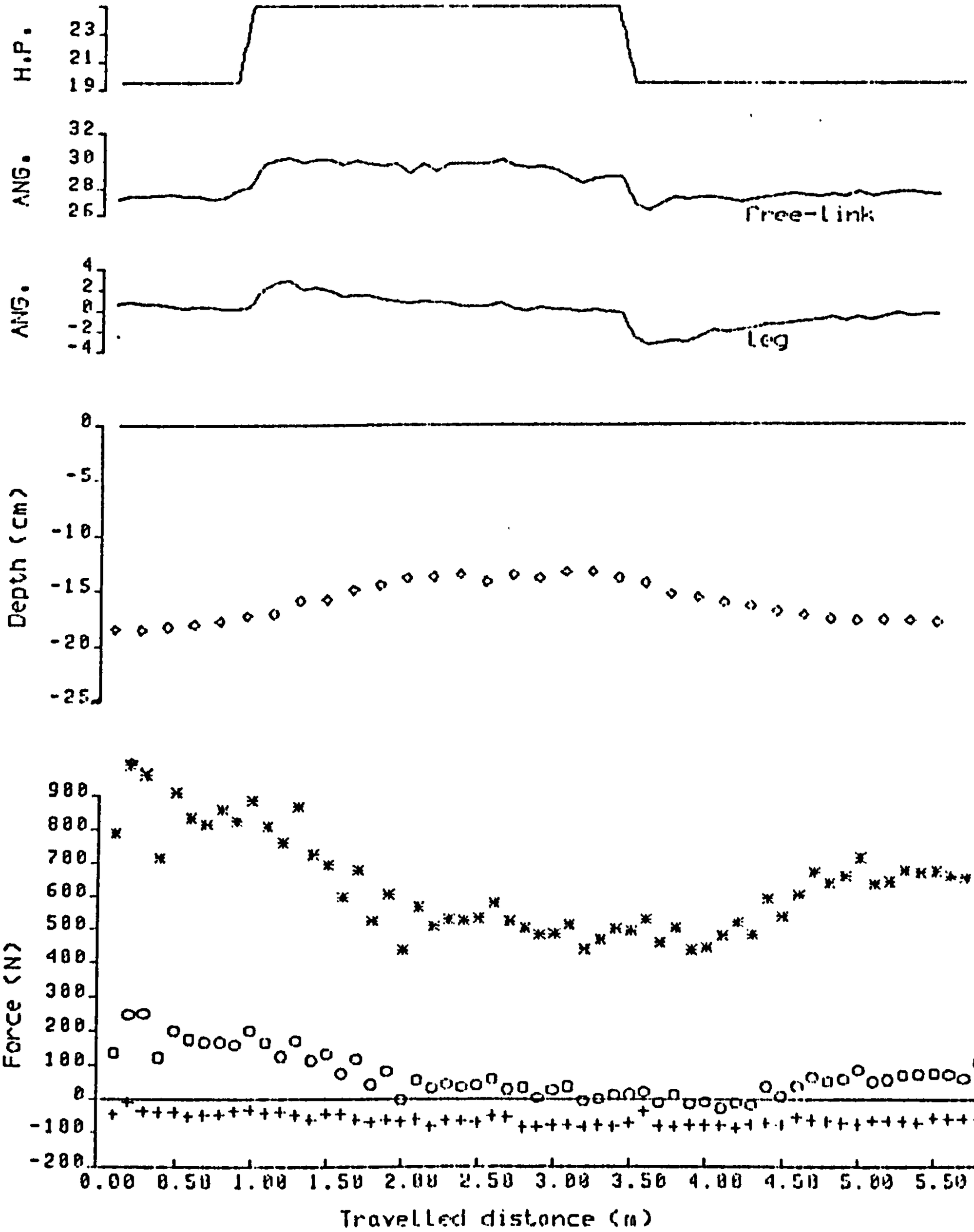

FIG. 6.7 Results of soil bin tests with a step movement of the hitch-point, upwards and downwards

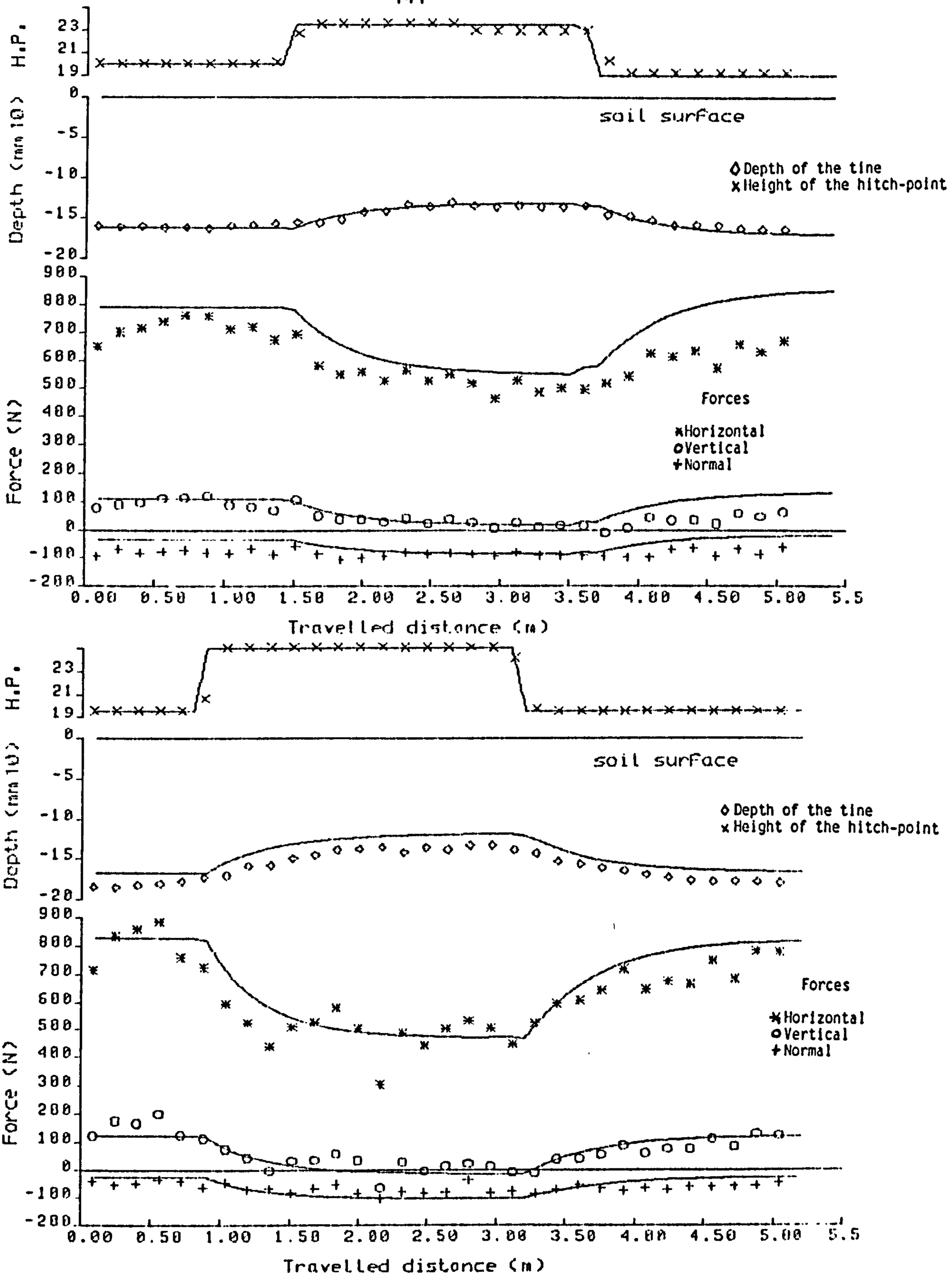

FIG. 6.8 Step input displacement of the hitch-point. Top: 30 mm upwards and 50 mm downwards. Bottom: 50 mm upwards and downwards

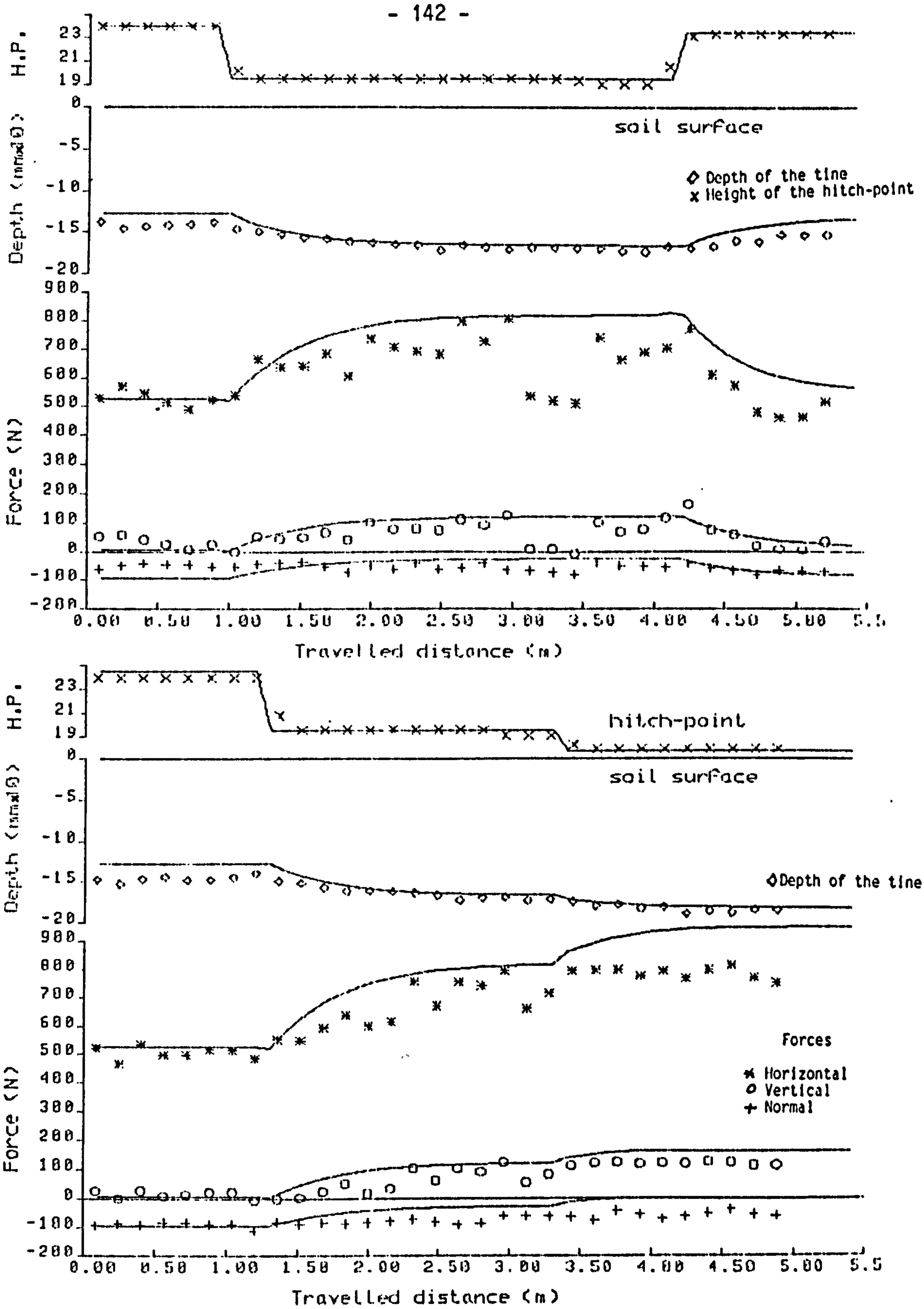

FIG. 6.9 Step displacement of the hitch-point. Top: 50 mm downwards and upwards. Bottom: 50 mm downwards and 20 mm downwards

agreement, suggesting that the approach used is valid and giving confidence to continue with the same analysis.

Fig. 6.10 shows the depth response of the implement during the upwards or downwards movement of the implement. It is possible to observe in this figure that the distance necessary for the implement to re-establish its equilibrium position is almost the same, where the rate of raising seems to be bigger than the penetration at the beginning of the movement. However, the time for the tine to achieve 63.2% of its equilibrium condition, i.e. ratio equal to 0.35, is not significantly different from the upwards or downwards movement of the hitch-point. This confirms the assumption that there is no significant difference between the ratio of the vertical displacement/travel distance for a given difference in depth of work.

In all the tests conducted by raising or lowering the hitch-point, it was observed that the implement reachieved a stable position, independent of the height of the hitch-point, and at that point the angle of the tine in relation to a vertical line was between 0-0.5^{o}. This confirms the assumption used in the development of the theoretical analysis, that the desired position of the plough, with its bottom parallel to the horizontal line, is the equilibrium position of the system when working above the maximum working depth. This result differs from the findings of Ede (1961) for the mole plough. He reported that there was only one true operational depth for a plough-beam arrangement. This may be explained by the use of a different arrangement

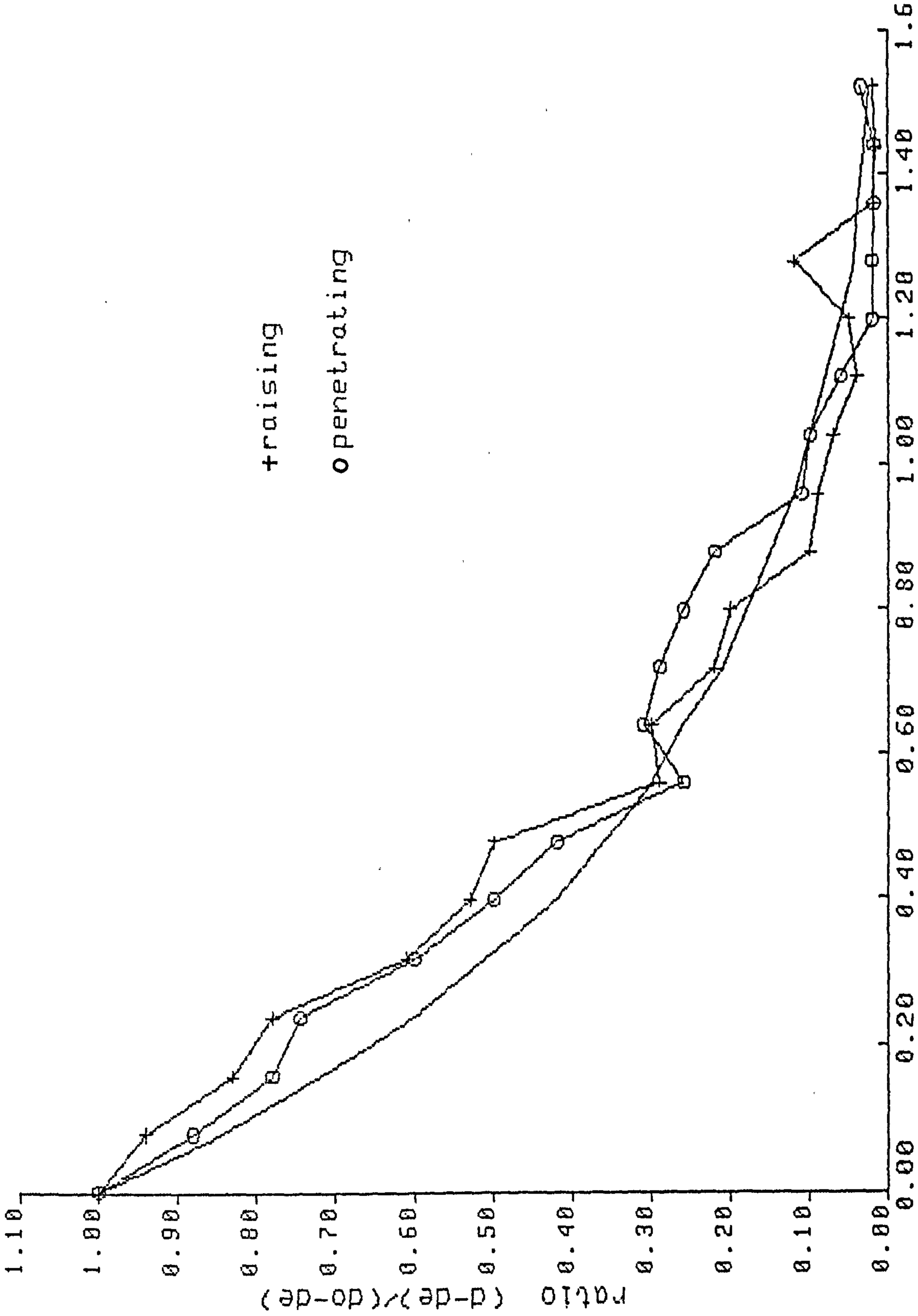

FIG. 6.10 Ratio of penetration and raising against the travelled distance. Predicted and experimental values.

for assembling the system not including the free-link between the hitch-point and the pivot point of the long beam, but this is not specified by him.

One important factor observed in these results (Fig. 6.7) is the angle of the free-link. Although the displacement of the hitch-point is 50 mm, i.e. 30% of the original working depth, the difference in the angle of the free-link is only 2^{o}. The angle changed almost instantaneously, and tended to stay constant during the time that the tine was re-establishing its equilibrium position. The difference in the direction of the resultant force between points a and c is the reason why the angle of the free-link changed, since at the equilibrium position the free-link and the resultant force acting on the implement have the same angle. This difference in the direction of the resultant force and the alteration in the position of the centre of resistance as the tine changes its working depth, is the reason why the relationship between the hitch-point height and depth of work of the implement not to one to one. This agrees with the results obtained by Singh (1982), where although he assumed a linear relationship between the soil reaction forces and depth of work, he shows that the inclination of the resultant force increases slightly with depth, and its position shifts slightly rearwards and deeper with increasing working depth and vice-versa.

The behaviour of the normal soil reaction force is very similar to the one described in the previous section as it varies with the depth of the tine, but does not have the peak value, even when the tine is tilted 3

to 4 degrees backwards as shown in Fig. 6.7.

Figs. 6.8 and 6.9 show the results of these tests compared with the results predicted by the mathematical model. The model presented excelent agreement especially in respect to prediction of the path of the implement. The prediction of the force presented some over estimation, particularly when the implement was at the end of the run. This could be explained by the fact that at that point the implement was very close to the edge of the prepared soil, where sometimes the soil density differs from the rest of the packed bin.

6.3.3 The sinusoidal movement of the hitch-point

The sinusoidal movement of the hitch-point was selected to simulate the continuous movement of the tractor over a field with an uneven soil profile. These tests were conducted with four different paths of the hitch-point, which consisted of two different wavelengths, 1.75 and 3.00 m, and two different amplitudes, 0.04 and 0.06 m, similar to the ones used in the study of the soil profile. During these tests the soil surface was levelled. Before starting the sinusoidal variation of the hitch-point, a short run was carried out with a fixed hitch-point, so that the implement could adjust itself to the equilibrium depth. Then the carriage had to stop, and the equipment necessary to simulate the movement of the hitch-point was connected before the run could restart.

The results shown in Fig. 6.12 are for the long wavelength with

amplitudes of 0.04 and 0.06 m, top and bottom respectively. Fig. 6.13 shows the results of the short wavelength with the same amplitude, 0.04 m, and different height of the hitch-point in relation to soil surface. In these figures it is possible to observe the following:

Although the response of the implement is in a sinusoidal form, and has the same wavelength as the hitch-point, it differs in amplitude and phase, as it is possible to observe in the Table below:

Soil amplitude (mm)	Amplitude attenuation wavelength (m)		Phase lag wavelength (m)	
	1.75	3.00	1.75	3.00
40	0.43 (1/2.3)	0.56 (1/1.8)	60^{o}	60^{o}
60	0.43 (1/2.3)	0.56 (1/1.8)	60^{o}	60^{o}

The reasons for these variations in the amplitude and phase are explained below:

When a system is excited by means of cyclic variation of the support, the response of this system is dependent on the frequency ratio (w/wn) and the damping ratio (c/c_c), as can be observed in Fig. 6.11 (Thomson 1973). For the particular case of the trenchless plough, which has a very large damping effect (the value of $c/c_c \gg 1$, as mentioned in section 4.3.4 and discussed in section 5.2), when a harmonic movement is imposed to the hitch-point $x=Xosinwt$, where Xo is the amplitude of the hitch-point, the ratio between Xo and the implement amplitude Y will be dependent on the frequency of excitation, or in other words the

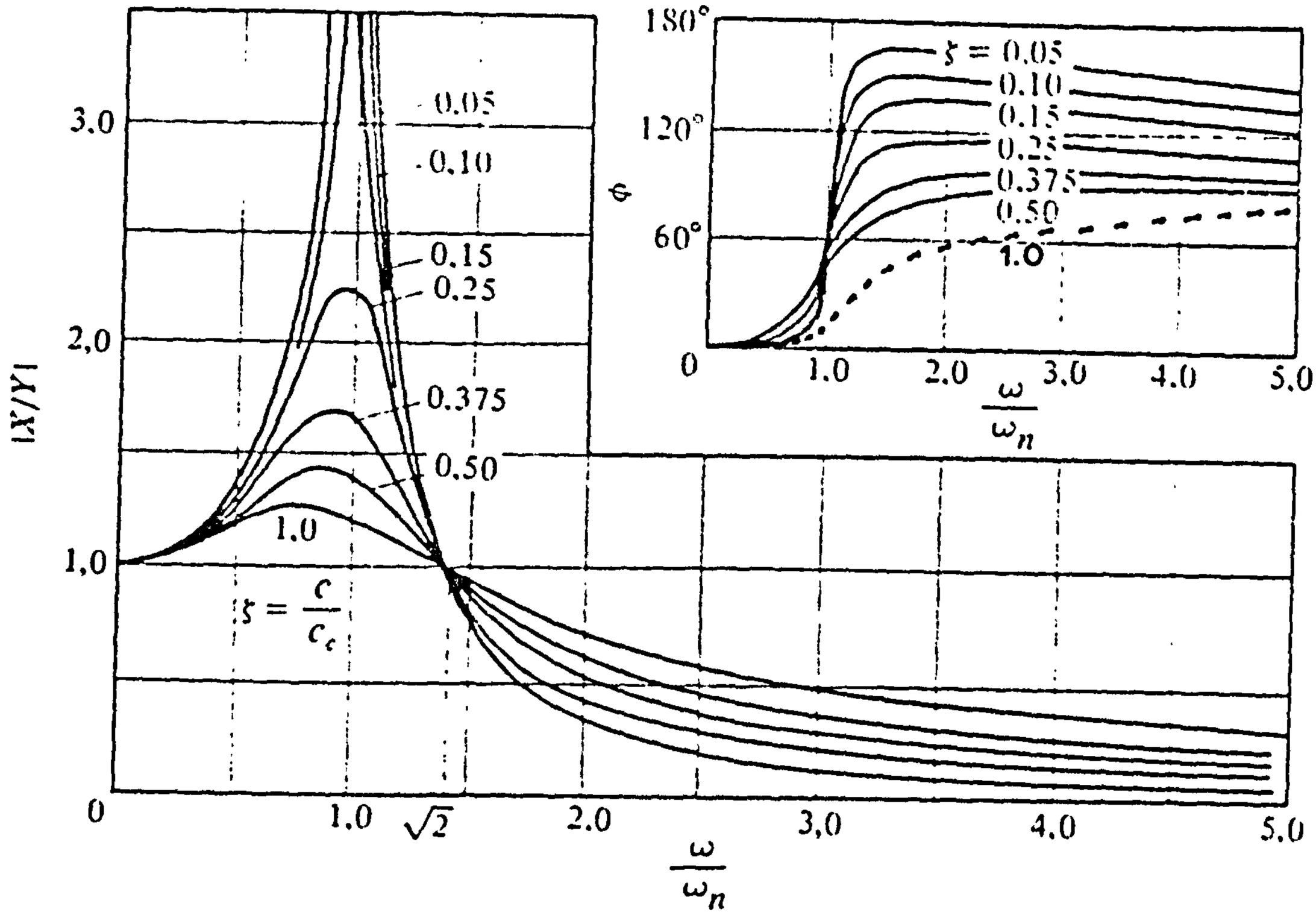

FIG. 6.11 Response of a system excited by the movement of the support. Bottom: frequency ratio (w/wn) against attenuation x/y. Top right: frequency ratio against phase angle ϕ

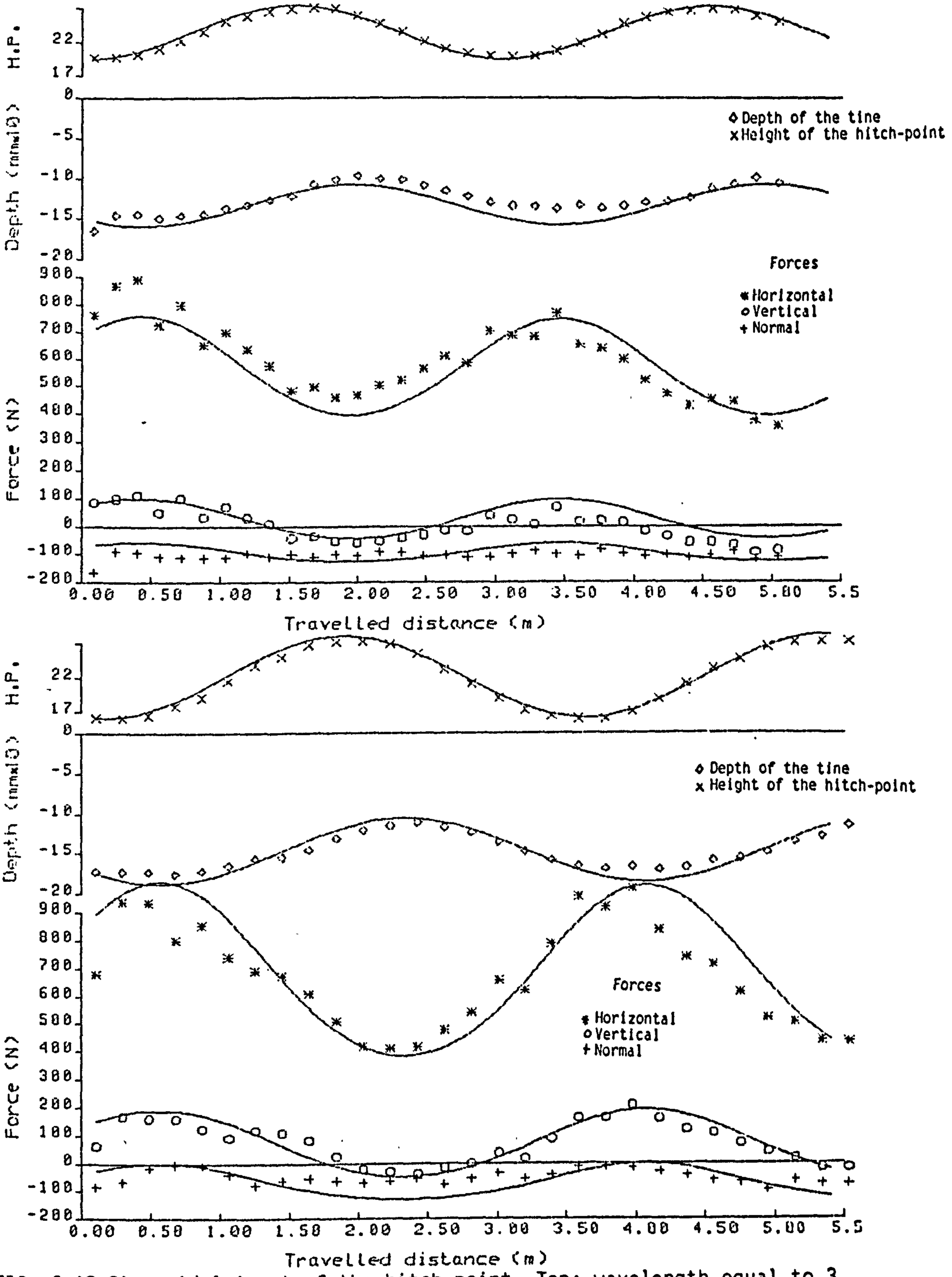

FIG. 6.12 Sinusoidal input of the hitch-point. Top: wavelength equal to 3 m and amplitude of 40 mm. Bottom: wavelength equal to 3 m and amplitude of 60 mm

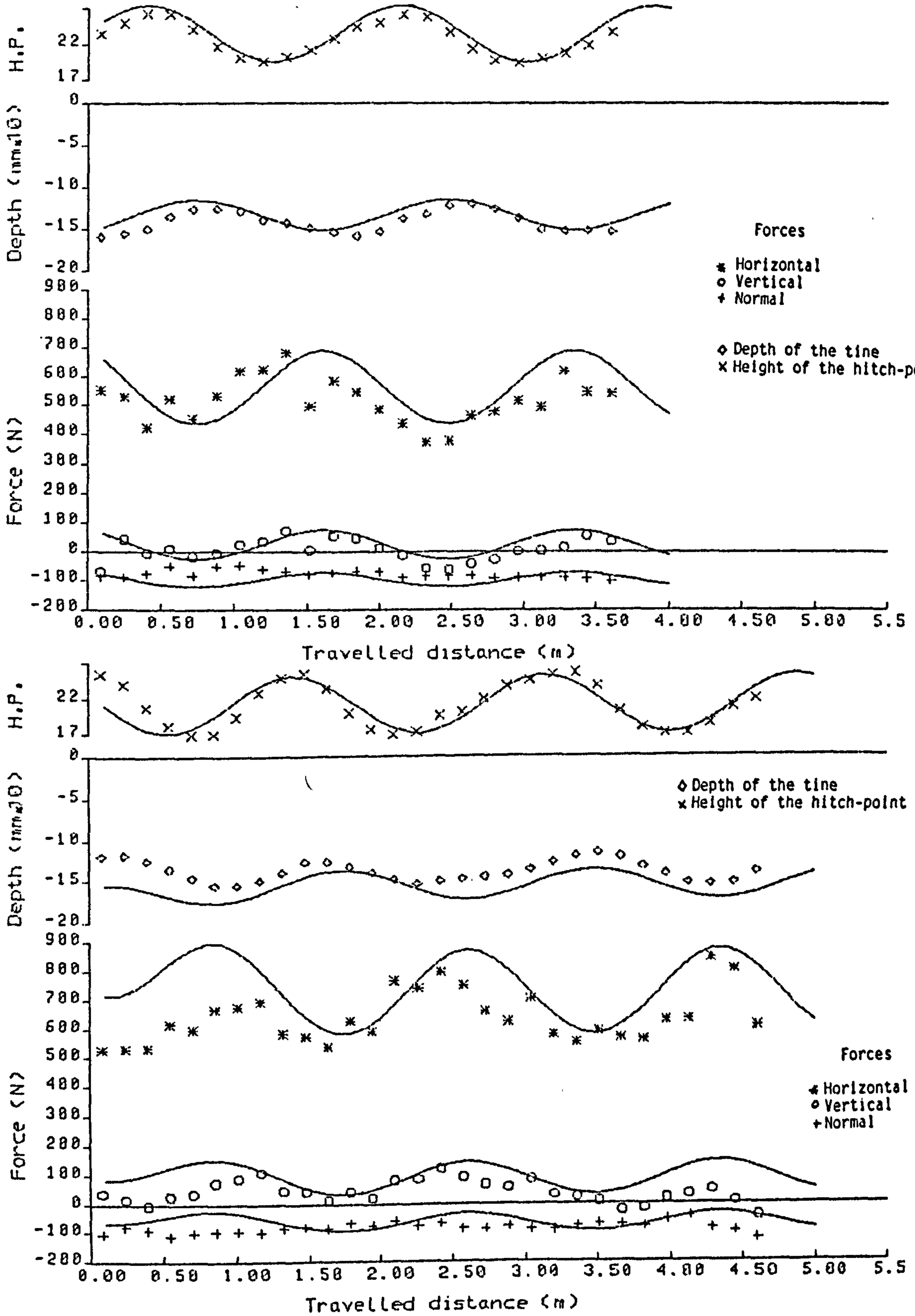

FIG. 6.13 Sinusoidal input of the hitch-point. Wavelength equal to 1.75 mm and amplitude of 40 mm

wavelength of the hitch-point. Since the results showed that the ratio X/Y (the response attenuation) is less than 1, it means that the system has a frequency ratio bigger than $\sqrt{2}$.

Fig. 6.11 (top-right) shows the phase angle Ø, the angular amount out of phase between the movement of the hitch-point and the implement depth response. There it is possible to observe that for frequency ratios bigger than 1 the out of phase angle of the implement movement in relation to the hitch-point movement becomes independent of the frequency ratio, and for damping ratio bigger than 1 its value will come close to 60^{o} (see broken line Fig. 6.11).

This means that the attenuation of the implement movement is always dependent on the frequency of the hitch-point, where better results are obtained as frequency values increase. Since the damping ratio is very large, there is not a critical value for the hitch-point frequency, but the biggest displacements of the implement will occur in case of very low frequency of the hitch-point (very long wavelength). The phase lag of the implement, in relation to the hitch-point movement, will always be 60^{o} independent of the frequency of the hitch-point, as long as it is bigger than the natural frequency, otherwise it will tend to be in phase with the hitch-point.

The response of the soil reaction forces have, as expected, a sinusoidal form. Since they are proportional to the depth of the implement, the forces response curves are in phase in relation to the path of the

implement (as can be observed in Figs. 6.12 and 6.13, they seem out of phase because the depth of the implement is plotted in a negative form). The magnitude of the forces, as shown in these figures, is in close agreement with the values estimated by the method proposed in chapter 5, especially in the vertical and horizontal directions.

It is also noticeable in these figures that the normal soil reaction force has a smaller amplitude than the other soil reaction forces. The reason for this is (as explained earlier in section 6.2.3) that this force only exists to compensate for the balance of moment about the beam hitch-point, and its magnitude is dependent upon the relation between the horizontal and vertical force.

Fig. 6.13 (bottom) shows that the results predicted by the theory and those obtained from the experimental tests do not totally agree. This is due to the fact that for some external reason the movement of the cam, which transmitted the motion to the hitch-point, did not have a sinusoidal displacement. This could be due either to a lack of lubrication, or to a error in the assembly of the system, for e.g. the shaft was out of centre in relation to the guide bearings, which could cause a slip in the cam. As can be observed in the other figures this did not happen, and the movement of the hitch-point was a perfect sinusoidal response.

6.3.4 Conclusions

From the tests explained above the following conclusions can be drawn:

a) For each position of the hitch-point, in relation to the soil surface, there is one equilibrium position for the implement to operate.

b) The slow response of the trenchless plough to movement of the hitch-point, due to its damped characteristics, prevents any sudden movement of the tine, and smooths the path of the drainage line.

c) The attenuation of the hitch-point movement is dependent on frequency ratio (w/wn), with better results obtained for larger values of (w/wn). In the case of a single displacement of the hitch-point, i.e. step input, the evidence shows that the path of the implement will be attenuated at a ratio of 1/1.50.

d) It was found that the depth response of the drainage implement is 60^{o} out of phase in relation to the movement of the hitch-point, and this value is independent of the frequency ratio for $w/wn > 1$.

e) The mathematical approach to predict the response of the implement in relation to the movement of the hitch-point was demonstrated to be reasonably accurate, being able to estimate the soil reaction forces and the path of the implement for all the situations tested.

CHAPTER 7

CONCLUSIONS

From the studies conducted and explained here with respect to the behaviour of a scale model of the trenchless plough drainage machine working under both restricted motion and dynamic conditions, in a soil bin filled with a sand loam soil, the following conclusions can be drawn:

i. The initial analyses of the implement revealed that:

   a. Due to its geometric characteristics and working conditions, the trenchless plough cutting blade can be considered a narrow tine. For that the model presented by Godwin and Spoor to predict the forces acting on the tine face, (based on the assumption that the soil worked by the tine obeys the Mohr-Coulomb failure criterion) extended to estimate the soil reaction forces acting on the sides of the tine can be used to predict the soil reaction forces on the tine.

   b. The centre of resistance, cr, the point of action of the soil reaction force on the implement tine face, is dependent on the depth of work of the implement. However it was found that the ratio between cr and depth of work can be considered constant and has the value of 0.88.

   c. The effect of moment of inertia on the system can be neglected although the equilibrium depth is a function of the system weight.

   d. Irregularities in the soil profile cause alteration in the

angle of the shear plane, and consequently in the length of the forward soil rupture distance ahead of the cutting blade. The angle of the shear plane, for different soil profiles can be estimated using the theory of Passive Earth Pressure proposed by Coulomb.

ii. The study of the implement behaviour under dynamic situations, i.e. when the implement is working over an uneven soil surface, or when the hitch-point of the system simulates the pitch action of the crawler tractor, demonstrated that:

a. The use of two pivoted points in the plough-beam system; one at the hitch-point and one at the end of the beam; connected through the free-link, enables the tine to find a desired equilibrium position, with its bottom parallel to the drainage line, for any position of the hitch-point in relation to the soil surface, as long as there is sufficient downwards vertical force to compensate for the moment generated by the horizontal soil reaction force.

b. The relationship between the height of the hitch-point and the equilibrium depth of the implement can be considered linear between the limits of the operational depth. However, since it was proven that is not a 1:1 relation, the grade of the line described by the hitch-point will differ from the grade of the drainage line.

c. In field situations where soil irregularities are in a

frequency up to three beam lengths, a better grade control of the trenchless plough drainage machine can be obtained if the hitch-point of the implement can be maintained parallel to a desired line, without being affected by the pitch action of the tractor.

d. In field situations where the soil irregularity is less frequent, or persists for a long distance (step inputs), the height of the hitch-point has to be correct in order to avoid the change in the grade of the drainage line, where the amount of correction of the hitch-point should obey the proportion ratio between it and the implement depth.

e. When it is impossible to exert control over the hitch-point, the damping reaction of a trenchless tine will smooth the displacement of the hitch-point. The attenuation of implement depth response in relation to the hitch-point is dependent on the frequency of the latter, where the phase angle is constant for values of frequency ratio (w/w_n) bigger than one.

iii. The mathematical model proposed, based on the dynamic balance of the forces involved in the system and on the findings explained above, proved to predict the dynamic behaviour of the implement adequately for the circumstances tested in this experiment.

vi. The computer programme developed to simulate the dynamic response of the implement (based on the mathematical model), can be a useful tool in the development of further improvements in the trenchless plough drainage machines, where several parameters can be easily tried and quickly evaluated in order to optimize its performance. Although it does not eliminate the need for the field test, it could simplify and minimize the number of tests required.

CHAPTER 8

SUGGESTIONS FOR FURTHER WORK

The dynamic behaviour of the trenchless plough drainage implement, although it has been clarified to a certain extend and the soil and tractor action on it explained, the problems involved in its performance are still far from being solved.

As revealed by the results obtained in this study, the influence of the soil irregularity in the path of the implement is very small, specially in fields with constant soil profile variation. In this case a better grade control can be obtained when the hitch-point of the system is maintained at constant level in relation to a reference plane. In certain cases where the field irregularity persists for long, then correction in the hitch-point height might be necessary. Due to the fact that there is not a 1:1 ratio between the depth of work and hitch-point height, the necessary amount of correction in the level of the hitch-point is not equal to the difference in the level of the soil profile.

In the light of these facts the following suggestions for further work are made, with the hope that a better grade control system for the drainage plough implement can be obtained in the future.

i. The commercially available linkage systems for the trenchless

plough should be studied, and the problems involved in its performance identified. This analysis will probably reveal the difficulties that exist in controlling the path of the hitch-point in reference to a desired level.

ii. a) The analysis for the trenchless plough conducted for the long floating beam arrangement with a real hitch-point should be extended and verified to include the virtual hitch-point and complex linkage cases.

b) With the results obtained from this linkage investigation, and using the mathematical model developed here for the real hitch-point and/or an extended model for the virtual hitch-point, it would be possible then to investigate the possibility of improvement in the linkage system and find a way to provide control over the hitch-point height in relation to a reference level.

iii. To compensate for the pitch motion of the power unit with regard to the implement when crossing uneven soil surfaces, it will be necessary to develop a control unit capable of sensing the soil profile ahead of the implement and conduct some calculations before sending the right information to the unit responsible for adjusting the hitch-point level. It will be essential that all the adjusting operations are done as a preventive method, i.e. to keep the implement at its desired level. This will considerably

improve the actual grade control method, which is currently only capable of correcting the path of the implement after it has already moved out of the desired drainage line.

iv. The difference in soil shear strength during the course of the implement shows very little effect on the implement behaviour, in the tests conducted here. This may be due to the fact that this small scale model of the trenchless plough does not have sufficient weight to overcome the bearing capacity of the soil. Therefore, further tests should be conducted with bigger models in order to check if these findings are still valid for a full scale model of the trenchless plough.

REFERENCES

ASRAFALI, H. (1980) An investigation of the soil forces acting on a scale model of a mole-plough. Bs.C dissertation, National College of Agricultural Engineering: Silsoe.

CASE, J. and CHILVER, A.H. (1971) An introduction to the mechanics of solids and structures. Edward Arnold (publishers) Ltd. (second edition), London.

CENTER NATIONAL DU MACHINE AGRICOLE, DU GENIE RURAL, DES EAUX ET DES FORESTS (1982) Technologies de l'Agriculture, mole drainage. Cemagref Report, etude No 485/486, France.

CHILDS, E.C. (1942) The mechanics of mole-draining. Empire Journal Exp. Agric., 169-181.

CLARK, S. J. and LILJEDAHL, J.B. (1968) Soil Bin, Artificial soils and scale-model testing. Transaction of the Amer. Soc. of Agric. Engr., 11(2): 198-202.

COOK, N.H. and RABINOWICZ, E. (1963) Physical measurement and analysis. Addison-Wesley Publishing Company, Inc., Massachusetts: U.S.A.

COWELL, P. and MAKANJOULA, G. A. (1966) The lateral dynamic behaviour of tractor-mounted implements, with particular reference to the three-point-linkage. J. Agric. Engng. Res., 11(3): 152-169.

COWELL, P. and LEN, S. C. (1967) Field performance of tractor draught control systems. J. Agric. Engng. Res., 12(3): 205-221.

COWELL, P. (1970) Automatic control of tractor mounted implements. Conference on agricutural and allied industries tractors, Inst. of Mech. Engr., London.

COWELL, P. and MILNE, M.J. (1977) An implement control system using pure draught force sensing and modified linkage geometry. J. Agric. Engng. Res., 22: 353-371.

COWELL, P. and SIAL, F.S. (1976) Theory of the dynamic behaviour of mouldboard ploughs during penetration. J. Agric. Engng. Res., 21(3): 313-323.

CROLLA, D.A. and PEARSON, G. (1975) Response of tractor draught controls to randon inputs. J. Agric. Engng. Res., 20(2): 181-197

CROS, P.L.; LECHAUX, H. and WOLSACK, J. (1978) Drain laying quality survey. Proceedings of the International Drainage Workshop, Wageningen, The Netherlands. May 16-20

CULPIN, C. (1971) Mechanical equipment for field drainage and ditching. United Nations, Economic Commission for Europe, Agric. Mechanization.

DRANSFIELD, P.; WILLATT, S.T. and WILLIS, A.H. (1964) Soil-to-implement reaction experienced with simple-tines at various angles of attack. J. Agric. Engng. Res., 9: 220-224.

EDE, A.N. (1961) Experimental land drain installation and function of field drainage. Ph.D. Thesis (unpublished) University of Cambrige

EDE, A.N. (1965) New materials and machines for drainage. Proceedings Amer. Soc. of Agric. Engr., Conference: Drainage for efficient crop production. pp 58-61. Chicago, Illinois, December 6-7.

FOOD AND AGRICULTURAL ORGANIZATION (1973) Drainage machinery. European Comission on Agric. Working Party on Water Resources and Irrigation. Irrigation and Drainage Paper 15. Bucharest, Romania.

FOUSS, J.L. (1971) Dynamic response of automatically controlled mole-drain plow. Ph.D. Thesis (unpublished) The Ohio State University, USA.

FOUSS, J.L.; HOLMES, R.G. and SCHWAB, G.O. (1964) Automatic grade control of subsurface drainage equipment. Transactions of Amer. Soc. of Agric. Engr., 7(2): 111-113.

FOUSS, J.L. and ALTERMATT, W.E. (1982) Drainage-plow "boot" design to improve installations of corrugated plastic tubing. Proceedings of the Amer. Soc. of Agric. Engr., Fourth Nat. Drainage Symp., Dec 13-14.

FREITAG, D.R.; SCHAFER, R.L. and WISMER, R.D. (1970) Similitude studies of soil-machine systems. J. of Terramechanics 7(2): 25-59.

GODWIN, R.J. (1974) An investigation into the mechanics of narrow tines in frictional soils. Unpublished Ph.D. Thesis, University of Reading.

GODWIN, R.J. (1975) An extended octagonal ring transducer for use in tillage studies. J. Agric. Engng. Res., 20(4): 347-352.

GODWIN, R.J. (1982) Forces measurement on tillage implements. 9th Conference of International Soil Tillage Research Organization, Yugoslavia.

GODWIN, R.J. and SPOOR, G. (1977) Soil failure with narrow tines. J. Agric. Engng. Res., 22: 213-228.

GODWIN, R.J.; SPOOR, G. and KILGOUR, J. (1980) The design and operation of a simple low cost soil bin. J. Agric. Engng. Res., 25: 99-104

GODWIN R.J.; SPOOR, G. and LEEDS-HARRISON, P. (1981) An experimental investigation into the forces mechanics and resulting soil disturbance of the mole-ploughs. J. Agric. Engng. Res., 26: 447-497.

GODWIN, R.J.; SPOOR, G. and SOOMRO, M.S. (1984) The effect of tine arrangements on soil forces and disturbance. J. Agric. Engng. Res., 30(1): 47-56.

HETTIARATCHI, D.R.P. and REECE, A.R. (1967) Symetrical three-dimensional soil failure. J. of Terramechanics, 4(3): 45-67

HETTIARATCHI, D.R.P. and REECE, A.R. (1974) The calculation of passive soil resistance. Geotechnique, 24: 289-310.

HETTIARATCHI, D.R.P.; WITNEY B.D. and REECE A.R. (1966) The calculation of passive pressure in two-dimensional soil failure. J. Agric. Engng. Res., 11(2): 89-107.

HUDSON, A.W.; HOPEWELL, H.G.; BOWLER D.G. and GROSS M.W. (1962) The drainage of farm lands. Bulletin no.18, Massey College Palmesston North, New Zealand.

JOHNSTON, M. (1982) Mole-plough performance in relation to surface undulation. Bs.C. Thesis (unpublished), Nat. College of Agric. Engineering, Silsoe.

KOSTRITSYN, A.K. (1956) Cutting of a cohesive medium with knives and cones. National Institute of Agricultural Engineering, Translation No. 58, Silsoe.

McKYES, E. and ALI, O.S. (1977) The cutting of soil by narrow blades. J. of Terramechanics, 14(2): 43-58.

MEYERHOF, G.C. (1951) The ultimate bearing capacity of fundations. Geotechnique, 2(4): 310-332

NAARDING, W.H. (1978) Trenching and trenchless drainage techniques. Proceedings of Int. Drain. Workshop, Wageningen, May 16-20.

O'CALLAGHAN, J.R. and FARRELLY, K.M. (1964) Cleavage of soil by tined implements. J. Agric. Engng. Res., 9: 259-270.

O'CALLAGHAN, J.R. and McCULLEN, P.J. (1965) Cleavage of soil by inclined and wedge-shaped tines. J. Agric. Engng. Res., 10: 248-254.

PAYNE, P.C.J. (1956) The relationship between the mechanical properties of soil and the performance of simple cultivation implements. J. Agric. Res., 1(1): 23-50.

PAYNE, P.C.J. and TANNER, D.W. (1959) The relationship between rake angle and performance of simple cultivation implements. J. Agric. Engng. Res., 4(4): 312-325.

PERRY, C.C. and LISSNER, H.R. (1962) The strain gauge primer. McGraw-Hill Book Company, 2nd. edition, USA.

REECE, A.R. (1965) The fundamental equation of earth-moving mechanics. Proceedings of the Symp. Earthmoving Machin. (Inst. Mech. Engineers.), London, March 16-17.

REECE, A.R.; GUPTA, R. and TAYAL, S.S. (1966) The lateral stability of tractor implements. J. Agric. Engng. Res., 11(2): 80-88.

REEVE, R.C. (1978) Trenchless drainage. Proceedings of Int. Drain. Workshop, Wageningen, May 16-20

ROADSMA (1974) Drainage for agriculture agronomy. American Soc. Agron. (17), Madison, Wis., U.S.A.

RYCROFT, D.W. (1983) Land drainage planning and design of agricultural drainage system. Basford Academic and Educational Ltd., London.

SCHAFER, R.L.; REAVES, C.A. and YOUNG, D.F. (1968) An interpretation of distortion in the similitude of certain soil machine system. Transactions of the Amer. Soc. of Agric. Engr., 12(1): 145-149.

SCHOLTZ, D.C. (1966) A three-point linkage dinamometer for restrained linkages. J. Agric. Engng. Res., 11(1): 33-37.

SCHURING, D.J. (1977) Scale model in engineering fundamentals and applications. Pergamon Press, Great Britain.

SIEGEL, M.; MALEEV, V.L. and HARTMAN, J.B. (1965) Mechanical design of machines. International Text Book Company Scranton, Pensylvania, USA.

SIEMENS, J.C. and WEBER, J.A. (1964) Soil bin for model studies on tillage tools and traction devices. J. Terramechanics, 1: 56-57.

SINGH, L.P. (1982) Vertical dynamic behaviour of trenchless drainage ploughs. Ph.D. Thesis (unpublished), National College of Agricultural Engineering, Silsoe.

SOLTYNSKI, A. (1968) Physical similarity and scale effects in soil machine system. J. Terramechanics, 5(2): 31-43

SPOOR, G. (1969) Design of soil engaging implements. Farm Machin. Design Engng. Sept.: 22-25.

SPOOR, G. and GODWIN, R.J. (1978) An experimental investigation into the deep loosening of soil by rigid tines., J. Agric. Engng. Res., 23: 243-258.

SPOOR, G.; LEEDS-HARRISON, P.B. and GODWIN, R.J. (1982) Some fundamental aspects of the formation stability and failure of mole drainage channels. J. of Soil Sci., 33: 411-425.

SPOOR, G. and FRY, R.K. (1983a) Field performance of trenchless drainage tines and implications for drainage system efficiency. J. Agric. Engng. Res., 28:319-335.

SPOOR, G. and FRY, R.K. (1983b) Soil disturbance generated by deep-woking low rake angle narrow tines. J. Agric. Engng. Res., 28:217-234.

STAFFORD, J.V. (1979) The performance of a rigid tine in relation to a soil properties and speed. J. Agric. Engng. Res., 24:41-56.

TERZAGHI, K. and PECK, R.B. (1967) Soil mechanics in engineering practice. John Wiley & Sons (2nd edition), N.Y., USA.

THEOBALD, G.H. (1963) Methods and machines for tile and other tube drainage. Food and Agricultural Organization, (Agriculture Develop. Paper No. 78).

THOMSON, W.T. (1973) Theory of vibration with applications. Prentice-Hall Inc., New Jersey, U.S.A.

VERMA, B.P. and SCHAFER, R.L. (1968) Compensated model theory in the similitude of soil-chisel system. Paper No. 68-656. Presented at the 1968 winter meeting of the Amer. Soc. of Agric. Engr., Chicago, Illinois, U.S.A.

VERMA, P.B. and SCHAFER, R.L. (1969) A distorted-model theory for non-uniform soil strength profile. Amer. Soc. of Agric. Engr, Indiana. June 22-25

WELLS, A.A. (1951) Soil mechanics and tillage . Ph.D. Thesis (unpublished), University of Cambridge.

YOUNG, D.F. (1968) Similitude of soil-machine system. Transactions of the Amer. Soc. of Agric. Engr., 11(5): 653-657.

Table 4.1
Resuts of tests to determine the position of the resultant force

Depth mm	Resultant newtons	Angle deg	centre of res. mm	ratio cr/d
198.0	888.41	23.75	161.2	0.814
196.8	889.13	24.95	172.6	0.876
194.7	843.10	24.30	165.4	0.849
191.0	831.20	26.29	167.5	0.877
188.1	808.25	24.01	155.2	0.824
186.2	843.30	25.45	160.9	0.864
183.7	742.89	24.76	164.2	0.893
183.2	826.31	24.06	156.7	0.855
180.8	726.03	24.56	155.9	0.862
180.4	701.26	24.24	160.3	0.888
180.0	805.75	25.45	160.9	0.863
177.7	789.29	26.58	166.3	0.920
176.9	777.16	23.86	152.3	0.860
177.3	769.72	23.54	146.7	0.827
173.2	840.72	25.16	147.9	0.853
171.8	840.01	24.79	145.3	0.853
170.5	769.92	23.97	155.1	0.886
169.2	664.97	24.42	163.7	0.967
167.7	667.58	23.98	157.3	0.937
166.2	693.62	26.18	142.5	0.864
164.4	548.03	27.97	147.3	0.896
164.1	689.90	24.12	147.2	0.896
163.0	673.26	27.61	129.1	0.791
158.1	633.91	27.06	140.5	0.888
157.8	566.20	26.85	139.7	0.885
156.9	580.73	27.77	143.9	0.917
154.5	525.87	23.35	141.0	0.919
150.8	602.06	27.79	130.7	0.866
150.0	489.64	28.03	132.4	0.851
149.1	585.51	26.87	132.7	0.889
147.7	595.51	27.25	126.6	0.857
147.1	608.41	26.39	134.1	0.893
146.9	585.51	26.70	131.8	0.897
144.7	592.18	26.37	130.5	0.962
141.7	573.25	28.17	130.4	0.919
140.9	491.47	26.71	127.1	0.900
138.8	514.11	26.02	120.3	0.860

sample meam = 0.877
standard deviation = 0.0353
variance = 0.0012

TABLE 4.2
Angle of inclination and depth of the implement during penetration and raising

Penetration			Penetration			Raising		
Depth mm	Angle deg	Ratio 0/0o	Depth mm	Angle deg	Ratio 0/0o	Depth mm	Angle deg	Ratio 0/0o
87.4	5.35	--	104.8	5.63	--	169.6	-5.47	--
97.9	4.26	0.796	103.2	5.27	0.936	156.9	-4.08	0.746
107.1	4.17	0.779	112.6	4.17	0.741	138.9	-3.65	0.667
102.2	3.24	0.606	112.1	4.08	0.725	139.5	-3.67	0.671
102.9	3.13	0.585	120.4	3.40	0.604	126.8	-2.80	0.512
110.2	2.40	0.449	124.8	2.93	0.520	132.2	-3.10	0.567
108.7	2.28	0.426	124.8	2.70	0.480	119.9	-2.29	0.419
112.3	1.95	0.364	125.7	2.36	0.419	124.1	-2.47	0.452
116.7	1.61	0.301	138.6	1.61	0.286	117.9	-2.15	0.393
118.8	1.38	0.258	134.1	2.06	0.366	111.0	-1.72	0.314
114.9	1.51	0.282	136.3	1.35	0.240	109.9	-1.72	0.314
120.6	1.11	0.207	140.5	0.97	0.172	110.9	-1.70	0.311
122.5	1.02	0.191	140.7	0.85	0.151	106.4	-1.54	0.282
123.3	0.95	0.178	139.7	1.05	0.187	102.6	-1.28	0.234
125.2	0.66	0.123	143.8	0.70	0.124	95.4	-0.81	0.148
128.3	1.41	0.077	140.0	0.99	0.176	98.7	-0.94	0.072
130.8	0.15	0.028	148.0	0.41	0.073	102.0	-1.11	0.203
125.2	0.46	0.086	140.9	0.82	0.146	93.7	-0.70	0.128
123.8	0.53	0.099	150.2	-0.14	0.025	88.7	-0.35	0.064
130.6	0.07	0.013	141.5	0.65	0.115	96.1	-0.72	0.132
126.1	0.31	0.058	151.0	-0.04	0.007	91.3	-0.47	0.086
128.0	0.13	0.024	146.6	0.29	0.052	91.5	-0.33	0.060
128.3	0.10	0.019	147.6	0.22	0.039	91.8	-0.35	0.064
124.5	0.37	0.069	152.6	-0.13	0.023	91.0	-0.34	0.062
130.0	0.03	0.006	150.4	-0.02	0.004	89.3	-0.33	0.060
128.9	0.08	0.015	146.7	0.22	0.039	91.4	-0.41	0.075
129.8	-0.05	0.009	147.8	0.05	0.009	86.2	-0.13	0.024
129.8	-0.02	0.000	147.7	-0.06	0.011	86.9	-0.01	0.002

Note: (-) the implement is turned backwards
(+) the implement is turned forwards

TABLE 4.3
Results of tests with implements of different weights

Total weight 432 (N)			Total weight 186 (N)			Total weight 142 (N)		
Depth mm	Leg angle Deg	Ratio 0/0o	Depth mm	Leg angle Deg	Ratio 0/0o	Depth mm	Leg angle Deg	Ratio 0/0o
103.2	6.90	--	97.2	5.78	--	83.7	6.04	--
100.1	6.65	0.96	92.4	4.60	0.88	97.6	4.74	0.78
118.7	5.16	0.77	109.9	4.14	0.72	99.1	4.58	0.76
118.6	4.50	0.67	114.2	3.82	0.66	104.3	40.8	0.68
121.5	4.16	0.62	118.9	3.40	0.59	107.2	3.78	0.63
132.0	3.12	0.47	122.9	3.02	0.52	109.9	3.48	0.58
130.4	3.30	0.50	122.7	2.89	0.50	111.9	2.83	0.47
136.2	2.50	0.38	127.1	2.49	0.43	116.5	2.43	0.40
138.5	2.26	0.34	130.4	2.19	0.38	114.2	2.58	0.43
141.1	1.91	0.29	129.2	2.08	0.36	120.6	2.13	0.35
143.8	1.68	0.25	134.1	1.88	0.33	123.1	1.95	0.32
144.8	1.41	0.21	133.7	1.52	0.26	123.1	1.95	0.32
149.4	1.25	0.19	132.0	1.79	0.31	121.0	2.02	0.33
149.6	0.99	0.15	138.1	1.05	0.18	125.7	1.80	0.30
150.1	0.78	0.12	132.3	1.38	0.24	127.7	1.52	0.25
151.1	0.67	0.15	141.1	0.65	0.11	125.5	1.68	0.28
148.9	0.73	0.11	136.7	0.93	0.16	131.3	1.11	0.18
155.8	0.09	0.01	137.4	0.86	0.15	123.9	1.61	0.27
153.0	0.23	0.03	136.4	0.90	0.16	130.7	1.08	0.18
148.0	0.56	0.08	137.3	0.72	0.12	132.3	0.93	0.15
158.2	-0.10	-0.02	135.3	0.88	0.15	131.9	0.99	0.16
155.7	0.21	0.03	137.6	0.71	0.12	132.9	0.88	0.15
159.0	0.05	0.01	135.7	0.68	0.12	130.8	1.05	0.17
159.3	0.23	0.03	138.7	0.49	0.08	132.1	0.88	0.14
			136.6	0.77	0.13	136.5	0.51	0.08
			137.2	0.66	0.11	132.9	0.82	0.13
			138.7	0.61	0.12	135.4	0.57	0.09
			137.5	0.61	0.11	132.6	0.75	0.12
			136.8	0.69	0.12	135.3	0.70	0.08
			135.8	0.52	0.09	135.9	0.40	0.06

TABLE 4.4
Results of tests conducted in the soil bin prepared with two different soil densities in the same run

	Forces		Resultant			
	H (N)	V (N)	Leg (N)	Total (N)	Ang. (Deg.)	Depth (mm)
	1013.0	208.10	1034.25	1106.16	23.67	158.4
	952.10	181.03	969.15	1039.42	23.65	157.4
	991.46	199.17	1011.27	1082.76	23.69	151.7
a	878.19	147.72	890.53	958.37	23.60	154.2
	939.13	176.03	955.49	1025.54	23.68	159.4
	932.34	180.49	949.65	1021.14	23.07	155.4
	869.99	148.25	888.53	951.07	23.63	158.4
	842.01	134.55	822.70	919.94	23.75	156.8
	763.33	104.32	770.42	835.75	24.03	163.8
	721.12	64.56	714.01	781.25	22.62	157.8
	637.03	45.83	638.68	696.60	23.86	163.2
	688.99	56.21	691.28	748.39	22.98	163.8
	710.05	67.71	713.27	772.28	23.15	160.6
	753.53	94.92	759.48	822.99	23.70	165.8
	738.87	104.23	746.79	813.44	24.72	163.8
	776.72	125.71	786.83	856.22	24.97	164.5
b	774.76	123.74	784.58	854.20	24.90	164.5
	749.11	123.74	784.58	854.20	24.90	164.5
	730.71	83.44	725.46	797.48	23.61	166.0
	692.75	66.56	695.95	755.95	23.59	165.1
	773.47	110.50	781.32	847.54	21.13	166.4
	753.99	100.13	760.61	825.52	24.02	168.1
	726.52	84.31	731.48	794.00	23.79	165.1
	773.83	135.29	780.96	854.75	23.79	167.7
	722.08	77.54	726.23	787.22	23.47	167.5
	750.36	83.81	755.03	815.07	23.08	169.0

Soil density = a) 1680 kg/m^3
b) 1350 kg/m^3

	Forces		Resultant			
	H (N)	V (N)	Leg (N)	Total (N)	Ang. (Deg.)	Depth (mm)
	789.60	100.03	795.91	858.13	23.05	139.5
	799.56	103.80	806.27	868.77	23.02	139.7
	749.42	78.99	753.57	812.93	22.79	136.3
	832.54	124.07	841.74	907.07	23.38	140.3
	779.10	91.06	784.41	844.94	22.77	134.5
	829.12	115.16	837.08	900.42	22.95	136.8
	680.46	69.21	683.97	745.77	24.15	136.8
	784.47	93.90	790.07	851.02	27.80	137.8
a	851.56	123.62	860.58	924.47	22.89	134.3
	731.42	70.77	743.83	793.11	22.74	136.4
	822.43	113.10	813.46	894.38	22.97	138.2
	809.83	93.42	815.30	874.36	22.13	128.4
	723.31	81.97	727.95	790.12	23.73	146.5
	647.43	31.67	648.20	700.58	22.46	133.1
	605.76	18.56	606.04	657.07	22.79	135.6
	629.65	42.57	631.09	682.52	23.86	137.5
	604.76	11.40	604.87	653.41	22.24	134.2
	635.77	38.76	636.95	692.61	23.37	139.1
b	606.60	21.08	607.08	660.01	23.20	135.3
	617.71	29.15	615.40	669.46	23.33	138.0
	635.24	41.13	636.57	693.06	23.57	133.7
	631.45	39.02	632.35	688.74	23.53	136.7
	664.41	54.87	666.67	725.29	23.64	137.7
	629.43	31.28	630.37	685.01	23.33	136.0
	528.95	-4.64	528.98	577.34	23.62	136.1
	603.75	25.38	604.28	657.90	25.41	138.5

Soil density = a) 1500 Kg/m^3
b) 1350 kg/m^3

	Forces		Resultant			
	H (N)	V (N)	Leg (N)	Total (N)	Ang. (Deg.)	Depth (mm)
	374.41	-58.17	378.81	414.41	25.41	162.2
	364.52	-63.34	369.82	403.67	25.47	158.7
	379.48	-52.09	383.15	421.34	25.75	158.0
	383.36	-51.96	386.87	425.25	25.64	161.6
a	356.51	-64.06	362.22	395.80	25.74	160.8
	365.52	-60.44	370.48	405.49	25.65	159.6
	359.54	-64.30	365.25	398.43	25.52	160.3
	369.48	-53.75	347.37	411.99	26.25	159.7
	728.48	98.75	735.09	801.55	24.65	158.3
	760.95	108.25	768.61	835.20	24.34	151.5
	784.82	163.17	794.16	862.92	24.59	161.9
	735.66	88.43	740.96	804.03	23.79	144.1
	804.04	132.29	813.29	880.26	24.01	155.2
	694.84	73.92	698.78	760.81	24.03	151.7
	732.34	84.26	735.37	799.49	23.61	149.9
	699.76	73.87	703.65	765.30	23.88	152.4
	746.34	108.74	754.22	822.11	24.79	150.6
b	702.65	72.84	706.41	767.53	23.72	149.6
	642.73	46.64	644.41	702.13	23.73	148.0
	763.41	93.55	769.12	831.51	23.34	149.3
	632.86	35.77	633.87	688.75	23.24	150.0
	694.44	65.77	697.55	757.18	23.48	147.3
	684.51	64.34	687.53	747.51	23.69	148.7
	704.10	77.90	708.40	770.91	24.02	146.3
	632.81	48.69	634.68	693.90	24.22	146.6

Soil density = a) 1200 Kg/m^3
b) 1500 kg/m^3

TABLE 6.1
Time response for the implement to reachieve its equilibrium position when the hitch-point is moved.

Raising	Predicted		Experimental	
displacement m	Depth mm	ratio (d-de)/(do-de)	Depth mm	ratio (d-de)/(do-de)
0.0	176.8	1.00	180.1	1.00
0.1	167.3	0.80	---	---
0.2	159.7	0.64	---	---
0.3	153.5	0.51	---	---
0.4	148.6	0.41	158.7	0.53
0.5	144.6	0.33	---	---
0.6	141.4	0.26	---	---
0.7	138.9	0.21	---	---
0.8	136.8	0.16	144.8	0.20
0.9	135.2	0.13	---	---
1.0	133.8	0.10	---	---
1.1	132.8	0.08	---	---
1.2	132.0	0.06	137.1	0.05
1.3	131.3	0.05	---	---
1.4	130.7	0.04	---	---
1.5	130.3	0.02	---	---
1.6	130.0	0.02	135.7	0.02

Penetration	Predicted		Experimental	
displacement mm	Depth mm	ratio (d-de)/(do-de)	Depth mm	ratio (d-de)/(do-de)
0.0	129.0	1.00	133.3	1.00
0.1	138.0	0.81	---	---
0.2	145.6	0.65	---	---
0.3	151.7	0.53	---	---
0.4	156.5	0.42	156.8	0.45
0.5	160.5	0.34	---	---
0.6	163.6	0.27	---	---
0.7	166.2	0.21	---	---
0.8	168.2	0.17	164.7	0.26
0.9	169.9	0.13	---	---
1.0	171.2	0.11	---	---
1.1	172.3	0.08	---	---
1.2	173.1	0.07	172.8	0.07
1.3	173.8	0.05	---	---
1.4	174.4	0.04	---	---
1.5	174.9	0.03	---	---
1.6	175.2	0.02	173.8	0.05

APPENDIX 1

Detailed drawings of the equipment designed for the study

APPENDIX 2

The trenchless tine transducer design

Material EN24	1½ Nickel Chromium Molybdenum Steel
Tensile Strenght	55/65 T.S.I
Yield Strength	44 T.S.I
Modulus of elasticity	2.1×10^5 N/mm^2

Design requirement

Estimated maximum applied moment	90 KN mm
Estimated maximum applied force	600 N (uniform load)
Safety factor	K = 2.5

Design details

a) Tension

Allowable tension σal = 44 T.S.I. = 600 N/mm^2

Maximum tension $\sigma max = al/K$ = 240 N/mm^2

at the weakest point 

b = 10 mm; h = 15 mm; y = 7.5 mm

APPENDIX 2

The trenchless tine transducer design

Material EN24	1½ Nickel Chromium Molybdenum Steel
Tensile Strenght	750/890 N/mm^2
Yield Strength	600 N/mm^2
Modulus of elasticity	2.1×10^5 N/mm^2

Design requirement

Estimated maximum applied moment	90 KN mm
Estimated maximum applied force	600 N (uniform load)
Safety factor	K = 2.5

Design details

a) Tension

Allowable tension $\sigma al = 600\ N/mm^2$

Maximum tension $\sigma max = \sigma al/K = 240\ N/mm^2$

at the weakest point 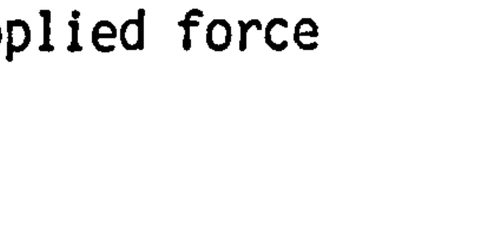

b = 10 mm; h = 15 mm; y = 7.5 mm

$$Mmax = \frac{Ix.\sigma max}{y} = 90 \text{ KN mm}$$

b) Deflection

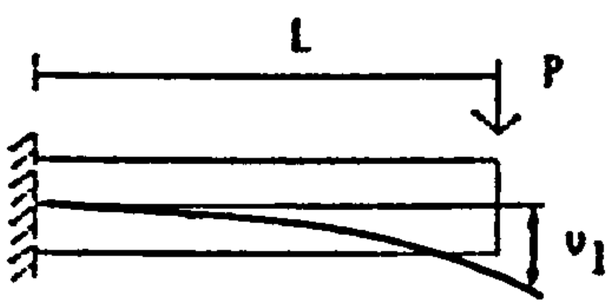

$$v_1 = \frac{P\ L^3}{8\ E\ I} \text{ (uniform load)}$$

$$v_1 = 0.43 \text{ mm}$$

APPENDIX 3

Details of the Strain Gauge Bridge Network

The strain gauges were wired in three four arm bridge network, one for each of the two forces, Fx and Fy, and one for the moment Mz, as shown in Fig. A3.1.

The strain gauges in each bridge have the same physical characteristics and their position were determined in order to give the maximum sensitivity and less interference from the other circuits.

Considering a simplified section of the "L-shaped" transducer, Fig. A3.1, the analysis of the effect of the forces and their position on the bridge composed by the gauges 1 to 4 are as follows:

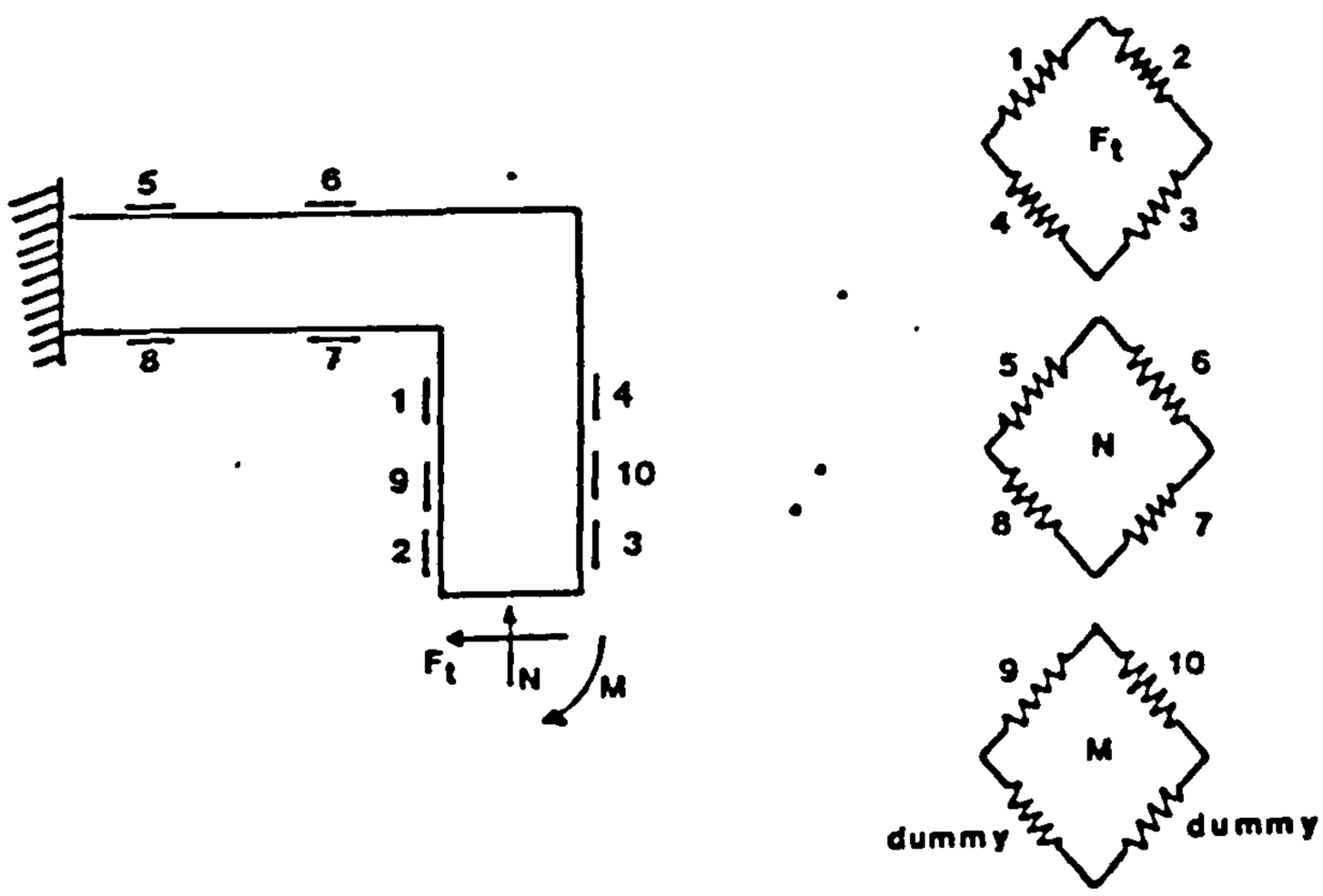

Since the strain gauges have the same resistance (Ro), force F1 causes deformation of the strain gauge

$S1 = Ro + \Delta R$; $S2 = Ro + \mu R$; $S3 = Ro - \mu \Delta R$; $S4 = Ro - \Delta R$

where the voltage meter is

$$\frac{\Delta V}{Vo} = \frac{(R1.R3) - (R2.R4)}{(R1+R4) . (R2+R3)} \qquad (A3.1)$$

$$\frac{\Delta V}{Vo} = \frac{2\ Ro\ \ R\ (1 - \mu)}{4Ro^2} = \frac{\Delta R}{2Ro}(1-\mu) \qquad (A3.2)$$

The bridge constant K is given by:

$$K = \frac{\Delta V/Vo}{\frac{1}{4}\ R/Ro} = 2\ (1-\mu) \qquad (A3.3)$$

and

$$\frac{\Delta V}{Vo} = \frac{K}{4}\ GF\ \ \varepsilon \qquad (A3.4)$$

where

$$\varepsilon = \frac{P\ L\ \ t}{E\ I\ \ 2} \qquad \text{and} \qquad I = \frac{b\ t^3}{12}$$

$$\frac{\Delta V}{Vo} = \frac{2(1 - \mu)}{4}\ GF\ \frac{F1\ L\ t}{2\ E\ \frac{b\ t}{12}^3} \qquad (A3.5)$$

Since $L - a = l$ and $\mu = a/L$ substituting then in the equation A3.5

$$\frac{\Delta V}{Vo} = \frac{3\ GF\ F1}{E\ b\ t^2}\ l \qquad (A3.6)$$

Therefore, the circuit is sensitive to any force in the F1 direction ($K \neq 0$) and it is independent of its position.

The draught force F2 would affects the strain gauges uniformly given: $S1 = S2 = S3 = S4 = Ro - \Delta R$, thus given zero $\Delta V/Vo$ output. Consequently the bridge is insensitive to forces in that direction.

The moment M will provide

$S1 = S2 = Ro + \Delta R$; $S3 = S4 = Ro - \Delta R$ so,

$$\frac{\Delta V}{Vo} = \frac{(Ro^2 - \Delta R^2) - (Ro^2)}{4Ro - 4R^2} = 0 \qquad (A3.7)$$

Therefore, the circuit is not sensitive to the moment M.

The same analusis is valid for the second bridge circuit (strain gauges 5,6,7 and 8), which is sensitive only to the force Fy and not to Fx or any couple genereted by its eccentricity.

The third bridge, formed by the strain gauges 9,10,11 and 12, where the strain gauges 11 and 12 are dummy, is proportional to the sum of each acting strain gauge output, for moments arising from applied eccentric loads.

Fx and Fy eccentric give $S9 = Ro + \Delta R$; $S10 = Ro - \Delta R$; $S11 = S12 = Ro$

$$\frac{\Delta V}{Vo} = \frac{(Ro + \Delta R)\ Ro - (Ro - \Delta R)\ Ro}{4\ Ro} = \frac{R}{2Ro} \qquad (A3.8)$$

$$K = \frac{\Delta V/Vo}{R/Ro} = 2 \qquad (A3.9)$$

from equation A3.4

$$\frac{V}{Vo} = \frac{1}{2} GF\ E = \frac{1}{12} GF \frac{F\ L}{E\ b\ t^2} = \frac{1}{12} GF \frac{M}{E\ b\ t^2} \qquad (A3.10)$$

Therefore, the bridge is sensitive to any eccentric force and the output is proportional to the eccentricity L.

APPENDIX 4

DETERMINATION OF THE INSTRUMENTS CHARACTERISTICS

A4.1 Introduction

The transducers used in the experimental work during this project had to be calibrated to determine their response to different loading systems. In order to minimize the error during the calibration, the strain gauge amplifiers were not used. A 9 volts stabilized D.C. was used as a source of energy for the bridge and the output signal recorded using a high precision digital voltmeter.

Static load was applied in increments at different positions within the working range dependent upon which the transducer bridge was being calibrated.

A4.2 The extended octagonal ring transducer.

Details of construction of the extended octagonal ring transducer, (Fig A4.1) are given by Godwin (1975), therefore only the calibration characteristics are presented here.

A4.2.1 Fx bridge

Table A4.1 and Fig. A4.2 show the results of the transducer submitted to

a horizontal load where the following can be observed:

i. Linear response with coefficient of regression analysis of r^2=0.9983.

ii. The hysteresis effect on the output; due to difference in the characteristics of the transducer material and strain gauge, and the bonding material, was found to be a maximum deviation of:

$$\pm \frac{10.11 - 9.99}{10.11 + 9.99} \times 100\% = 0.60\%$$

iii. The maximum error between the output due to application of load at different position was no greater than 2.9%.

A4.2.2 Fy bridge

The results of load application in the vertical direction are presented in Table A4.2 and Fig. A4. 1, where the following can be observed:

i. Linear response with coefficient of regression analysis of r^2 = 0.99998.

ii. The hysteresis effect on the output results was found to be the maximum value of: $\pm \frac{7.58 - 7.53}{7.58 + 7.53} \times 100\% = 0.33\%$

A4.2.3 Mz bridge

The results for the Mz bridge for load in the horizontal direction are shown in Table A4.1 and Fig. A4.4, and in Table A4.2 for load in the vertical direction, where the following can be observed:

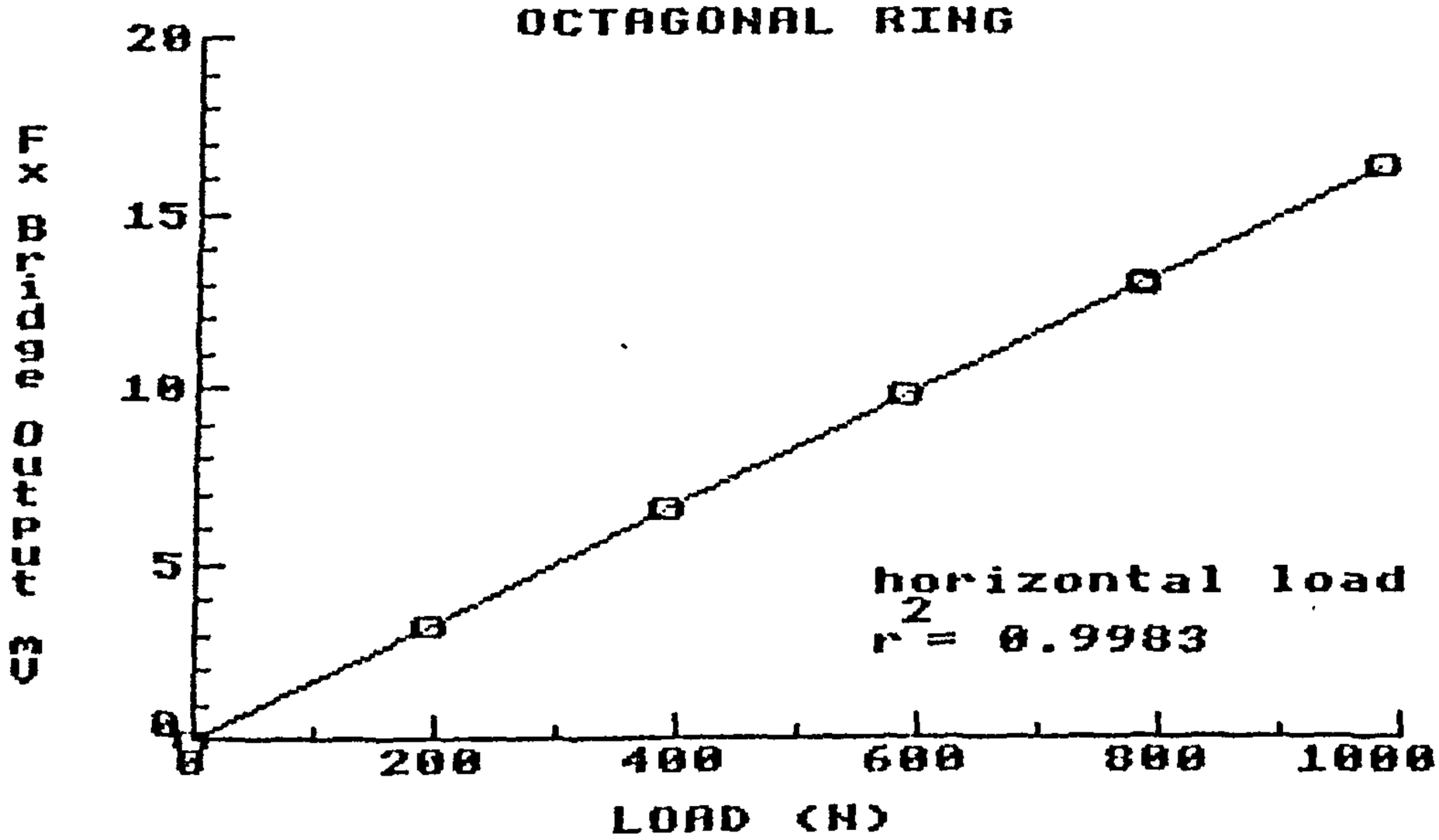

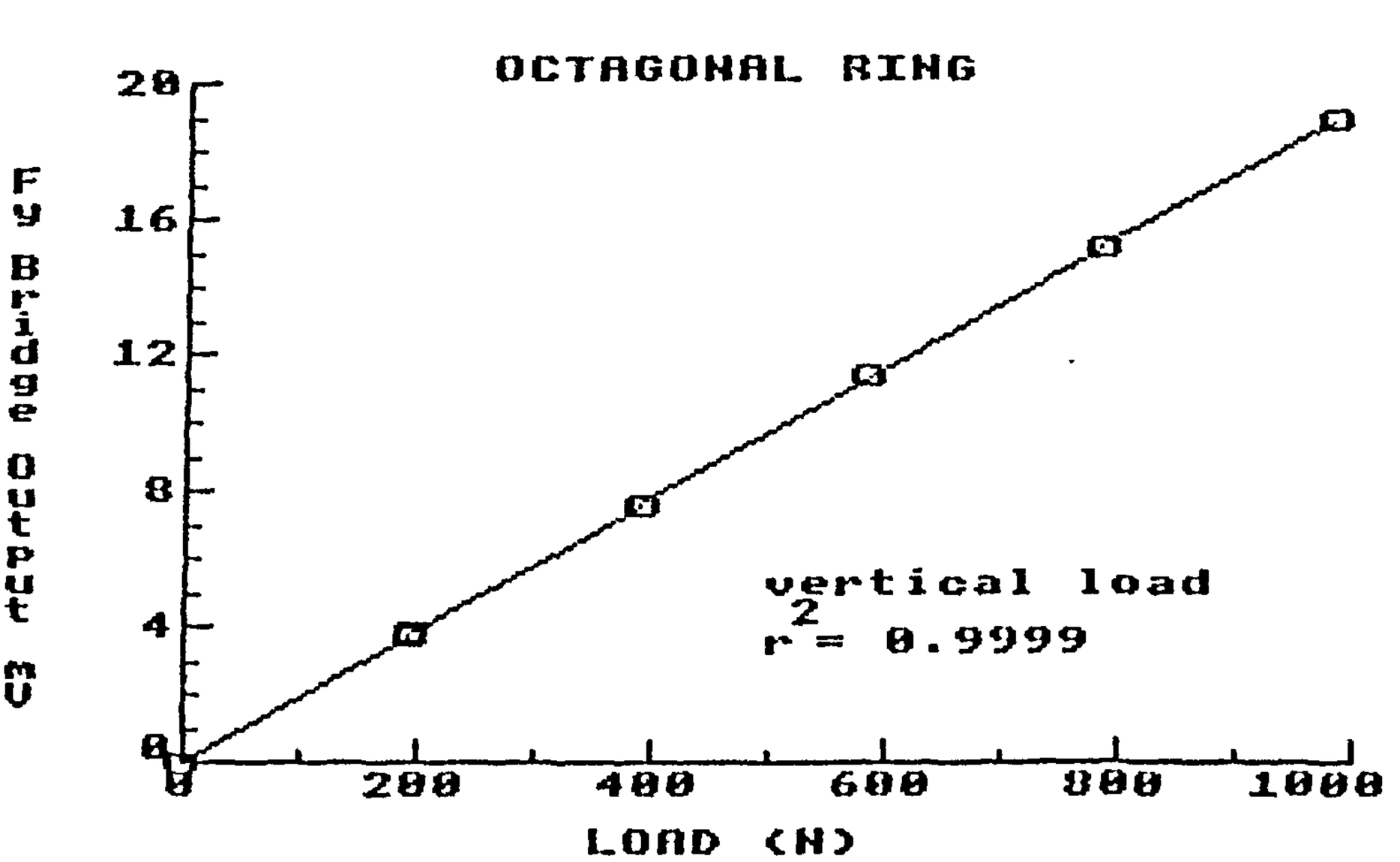

FIG. A4.1 Calibration of the extended octagonal ring transducer. Fx bridge (top) and Fy bridge (bottom)

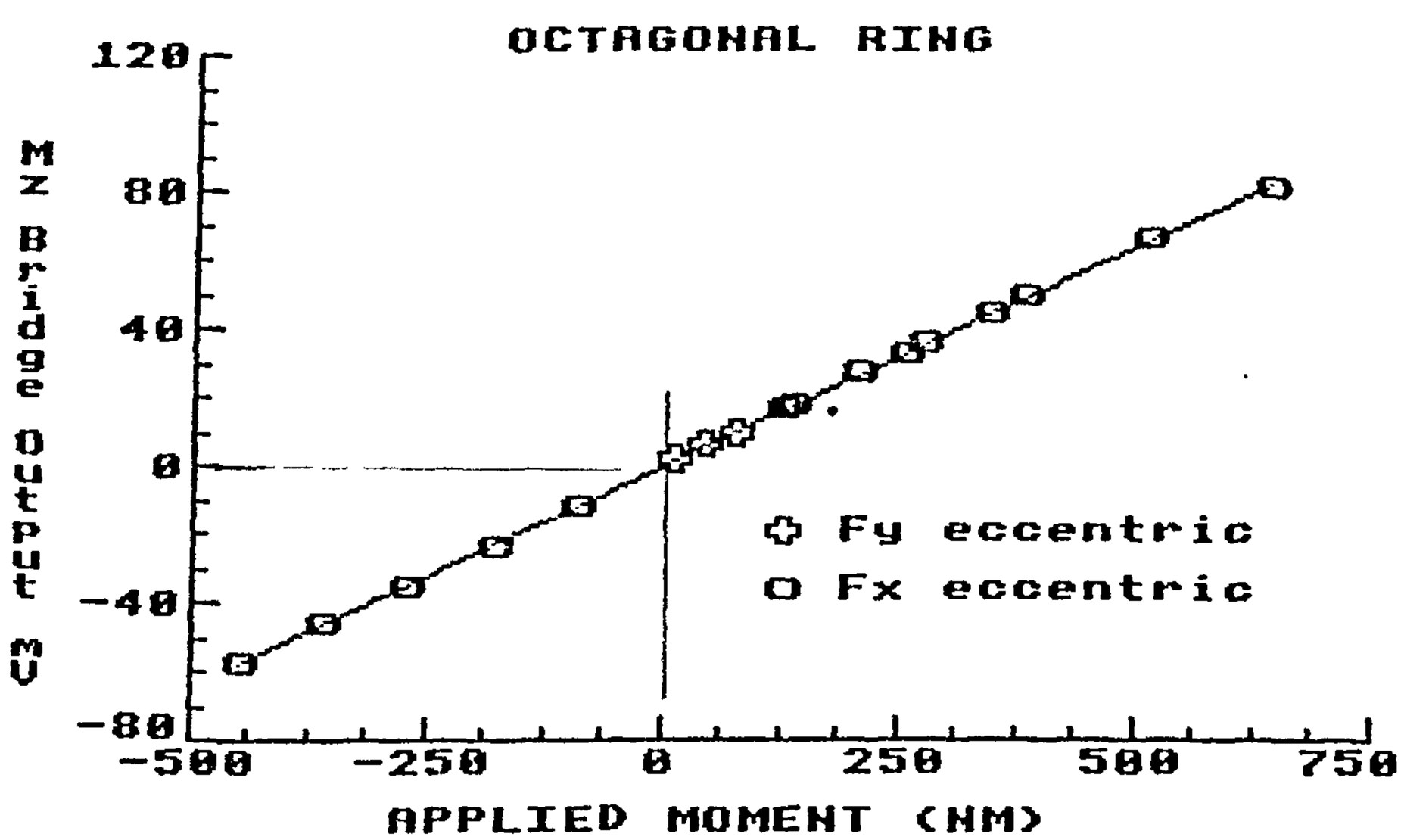

FIG. A4.2 Calibration of the extended octagonal ring transducer Mz bridge

TABLE A4.1
Extended octagonal ring transducer, bridge output for horizontal load

Fx Bridge Output mV

Load (N)	lx = 0.0 mm Loading	lx = 0.0 mm Unloading	lx = +655 mm Loading	lx = +655 mm Unloading	lx = +355 mm Loading	lx = +355 mm Unloading	lx = -455 mm Loading	lx = -455 mm Unloading
196.2	3.24	3.24	3.41	3.41	3.35	3.31	3.18	3.18
392.4	6.48	6.46	6.86	6.86	6.64	6.62	6.34	6.33
588.6	9.73	9.72	10.11	9.99	9.98	9.92	9.50	9.49
784.8	12.95	12.98	13.41	13.33	13.24	12.25	12.66	12.65
981.0	16.24	---	16.72	---	16.58	---	15.79	---

Fy and Mz Bridge outputs mV

Load (N)	lx = 0.0 mm Fy Bridge	Moment (Nm)	lx = +655 mm Mz Bridge	lx = +655 mm Fy Bridge	Moment (Nm)	lx = +355 mm My Bridge	lx = +355 mm Fy Bridge	Moment (Nm)	lx = -455 mm Mz Bridge	lx = -455 mm Fy Bridge
196.2	0.02	128.51	16.40	0.08	69.65	8.62	0.04	-89.27	-11.63	0.08
	(0.04)		(16.35)	(0.08)		(8.87)	(0.01)		(-11.55)	(0.05)
392.4	0.03	257.02	32.57	0.11	139.30	17.81	0.06	-178.54	-23.01	0.15
	(0.06)		(32.78)	(0.14)		(17.66)	(0.03)		(-22.97)	(0.10)
588.6	0.05	385.53	49.27	0.29	208.35	26.60	0.08	-267.81	-34.55	0.19
	(0.05)		(49.29)	(0.29)		(26.58)	(0.06)		(-34.44)	(0.16)
784.8	0.03	514.04	65.73	0.28	278.60	35.58	0.11	-357.08	45.84	0.24
	(0.04)		(65.28)	(0.26)		(35.32)	(0.07)		(45.84)	(0.20)
981.0	0.03	642.56	81.16	0.26	348.26	44.26	0.04	-445.35	57.13	0.23

lx = distance form the center of transducer to point of application of the load.

TABLE A4.2

Extended octagonal ring transducer, Bridge Output for Vertical Load

Fy, Fx and Mz Bridge Output mV

Load (N)	Fy Bridge output Loading	Unloading	Fx Bridge output Loading	Unloading	Mz Bridge output Loading	Unloading	Moment (Nm)
196.2	3.80	3.77	0.04	0.03	1.89	1.89	15.70
392.4	7.58	7.53	0.03	0.03	3.79	1.89	31.39
586.6	11.35	11.33	0.04	0.10	5.70	5.69	46.93
784.8	15.16	15.12	0.16	0.17	7.60	7.60	62.93
981.0	18.92	---	0.16	--	9.49	--	78.48

i. Linear response with coefficient of regression analysis of $r^2 = 0.9998$.

ii. The response proved to be independent of the origin of the eccentricity of the force.

iii. The hysteresis effect on the output result was found to be the maximum value of: $\pm \frac{17.81 - 17.66}{17.81 + 17.66} \times 100\% = 0.42\%$

A4.2.4 Cross sensitivity

Cross sensitivity is the determination of the percentage of output sensed in one bridge due to load in the other bridge. The results presented below show that the cross sensitivity was less then 1.85% at the load of 784 N. These figures would be more accurate with forces lower than 784 N.

	Fx	Fy
Fx	12.96	0.28
Fy	0.17	15.14

% of cross sensitivity of Fx in Fy = 1.85%

% of cross sensitivity of Fy in FX = 1.31%

A4.3 The "L-Shaped" tine transducer

A4.3.1 Introduction

A similar procedure, as described above for the calibration of the

extended octagonal ring transducer, was used in the calibration of the trenchless tine "L-shaped" transducer.

A4.3.2 Fy bridge

Table A4.3 and Fig. A4.3 show the results of the trenchless tine submitted to a vertical load at a different position from the centre of the transducer, where the following was possible to be observed:

i. Linear response with a coefficient of regression analysis of $r^2 = 0.99988$.

ii. The hysteresis effect on the output result was found to be the maximum value of: $\pm \frac{5.92 - 5.84}{5.98 + 5.84} \times 100\% = 0.68\%$

iii. The error between the output of the response for the load position of lx = 75 mm was no greater than 1.3% at 392.4 N.

A4.3.3 Fx bridge

Table A4.4 and Fig. A4.3 show the results of load application in the horizontal direction, where the following was possible to be observed:

i. Linear response with a coefficient of regression analysis of $r^2 = 0.9998$

ii. The hysteresis effect on the output result was found to be the

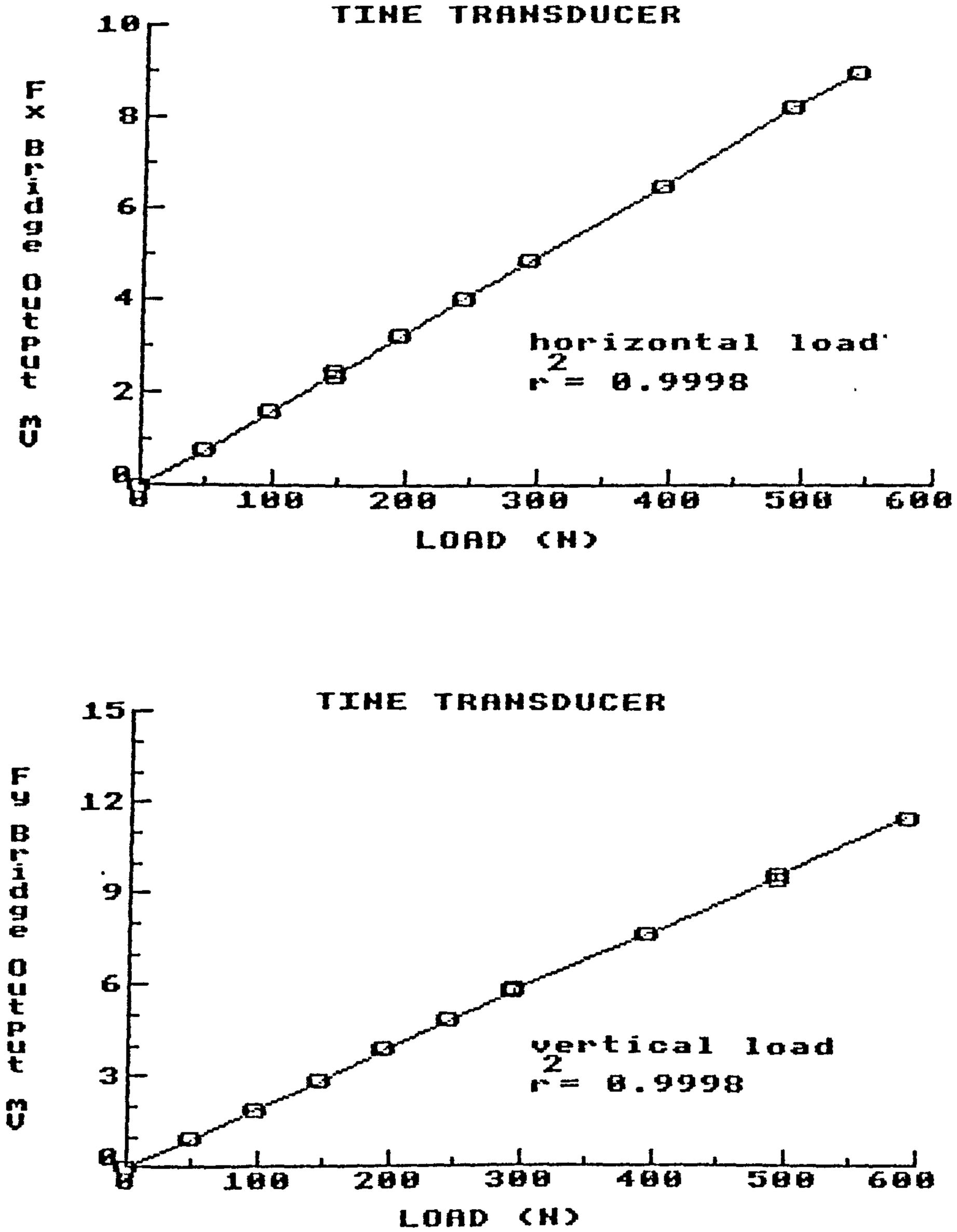

FIG. A4.3 Calibration of the tine transducer. Fx bridge (top) and Fy bridge (bottom)

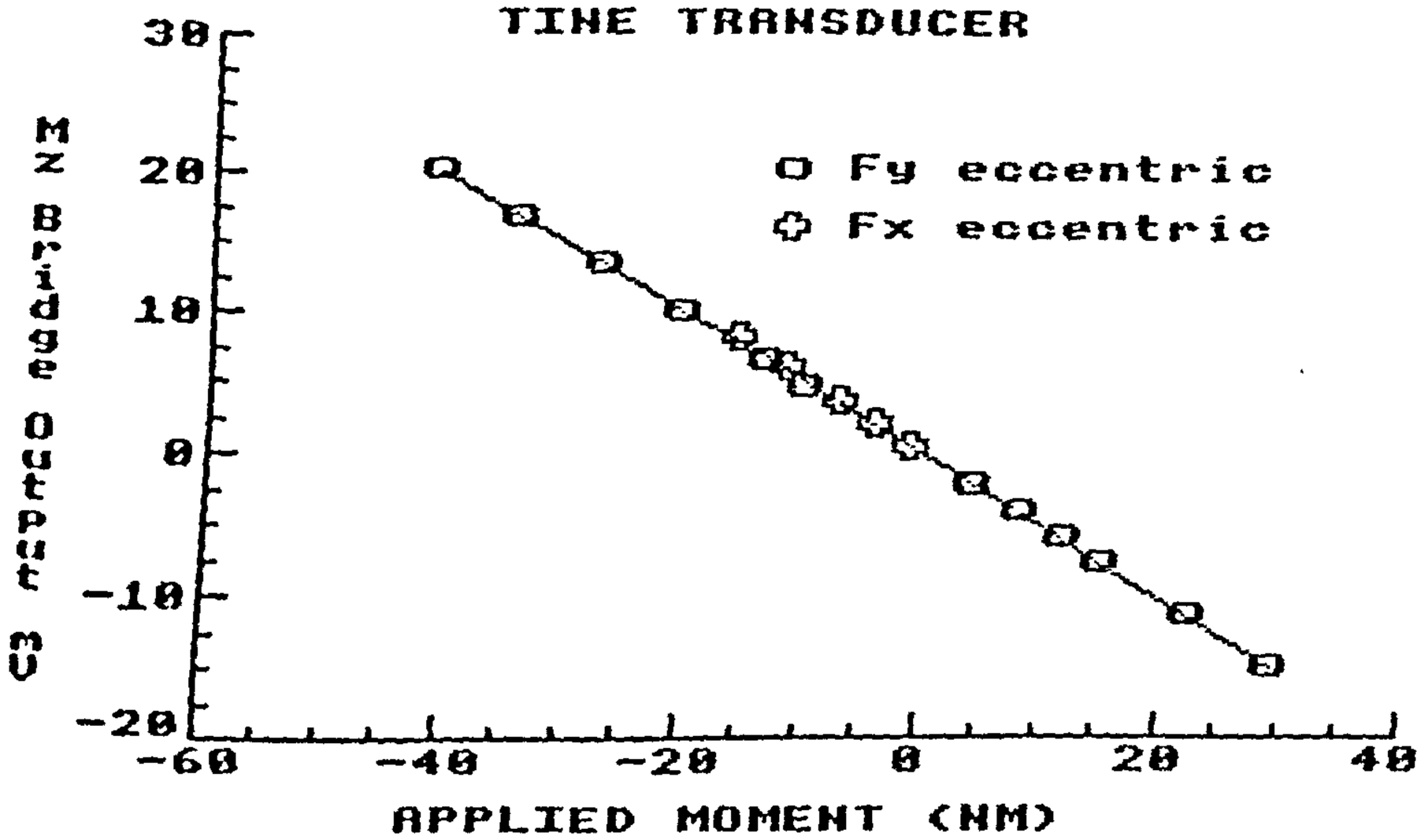

FIG. A4.4 Calibration of the tine transducer Mz bridge

TABLE A4.3
Tine transducer, Bridge Output to Vertical Load

Fy Bridge output mV

Load (N)	lx = 0.0 Loadind	Unloading	lx = -70 mm Loading	Unloading	lx = 30 mm Loading	Unloading	lx = 75 mm Loading	Unloading
49.05	0.94	0.98	0.94	0.96	0.97	0.97	0.96	0.95
98.10	1.90	1.95	1.89	1.90	1.93	1.91	1.93	1.92
147.15	2.83	2.88	2.82	2.85	2.87	2.88	2.89	2.87
196.20	3.81	3.86	3.82	3.80	3.85	3.83	3.85	3.83
245.25	4.76	4.80	4.74	4.73	4.81	4.78	4.82	4.80
294.30	5.71	5.79	5.92	5.84	5.78	5.85	5.78	5.86
392.40	7.46	7.70	7.79	7.81	7.72	7.76	7.72	7.74
490.05	9.48	9.59	9.68	9.71	9.66	9.67	--	--
580.60	11.46	--	11.53	--	11.57	--	--	--

Fx and Mz Bridge output mV

Load (N)	lx = 0.0 Fx Bridge	Moment (Nm)	lx = -70 mm Mz Bridge	Fx Bridge	Moment (Nm)	lx = +75 mm Mz Bridge	Fx Bridge
49.05	0.01 (0.00)	-3.43	1.71 (1.68)	0.04 (0.03)	3.68	-1.83 (-1.85)	0.00 (0.02)
98.10	0.02 (0.03)	-6.87	3.36 (3.41)	0.01 (0.01)	7.63	-3.71 (-3.74)	0.05 (0.01)
147.15	0.05 (0.05)	-10.30	5.00 (5.05)	0.02 (0.01)	11.40	-5.60 (-5.57)	0.05 (0.01)
192.20	0.07 (0.07)	-13.73	6.86 (6.82)	0.01 (0.06)	14.72	-7.43 (-7.43)	0.07 (0.09)
294.30	0.10 (0.10)	-20.60	10.21 (10.30)	0.00 (0.06)	14.72	-11.16 (-11.13)	0.10 (0.14)
392.30	0.16 (0.14)	-27.47	13.63 (13.73)	0.01 (0.04)	29.43	-14.86 (-14.85)	0.14 (0.12)
490.05	0.18 (0.17)	-34.30	17.04 (17.06)	0.02 (0.04)	36.75	--- ---	0.16 (0.13)
588.60	0.20	-41.20	20.33	0.03	44.15	---	0.16

Values between brackts are for unloading

TABLE A4.4

Tine transducer, Bridge Output to Horizontal Load

Fx, Fy and Mz Bridge output mV

Load (N)	Fx Bridge output Loading	Unloading	Fy Bridge output Loading	Unloading	Mz Bridge output Loading	Unloading	Moment (Nm)
49.05	0.78	0.78	0.01	0.07	0.78	0.78	-1.47
98.10	1.61	1.57	0.02	0.07	1.56	1.56	-2.94
147.15	2.44	2.38	0.03	0.03	2.33	2.38	-4.41
196.20	3.21	3.21	0.05	0.10	3.10	3.08	-5.89
245.25	4.01	4.01	0.02	0.06	3.89	3.88	-7.36
294.30	4.84	4.82	0.04	0.06	4.64	4.62	-8.83
392.40	6.46	6.46	0.05	0.06	6.17	6.15	-11.77
490.05	8.19	8.18	0.07	0.05	7.60	7.63	-14.70
539.55	8.92	--	0.05	--	8.33	--	-16.19

$$\text{maximum value of: } \pm \frac{4.84 - 4.82}{4.84 + 4.82} \times 100\% = 0.21\%$$

A4.3.4 Mz bridge

Tables A4.3, A4.4 and Fig. A4.4 show the results of eccentric load application in the horizontal and vertical directions, where the following was possible to be observed:

i. Linear response, with a coefficient of regression analysis of $r^2 = 0.9992$

ii. The response proved to be independent of the origin of the eccentricity of the force.

iii. The hysteresis effect on the output result was found to be the

$$\text{maximum value of: } \pm \frac{13.63 - 13.73}{13.63 + 13.73} \times 100\% = 0.42\%$$

A4.3.5 Cross sensitivity

The cross sensitivity resulting from force channel Fx, Table A4.4 and from force channel Fy, Table A4.3 at load of 490.5 N gives the following results:

	Fx	Fy
Fx	9.48	0.18
Fy	0.07	8.19

% of cross sensitivity of Fy in Fx = 0.74%

% of cross sensitivity of Fx in Fy = 2.20%

APPENDIX 5

Theory of Narrow Tines

Godwin and Spoor (1977) developed a force prediction model for tines of a wide range of working depth/width ratio. The model is based upon Mohr-Coulomb soil mechanics.

The authors identified two failure mechanisms:

i) an upper failure zone where the displaced soil has forward and upward components, termed crescent failure.

ii) a lower failure zone where the displaced soil has components both in the direction of travel and sideways, termed lateral failure.

The force prediction equation in the crescent failure is based on the fundamental soil equation to estimate the forces in front of the wide cutting blades, given by Hettiaratchi et al (1966). The model was later modified by Godwin et al (1984), where the following equation was given:

$$H = (\gamma.dc^2.N\gamma + c.dc.Nc + q.dc.Nq)\ [w + dc\ (m - \tfrac{1}{3}(m - 1))]$$
$$\sin(\alpha+\delta) + ca.w.dc\ (Na \sin(\alpha+\delta) + \cos\alpha) \qquad (A5.1)$$

which could be extended to the vertical direction

$$V = (\gamma.dc^2.Ny + c.dc.Nc + q.dc.Nq)\ [w + dc\ (m - \tfrac{1}{3}(m - 1))]$$
$$\cos(\alpha + \delta) - ca.w.dc\ (Na \cos(\alpha + \delta) - \sin\alpha) \qquad (A5.2)$$

The N factors in each of the terms are dimensionless numbers and whose magnitudes are dependent upon the magnitude of α, ϕ and δ. Their values can be determined using the graphic given by Hettiaratchi et al (1966), and presented in the following pages:

$$N_{\delta = \delta} = N_{\delta = 0} \left[\frac{N_{\phi, \alpha}}{N_{\delta: 0}}\right]^{\delta/\phi} \qquad (A5.3)$$

Where :

$N_{\delta = \delta}$ is N factor for a friction angle of δ^o

$N_{\delta = 0}$ is N factor for a friction angle of 0^o

$N_{\delta = \phi}$ is N factor for a friction angle of ϕ^o

and applies for N_γ, Nc, Na and Nq above.

For the force prediction model in the lateral failure zone the model was developed based on the Meyerhof (1951) technique to calculate the resultant force acting on a footing orientated at 90^o to the normally accepted direction of application.

Therefore the following equation was given by Godwin and Spoor (1977) to estimate the forces in the lower zone, between the limits of the critical depth and the total working depth.

$$Q = w\ c\ Nc'\ (d - dc) + 0.5\ Ko\ Y\ w\ Nq'\ (d^2 - dc^2) \qquad (A5.4)$$

Where the values of Nc' and Nq' can be determined from the equations below, Meyerhof (1951), or from graphic presented (Godwin 1974).

$$Nc' = \cot \phi \left[\frac{(1 + \sin \phi)\ e^{2\theta \tan \phi}}{(1 - \sin \phi \sin\ (2n + 0))} - 1 \right] \qquad (A5.6)$$

$$Nq' = \frac{(1 + \sin \phi)\ e^{2\theta \tan \phi}}{1 - \sin \phi \sin\ (2\eta + \phi)} \qquad (A5.7)$$

Where η, and ϕ are defined in Fig. A5.1

So, the total horizontal force component of the soil reaction on the face of the tine is give by:

$$H_T = H + Q \qquad (A5.8)$$

Where H is given by equation A5.1 and Q by equation (A5.5). The vertical force component is evaluated from equation (A5.2).

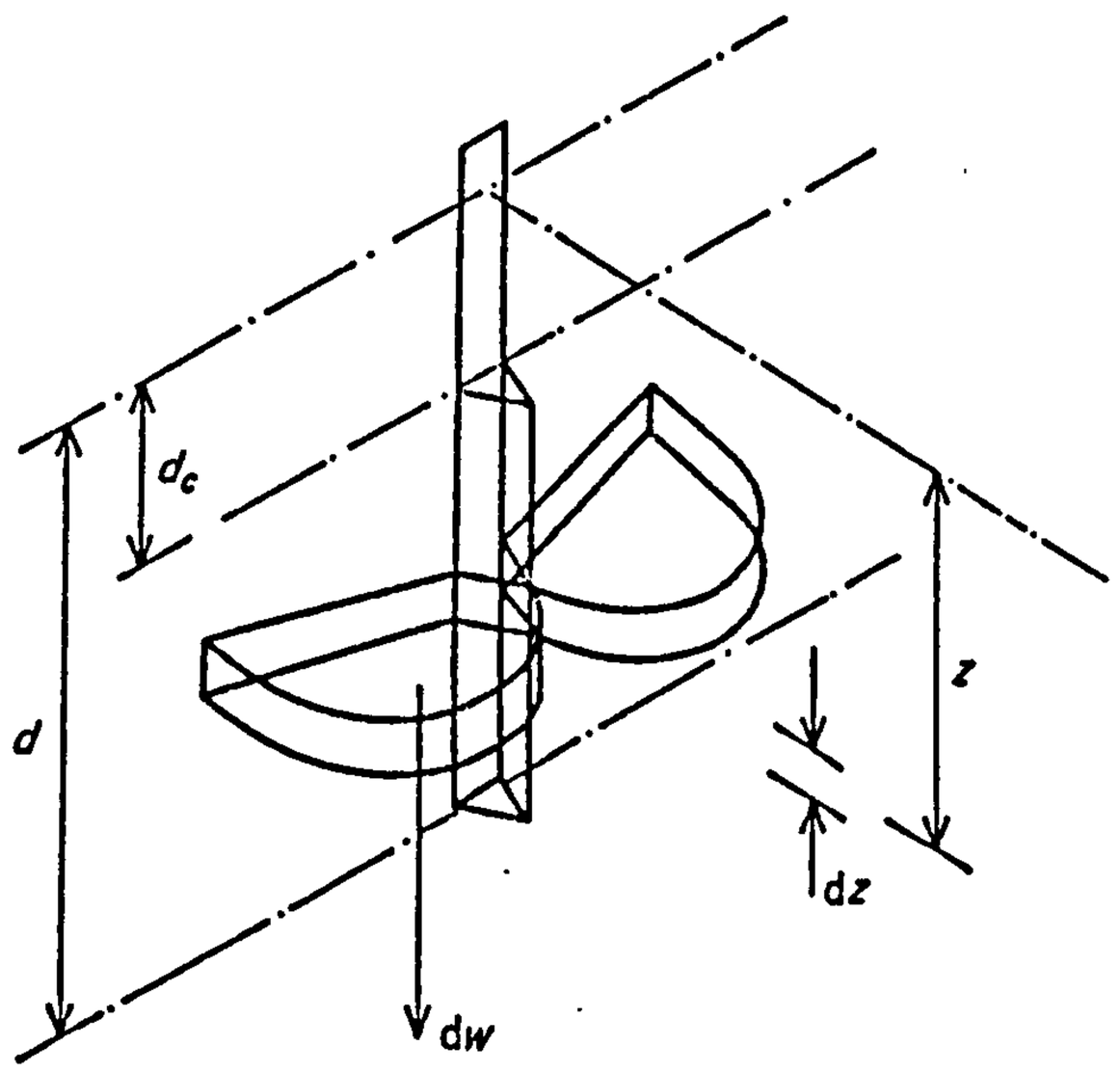

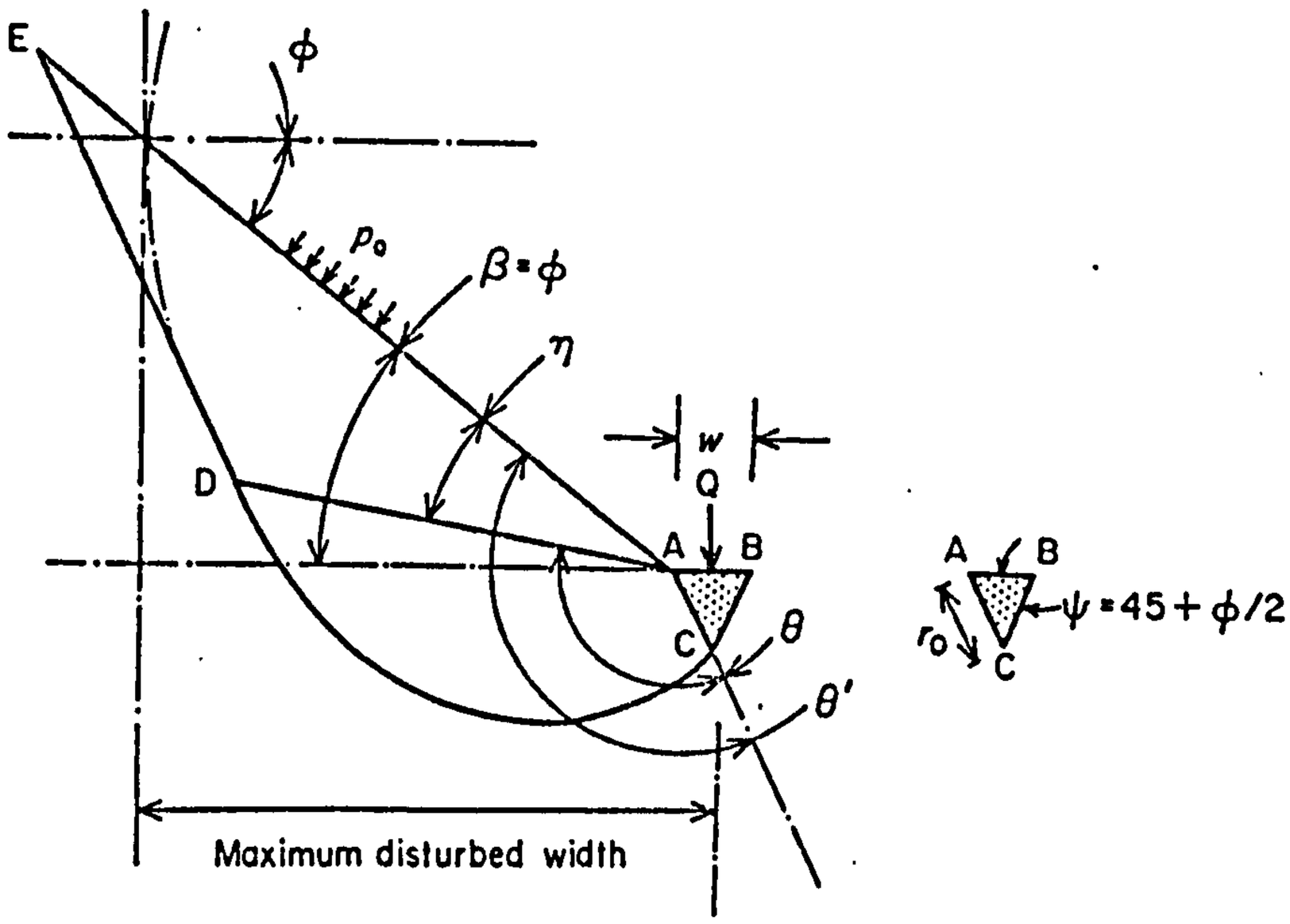

FIG. A5.1 Lateral soil failure mechanism (Godwin and Spoor, 1977)

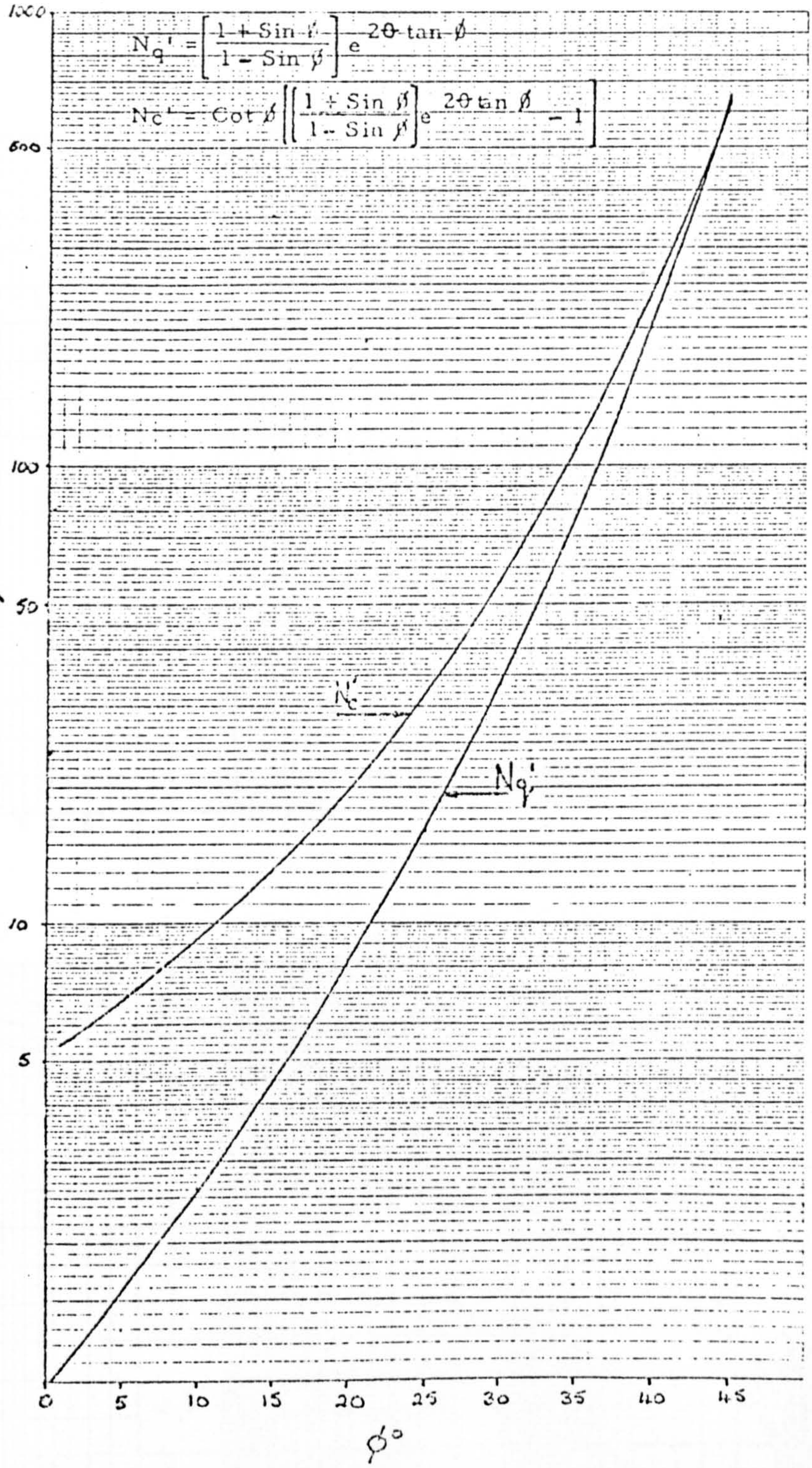

FIG. A5.2 The relationship between the dimensionless factors Nq' and Nc' and the angle of internal shearing resistance

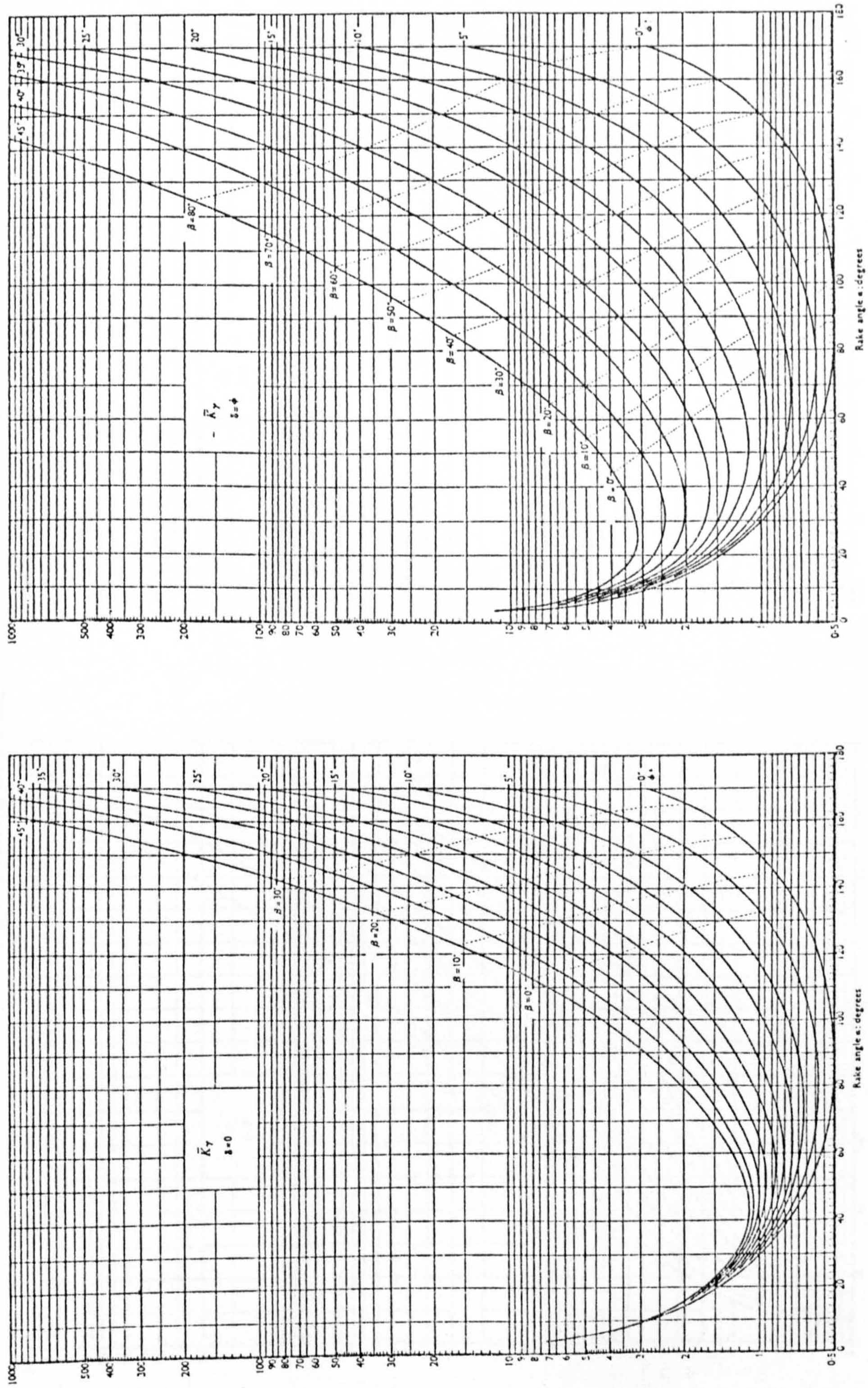

FIG. A5.3 Coefficient **N** (K=N); N_γ = 0 (left) and $N_\gamma = \mathscr{J}$ (right)

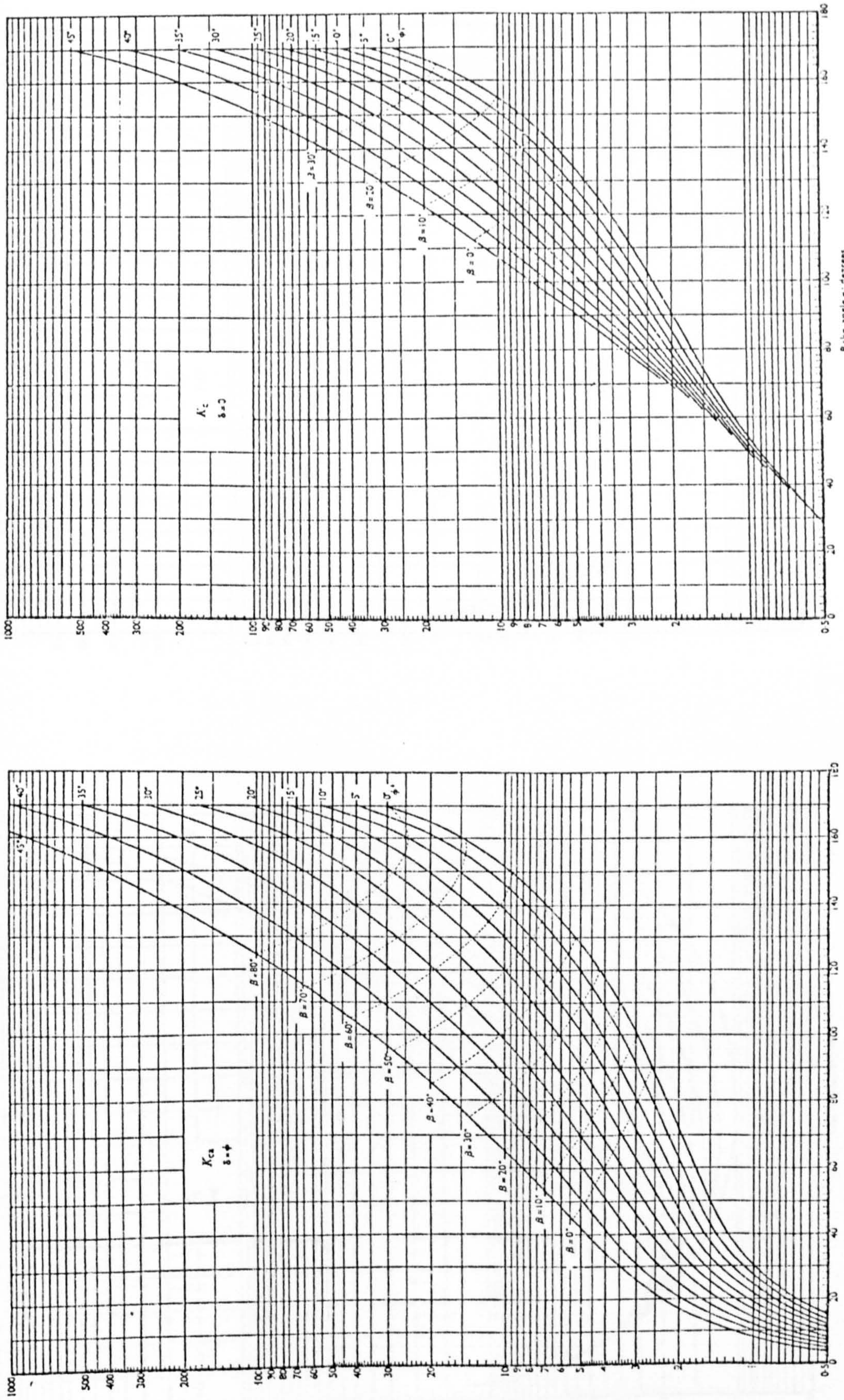

FIG. A5.4 Coefficient N (K=N); N_c = Ø (left) and N_c = 0 (right) c_a = c

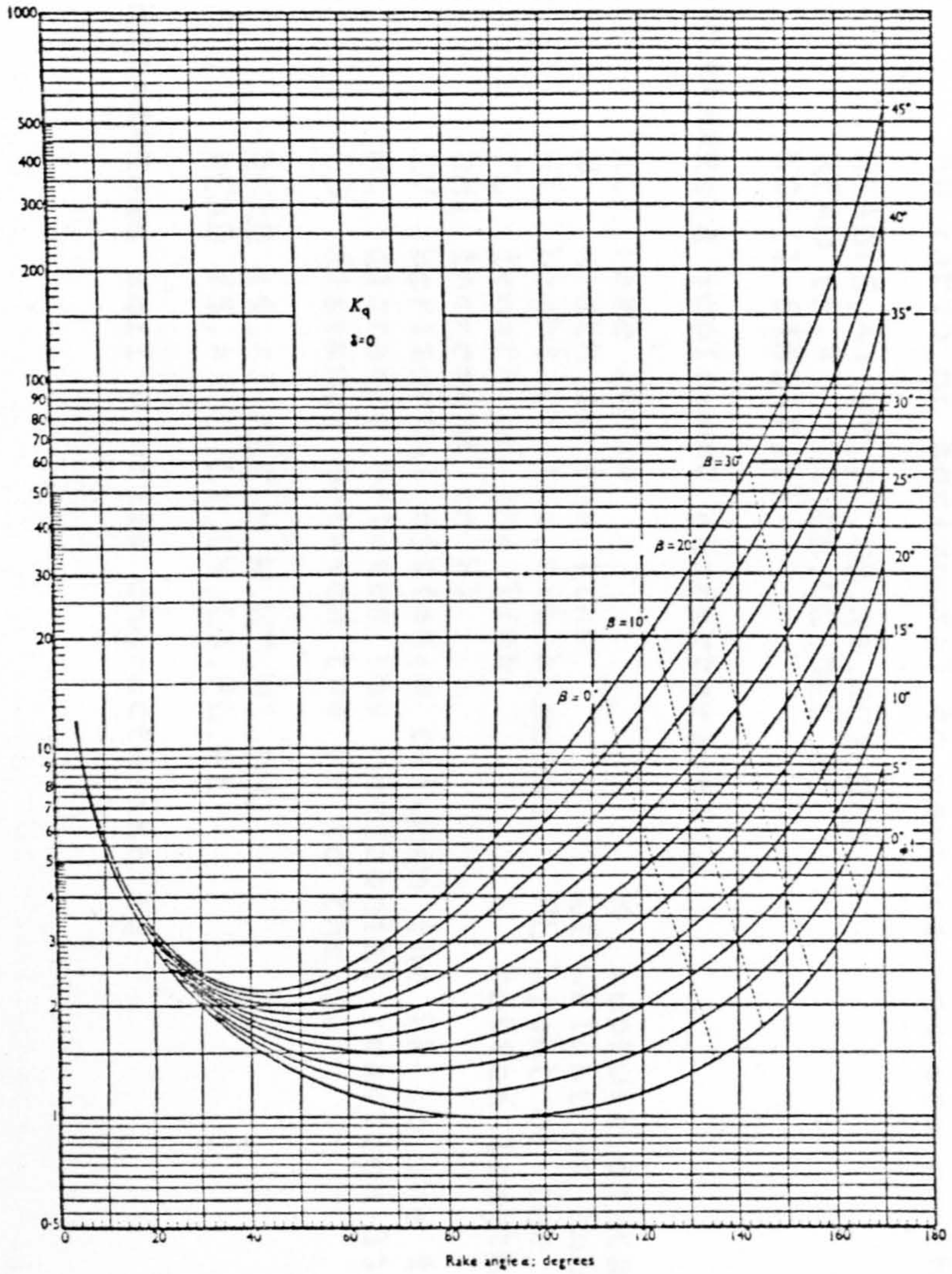

THE CALCULATION OF PASSIVE SOIL RESISTANCE

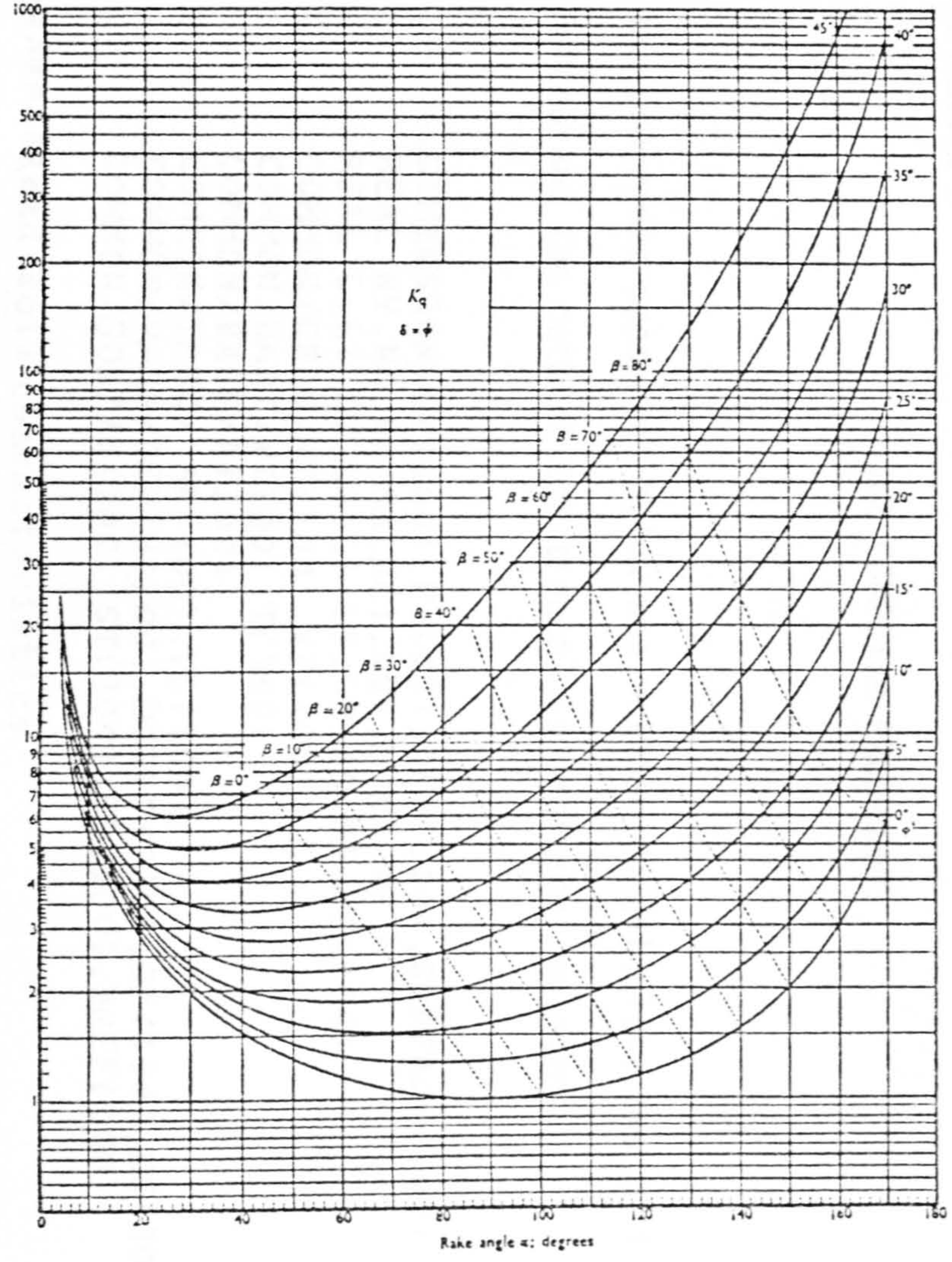

FIG. A5.5 Coefficient **N** (K=N); $N_q = 0$ (left) and $N_q = \phi$ (right)

APPENDIX 6

THE COMPUTER PROGRAMME

The programme presented below was written to calculate the soil reaction forces and the path of the trenchless drainage implement.

```
      DIMENSION GT(100),F(100),DEO(100),SURFACE(100)
      REAL NY,NC,NQ,NA,NC1,NQ1,M,NI,NF,N
      REAL L,L1,LV,L3,L4,L5,L6,KO,MI,MS(100)
      COMMON/CRAC/HT(100),VT(100)
      COMMON/DART/N(100),T(100)
      COMMON/BASF/R(100)
      COMMON/TASC/ AR(100),VL(100)
      COMMON/VASP/DEPTH(100),DCRIT(100),DP(100),DC(100)
      COMMON/GOST/S(100),ST(100),SP(100),DREF(100)

c******Read soil characteristics

c       N dimensionless numbers       QS surcharge
c       C cohesion                    FI angle of shearing resistence
c       CA adhesion                   DEL angle of soil interface friction
c       Y bulk density
c       KO ratio of horizontal to vertical strees on the soil at rest

      READ(5,*) NY,NC,NQ,NA,NC1,NQ1
      READ (5,*) Y,C,CA,QS,DEL,FI
      KO=(1-SIND(FI))

c******Read implement characteristics

c       ALF rake angle                M  rupture distance ratio
c       W   width of the tine         WT weight of the system
c       H1  hight of the hitch point  PL hight of the tine
c       FL  length of the link        L  bottom length
c       DH1 increment in H1
c       LV  horizontal distance between the PP to the tine tip
c       HL  distance between the horizontal reaction line and the PP
c       L3  distance between the PP to the GC

      READ (5,*) ALF,M,W,WT,H1,DH1
      READ (5,*) L,L1,LV,L3,PL,FL

c******Read soil profile characteristics
```

TEXT CUT OFF IN ORIGINAL

```
C       WL wavelenght                   AMP wave amplitud
C       SL length of the run            STP step input height
C       SIS step location

        READ (5.*) WL.AMP,SL,STP,SIS

        IF (AMP.EQ.0.0) GOTO 5
        WRITE(6,100) WL.AMP
        GOTO 15
   5    WRITE(6,102)
  15    WRITE(6,105) NY.NC,NQ,NA,NC1,NQ1
        WRITE(6,370) C,CA,QS,Y

C******Read hitch-point movement characteristcs

C       HWL wavelenght          HAMP wave amplitude
C       SPT step input          SIL inicial plateau or position of the ste
C

         READ (5,*) HWL,HAMP,SIL,STP
         IF (AMP.EQ.0.) GOTO 25
         WRITE(6,100) WL.AMP
   25    IF (STP.EQ.0.) GOTO 16
         WRITE (6,107) STP
C*************************************************************************

C******Calculations

C^^^^^First depth
         I=1
         S(I)=0.00
         DP(I)=0.1
   52    DC(I)=CRIT(DP(I))
         SURFACE(I)=0.15
         F(I)=M*DC(I)
         HL=(PL-DP(I)*0.10)
         MS(I)=M
         CALL FORCE1 (Y,C,QS,NC,NY,NQ,I,W,M,ALF,DEL,NA,CA,NQ1,NC1)
         CALL FORCE2 (W,C,NC1,KO,Y,NQ1,L,CA,ALF,DEL,I,LV,L3,HL,PL,WT)
         HTEST=SIND(T(I))*FL+(PL-DP(I))
         IF(ABS(H1-HTEST).LE.0.0001) GOTO 61
   53    DP(I)=DP(I)-(H1-HTEST)
         GOTO 52
   61    DEPTH(I)=DP(I)
         DCRIT(I)=DC(I)
         WRITE (6,234) DEPTH(I),DCRIT(I)
         DREF(I)=DP(I)
         H0=H1
         HII(I)=H0*100
         WINT=S(I)
         WEND=S(I)+WL*3
```

```
c*******Hitch-point position
 65       I=I+1
          S(I)=S(I-1)+0.1
          ST(I)=S(I)
          DC(I)=DC(I-1)
          DP(I)=DP(I-1)
          H1=HO+SEN((S(I)+SIL),HNL,HAMP)
          DREF(I)=DREF(I-1)+DCOR
          DP(I)=DREF(I)
          DC(I)=CRIT(DP(I))
          DEPTH(I)=DP(I)

C*******Estimation of M
          IF (AMP.NE.0.0) GOTO 79
          WINT=0.0
          WEND=WL
 79       CALL FAILURE (I,WL,AMP,Y,C,M1,FI,ALF,DEL,L1,WINT,WEND,SIS,STP)
          MS(I)=M1
          SURFACE(I)=SEN((ST(I)-WINT),WL,AMP)
          F(I)=M1*DCRIT(I)
          HL=(PL-DP(I)*0.1)
          HIT(I)=H1*100

c*******Main forces determination
          CALL FORCE1 (Y,C,QS,NC,NY,NQ,I,W,M1,ALF,DEL,CA,NA,NQ1,NC1)
          CALL FORCE2 (W,C,NC1,KO,Y,NQ1,L,CA,ALF,DEL,I,LV,L3,HL,PL,WI)
          H2=H1-SIND(T(I))*FL
          DEQ(I)=PL-H2
          DCOR=DEQ(I)+(DREF(I)-DEQ(I))*EXP(-(S(I)-S(I-1))/LV)-DREF(I)
          GT(I)=ATANDL(DEQ(I)-DREF(I))/LV)
          IF(S(I).LE.SL) GOTO 65

c*******Results output
 85       WRITE (6,440)
          DO 10 J=1,I
          N(J)=-N(J)
          T(I)=-T(I)
          DREF(J)=-DREF(J)*100
          WRITE (6,*) S(J),SL,J,DC(J),DP(J)
          WRITE(7,500) HT(J),N(J),VT(J),DREF(J),HT1,GT(J)
          WRITE(6,450) HT(J),N(J),VT(J),T(J),DREF(J),ST(J),GT(J)
     *    ,F(J),MS(J),S(J),SURFACE(J)
 10       CONTINUE
          WRITE(6,460)

c*******Format
100       FORMAT(//,2X,'Soil profile: ',2x,'wavelength=',f6.3,' m',5x,
     *    'wave amplitude=',f5.2,' cm')
102       FORMAT(//,2x,'Flat surface')
```

```
105     FORMAT(/,2X,'NY=',F6.3,3X,'NC=',F6.3,3X,'NQ=',F6.3,3X,'NA='
     *  ,F6.3,5X,'NC1= ',F5.1,3X,'NQ1= ',F5.1)
234     FORMAT (2X,'DP=',F7.3,' m',3x,'dcrit=',f7.3,' m')
300     FORMAT(/,2X,'PL=',F6.3,' cm',2X,'H1=',F6.3,' cm')
370     FORMAT(/,2X,'COHESION=',F8.2,' N/m2',2X,'ADHESION=',F5.3,' N/m2
     *  ,2x,'SURCHARGE=',F4.2,' N/m2',4X,'BULK DENSITY=',F10.3,' N/m3')
400     FORMAT(/,3X,6F10.3,F13.6)
420     FORMAT(/,3X,5F10.3)
430     FORMAT(//2X,'CRESCENT FAILURE',F7.3)
440     FORMAT(//,8X,'HT',9X,'N',8X,'VT',8X,'ALFA',6X,'DEPTH',8X,' ST
     *  ,6X,'TETA',8x,'F',9x,'M',8x,'DIST',3x,'SURFACE')
450     FORMAT(/,3X,4F10.3,2F12.5,5F10.3)
460     FORMAT(/,3X,'SUCCESSFUL')
500     FORMAT(3X,6F12.4)

        STOP
        END

        FUNCTION SEN(X,Y,AMP)
        P=4*ATAN(1.)
        SEN=-AMP*SIN(2*P*X/Y)
        END

        FUNCTION COSE(A,B,AMP)
        P=4*ATAN(1.)
        COSE=-AMP*COS(2*P*A/B)
        END

        FUNCTION CRIT (DP)
        CRIT=(-8)*DP**3+0.6*DP**2+0.9*DP
        END


        SUBROUTINE FORCE1 (Y,C,QS,NC,NY,NQ,J,W,M,ALF,DEL,CA,NA,NQ1,NC1)
        COMMON/CRAC/HT(100),VT(100)
        COMMON/VASP/DEPTH(100),DCRIT(100),DF(100),DC(100)
        REAL NY,NC,NQ,NA,NQ1,NC1,M
        S5=(Y*DC(J)**2*NY+C*DC(J)*NC+QS*DC(J)*NQ)*
     *  (W+DC(J)*(M-1/3.*(M-1)))
        HT(J)=S5*SIND(ALF+DEL)+(CA*W*DC(J)*(NA*SIND(ALF+DEL)+COSD(ALF)))
        VT(J)=S5*COSD(ALF+DEL)-(CA*W*DC(J)*(NA*COSD(ALF+DEL)-SIND(ALF)))
        RETURN
        END

        SUBROUTINE FORCE2 (W,C,NC1,KO,Y,NQ1,L,CA,ALF,DEL,J,LV,L3,HL
     *  ,PL,WT)
        COMMON/CRAC/HT(100),VT(100)
        COMMON/DART/N(100),T(100)
        COMMON/VASP/DEPTH(100),DCRIT(100),DP(100),DC(100)
        REAL KO,L,LV,L3,NQ1,NC1,N
        VL=(LV+DP(J)*0.10)
```

```
      Q=(WAC*NC1*(DP(J)-DC(J))+0.5*KO*WAY*NQ1*(DP(J)**2-DC(J)**2))
      FS=(CA*DP(J)*(2*L-DP(J)*COTD(ALF),+TAND(DEL)*KO*Y*
     *  (L*DP(J)**2-COTD(ALF)*1/3.*DP(J)**3))
      N(J)=(VT(J)*VL+WT*L3-(HT(J)+Q)*HL+FS*(PL-1/4*DP(I))/
     *  (TAND(DEL)*PL+LV+L/2.)
      IF(N(J).LE.0.) N(J)=0.
      FT=TAND(DEL)*N(J)
      HT(J)=HT(J)+FS+FT+Q
      VT(J)=VT(J)-N(J)
      T(J)=ATAND((WT+VT(J))/HT(J))
      RETURN
      END



c*******Subroutine to calculate the value of M
      SUBROUTINE FAILURE (I,WL,AMP,Y,C,M1,FI,ALF,DEL,L1,WINT,WEND,SIS,STP
      COMMON/VASP/DEPTH(100),DCRIT(100),DP(100),DC(100)
      COMMON/GOST/S(100),ST(100),SP(100),DREF(100)

      REAL M1
      HMIN=9999999.99
      P=4*ATAN(1.)
      AMP1=AMP
      IF(ST(I).GE.WINT) GOTO 1
      AMP1=0.0
1     SP(I)=SEN((ST(I)-WINT),WL,AMP1)
2     DP(I)=DREF(I)+SP(I)
      DC(I)=CRIT(DP(I))
      IF (AMP.EQ.0.0) GOTO 15
      SO=ST(I)-(DP(I)-DC(I))
      S2=L
3     IF((ST(I)-S2).LE.WINT) AMP2=0
      GS=SEN((ST(I)-S2-WINT),WL,AMP2)+(DP(I)-SP(I))
      GD=TAND(ALF+INC)*S2
      IF (ABS(GS-GD).LE.0.0001) GOTO 5
4     S2=S2+GS-GD
      GOTO 3
5     SV2=(ST(I)-S2)
      GDI=TAND(ALF+INC)*S2**2/2
      GSI=AMP*WL/(2*P)*(-COSE((SO-WINT),WL,AMP1)+COSE((SV2-WINT),
     *  WL,AMP2))+(DC(I)-SP(I))*S2
      A1=GSI-GDI
      SF=SO
      IF(SO.LE.WINT) AMP1=0.0
      IF(SO.GT.WEND) AMP1=0.0
15    BETA=50.0+FI/2.
      DO 11 J=1,50
      BETA=BETA-1.
      IF (AMP.EQ.0.0) GOTO 25
6     AMP3=AMP
```

```
      IF(SF.LE.WINT) GOTO 7
      IF (SF.LE.WEND) GOTO 8
 7    AMP3=0.0
 8    GD=TAND(BETA)*ABS(SF-SO)
      GS=SEN((SF-WINT).WL.AMP3)+(DC(I)-SP(I))
      IF(ABS(GS-GD).LE.0.0009) GOTO 10
 9    SF=(SF+(GS-GD))
      GOTO 6
10    GDI=TAND(BETA)*(SF-SO)**2/2
      GSI=AMP*WL/(2*P)*(-COSE(SF,WL,AMP3)+COSE(SO,WL,AMP1))+(DC(I)-
     *SP(I))*SF
      A2=GSI-GDI
      AT=A1+A2
      CL=(SF-SO)/COSD(BETA)
      GOTO 40
25    F1=DC(I)/TAND(ALF)
      F2=DC(I)/TAND(BETA)
      A=F1+F2
      SF=S(I)+F2
      SV2=S(I)-F1
      IF (SF.GT.SIS) GOTO 30
28    B=0
      DC2=DC(I)
      DP2=DP(I)
      CP=0
      CL=DC(I)/SIND(BETA)
      GOTO 40
30    CP=SF-SIS
      IF (CP.GT.A) CP=A
      CL=(DC(I)+STP)/SIND(BETA)
      B=(DC(I)+STP)/TAND(BETA)-(F2-CP)
      PSA=CP/A
      DPF=DP(I)+STP
      DP2=DPF*PSA+DP(I)*(1-PSA)
      DC2=CRIT(DP2)
      AT=(F1+F2)*DC(I)/2+(B+CP)*STP/2
      SF=SF+(B-CP)
40    HI=Y*AT+C*CL*(SIND(BETA)+COSD(BETA)*(COSD(BETA+FT)/SIND(BETA+FI)))
     */((COSD(BETA+FI)/SIND(BETA+FI))+(1/TAND(ALF+DEL)))
      IF(HMIN.LT.HI) GOTO 11
      IF (AMP.NE.0.0) GOTO 41
      DC2F=DC2
      DP2F=DP2
41    SFF=SF
      SV2F=SV2
      AMP4=AMP3
      BETAF=BETA
      HMIN=HI
11    CONTINUE
      DC(I)=DC2F
```

```
      DP(I)=DP2F
      M1=(SFF-SV2F)/DC(I)
      WRITE (6,*) S(I),SFF,DP(I),DC(I),I
      DEPTH(I)=DP(I)
      DCRIT(I)=DC(I)
      RETURN
      END
```